Towards a more efficacious treatment for Oropharyngeal Candidiasis (OPC): Hydrogel-forming tablets for the controlled release delivery of Chlorhexidine diacetate

Enas Atallah Al-Ani (BSc, MSc)

A thesis submitted in partial fulfilment of the
requirements of the University of Wolverhampton
for the degree of Doctor of Philosophy

April 2018

Signature……..
Date……..

Abstract:

Oropharyngeal candidiasis is a localised infection in the oropharynx region caused by *Candida* species, predominately *C. albicans.* It is commonly spread among immunocompromised patients and aggravated by hyposalivation or xerostomia. Current treatment is by systemic antifungals, which might be accompanied by gastrointestinal tract disorders, headache, allergic reactions and drug interactions or *Candida* becoming resistant to them. In the present work, the *anti-candida* activity of chlorhexidine diacetate (CHD) was tested as the drug of choice, it has no systemic side effects and microorganisms do not develop resistance against it. Thymol and farnesol were also tested individually and in combination with CHD to investigate a synergistic effect against *Candida* planktonic cells. The effects of CHD and thymol were investigated against *C. albicans* biofilm after two hours exposure by testing the metabolic stress, vacuolar activity and protein content. The results of the *anti-Candida* activity of CHD and thymol based on the minimum inhibitory concentration (MIC) and the minimum biocidal concentration (MBC) were 2.5 and 5 µg/ml for the former and 125 and 250 µg/ml for the later. Farnesol did not show an MIC and MBC at the investigated concentrations, however, it increased the MIC and MBC of CHD to 5 and 40 µg/ml and of thymol to 250 and >250 µg/ml, respectively. The antibiofilm activity of CHD and thymol was concentration dependent and CHD was more potent than thymol. A concentration of 20 µg/ml and 2 hours treatment of *Candida* biofilm grown for 24 hours showed an 85% decrease in oxidative stress, 78% and 60% loss of vacuolar activity and protein content, respectively. The combination of both drugs showed a limited increase in the activity. The cytotoxic effects of CHD and thymol were tested on human embryo kidney epithelial cell line (HEK 293); the metabolic stress, lysosomal activity and protein content were tested. The cytotoxic effects were also concentration dependent and the combination have increased the cytotoxicity. A concentration of 20 µg/ml and 2 hours treatment showed a 40% decrease in oxidative stress and neither the lysosomal activity nor protein content of HEK 293 cells was affected by the treatment

Finally, a mucoadhesive hydrogel buccal tablets for the controlled release of CHD were designed and prepared to increase the residence time of an effective concentration of CHD in the oral cavity for two hours. They were prepared using

Poloxamer 407 (P407), hydroxypropyl methylcellulose (HPMC) and either sorbitol, mannitol or xylitol at different ratios. The tablets were investigated for their physical properties, *ex vivo* mucoadhesion, the rate of hydration, gelling efficiency using image analysis, differential scanning calorimetry (DSC), Fourier transforms infrared spectroscopy (FTIR), X-ray diffractometry (XRD) and *in vitro* dissolution using Apparatus I and a novel method based on controlled flow rate to mimic salivary drug delivery in the oral cavity.

Based on the antibiofilm activity and the cytotoxic effect of CHD a concentration of 20 µg/mL was chosen to be released from the tablets to maintain both efficacy and safety. Accordingly, to maintain this concentration the final formulations were prepared with a 2.5 mg dose of CHD. Tablets analysis showed no chemical interaction with the excipient based on DSC, FTIR and XRD. Furthermore, a novel dissolution method was developed based on a constant flow rate of the dissolution media to mimic oral salivary flow. By comparing CHD release using App I and the flow rate method it was shown that hydrogel-forming tablets successfully controlled the release of CHD regardless of the volume of the dissolution media with approximately 90% release and an average release concentration of 19 µg/ml and 1 ml/min flow rate. This making it a potential candidate for future application for treatment of candidiasis in all types of patients.

Table of Contents

List of Figures

Appendices Figures

List of Tables

Appendices Tables

List of Abbreviations

AGS	**Human gastric carcinoma cells**
AIC	**Akaike information criterion**
ANOVA	**Analysis of variance**
App I	**Apparatus I (basket method)**
AUC	**Area under the curve**
BNF	**British National Formulary**
BP	**British Pharmacopoeia**
CFR	**Controlled Flow Rate**
CHD	**Chlorhexidine diacetate**
CI	**Carr's (compressibility) index**
cm	**Centimetre**
CMC	**Carboxymethyl cellulose**
CV	**Crystal violet**
D.E.	**Dissolution efficiency**
DMEM	**Dulbecco's modified eagle's medium**
DMSO	**Dimethyl sulfoxide**
DNA	**Deoxyribonucleic acid**
DNase	**Deoxyribonuclease**
DSC	**Differential scanning calorimetry**
EDTA	**Ethylenediaminetetraacetic acid**
EDX	**Electron dispersive x-ray analysis**
EO	**Polyethylene oxide**
FBS	**Foetal bovine serum**
FIC	**Fractional inhibitory concentration**
FTIR	**Fourier transforms infrared spectroscopy**

GIT	**Gastrointestinal tract**
GSH	**Glutathione**
HEK 293	**Human embryo kidney epithelial cells**
HEC	**Hydroxyethyl cellulose**
HLB	**Hydrophilic lipophilic balance**
HPC	**Hydroxypropyl cellulose**
HPMC	**Hydroxypropyl methylcellulose (Dow-Colorcon)**
HPMC-S	**Hydroxypropyl methylcellulose (Sigma)**
HR	**Hausner Ratio**
M	**Mannitol**
MBC	**Minimum biocidal concentration**
MEB	**Malt extract broth**
MgSt	**Magnesium stearate**
MHB	**Muller Hinton Broth**
MIC	**Minimum Inhibitory Concentration**
min	**minute(s)**
MOPS	**3-(N-Morpholino) propane sulfonic acid, 4-Morpholinepropanesulfonic acid**
MTT	**3-(4,5-Dimethyl-2-thiazolyl)-2,5-diphenyl-2H-tetrazolium bromide**
NR	**Neutral red uptake**
OPC	**Oropharyngeal Candidiasis**
P407	**Poloxamer 407**
PAA	**Polyacrylic acid**
PBS	**Phosphate buffer saline**

PO	**Polypropylene oxide**
PVA	**Polyvinyl alcohol**
PWL2	**piecewise linear regression 2**
RNase	**Ribonuclease**
RPM	**Rotation per minutes**
RPMI-1640	**Roswell Park Memorial Institute medium**
QSM	**Quorum sensing molecules**
s	**Second**
S	**Sorbitol**
SCMC	**Sodium carboxymethyl cellulose**
SD	**Standard deviation**
SDA	**Sabauroud dextrose agar**
SE	**Standard error**
SGH	**salivary glands hypofunction**
SEM	**Scanning electron microscopy**
SGH	**Salivary glands hypofunction**
SI	**Swelling index**
SRB	**Sulforhodamine B**
TCA	**Trichloroacetic acid**
X	**Xylitol**
XRD	**X-ray diffractometry**
XTT	**2,3-bis(2-methoxy-4-nitro-5-sulfophenyl)-2H-tetrazolium-5-carboxanilide**

Acknowledgement

All praise to almighty ALLAH for giving me the blessing, strength, patience to complete this work.

I express my deepest gratitude to my supervisory team, to Professor David Hill, Dr Claire Martin and Professor Stephen Britland for their constant encouragement, continuous support, immense knowledge, inspiring suggestion and critical discussion. I am grateful to Dr Claire Martin, my first director of study, for the confidence and freedom she gave me to do this work. Moreover, I am grateful to Professor David Hill, my current director of study, for his patience in proofreading my thesis and for his unlimited support.

I would also like to take this opportunity to express my gratitude to my wonderful colleagues, Dr Joanne Skidmore, Clare Murcott, Nadia Ahmad, Henrick Townsend, Lawrence Eagle and Colin Hill for their support and encouragement.

Special thanks to Nick Skidmore for training me to use the tablet press, David Locust for helping in microscopical imaging, Dr Keith Jones (SEM images), David Townrow (Particle size and XRD analysis) and Dr. Angela Williams for her support and for ordering the chemicals. Many thanks to the microbiology technical staff Andrew Brooke, Ann Dawson and Balbir Bains for their kind support.

My sincere gratitude goes to Dr Angel Armisella for tissue culture training and the generous gift of HEK293 cells and to Dr Khalid Doudin (Aston University) for helping in DSC analysis. My sincere thanks go to my wonderful lab-mates Fatima Buba, Dr Ibrahim Khalil, Hussaini Bello, Abhishek Gupta, Parmjit Dosanjh and Dr Olajumoke Adebayo for the stimulating discussion and wonderful time.

Most of all, I am fully indebted to my beloved parents for their unlimited love, support and encouragement.

Dedication

This Thesis is dedicated to my parents, my sisters, my brothers and my little nephew Mimi for their love, endless support, encouragement and guidance

Words cannot express my sincere gratitude to you. I pray that Almighty ALLAH bless you exceedingly

Chapter One
Introduction

Chapter 1 : Introduction

1.1 Oropharyngeal Candidiasis (OPC)

Oropharyngeal Candidiasis (OPC) is a localised *Candida* spp. infection of the oral cavity and pharynx, characterised by inflammation and superficial, elevated white plaques resembling milk curds. Lesions may develop and spread to cover most of the mouth, accompanied by pain, burning or dryness, loss of taste and pharyngeal dysphagia (Hoepelman and Dupont, 1996). Although *Candida albicans* predominates, OPC is associated with a range of commensal *Candida* species (Kamikawa *et al*., 2013), including *C. tropicalis*, *C. glabrata*, *C. dubliniensis, C. parapsilosis, C. krusei*, *C. utilis*, *C. guilliermondii, C. ciferrii* and *C. norve* (Lin *et al*., 2013). In healthy individuals, protection against *Candida* spp. overgrowth and colonisation are achieved by the presence of bacterial flora which limits the opportunity for attachment and proliferation; the host's epithelial cell barrier and defensive immune system activities are also implicated (Gow and Hube, 2012).

The global annual incidence of oral and oesophageal candidiasis are approximately 2 and 1.3 million respectively, oral candidiasis might be proliferating to invasive candidiasis with an annual incident rate of 5142 in the UK. The estimated mortality rate from invasive candidiasis is >40% despite the introduction of new antifungals (Bongomin *et al.,* 2017). This can be explained by the resistance of *Candida* to antifungal medications.

1.2 Host factors and OPC

1.2.1 Normal flora

Normal commensal oral flora, including *Streptococcus sanguis, S. salivarius, E. coli* and *Porphyromonas gingivalis,* effectively decrease *Candida* (*C. albicans* and *C. krusei*) colonisation on buccal epithelium in a species and concentration-dependent manner (Nair and Samaranayake, 1996). Commensal microbial flora competes with pathogenic microorganisms for binding sites on the anionic biopolymer mucin a major component of the mucous membrane and secreted by epithelial cells (Derrien *et al*., 2010).

1.2.2 From commensalism to pathogenesis

Although *C. albicans* is commensal fungi on human mucosal surfaces, it invades the skin, oral cavity, oesophagus, gastrointestinal tract, vagina and vascular system (Calderone and Fonzi, 2001). It is a polymorphic fungus; it grows from oval unicellular budding yeast to a pseudohyphal form consisting of an elongated chain of budding cells that subsequently develop to hyphae, which are formed of parallel sided filaments. The transition of *C. albicans* from a commensal yeast to pathogenic pseudohyphal (intermediate stage) and hyphal forms is reversible (Bastidas and Heitman, 2009). This process is regulated by quorum sensing molecules (QSM) synthesized by *C. albicans.* They are involved in cell-to-cell communication and signaling, including 1) tyrosol (accelerates hyphal transition) (Brilhante *et al*., 2016), and 2) farnesol (suppresses transition to the hyphal form) (Han *et al*., 2011). *Candida* spp. transition from yeast to hyphal form can also be suppressed by 3-oxo-C12-homoserine lactone, a QSM secreted by *P. aeruginosa* (Lu *et al*., 2014). *C. albicans* pathogenicity can also be triggered by

the secretion of hydrolytic enzymes, including proteinase, phospholipase and lipase (Owotade and Patel, 2014).

1.2.3 Epithelial cell activity

The oropharynx is lined by mucosa or mucous membrane, which consists of epithelial cells and the underlying connective tissue that contains blood supply (Squier, 1991). Epithelial cells taken from healthy volunteers display anti-*Candida* activity *in vitro*, a feature which is also seen with epithelial cells taken from HIV positive (HIV+) patients without OPC infection. Epithelial cells appear to prevent the growth of *Candida* in the oral cavity by stimulating the release of cytokines in response to the presence of *C. albicans.* (Lilly *et al*., 2006). Cytokines are proinflammatory agents activating cell phagocytic potential and generating a long-lasting immune response. Moreover, some cytokines promote a direct *anti-candida* killing activity of epithelial cells, this requires a direct contact between epithelial cells and *Candida* (Dongari-Bagtzoglou and Fidel Jr, 2005). HIV+ patients with concurrent OPC infection display epithelial cells with lower anti-*Candida* activity (Steele *et al*., 2000); interestingly this feature of a weakened epithelial cell response to the presence of *C. albicans* in HIV+ patients is observed regardless of their OPC infection status.

1.2.4 Saliva

Saliva is a clear, slightly acidic, dilute aqueous liquid composed of more than 99% water that is secreted from the major (parotid, sublingual and submandibular) and minor salivary glands located around the mouth, and from the gingival fluid. The normal salivary flow rate is ≥0.1mL/min for unstimulated and ≥0.7 mL/min for

stimulated saliva, respectively (Cho *et al*., 2010). A thin mobile layer of saliva covers the mucous membrane and forms an 8-40 μm thick pellicle over the teeth by selective adsorption by salivary protein molecules (Schipper *et al*., 2007). Saliva and its flow rate have a prominent role in controlling OPC (Akpan and Morgan, 2002).

Saliva has different functions depending on its composition (Slomiany *et al*., 1996):

1. Lubrication and humidification
2. Buffering and clearance
3. Maintenance of tooth integrity
4. Antibacterial activity
5. Taste and digestion

The organic and inorganic components of saliva are detailed in Table *1.1*

Table 1.1 Saliva composition.

Component	Function	Reference
Inorganic ions and salts (*e.g.* sodium, chloride, calcium, phosphate and bicarbonate)	• Enhances taste sensation • Maintains dental structure • Buffering capacity	Dodds *et al*., 2005
Mucin	• Promote bacterial aggregation and clearance from the oral cavity • Protect the buccal epithelial from the pathogenic microorganisms • Lubricant	Slomiany *et al*., 1996 Derrien *et al*., 2010
Salivary Agglutinin	Promote bacterial aggregation and clearance from the oral cavity	Reichhardt *et al*., 2014
Cystatin-cysteine proteinase inhibitor	Control the degradation of proteins by inhibiting proteinase enzyme produced by host and colonising microorganisms	Baron *et al*., 1999
Von Ebner glands protein (VEGh) - cysteine proteinase inhibitor	• Bitter taste perception • Proteinase inhibitor similar to cystatin	Van't Hof *et al*., 1997

Secretory leucocyte proteinase inhibitor	• Inhibit protease enzyme • Antibactericidal and antifungal activity which may be attributed to its positive charge	Doumas *et al*., 2005
Histatins	• Anti-candida (kill candida or inhibit its germination) • Inhibit the protease enzymes of the host and the bacteria	Xu *et al*., 1991) Paul *et al*., 2011
Lactoferrin	• Bacteriostatic, bactericidal activity and marker in periodontal disease • Inhibit the adhesion of microorganisms to host cells	Valenti and Antonini, 2005
Defensins	Antimicrobial, antifungal and cytotoxic activity.	Abiko *et al*., 2003
Proline-rich Proteins	• Lubricant and bind to bacteria • Maintain the homeostasis of calcium • Responsible for astringent sensation in food and beverage	Pascal *et al*., 2006
Statherin	• Inhibit calcium phosphate precipitation in the saliva • Maintain the mineralisation of the enamel surfaces • Anti-candida activity (inducing the conversion of *C. albicans* from hyphae to the yeast form)	Sarode *et al*., 2014 Leito *et al*., 2009
Salivary IgA	• Inhibit bacterial colonisation and adhesion to the mucosal epithelial cell • Neutralize toxins and enzymes produced by bacteria • Enhance the defence activity of lactoferrin and lysozymes	Kilian *et al*., 1988
Calprotectin	• Antimicrobial (competitive binding to zinc metal) • Anti-candida (by inhibiting yeast growth phase and transforming to hyphal phase)	Kleinegger *et al*., 2001
Peroxidase	• Antibacterial, antifungal and antiviral activity (achieved by the oxidation of thiocyanate by hydrogen peroxide) • Protect the human cells from the carcinogenic and mutagenic activity of hydrogen peroxide	Ihalin *et al*., 2006
Lysozyme	Antibacterial, antifungal and antiviral activity (by enzymatic and non-enzymatic activity)	Yeh *et al*., 1997

Chitinase	Defence mechanism against chitin containing pathogen such as *C. albicans*	Van Steijn *et al*., 1999
α-Amylase	Break down starch and glucose to maltose	Mese and Matsuo, 2007
Lipase enzyme	• Digest small fraction of triglyceride • Responsible for triglyceride taste in the human	Mese and Matsuo, 2007

1.3 OPC Predisposing factors

Whilst OPC is prevalent among immunocompromised patients, there are also several underlying conditions that can act as predisposing factors:

1.3.1 Local factors

Xerostomia and Sjögren's Syndrome: Xerostomia is a subjective sensation of oral dryness which might be attributed to salivary glands hypofunction (SGH), although it may occur with normal salivary glands function. SGH is characterised by a pronounced decrease in salivary flow rate (Plemons *et al*., 2014, Närhi *et al*., 1999). The prevalence of xerostomia and SGH is increased by the effect of systemic diseases and its related pharmacotherapy and/or radiotherapy (Holmes, 1998). For instance, antihistamines, anticholinergics, antihypertensives, antidepressants and opioids (Bergdahl and Bergdahl, 2000) radiotherapy for head and neck cancer (Lovelace *et al*., 2014), anxiety, depression, stress (Bergdahl and Bergdahl, 2000), Sjogren's syndrome, diabetes (Moore *et al*., 2001) and HIV infection (Islam *et al*, 2012) have been shown to be linked to xerostomia and or SGH a condition that increases with age (Närhi *et al*., 1999). It results in dry mouth, difficulty swallowing and increased susceptibility to infection. The oral carriage of *Candida* is directly related to the salivary flow rate,

although there is no linear relationship between candidiasis and salivary flow rate (Navazesh *et al*., 1995). Sjögren's syndrome is an autoimmune disease characterised by inflammation of lachrymal and salivary glands, results in xerostomia and viscous saliva with a concurrent rise in *Candida* colonisation (Plemons *et al*., 2014). The prevalence of this syndrome in Europe is 0.1-4.8% of the population (Both *et al.,* 2017).

The normal salivary flow rate is ≥ 0.1 mL/min for unstimulated and ≥ 0.7 mL/min for stimulated saliva, respectively (Cho *et al*., 2010). In fact, the number of *Candida* colony forming units is inversely proportional to the salivary flow rate. CFU of 400/ml was set as a cut of value, thus patients, with a history of xerostomia, who had a low salivary flow rate of 0.71 ml/min had a high *Candida* CFU/ml (≥ 400), whilst those with a higher salivary flow rate of 0.96 ml/min gave counts of < 400 ml/min (Torres *et al*., 2002, Holmes, 1998).

For the relief of the dryness symptoms of the mouth many salivary substitute formulations have been used, for example, Biotène Oralbalance® gel Xerotin® spray, BioXtra® gel, Glandosane® spray, Saliva Orthana® spray or lozenges, Saliveze® spray and Salivix® pastilles (BNF, 2017). Muscarinic receptor agonists; pilocarpine (Leek and Albertsson, 2002) (BNF, 2017), and cevimeline (Petrone *et al*., 2002) are used to stimulate the release of saliva in patients with residual activity in their salivary glands.

Radiotherapy of head and neck cancers: Radiotherapy results in damage to the mucosa, jaw muscles, alveolar bone and salivary glands, causing xerostomia (Bulacio *et al*., 2012).

Dentures Immunosuppressed patients with dentures are more prone to *Candida* spp. infections. The acrylic resin found in dentures can control yeast adhesion by

increasing surface hydrophobic interaction between *Candida* and the surface of the denture (Yoshijima *et al*., 2010). *Candida* colonisation also increases by co-aggregation with certain Streptococcus spp. that also adhere to dentures (Jenkinson *et al*., 1990).

Carbohydrate intake: *Candida* spp. adherence to buccal epithelial cells is enhanced by higher carbohydrate intake (Samaranayake and Macfarlane, 1982). Abu-Elteen (2005) reported the effect of different carbohydrates (galactose, glucose, sucrose, fructose, maltose, sorbitol, lactose, trehalose and xylitol) on *C. albicans, C. tropicalis, C. glabrata and C. parapsilosis* adhesion to buccal epithelial cells. Galactose, glucose, sucrose, fructose and maltose were considered as a risk factor for candidiasis, by enhancing yeast adhesion when associated with poor oral hygiene, xylitol showed an inhibitory effect. As *Candida* spp. are unable to catabolise xylitol which leads to an increase in osmotic pressure, cell swelling and eventually death.

1.3.2 Systemic factors

HIV+ patients: The prevalence of HIV in the UK is estimated to be 0.16% in 2016 (Public Health of England, 2016) and OPC is the first clinical sign of HIV+ patients with an incidence of 50-90% (Fidel., 2006). The prevalence is increased when the CD4+ T helper cell count is < 200/µl (Lin *et al*., 2013), these cells are considered as the predominant host defence mechanism against OPC (Fidel., 2006). Although treatment with antiretroviral therapy (ART) increases CD4 cells, it was reported that there was no relationship between the extent of *Candida* infection for patients receiving ART (Katiraee *et al*., 2010). This might be attributed to HIV viral load, which has an equal importance of CD4 cells count. It

was found that OPC development increases with a viral load of >10000 copies/ml, which might have a role in host susceptibility to the infection (Thompson *et al.,* 2010).

Moreover, in HIV patients there is also a significant reduction in saliva flow rate and the secretory proteins from the salivary glands, which possess antibacterial, anti-Candidal and antioxidant activity. (Leigh, 2004).

Smoking: Smoking is a high-risk factor when combined with other predisposing factors for *Candida* infection (Shiboski and Shiboski, 2013). In tobacco smokers the population of oral leukocytes and immunoglobulins are decreased by the effect of nicotine, thus aggravating *Candida* infection (Soysa and Ellepola, 2005). The proportion of keratinised epithelial cells is also raised, which increases *C. albicans* tissue adherence and hence leads to greater yeast colonisation in smokers (Williams *et al*., 1999). Furthermore, secretion of histolytic enzymes and *Candida* spp. adherence increases *in vitro* following exposure to cigarette smoke condensate (Baboni *et al*., 2009).

Malignancy: Patients with malignancy, specifically haematological ones, have a higher incidence of Candidiasis (resulting from neutropenia) even before starting treatment (Epstein and Polsky, 1998). In addition, cytotoxic drugs can cause atrophy of oromucosal epithelial cells which increases inflammation, ulceration and xerostomia and decreases the number of lymphocytes and neutrophils resulting in reducing the defence mechanism. All the above conditions are aggravated by the concurrent administration of antibiotics. (Soysa *et al*., 2004)

Diabetes: Poor glycaemic control is the major reason behind diabetic related oral disorders, including gingivitis, periodontitis, dental caries salivary dysfunction,

oral mucosal disorders, oral candidiasis and other neurosensory disorders (Lamster *et al.,* 2008). The incidence of candidiasis is five times higher in diabetic patients than in non-diabetics (Guggenheimer et al., 2000) and OPC incident in diabetic patients is increased with cigarette smoking, use of denture and salivary hypofunction (Ship, 2003). Moreover, Type II diabetics are more susceptible to *Candida* spp. infections resulting from neuropathic salivary gland impairment and consequently reduction in saliva flow rate (Mata *et al*., 2004). Another factor is the salivary glucose level which is higher in diabetic patients, the glucose resulting in glycosylated proteins which promote *Candida* adhesion (Soysa *et al.,* 2006)

Elderly: Geriatric patients are more prone to *Candida* infections due to changes in normal flora and microenvironment, denture wearing, decreased salivary flow rate, decreased the immune response, the use of medications and systemic diseases (Zakaria *et al.,* 2017, Ai *et al.,* 2017). Wu *et al.,* (2013) investigated the prevalence of *C. albicans* among ethnic eastern Chinese patients with leukoplakia and epithelial dysplasia. Finding that the incidence of candidiasis was higher amongst geriatric patients, this population group were also more prone to chronic conditions such as diabetes, bronchial asthma, xerostomia, the requirement for dentures and regular administration of polytherapeutics, all of which encourage *Candida* infections (Gonsalves *et al.,* 2008).

Low Body Mass Index (BMI): Low BMI is strongly related to malnutrition (Shahin *et al.,* 2010) that can result in decreased salivary flow rate and reduced cytokines level, both of which are associated with candidiasis (Van Lancker *et al.,* 2012). Patients with protein-energy malnutrition, have iron, folate Vitamin B12 and Vitamin C deficiencies may also result in a decrease in natural defence

mechanisms, loss of the mucosal integrity and thus aggravate *Candida* invasion (Farah *et al.,* 2010). Amiri *et al*., (2012) also showed that patients with low BMI and malnutrition are more prone to *Candida* infection resulting from immune system suppression.

1.3.3 Effect of medications

Antimicrobials: Several mechanisms explain the effect of antimicrobials on Candida spp. virulence including reduced neutrophil activity, increased antibacterial activity against normal antagonistic flora (Soysa *et al*., 2008) and the subsequent reduction of these florae that increase nutrient availability (Seelig, 1966).

Inhaled Corticosteroids: The incidence of OPC in asthmatic patients treated with inhaled corticosteroids is 5% and positive mouth culture of *Candida* was found in 25% of patients treated with inhaled corticosteroids. This has been attributed to suppression of T lymphocytes, macrophages and neutrophils in the oral cavity and oesophagus, accompanied by increased salivary glucose levels. The extent of OPC is related to the type, dosage and form, as well as the dosing interval of the corticosteroid (Buhl, 2006).

Chemotherapy: Direct mucosal epithelial loss and indirect suppression of bone marrow that leads to neutropenia, both increase the prevalence of OPC. The severity of OPC is directly related to the chemotherapeutic treatment regimen but also varies from patient to patient as a result of genetic factors (Brown and Wingard, 2004).

Proton pump inhibitors (PPI): Amiri *et al*., (2012) reported an increased incidence of *Candida* spp. colonisation amongst critically ill ICU patients receiving proton pump inhibitor (PPIs) treatment. The authors suggested that OPC may be

facilitated by the anti-oxidant effects of PPIs that reduce the anti-inflammatory response by acting on neutrophils, monocytes, endothelial and epithelial cells.

1.4 Treatment of OPC

First-line treatment for OPC involves fluconazole tablets or intravenous injection, clotrimazole troches or nystatin suspensions (Thompson *et al*., 2010). Chlorhexidine and bicarbonate mouthwashes are also prescribed as adjuvant treatments (Ferreirós *et al*., 2012).

Based on the British National Formulary (BNF), (Joint Formulary Committee, 2017) OPC is treated with nystatin suspension, miconazole (gel or buccal tablet), fluconazole (tablets or suspension), posaconazole (tablet or suspension), itraconazole (oral liquid or capsules), voriconazole (tablet or suspension) and ketoconazole (tablet or suspension). The mechanism of action of currently used antifungals is illustrated in Table 1.2.

Table 1.2: The mechanism of action of currently used antifungals.

Group	Drugs	Mechanism of action	Reference
Polyenes	Nystatin	Bind to ergosterol on candida cell wall leading to leakage of cell constituent.	(Odds *et al.*, 2003)
Azoles	Fluconazole Voriconazole Posaconazole Ketoconazole Itraconazole	Block ergosterol synthesis the major component of the cytoplasmic membrane.	(Kathiravan *et al*., 2014)
Echinocandins	Caspofungin	Glucan synthesis Inhibitors leads to damage the cell wall of the fungi.	(Denning, 2003)

Degregorio *et al.,* (1982) found that nystatin was ineffective in the treatment of OPC in immunocompromised patients, the latter will be under a significant risk of the development of systemic candidiasis. In OPC patients, *C. albicans* is the most

common species resistant to fluconazole (Revankar *et al*., 1998). Cross-resistance between fluconazole and itraconazole can lead to refractory infection by non-albicans spp. such as *C. glabrata* and *C. tropicalis*. Posaconazole (a triazole) however, have a potent *in vitro* activity against these strains (Skiest *et al*., 2007). The development of the resistance to azoles is considered as the major drawback in the treatment of OPC which is most likely attributed to the incomplete eradication of *Candida* due to its fungistatic activity rather than fungicidal (Morschhäuser, 2002, Campoy and Adrio, 2017). Capsofungin is a second line treatment for patients show refractory to azoles and polyenes, its effectiveness resulting from the different drug mechanisms of action (Kartsonis *et al*., 2004). Caspofungin is available as Intravenous infusion only due to its poor intestinal absorption and short half-life, this led to its limited usage to hospitalised patients only (Campoy and Adrio, 2017). Based on these findings, CHD was chosen to be investigated for the treatment of OPC because it has no drug resistance, systemic side effects and drug interactions.

1.4.1 Local Treatment of OPC

Local oral drug delivery for the treatment of OPC is a targeted drug delivery for the treatment of *Candida* infection in the oral cavity. The advantages of this mode of drug delivery are that it: reduces the systemic side effects of the drug; minimizes the dose of the drug required; and provides a targeted drug delivery (Sankar *et al*., 2011). Moreover, it is regarded as cost-effective as treatment is achieved by the lower amounts of the drug used. For these reasons, this mode of drug delivery was adopted in this work to prepare the local delivery of CHD in the oral cavity.

Clinical investigation has been conducted by researchers for the local treatment of candidiasis by different antifungals. Fluconazole mouth rinses (2 mg/mL) were used by patients with oral candidiasis three times daily for one week. Seventeen patients out of 19 showed complete recovery after the end of the treatment (Epstein *et al*., 2002). Cardot *et al*., (2004) compared salivary concentration and the residence time of miconazole mucoadhesive tablets (50 and 100 mg) and miconazole 125 mg gel in healthy volunteers. The tablets were administered once daily whilst the gel was applied three times daily, they found that both tablets (50 and 100 mg) gave a prolonged detectable concentration even after the six-hour application. However, a similar comparison was conducted on cancer patients with OPC. Lauriad® (50 mg miconazole) applied once daily and Daktarin® (125 mg miconazole) applied four times daily and were used for fourteen days. The responses to the treatment were nearly similar, taking in account that the tablet taken once daily in one-tenth of the concentration of the gel made it superior to the gel (Bensadoun *et al*., 2008).

Another study compared the effect of the local mouthwash of Itraconazole (200 mg) oral solution and systemic tablets of fluconazole (100 mg) in OPC patients, both treatments were given once daily. The solution had the same effectiveness of the tablet, but it is preferable due to ease of use and avoidance of systemic side effects (Graybill *et al*., 1998). Although azole formulations showed a promising effect for the treatment of OPC, the resistance of *C. albicans* to azoles cannot be overcome (Revankar *et al*., 1998). Whereas, resistance to miconazole is very limited (Fothergill, 2006), GIT disturbances obtained from the administration of miconazole mucoadhesive buccal tablet is common. Moreover, It shows unfavourable drug interaction with a drug metabolised by CYP2C9 and

CYP3A4, such as oral hypoglycaemics, phenytoin and ergot alkaloids, due to the enzyme inhibitory activity of miconazole (Lalla and Bensadoun, 2011).

Moreover, Lamfon *et al.,* (2004) investigated the effect of fluconazole, miconazole and CHD on *C. albicans* biofilm, they found that the MIC for planktonic cells and 72 hours biofilm increased from 0.25 to >256 µg/ml for fluconazole and miconazole, while for CHD from 400 to 3000 µg/ml.

1.4.2 Biguanide Disinfectants

Biguanides are synthetic cationic compounds, widely used as antiseptics, disinfectants and preservatives. Polyhexamethylene biguanide (PHMB) and chlorhexidine are the most common salts used as disinfectants.

1.4.2.1 Polyhexamethylene biguanide (PHMB)

PHMB or polyhexanide is a linear polymeric biguanide, available as a 20% concentrated solution (Carrijo-Carvalho *et al.,* 2017). Although it has a higher *anticandida*l activity than CHD (Koburger *et al*, 2010) the powdered form of PHMB produces acute toxicity if inhaled (Bernauer, 2015), which limits its preparation into tablet dosage forms.

1.4.2.2 Chlorhexidine (CHD)

CHD is 1:6-di-4'-Chlorophenyldiguanidohexane (Figure 1.1), it was first investigated by the Imperial Chemical Industries, Limited (Manchester, UK). The company proved its high antimicrobial potency against a wide range of microorganisms (Davies *et al*., 1954), with the MIC ranging from 2.67 to 4 µg/ml for bacteria (*Staphylococcus aureus, Enterococcus faecalis, Escherichia coli, C. albicans, Prevotella intermedia, Porphyromonas gingivalis, Porphyromonas endodontalis, Prevotella denticola* and *Prevotella melaninogenica)* (Amorim *et*

al., 2004) and MIC values for thirty-two *C. albicans* species were found to be from 0.78 µg/ml – 6.25 µg/ml (average 3.125 µg/ml) (Salim *et al*., 2013). It is an odourless, hygroscopic, white crystalline powder with a bitter taste (Rowe *et al*., 2006, Lim and Kam, 2008) with established topical disinfectant properties and no systemic effects (Davies *et al*., 1954). CHD's optimal antimicrobial activity occurs between pH 5-7; above pH 8 precipitation and hence inactivation is observed (Rowe *et al*., 2006). CHD is available as a gluconate salt (liquid), making it unsuitable for tablet preparation, or as acetate and hydrochloride salts. Acetate is ten times more soluble than the hydrochloride salt (Zeng *et al.,* 2010), hence its suitability for inclusion in buccal tablet formulations (used in this study).

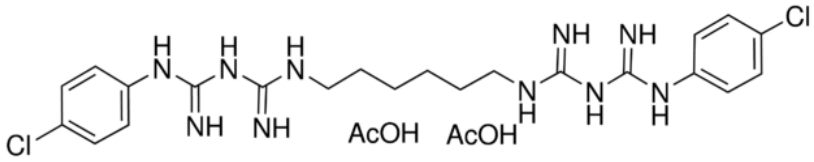

Figure 1.1 Chemical structure of CHD.

CHD is used topically for localised antiseptic and disinfection activity in the oral and nasal cavities, skin, wounds and burns. For treatment of oral infections, CHD is available as a 0.2 % w/v mouthwash, 0.2 % w/v oral spray and 1 % w/v dental gel (Joint Formulary Committee, 2015). The main advantage of these oral formulations is the unspecific cellular target for microbiocidal activity that retards the development of resistance against CHD (Ankola *et al*., 2008).

Mechanism of action: The antifungal activity is achieved by the binding of the CHD cation to the anionic surface charge of the fungal cell wall surface, leading to a decrease in the adhering capacity, losing the structural integrity, and finally disrupting the cell wall (Williams *et al.,* 2011). CHD activity is concentration and time-dependent. It produces cell coagulation at high concentration, it also

irreversibly precipitates adenosine triphosphate (ATP) and nucleic acids resulting in cell death. However, at low concentration, it distorts the plasma membrane followed by cytoplasmic leakage and coagulation of nucleoprotein (Bobichon and Bouchet, 1987).

At low concentration, it has a direct effect on yeast hydrolases activity, inactivates proteases (Grenier, 1993) and decreases the activity of phospholipase produced by *C. albicans* (Kadir *et al*., 2007).

Effect on Normal Flora: Sreenivasan and Gittins (2004) investigated the effect of chlorhexidine on oral flora; they found that it has a significant effect against Gram-positive, Gram-negative and anaerobic bacteria after treatment with CHD mouth rinse. Jones (1997) found that a single rinse with CHD can decrease oral flora by up to 90% for several hours. However, oral biofilms show a greater resistance toward antifungals, for instance, the MIC of chlorhexidine against *C. albicans* strain GDH-2346 was increased from 8 to 128 µg/ml for planktonic and biofilm cells respectively (Mukherjee and Chandra, 2004). Furthermore, the sensitivity of planktonic cells towards antifungals is higher than of biofilm cells, because there is a more uniform distribution of the drug in planktonic cell culture media whereas a concentration gradient of extrinsic and intrinsic material results from the uneven thickness and cell density in the biofilm, hence their different responses (Suci and Tylor, 2002). The growing biofilms produce extracellular polysaccharide materials composed of mannose and glucose, and this might cause a physical interaction between the drugs and the extracellular materials and decrease their effectiveness. Moreover, it has been suggested that in the biofilm there is a differential regulation of the gene encoding for the enzymes

involved in carbohydrate biosynthesis for the formation of extracellular material which resulted in decreasing drug activity (Chandra *et al*., 2001).

CHD shows superior activity *in vitro* compared to fluconazole against different *Candida* spp. with a geometric mean MIC (minimum inhibitory concentration) of 3.03 µg/ml and 19.12 µg/ml, respectively with no cross-resistance between them (Salim *et al*., 2013).

Oral hygiene: It is used for the treatment of periodontics, caries prevention, oral and maxillofacial surgery, prosthodontics and endodontics (Ankola *et al*., 2008). It binds to the oral mucosa via electrostatic forces inhibiting plaque formation and promoting prolonged bacteriostatic activity (Lim and Kam, 2008).

Stability of chlorhexidine in the oral cavity: Because it has a high binding capacity to compounds, it binds to both soft and hard oromucosal tissues resulting in prolonging its activity (Ankola *et al*., 2008). Musteata and Pawliszyn (2005) reported that the oral cavity acts as a reservoir for CHD because of its high protein binding capacity; CHD continues to release in the oral cavity up to 8 hours with a final concentration equal to 2 µg/mL after a single mouthwash rinse of 1 mg/mL. Furthermore, the stability of chlorhexidine in the oral cavity is at least 9 hours. A single mouth rinse with chlorhexidine maintains its activity for 5 hours in saliva and 12 hours at the oral surfaces (Jones, 1997). However, the concertation of chlorhexidine cannot be considered as an effective concentration against *Candida* biofilm. This can be overcome by preparing a controlled release dosage form to maintain the release of a higher effective concentration of CHD.

Side effects: CHD has a reversible effect on taste perception, it decreases the intensity of salty and bitter perceptions, but it has no effect on sweat and sour

tastes (Helms *et al*., 1995). Another common side effect is tooth staining, which is enhanced by chromogenic drinks such as tea and coffee (Leardand and Addy, 1997) as well as rare transient dulling of taste (Lim and Kam, 2008).

Cytotoxicity: The cytotoxicity of CHD is concentration and time-dependent (Hidalgo and Dominguez, 2001). The mechanism of cell death, changes from apoptosis to necrosis with increasing concentration of CHD (Li *et al*., 2014), although the precise mechanism of cytotoxicity is not well defined. A study on human blood lymphocyte found that CHD produces toxic effects through oxidative stress and damage to the mitochondria and lysosomes has been observed. Finally, depletion of Glutathione (GSH) precedes apoptosis or necrosis (Salimi *et al*., 2017). Osteoblast has been found to be more vulnerable to CHD toxicity than endothelial or fibroblast cells although once initiated all showed the same mechanism of cytotoxicity (Giannelli *et al.*, 2008).

Based on the above finding, the cytotoxic effect of CHD has been investigated in this work to find safe concentration on human cells for the treatment of OPC.

1.5 Hydrogels and OPC

Currently, the greatest disadvantage of CHD formulations (mouthwashes, gels) is their short retention and activity time in the oral cavity. Consequently, there is a genuine need for a new approach to the localised, prolonged delivery of antifungal agents for enhanced OPC therapy. Hydrogel polymers were used to formulate the mucoadhesive buccal tablet to prolong and control the release of CHD in the oral cavity.

Localised drug delivery can be used to treat a range of oral conditions including xerostomia, oral cancer, fungal and bacterial infection, periodontal disease,

toothache, aphthous stomatitis *etc.* (Smart, 2005). The advantages of local delivery are fewer systemic side effects and more targeted drug activity (Sankar *et al*., 2011); disadvantages include drug loss by swallowing and unpleasant taste that can lead to issues with patient compliance.

To control localised drug delivery in the oral cavity mucoadhesive controlled release hydrogel dosage forms were recently investigated. Hydrogels are a three-dimensional crosslinked structure of hydrophilic homopolymer, copolymer, multipolymer or interpenetrating hydrogels, they can retain water and form porous structures (Roy *et al*., 2009), They are either ionic or nonionic depending on the pendant group, the network structure of the hydrogel are either amorphous or crystalline. They are used as drug delivery systems due to their resemblance to natural tissue because they retain large quantities of water and they have smooth and soft texture (Peppas *et al*., 2000) this make hydrogels a good candidate for drug delivery.

1.3.1 Hydrogel in drug delivery: advantages and limitations

Advantages of using hydrogel in buccal drug delivery (Hoare and Kohane, 2008):

1. Biocompatibility due to its high-water content
2. Drug loading, the highly porous structure enables drug loading followed by subsequent disintegration and dissolution
3. Biodegradability or dissolution by the effect of enzyme, temperature and pH.
4. Deformability (takes the shape of the surface applied to).

Limitations of using hydrogel in buccal drug delivery (Hoare and Kohane, 2008):

1. Low tensile strength leads to premature dissolution or detachment from the site of application.
2. Drug loading and homogeneity of hydrophobic drug is limited.
3. High porous structure and high-water content may result in the rapid dissolution of the drug.

1.6 Mucoadhesion

Mucoadhesive dosage forms can be applied to various parts of the oral cavity (*e.g*. palate, gingiva, buccal mucosa or periodontal pocket) to localise and retain the drug (Bruschi and De Freitas, 2005).

Bioadhesion is defined as the adherence of polymeric material to the biological surfaces, while mucoadhesion is the adherence of the polymeric material to the mucosal surfaces (Salamat-Miller *et al*., 2005; Smart, 2005). In the oral cavity mucin at the physiological pH 5.8-7.4 is negatively charged due to the ionization of sialic acid and ester sulphate residues, which may have a considerable role in the process of mucoadhesion. At this pH, it forms a strongly cohesive viscoelastic hydrogel (mucus), which binds to the epithelial cells with a 10-100 μm thickness and due to the abundance of positive and negative charge it acts as a protective layer by forming electrostatic attractions with the charged molecules. The turnover of the mucus in the human oral cavity is 12-24 hours (Campisi *et al*., 2010).

Mucoadhesive polymers are widely used in the preparation of salivary substitute due to its lubrication activity, they decrease the friction in the oral cavity (Partenhauser and Bernkop-Schnürch, 2016), (Dost and Farah, 2013). For example, carbomer, hydroxypropyl cellulose, poloxamer,

carboxymethylcellulose, sodium carboxymethylcellulose and acacia (BNF, 2017). Mucoadhesive hydrogel formulations have been used for the treatment of hyposalivation due to their hydration capacity and long residence time in the mouth (Tsibouklis *et al*., 2013).

The use of mucoadhesive tablets as a prolonged dosage form has been successfully utilised. In the BNF miconazole buccal tablet (Loramyc®) is used for the treatment of OPC, each 50 mg miconazole tablet applies for 7 hours daily.

1.6.1 Factors affecting mucoadhesion

Factors affect mucoadhesion are:

Molecular weight (MW) of the polymer: the optimum MW ranging from around 10^4 Da to 4 x 10^6 Da. Low MW polymer will dissolve rapidly or make a loose gel, while high molecular weight polymer needs time to hydrate and make the functional groups ready for interaction (Kharenko *et al*., 2009).

Flexibility: is an important factor for interpenetration and entanglement, makes more binding group available for interaction. (Andrews *et al*., 2009).

Cross-linking density: this property of the polymer is inversely related to the degree of swelling, resulting in a decrease in the interpretation of the polymer with the mucous membrane (Salamat-Miller *et al*., 2005, Blanco-Fuente *et al*., 1996).

pH: affect the mucoadhesion of ionisable polymers, changing the pH change the degree of ionization. (Rahamatullah *et al*., 2011).

Hydrophilicity: polymers containing carboxyl, hydroxyl, amino and sulfate groups have the ability to form hydrogen bonds with the mucous membrane (Andrews *et al*., 2009). They can retain water, swelling, increase the flexibility and

improve drug release (Rahamatullah *et al*., 2011). However, polymer with low wettability may show weaker mucoadhesive properties such as chitosan and Eudragit® (Wong *et al*., 1999).

Concentration: there is a critical concentration of each polymer to achieve optimum adhesion, at low concentration the interaction between the polymer and the mucous membrane will be unstable. While at high concentration the degree of wetting of the polymer will decrease and this will either greatly decrease or not produce adhesion (Salamat-Miller *et al*., 2005).

Contact time and contact force: the force and the time provided by the patient to make the tablet adhere to the oral mucosa, furthermore the contact time is more influential than contact force and the latter when increased it may damage the mucosa (Wong *et al*., 1999).

Spatial conformation: linear conformation of Poly Ethylene Glycol with a molecular weight 200000 show the same adhesive properties as Dextran with a molecular weight 19500000. In the latter due to its helical conformation, not all of the functional group are exposed to attach to the mucosa (Rahamatullah *et al*., 2011).

1.6.2 Oral mucoadhesive dosage forms

The desired characteristics of bioadhesive dosage forms intended for application in the oral cavity are flexibility, smooth texture, ease of application and low irritancy (Salamat-Miller *et al*., 2005). Drug release from such systems can be affected by:

1. **Drug-polymer interaction:** depending on drug properties, it is sometimes occupying the functional group of the polymer leading to decrease its mucoadhesion (Blanco-Fuente *et al*., 1996)
2. **Site of application:** salivary flow rate varies in the oral cavity, resulting in variable drug release (Codd and Deasy, 1998).

In the oral cavity the mucus is thin and discontinuous, so the preferred dosage form should be dry or partially hydrated such as tablet or films and to a lesser extent semisolids (Smart, 2005).

1.6.2.1 Mucoadhesive tablets

By far the most commonly used mucoadhesive dosage form in the buccal cavity, mucoadhesive tablets can be applied to different sites within the mouth (Rahamatullah *et al*., 2011). After wetting of the solid matrix, mucoadhesive tablets soften and adhere to the mucosa until dissolved or removed (Salamat-Miller *et al*., 2005), their residence time depends on the site of application: 7-12 hrs for gingiva, and 4-6 hrs for palate (Bruschi and De Freitas, 2005). The major disadvantage is the lack of flexibility which leads to poor patient compliance upon repeated or prolonged use (Salamat-Miller *et al*., 2005), in addition to tablet detachment, swallowing and subsequent adherence to the œsophagus in geriatric and paediatric patient groups (Bruschi and De Freitas, 2005). There are several factors affecting the mucoadhesion of mucoadhesive buccal tablets, including:

1. **Force of compression:** Increasing the force of tablet compression can decrease *in vivo* and *in vitro* tablet mucoadhesion (Perioli *et al.,* 2008), this

might be explained by the production of smoother surfaces with a higher compression force, resulting in decreasing the surface area and consequently the contact point.

2. **Polymer ratio:** increasing polymer concentration in the tablet improves the mucoadhesion by increasing the sites of adhesion to the mucosa (Mohammadi-Samani *et al*., 2005).
3. **Type of excipients:** may affect the adhesion properties of the polymer, e.g. oils degrade the adhesion of polyacrylic acid (Peppas and Sahlin, 1996).

1.6.2.2 Mucoadhesive films

Soft, elastic and strong enough to withstand stress due to mouth movements, the swelling capacity of mucoadhesive films must be limited to avoid patient discomfort (Salamat-Miller *et al*., 2005). They have the advantage of adopting the shape of underlying structures (Kharenko *et al*., 2009). Its limitations are due to their methods of preparation, which is either by solvent casting method which results in poor content uniformity or by hotmelt extrusion which requires specific equipment (Morales and McConville, 2011).

1.6.2.3 Mucoadhesive semisolids or gels

Semisolid drug delivery systems have a major advantage in the treatment of oral infections resulting from their close contact with the oral mucosa and concurrently rapid drug release. However, it is difficult to control the dose of gel preparation, making them unsuitable for API's with a narrow therapeutic index (Kharenko *et al*., 2009).

Table 1.3 shows the conducted research investigating the mucoadhesive formulations for OPC treatment.

Table 1.3 OPC treatment using different antifungals incorporated in different mucoadhesive dosage forms.

Drug	Dosage form	Polymer	Reference
Chlorhexidine diacetate	Tablet	Sodium alginate Chitosan	(Giunchedi *et al*., 2002)
Chlorhexidine diacetate	Tablet	Polyacrylic acid (PAA), Hydroxyethyl cellulose (HEC)	(Irwin *et al*., 2003)
Chlorhexidine diacetate	Tablet	HPMC, Carbomer	(Ceschel *et al*., 2006)
Chlorhexidine diacetate	Film	Sodium alginate, chitosan	(Juliano *et al*., 2008)
Chlorhexidine digluconate	Gel	HPMC, Carboxymethylcellulose(CMC), Hydroxypropyl cellulose (HPC)	(Fini *et al*., 2011)
Lactoferrin	Tablet	Sodium alginate	(Kuipers *et al*., 2002)
Miconazole nitrate with or without Chlorhexidine diacetate	Lozenges	Acacia, Carbopol	(Codd and Deasy, 1998)
Miconazole	Patches	Sodium carboxymethyl cellulose(SCMC), chitosan, Hydroxyethyl cellulose (HEC), Polyvinyl alcohol (PVA), HPMC	(Nafee *et al*. 2011)
Metronidazole	Tablet	Hydroxypropyl cellulose (HPC), Hydroxyethyl cellulose (HEC), HPMC SCMC	(Perioli *et al*., 2004)

1.7 CHD mucoadhesive buccal tablet

Recently, investigations were conducted to examine the use of sustained release CHD to treat OPC. This is feasible because CHD has no systemic side effects like other antifungals and so an effective concentration of the drug equal to or above the minimum fatal *Candida* concentration can be maintained. For instance, Ceschel *et al*. (2006) prepared CHD buccal tablet using carbopol and/or HPMC with lactose. They found that 2.5 mg of CHD in a 60 mg tablet sustained the action of CHD more than a Corsodyl gel containing 1% chlorhexidine gluconate over an 8 hours period. In another study, Chitosan was used to formulate CHD in

a gel and a film format, in which the concentration of CHD in the gel was 1% or 2% while in the film 0.1% or 0.2%. In these formulations, the CHD release was maintained for 3 hours for the gel and 4 hours for the film (Şenel *et al*., 2000). Moreover, Juliano *et al*. (2008) used chitosan and sodium alginate to prepare a CHD mucoadhesive film using a solvent casting method, which when tested *in vivo* successfully maintained the concentration of CHD up to 3 hours. None of the investigated formulation showed a constant release over time, tested against *Candida* biofilm, or studied their cytotoxic effect over the intended time of application.

In this current work, CHD mucoadhesive buccal tablets were prepared using hydroxypropyl methylcellulose (HPMC) and Poloxamer 407 polymers and sugar alcohols (sorbitol, mannitol and xylitol).

1.7.1 Hydroxypropyl methylcellulose (HPMC)

HPMC is a non-ionic hydrophilic polymer with mucoadhesive and hydrogel-forming properties. It has widely been investigated in buccal drug delivery and is included in marketed products (Sudhakar *et al*., 2006).

HPMC or Hypromellose is a partly O-methylated and O-(2-hydroxypropylated) cellulose ether derivative (Figure 1.2). Based on the substitution, it is available in three groups which are commercially defined by codes (2208, 2906 and 2910) The first two digits refer to the approximate percentage content of the methoxy group, while the second two digits refer to the approximate percentage content of the hydroxypropoxyl group (Li et al., 2005). Moreover, each group is available in different molecular weights, the variation in the molecular weight and the degree of substitution affect the solubility, thermal gelation temperature in aqueous solution, swelling, diffusion, and drug-release rate (Brady et al., 2017).

In oral tablet dosage forms it is used as a binder, film-coating and as a matrix for controlled-release tablet formulations (Rowe *et al.*, 2006).

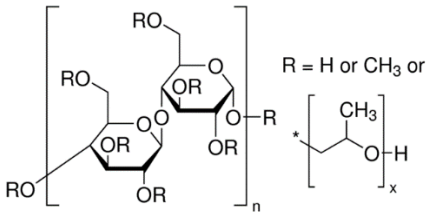

Figure 1.2 Chemical structure of HPMC.

Hypromellose 2906: In this current work, a high purity medium substituted HPMC, Hypromellose 2906, was used with an average viscosity of 4000 cp (2% aqueous solution). It has been used for its medium molecular weight and consequently its viscosity. The formulations prepared in this work were aimed to release CHD over two hours, rather than using the higher viscosity HPMC which is usually used for a minimum 8 hours sustained release formulations.

1.7.2 Poloxamer polymers:

Poloxamers are non-ionic block copolymers of polyethylene oxide (EO) and polypropylene oxide (PO) arranged in a basic structure EO_x -PO_y - EO_x (Figure 1.3). The hydrophilic nature of EO and the hydrophobic nature of PO results in an amphiphilic molecule with consequent surfactant properties. Poloxamers with different x and y values result in variation in the hydrophilic-lipophilic balance (HLB) (Kabanov *et al.,* 2002). Poloxamers are followed by three-digit number, the first two digits when multiplied by 100 represents the average molecular weight of EO and the third digit when multiplied by 10 corresponds to the PO percentage by weight. Their physical properties change from liquid to solid upon increasing

the molecular weight and are used as a solubilizing agent, emulsifying agent, wetting agent, binder and coating agent in formulations (Rowe *et al.*, 2006).

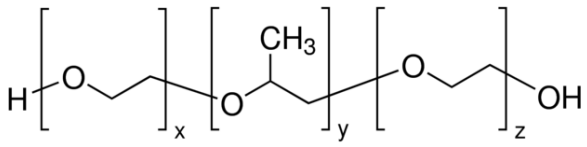

Figure 1.3 Chemical structure of P407.

Poloxamer P407 (P407)

P407 is a non-ionic copolymer of polyethylene oxide and polypropylene oxide, in solution, it forms a thermosensitive hydrogel at a concentration of ≥ 25 %. It has a wide application in drug delivery, for example, parenteral, ophthalmic, inhaler, oral solution, suspension, and topical formulation. Its mucoadhesive property was exploited in rectal and ophthalmic preparation (Dumortier *et al*., 2006). Poloxamer 407 (P407) has an average molecular weight of 12,600 (9,840-14,600) and HLB value of 22 at 22°C. It is used as an excipient in different formulations, for instance, Intravenous, inhalation, oral solution, suspension, ophthalmic and topical formulations (Dumortier *et al*., 2006). Alike other poloxamers, P407 has a thermoreversible hydrogel-forming ability with a mucoadhesive property, it gels at a concentration > 20% at 25°C (Ruel-Gariepy and Leroux, 2004). In the current work, P407 was chosen due to its pronounced gelling properties and high viscosity of 3100 cp which is attributed to its high molecular weight compared to other poloxamers and its availability as microprills (Matanović *et al.,* 2014). Although, it is not commonly used in controlling the release of the drug from solid dosage forms, in the current work it was formulated in tablet dosage form to

control the release of CHD alongside with HPMC by exploiting its thermoreversible hydrogel-forming properties.

1.7.3 Sugar alcohols (Polyols)

Polyols or sugar alcohols are naturally available in fruits and vegetables. They have a sweet taste, stimulate salivation, widely used as noncarcinogenic sweetening agents, make them the best candidates as a sweetener (Carocho *et al.,* 2017). Sorbitol, mannitol and xylitol are sugar alcohols, they either minimise or do not promote tooth decay and have a low glycaemic index (Gliemmo *et al.*, 2004). Sorbitol and Xylitol have humectant activity, which is attributed to the availability of the hydroxyl group in their chemical structure, which forms hydrogen bonding with water. As a consequence, this humectant property reduces water activity, a feature exploited in the food industry to improve the stability of food products (Ergun *et al.*, 2010).

Mannitol and sorbitol are isomers (Figure 1.4 a and b) with a molecular formula of $C_6H_{14}O_6$, however, xylitol (Figure 1.4 c) has one carbon atom less with a molecular formula of $C_5H_{12}O_5$. They have different physical properties (Table 1.4)

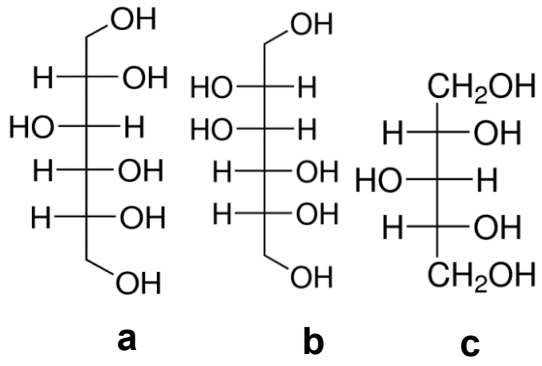

Figure 1.4 Chemical structure of a- sorbitol, b-mannitol and c-xylitol.

Table 1.4 Physical properties of sorbitol, mannitol and xylitol

Sugar alcohol	M. wt * g/mol	Solubility 20° C* mg/mL	Heat of Solution*	Sweetness ** Sucrose=100	Glycemic Index*** Glucose=100
Sorbitol	182.172	2000	-106.3	50-60	9
Mannitol	182.172	181	-120.9	50-60	0
Xylitol	152.15	625	-157.1	90-100	13

*(Rowe *et al*, 2006)
**(Ghosh & Sudha, 2012)
***(Livesey, 2003)

Due to their sweet taste, cooling sensation resultant from their negative heat of dissolution, low glycaemic index, non-cariogenic (Deshpande & Jadad, 2008), polyols are frequently used in oral dosage forms, such as orally disintegrating tablets, lozenges, chewable tablets, chewing gum toothpaste (Bolhuis *et al*, 2009) and as moisturizers in artificial saliva (Femiano *et al*, 2011).

Moreover, both xylitol and sorbitol due to their humectant property are used to relieve oral dehydration, for example; XyleMelts® is a marketed mucoadhesive buccal tablet which proofs its activity for the relief of oral dryness, especially during sleeping. The main ingredients are xylitol and cellulose gum and relief of the dryness might be attributed to the slow release of xylitol which stimulates saliva and to the activity of the mucoadhesive polymer which acts as a lubricant and a humectant (Burgess and Lee, 2012).

Biotine® oral balance gel, another marketed product, contains 2% HPMC, xylitol and sorbitol. Epstein *et al*., (1999) investigate the effect of the gel on xerostomia patients treated with head and neck radiation, the outcome of their study showed improvement in the dryness of the mouth, but it had no effect on the colonisation by *Candida.*

1.8 Thymol

The combined effect of Chlorhexidine with natural products has been previously investigated, for instance, eucalyptus oil and Chlorhexidine gluconate showed a synergistic effect against both the planktonic cells and the biofilm of *C. albicans, Staphylococcus aureus, and methicillin-resistant S. aureus* (Hendry *et al*., 2009).

Thymol (2-isopropyl-5-methylphenol) is a phenolic essential oil produced by plants belonging to *Lamiaceae* family, such as thyme. Its antifungal activity is associated with disruption of the lipid packing of the cell membrane, increasing its fluidity and changing its permeability. The damaging effect on the cell membrane interferes with hyphae production, which is considered one of the most important pathogenicity traits of *Candida* (Braga *et al*., 2007a). Both thymol and CHD affect the cell wall of *Candida*, their combined effect was tested in this work to check synergistic or additive anticandidal effect.

It has an antioxidant activity and is also used as a mouthwash (Dušan *et al*., 2006). It is toxic to human gastric carcinoma cells (AGS) inducing chromatin condensation and cleavage of DNA followed by apoptosis via depolarisation of mitochondrial membrane potentials (Kang *et al*., 2016). Moreover, in Caco-2 cells, it has been shown to cause lipid degeneration, mitochondrial damage, nucleolar segregation and apoptosis (Llana-Ruiz-Cabello *et al*., 2014). The antioxidant activity of thymol has been associated with protection from oxidative stress and mitochondrial damage produced by $HgCl_2$ in HepG2 cells (Shettigar *et al*., 2015). As mentioned earlier, CHD produces metabolic stress which might be overcome by the antioxidant activity of thymol, the combination of CHD and thymol were tested as an attempt to minimise the cytotoxic effect of CHD.

1.9 Farnesol

Quorum sensing is a process of microbial communication for intra and interspecies. It regulates growth, biofilm formation, virulence and competence (Lu *et al*., 2014). *C. albicans* releases different QSMs including tyrosol, farnesol, farnesoic acid, phenyl ethyl alcohol and tryptophol. It is believed that all these QSMs play a role in *Candida* morphogenesis (Kruppa, 2009). The release of these QSM is regulated by cell density (Han *et al*., 2011).

Farnesol is a quorum sensing molecule produced by *C. albicans* to control filamentation, it is released when the yeast cells concentration is below 10^6 CFU/mL (Albuquerque and Casadevall, 2012). It inhibits hyphal formation at a concentration of 10-250 μM but has no effect on cell elongation (Lu *et al*., 2014). It enhances the resistance of *Candida* to oxidative stress, and it plays an important role in the competence of *Candida* with other fungi by promoting apoptosis in *Saccharomyces cerevisiae*, *Aspergillus nidulans*, and *Penicillium expansum*), and suppresses the growth of *Paracoccidioides brasiliensis* (Han *et al*., 2011). In the current work, farnesol was investigated to be incorporated with CHD and thymol as an attempt to stop the filamentation of *Candida*, preventing the biofilm formation and consequently preventing the invasion of *candida* to new sites in the oral cavity.

To avoid the burden of medication systemic side effects of antifungals formulations, CHD was investigated for its applicability for local delivery as it has no systemic side effect and has a broad-spectrum biocidal activity. The dosage form was designed in the form of a mucoadhesive buccal tablet to provide a controlled release for two hours, the time being selected to minimise distress that might be obtained from tablet application. Moreover, thymol and farnesol were

preliminarily tested for their antifungal activity and cytotoxicity for evaluating potential incorporation into future formulations. Hydrogel polymers were used to formulate the mucoadhesive buccal tablet to prolong and control the release of CHD in the oral cavity.

1.10 Research aim and Objectives

OPC is an opportunistic infection commonly spread among immunocompromised patients which are normally under the treatment with potent drugs with a considerable side effect. For this reason, there is an immense need for an efficient treatment with a minimum side effect. Local targeted drug delivery will help in avoiding the systemic side effects that are normally accompanied by systemic drug delivery. To achieve this goal Hydrogel mucoadhesive buccal tablets were used to deliver and control the release of chlorhexidine locally to the oral cavity at a safe and effective concentration for the treatment of OPC.

This project was conducted to meet the following objectives:

1. To investigate the anticandidal activity of CHD on *C.albicans* planktonic cells and biofilms of different ages.
2. To study the effect of thymol and farnesol on the anticandidal activity of CHD.
3. Study the cytotoxicity of CHD on human epithelial cells (the model used in this study is HEK293)
4. To prepare CHD mucoadhesive buccal tablets using HPMC and P407 polymers
5. Study the effect of different flow rates of the dissolution media on the release of CHD to mimic the release in the oral cavity.

6. The prepared tablets will be optimised to comply with the British Pharmacopoeia standards.

Chapter Two

Anti-candida activity of CHD, Thymol and Farnesol

Chapter 2 : Anti-candida activity of CHD, thymol and farnesol

This chapter investigated the *anti-Candida* effects of CHD on planktonic cells and on biofilm cells with different maturity stages. Moreover, the effects of thymol and farnesol on the activity of CHD were investigated to check the feasibility of their incorporation into future formulations. CHD damages the cell wall of *C. albicans* (Williams *et al.,* 2011) and changes its lipid composition (Abu-Elteen and Whittaker, 1997), thymol disrupts the lipid packing of the cell wall resulting in increasing its fluidity (Braga *et al*., 2007b). Based on these findings the combined effect of CHD and thymol were investigated for a probable synergistic effect. Farnesol blocks the conversion of the yeast to a hyphal form, thus the combined effects with CHD or thymol were initially investigated to evaluate the potential of stopping *Candida* invasion via hyphae formation and the anticandidal effect of CHD and thymol. Furthermore, the effects of HPMC and P407 as the main polymers in future formulations were also investigated.

2.1 Materials and Methods

2.1.1 Preparation of growth medium and *C. albicans* culture

Preparation of growth medium

Malt extract broth (MEB), Muller Hinton broth (MHB) and Sabauroud dextrose agar (SDA) (Sigma-Aldrich, UK) were prepared according to manufacturer's instructions and sterilised by autoclaving at 121°C for 15 minutes. SDA was cooled to approximately 50°C then aseptically poured into sterile Petri dishes.

Preparation of *C. albicans* stock culture

C. albicans strains were obtained from the University of Wolverhampton. MEB (10 mL) was seeded with one colony of *C. albicans* and incubated in an orbital shaking incubator (Innova, New Brunswick Scientific, USA.) at 150 rpm and 30°C for 18-24 hours. The overnight culture was centrifuged at 1650 g for 5 minutes, the broth was decanted, and the cells were resuspended in 30:70 glycerol/MEB. Aliquots of 1 mL were transferred to sterile Eppendorf tubes and stored at -80°C. Subcultures were prepared from this stock by spreading onto SDA then incubating at 30°C for 48 to72 hours. The plate was stored in the fridge for 7-10 days as a stock for overnight culture.

Preparation of 0.5 McFarland standard solution

The standard solution was prepared by adding 0.5 mL of 0.48 M barium chloride to 99.5 mL of 0.18 M sulfuric acid. The turbidity of this suspension is equal to the absorbance of 0.12-0.15 at λ_{530nm} which is equivalent to the turbidity of *C. albicans* overnight culture at a concentration of 1-5x10^6 CFU/mL.

Preparation of *C. albicans* overnight culture

From an SDA plate incubated at 30°C for 18-24 hours, colonies of *C. albicans* were transferred to MHB and the absorbance was adjusted to 0.12-0.15 at λ_{530nm}.

2.1.2 Minimum Inhibitory concentration (MIC) and minimum biocidal Concentration (MBC)

MIC and MBC were performed for the two drugs under investigation, polymers and sugar alcohols which will be used for mucoadhesive buccal tablets preparation. Chlorhexidine diacetate salt hydrate (CHD) (Sigma Aldrich, Uk) and thymol (Alfa Aesar, UK). Three polymers were investigated namely Methocel™

F4M premium hydroxypropyl methylcellulose (HPMC, viscosity of 2663-4970 cps for 2% solution at 20°C, 27-30% methoxyl and 4-7.5% hydroxypropyl substitution) was kindly gifted by Colorcon, Uk. Hydroxypropyl methylcellulose (HPMC-S, Mn ~86,000, viscosity of 4000 cps for 2% solution at 20°C, 29% methoxyl and 7% hydroxypropyl substitution) (Sigma Aldrich, UK). Poloxamer 407 (P407) (Sigma Aldrich, Uk). Moreover, three sugar alcohols were investigated, Sorbitol (Sigma Aldrich, Uk), xylitol (Xylisorb XTAB 240) and mannitol (Pearlitol 200 SD), (kindly gifted by Roquette, UK) and farnesol, a quorum sensing molecule (Alfa Aesar, Uk).

The MIC test was performed using the broth tube dilution method, the tested compounds were serially double diluted in MHB to a final volume of 5 mL, and uninoculated MHB was used as a negative control. 200 µL of an overnight culture was transferred to each test tube and to the positive control (giving a final cell density of 10^4-10^5 CFU/mL, and the tubes were incubated at 30°C for 24-48 hours. The MIC is defined as the lowest concentration giving no visible growth.

The MBC was determined by inoculating SDA plates with 10 µL from MIC tubes showing no visible growth and incubating at 30°C for 24-48 hours. The MBC is the lowest concentration of the tested compound with no visible growth after subculture.

2.1.3 Time-kill assay

Time-kill studies were performed by the broth macro-dilution method, each drug was serially double diluted using MHB and seeded with 200 µL of a *C. albicans* overnight culture. All tubes (including positive and negative controls) were incubated in a shaking water bath (Mickle Laboratory Engineering Company,

Gomshall, Surrey, UK) at 30ºC and 80 rpm. Samples of 50 µL were withdrawn at time zero and 20 minutes intervals for four hours and at 24 hours, subcultured on SDA plates and incubated at 30ºC for 24-48 hours. The results were assessed qualitatively for the presence of the growth.

Quantitative time kill studies were performed at MIC and MBC concentrations for up to 2.5 hours. Samples of 100 µL were withdrawn every 30 minutes, serially tenfold diluted and a 50 µL were aliquoted from each dilution and spread onto SDA plates, the plates were incubated at 30 ºC for 24-48 hours. Colony counts were performed for plates with a growth of 30-300 colonies, and the viable count was calculated. This test was performed to check the degree of killing for two hours which is the proposed time of the tablet to be placed in the oral cavity.

2.1.4 Microdilution checkerboard assay

Using a 96 well microtiter plate, CHD stock solution of 10 µg/mL was serially double diluted horizontally and thymol 250 µg/mL was serially double diluted vertically in MHB. The wells (with the serial dilutions and positive controls) were inoculated with 8 µL of *C. albicans* overnight culture. Sterile MHB was used as a negative control. The plate was incubated at 30°C for 24 hours. The turbidity was measured using a microtiter plate reader (BioTec, EL800, UK) at $\lambda_{595\ nm}$. The fractional inhibitory concentration (FIC) was calculated as follows.

$$FIC = \frac{\text{MIC of drug A tested in combination}}{\text{MIC of drug A tested alone}} + \frac{\text{MIC of drug B tested in combination}}{MIC\ of\ drug\ B\ tested\ alone}$$

The interaction between the tested drugs was predicted from the FIC value: FIC ≤ 0.5 indicates synergy; FIC > 0.5–4.0 indicates no interaction; and FIC > 4.0 indicates antagonism (Odds, 2003).

2.1.5 Farnesol effect on *Candida*

Farnesol stock solution was prepared by adding 70 µL of the stock oily farnesol (3.79 M) to 10 mL of a 10% (w/v) solution of P407, the molarity of the prepared stock solution is 26.6 mM. Aliquots of 200 µL of *C. albicans* ATCC 10231 overnight culture (prepared as described above) was added to 5 mL MHB and to 5 mL of 2.66 mM of farnesol in MHB. The tubes were incubated at 30°C for 24 hours. After incubation, the cells were centrifuged (Centrifuge 5804R, Eppendorf, Germany) washed twice with Ringer's solution, stained with 1% crystal violet and examined at 1000x magnification using an optical microscope under oil immersion lens (Nikon Eclipse ME600, Japan).

2.1.6 *C. albicans* biofilm formation

Preparation of RPMI-1640

RPMI-1640 medium (dry powder, Sigma-Aldric, UK) was prepared as instructed by the manufacturer. The pH of the liquid medium was adjusted to 7.2 with 0.165 M MOPS (3-(N-Morpholino) propane sulfonic acid, Sigma-Aldrich, UK).

Growth of *C. albicans* biofilms

C. albicans ATCC 10321 was grown on SDA plates for 24 hours at 30°C; then colonies were harvested using sterile inoculating loops and seeded into RPMI-1640 medium. The turbidity of the fungal suspension was adjusted to give an absorbance of 1.7±0.3 at λ_{530nm}. *C. albicans* biofilms were formed in 96 well microtiter plates by placing 200 µL of the prepared suspension into the wells, 200 µL of medium (without cells) were used as a negative control. The plates were incubated at 37ºC for 4 hours (initial biofilm formation), 24 hours (biofilm) and 72 hours (mature biofilm) (Pierce *et al*., 2008).

2.1.7 Assessment of antibiofilm activity

The effect of the drugs used upon existing biofilm was evaluated for their effect upon biofilm removal and viability indicators of the remaining cells. To measure the antibiofilm activity of the tested drugs, the medium was removed from the wells and biofilms washed twice with 200 µL phosphate buffer saline (10 mM, pH=7.4), to remove planktonic and non-adherent cells. Pre-prepared serial double dilutions of the tested drug in RPMI-1640 medium were added to the washed biofilms and incubated for two hours at 37°C. The drug(s) were subsequently removed and the biofilm washed with 200 µL phosphate buffered saline and the antibiofilm activity was evaluated using the XTT, NR, CV assays or by viable counts. Different methods were used to evaluate the effect of the test compounds on the metabolic stress and lysosomal activity as indicators of the viability condition of the cells. However, the CV assay was used to measure the loss from the biofilm. Viable count was performed to check whether the treated biofilm cells were dead or alive.

2.1.7.1 XTT assay

XTT reduction assay measures the mitochondrial metabolic activity of the cells in the biofilm by the reduction of tetrazolium (XTT) to a water-soluble formazan with an orange colour. There is a good correlation between the metabolic activity using XTT and cell density, the assay adopted from Pierce *et al*., (2008). XTT is a water-soluble compound with a negative charge; this prevents its cell penetration. To promote its activity, intermediate electron coupling reagent was added to transfer electrons from the cytoplasm and plasma membrane to the medium and facilitate the reduction of the tetrazolium to formazan (Riss *et al*., 2004).

XTT (2,3-bis(2-methoxy-4-nitro-5-sulfophenyl)-2H-tetrazolium-5-carboxanilide, (Alfa Easer, UK)) was prepared by dissolving XTT-sodium salt in PBS (pH 7.4) at 0.5 mg/mL, followed by filter sterilisation through a 0.22 µm pore size filter. XTT stock solution was stored at -80°C in the dark. Menadione (2-Methyl-1,4-Naphthoquinone or vitamin K3, Alfa Easer, UK) solution was prepared in acetone (Sigma-Aldrich, UK) at three concentrations 1, 10 and 100 µM, then the minimum concentration with the better detection was used.

For the XTT assay, the selected menadione concentration was added to 10 mL of the XTT solution immediately before the assay, then a 100 µL of this XTT/menadione solution was added to each well of a microtiter plate containing *Candida* biofilms, then incubated for two hours at 37°C. Subsequently, 80 µL aliquots were pipetted from the supernatant of each well into a new microtiter plate and the absorbance was recorded at λ_{450nm} using a spectrophotometric plate reader (BioTec, EL800, UK). Biofilm viability was calculated based on the ratio of the treated cells to untreated cells (positive control) as shown below.

$$Biofilm\ Viability\% = \frac{Absorbance\ of\ the\ treated\ well - Absorbance\ of\ the\ control}{mean\ Absorbance\ of\ untreated\ wells - Absorbance\ of\ the\ control} \times 100$$

2.1.7.2 Neutral red uptake (NR) assay

Neutral red is a weekly basic dye, it penetrates cells by diffusion and accumulates in the lysosomes and staining them red, due to their low pH compared to the cytoplasm. In live healthy cells, the pH gradient was maintained, however when the cell dies lysosomes are not able to retain the dye due to the loss of the pH gradient (Repetto *et al*., 2008).

NR (3-amino-7-dimethylamino-2-methyl-phenazine hydrochloride, Sigma-Aldrich, UK) stock solution was prepared using ultrapure water at a concentration of 4 mg/mL and stored at room temperature in the dark for 1-2 months. A working

solution was prepared at a concentration of 80 µg/mL in PBS (pH 7.4), incubated at 37°C for 24 hours and then filtered through a 0.45 µm filter to remove precipitated dye crystals. Aliquot of 100 µL of this solution was added to each *Candida* biofilm well and the plate was incubated for two hours at 37°C. NR was removed, biofilms were washed with 150 µL PBS, followed by fixation with 100 µL 5% glutaraldehyde (Alfa Easer, UK) for 2 minutes in a fume hood. After the fixative solution was removed, 150 µL de-stain solution (50% absolute ethanol, 48% ultrapure water and 2% glacial acetic acid) was added to each well and the plate left for 30 minutes on an orbital shaker to extract NR from the biofilm. Finally, from each well, a 100 µL was transferred into a new microtiter plate and the optical density was measured at λ_{540nm} (Multiskan Ascent, Thermo Labsystems, Finland). The anti-biofilm activity was calculated as a percentage of untreated cells.

2.1.7.3 Crystal violet (CV) assay

Crystal violet is a basic compound which binds to the negative charge of both dead and live cells, it is used to measure the biomass of biofilms. It does not reflect the killing of the biofilm, but the mass left after treatment (Peeters *et al*., 2008).

Biofilms were fixed with 100 µL/well of absolute ethanol for 15 min, then ethanol was removed, and the microtiter plate left to air dry. A volume of 100 µL of 0.1% (w/v) CV (Chadwell Heath, UK) was added to each *Candida* biofilm well, after 20 minutes the stain was removed, and the plate was washed under a gentle stream of running tap water. CV was then extracted from the biofilm by adding 150 µL of 33% acetic acid (Sigma-Aldrich, UK). Then a 100 µL of the supernatant was transferred to a new plate, diluted as required and the absorbance was read at

λ_{595nm} using a plate reader (BioTec, EL800, UK). Antibiofilm activity was calculated as a percentage of untreated cells.

2.1.7.4 Viable count

Viable counting was used to determine the number of living (capable of reproduction) cells after treatment on SDA plates. To the washed biofilm 100 µL of MHB was added to each well, the biofilm was resuspended (by repeatedly pipetting up and down). The resultant suspension was serially tenfold diluted up to seven dilutions in sterile Eppendorf tubes and 50 µL was transferred from each dilution and spread onto SDA plate and incubated for 24-48 hours at 30°C. Plates with a count of 30-300 colonies were selected the viability was calculated as a percentage count of untreated biofilm.

2.1.7.5 Statistical Analysis

Tow-way ANOVA (analysis of variance) was obtained using Microsoft Excel to test the significant difference between the tested compounds.

2.2 Results

2.2.1 Minimum Inhibitory concentration (MIC) and minimum biocidal concentration (MBC)

MIC and MBC were conducted to test the *anti-Candidal* activity of CHD, thymol, and the additives of future formulations against planktonic cells.

CHD was studied over the range from 10 to 0.087 µg/mL and thymol from 250 - 1.95 µg/mL. The results are presented in Table 2.1. *C. albicans* ATCC 10231 strain showed more resistance toward CHD than the NCYC 854 strain. Therefore the former was chosen for testing other compounds.

Table 2.1 MIC and MBC of the tested compound at 30°C, n = 3.

Testing compounds (µg/mL)	*C. albicans* ATCC 10231		*C. albicans* NCYC 854	
	MIC	***MBC***	***MIC***	***MBC***
CHD	2.5	5	1.25	2.5
Thymol	125	250	-	-
HPMC, HPMC-S or P407	>500	>500	-	-
Sorbitol, Xylitol or Mannitol	>10000	>10000	-	-

The antifungal activity of the polymers (HPMC, HPMC-S and P407) and Sugar Alcohols (sorbitol, xylitol and mannitol) was investigated to check any future impact on the activity of the drug in the formulations. Each polymer was serially diluted from 500 to 0.005 µg/mL, and sugar alcohols from 10 to 0.0001 mg/mL. Neither the polymers nor the sugar alcohols showed any *anti-Candidal* activity against *C. albicans* ATCC 10231 at the investigated concentrations.

Due to the mucoadhesive nature of the polymers, polymer-CHD combinations were investigated, each polymer was co-dissolved with each drug at a ratio of 5:1. None of the polymers had an effect on the *anti-Candidal* activity of CHD against planktonic cells. Similarly, thymol-HPMC or HPMC-S showed no effect on the activity of thymol Table 2.2. However, P407 at 5:1 ratio increased the MBC of thymol above 250 µg/mL with no effect on the MIC. Due to the limited solubility of thymol, no further concentrations were investigated.

Table 2.2 MIC and MBC of drug-polymer combinations at 30°C, n = 3.

Testing compounds (µg/mL)	*C. albicans* ATCC 10231	
	MIC	***MBC***
CHD + HPMC, HPMC-S or P407 (5:1)	2.5	5
Thymol + HPMC or HPMC-S (5:1)	125	250
Thymol + P407 (5:1)	125	>250
Thymol + P407 (4:1)	125	>250
Thymol + P407 (2:1)	125	>250
Thymol + P407 (1:1)	125	≥250*

* 2 with no growth and 1 with growth.

The effect of P407 on the activity of thymol was further investigated at 4:1, 2:1 and 1:1 ratio. At 4:1 and 2:1 ratio, the MBC of thymol was >250 µg/mL, while at 1:1 ratio two out of three replicates showed no growth (Table 2.2). This means the effect of P407 on the antifungal activity of thymol is concentration dependent.

2.2.2 Time-kill assay

2.2.2.1 CHD

Qualitative time kill study was performed against ATCC 10231 and NCYC 854 strains, CHD was serially double diluted from 10 to 0.156 µg/mL.

The results (Table 2.3) show a complete inhibition of growth after one hour at 10 µg/mL CHD, however, the MBC (5 µg/mL) had no apparent kill until after 4 hours and before 24 hours for ATCC 10231. However, NCYC 854 strain was more susceptible with a loss of viability seen after 40 minutes at 10 µg/mL, after 3 hours at 5 µg/mL and for the MBC (2.5 µg/mL) the loss of viability was after 4 hours, up to 24 hours (Table 2.4). All other dilution showed no apparent loss of viability over the 24 hours period.

*Table 2.3 Time-kill results for CHD against C. albicans ATCC 10231 for 24 hours and 30°C in MHB, n = 4. (*results are 50%.)*

Time (min)	Concentration (µg/mL)							
	10	5	2.5	1.25	0.625	0.3125	0.15625	Negative control
20	+	+	+	+	+	+	+	-
40	+	+	+	+	+	+	+	-
60	+	+	+	+	+	+	+	-
80	-	+	+	+	+	+	+	-
100	-	+	+	+	+	+	+	-
120	-	+	+	+	+	+	+	-
150	-	+	+	+	+	+	+	-
180	-	+	+	+	+	+	+	-
210	-	+	+	+	+	+	+	-
240	-	-* +*	+	+	+	+	+	-
24 hours	-	-	+	+	+	+	+	-

Table 2.4 Time-kill results for CHD against C. albicans NCYC 854 for 24 hours and 30°C in MHB, n = 4.

Time (min)	Concentration (µg/mL)							
	10	5	2.5	1.25	0.625	0.3125	0.15625	Negative control
20	+	+	+	+	+	+	+	-
40	+	+	+	+	+	+	+	-
60	-	+	+	+	+	+	+	-
80	-	+	+	+	+	+	+	-
100	-	+	+	+	+	+	+	-
120	-	+	+	+	+	+	+	-
150	-	+	+	+	+	+	+	-
180	-	+	+	+	+	+	+	-
210	-	-	+	+	+	+	+	-
240	-	-	+	+	+	+	+	-
24 hours	-	-	-	+	+	+	+	-

The effect of CHD upon the viable cell count with time was studied (Figure *2.1*). The results show that at the MBC (5 µg/mL), cell viability was decreased within the first 60 minutes and eventually by 1 log, while both the MIC and the positive control showed no change in cell viability over the tested period. The time performed was chosen based on the proposed time for the tablet in the oral cavity.

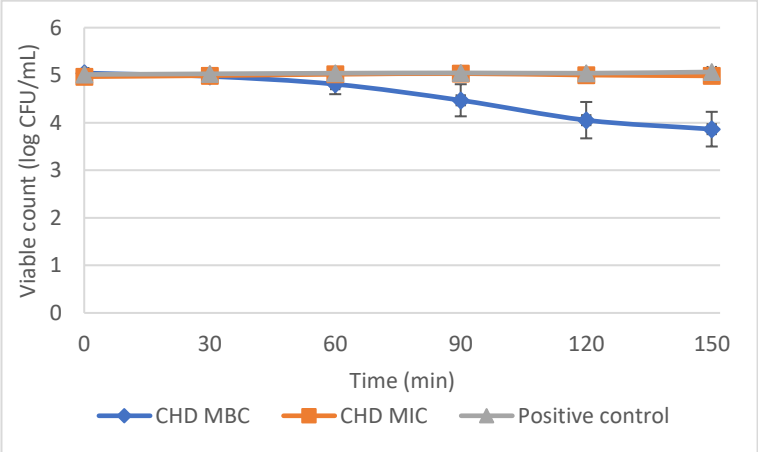

Figure 2.1 Time-kill curves for CHD against C. albicans ATCC 10231 strain, at the MBC (5 µg/mL), MIC (2.5 µg/mL) and positive control (0 µg/mL CHD) at 30°C and shaking at 80rpm in MHB. Data are expressed as mean percentage ± SD, n = 3.

2.2.2.2 Thymol

A thymol time kill study was performed against *C. albicans* ATCC 10231, at a concentration range from 250 µg/mL to 15.6 µg/mL. The results (Table 2.5) show that the only fungicidal activity was found at 24 hours for 250 µg/mL; which is the MBC concentration.

Table 2.5 Time-kill results for thymol against C. albicans ATCC 10231 for 24 hours and 30°C in MHB, n = 3.

Time (min)	Concentration (µg/mL)					
	250	125	62.5	31.25	15.625	Negative control
20	+	+	+	+	+	-
40	+	+	+	+	+	-
60	+	+	+	+	+	-
80	+	+	+	+	+	-
100	+	+	+	+	+	-
120	+	+	+	+	+	-
150	+	+	+	+	+	-
180	+	+	+	+	+	-
210	+	+	+	+	+	-
240	+	+	+	+	+	-
24 hours	-	+	+	+	+	-

A more detailed time kill study was undertaken which monitored the number of viable cells with respect to time of exposure to thymol (Figure *2.2*).

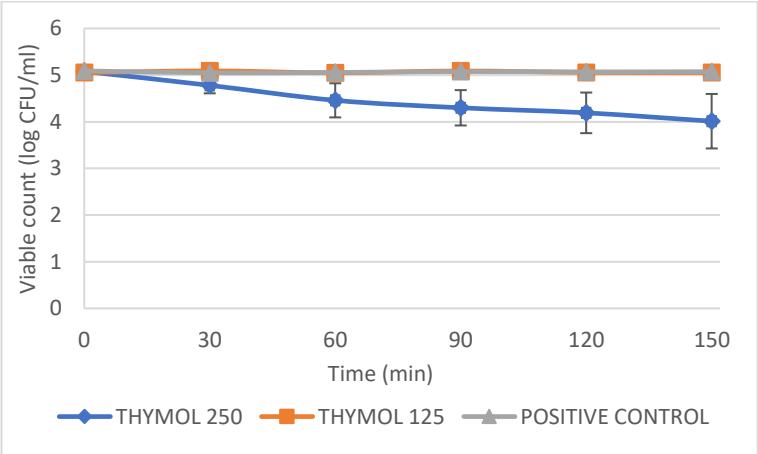

Figure 2.2 Time-kill curves for thymol against C. albicans ATCC 10231 strain, at the MBC (250 µg/mL), MIC (125 µg/mL) ad positive control (0 µg/mL thymol) at 30°C and shaking at 80rpm in MHB. Data are expressed as mean percentage ± SD, n = 3.

Quantitatively, thymol at the MBC (250 µg/mL) showed continuous loss of cell viability from 30 minutes leading to a 1 log reduction in viable cells, by 2.5 hours. There was no change in the cell viability at the MIC concentration (125 µg/mL) or the absence of thymol (control).

2.2.3 Microdilution checkerboard assay

C. albicans ATCC 10321 susceptibility to the combination of CHD and thymol was examined using a checkerboard assay, the results are presented in Table 2.6. Although there is a reduction in the MIC of both drugs, the MIC for the combination was 1.25 µg/mL CHD and 31.25 µg/mL thymol, the FIC value was equal to 0.75 which means there was no interaction (FIC =0.5-4) (Odds, 2003). However, the MBC of CHD did not change after the addition of thymol and was equal to 5 µg/mL.

Table 2.6 Checkerboard assay for the combination of CHD and thymol against C. albicans ATCC 1023 for 24 hours at 30°C in MHB, Data are expressed as mean percentage ± SD, n = 5.

Thymol concentration µg/mL	CHD concentration µg/mL								
	5	2.5	1.25	0.625	0.312	0.156	0.078	0.039	0.019
125	-	-	-	-	-	-	-	-	-
62.5	-	-	-	-	-	-	-	-	-
31.25	-	-	-	75.54±16.93	60.47±5.52	66.21±13.51	62.57±0.81	62.84±14.10	66.10±11.02
15.625	-	-	57.26±34.44	77.80±2.34	66.03±6.27	71.33±4.48	72.04±6.72	70.84±5.96	79.95±8.36
7.8125	-	-	75.56±15.97	77.75±8.46	74.29±10.47	76.66±17.51	76.23±3.10	68.61±9.31	75.06±8.59
3.906	-	-	90.94±24.29	88.28±14.81	75.41±13.56	80.33±14.08	82.11±0.94	78.41±8.19	79.37±8.58
1.953	-	-	77.19±9.22	85.07±7.78	86.19±14.92	88.87±20.30	83.67±9.60	91.53±11.09	88.15±5.87
0.977	-	-	90.34±16.47	84.12±9.09	82.71±13.04	86.61±18.30	88.16±5.69	89.32±6.68	90.60±5.75

2.2.4 Effect of farnesol on *C. albicans*

Farnesol is a quorum sensing molecule produced by *C. albicans* to stop hyphae formation. The MIC and MBC were tested by serially ten-fold dilution from 1.06 x 10^{-4} to1.06 mM. After incubation, all tubes showed turbidity which indicates no growth inhibition. The turbidity in the first three tubes was less than the control without farnesol, due to inhibition of hyphae formation, because cells showed less density. No MBC was attained at a concentration ≤1.06 mM against *C.albicans* ATCC 10231.

The morphological investigation was performed by taking the highest concentration of 1.06 mM farnesol in MHB and examined microscopically under oil immersion (1000x). Untreated cells showed long hyphae, however, treated cells had an oval shape (Figure 2.3), indicating that farnesol successfully inhibited the filamentation of *Candida*.

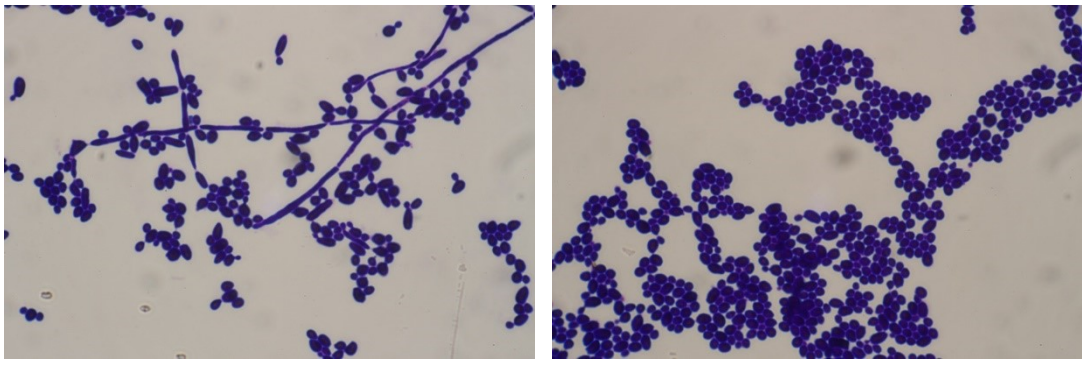

Figure 2.3 C. albicans stained with crystal violet, left grown in MHB, right grown in 1.06 mM of farnesol in MHB and incubated at 30°C for 24 hours (1000x).

2.2.4.1 Effect of farnesol on the activity of CHD and Thymol

The MIC and MBC for CHD were investigated in the presence of farnesol (1.06 mM). It was found that the MIC increased from 2.5 to 10 µg/mL and the MBC increased from 5 to 40 µg/mL. The MIC and MBC for thymol in the presence of

farnesol at 1.06 mM was similarly investigated. It was found that the MIC was increased from 125 to 250 µg/mL and MBC was >250 µg/mL. Due to the limited aqueous solubility of thymol, no further analysis was performed to estimate the MBC in the presence of Farnesol.

2.2.5 Effect of CHD and thymol on *C. albicans* biofilm

The major pathogenicity of *C. albicans* is attributed to its ability to form a biofilm, which is more resistant to antifungals. This explained by the upregulation of efflux pumps, the presence of extracellular matrix and persister cells (Gulati and Nobile, 2016). So, it is very important to study the effect of CHD and thymol on *C. albicans* biofilm. The antibiofilm effect of CHD and thymol and their combination were investigated for two hours which is the intended time of mucoadhesive buccal tablet application, for the treatment of OPC which is commonly available in the form of biofilms.

There are several methods to measure the viability of the biofilm, in this work XTT assay, CV assay and NR uptake assay were used.

2.2.5.1 XTT reduction assay

XTT reduction assay was selected to measure the metabolic activity of the cells in the biofilm (Pierce *et al*., 2008). Menadione was added to facilitate the reduction of the tetrazolium (XTT) to orange colour, water soluble formazan (Riss *et al*., 2004). In this experiment, the optimisation of menadione concentration (1, 10 and 100µM (n=24)) was performed on *Candida* biofilms which were grown in 96 well plates for 24 hours. Each concentration was added to XTT solution instantly before adding to the biofilm as a 100 µL of XTT/menadione solution, the

plate was incubated for 2 hours at 37°C and the colour change was measured. The absorbance values were 0.063±0.040, 0.470±0.041 and 0.685±0.193 for 1, 10 and 100 µM, respectively. 10 µM was chosen due to its reasonable detection with low standard deviation for subsequent experiments.

Anti-biofilm activity of CHD, CHD-HPMC and CHD-P407 were investigated at a 5:1 ratio of polymer to CHD. The concentrations of CHD were 160 to 0.63 µg/mL (serially double diluted). The percentages of the absorbance of the treated biofilms to the average of untreated cells represented the metabolic activity of the biofilms (4, 24 or 72 hours) after two hours exposure of the drug.

Candida in the 4-h biofilm, had started adhering to the plate and producing hyphae. After two hours treatment with CHD at a concentration of ≥10 µg/mL, XTT results show nearly 100% loss of the mitochondrial activity. Moreover, there was a considerable loss in the activity at 5 µg/mL and this loss is decreased with the decrease in CHD concentration (Figure *2.4*-a).

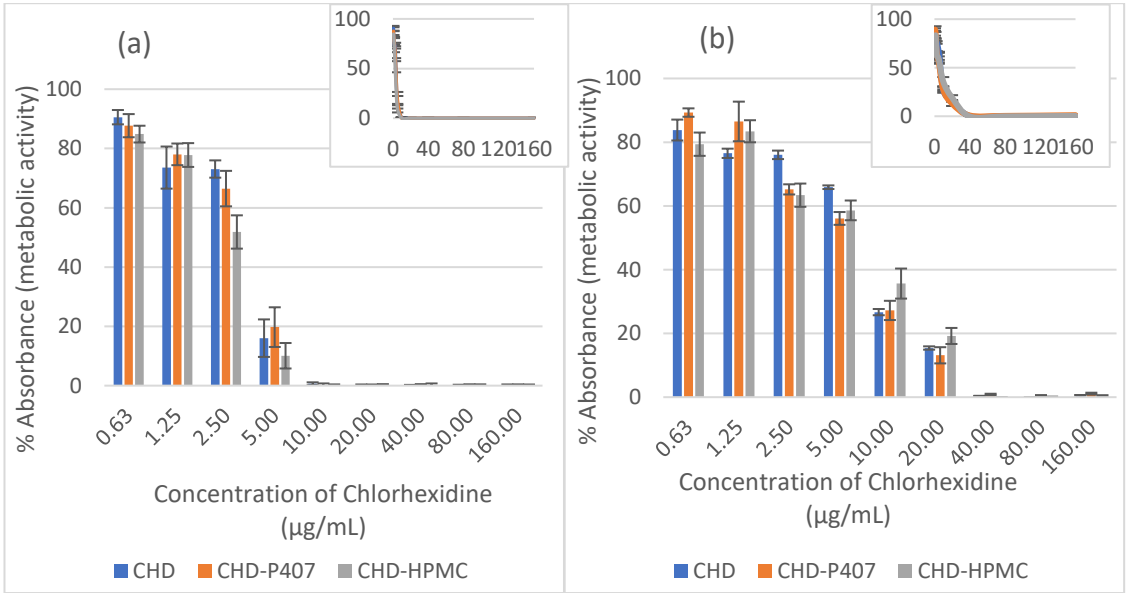

Figure 2.4 Effect of CHD on initial C. albicans biofilm, (a) 4 hours and (b) 24 hours, for 2 hours at 37°C using XTT assay. Data are expressed as mean percentage ± SE, n = 12.

With the increase in the maturity of the biofilm at 24 hours (Figure *2.4*-b), the resistance to CHD was increased. As evidenced by CHD concentration of ≥40 µg/mL showing nearly 100% suppression of metabolic activity, with a significant reduction to 15% and 26% at 20 and 10 µg/mL CHD, respectively. The reduction was decreased gradually with the decrease of CHD concentration. Furthermore, there is no apparent difference between the activity of CHD alone or in combination with the polymers for both biofilms.

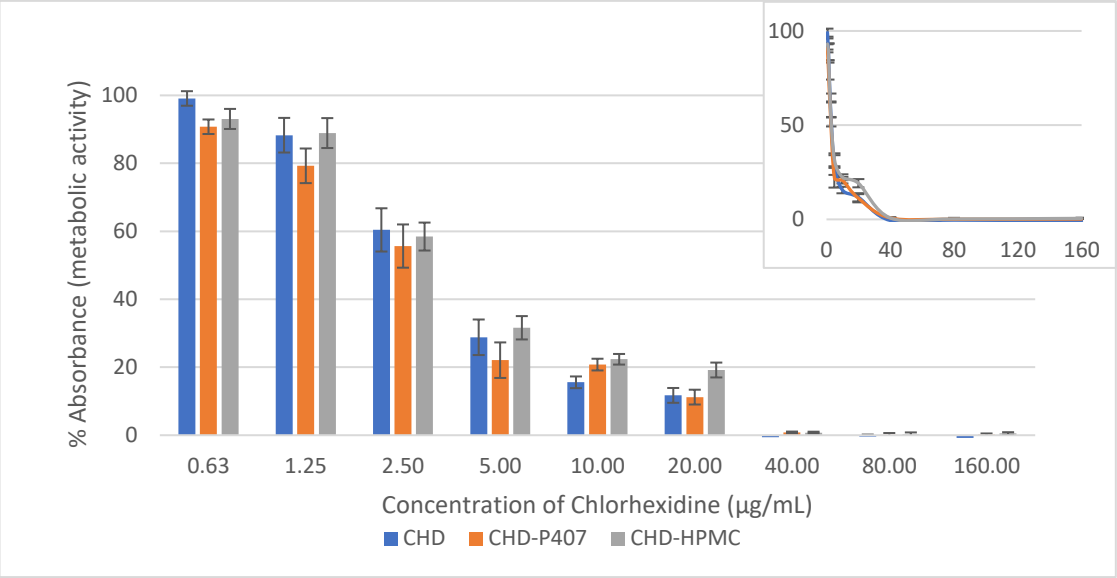

Figure 2.5 Effect of Chlorhexidine on C. albicans biofilm (72 hours), for 2 hours at 37°C using XTT assay. Data are expressed as mean percentage ± SE, n = 4.

Biofilms grown for 72 hours showed nearly 100% loss in activity at concentrations of ≥40 µg/mL. The loss was started from a concentration of 2.5 µg/mL and it was higher than 24-h biofilm. This explained by the fragile nature of the 72-h biofilm, a visual loss was noticed during the several washing steps, this might result in false negative results showing more sensitivity toward CHD than 24-h biofilm (Figure 2.5).

Similarly, thymol was investigated for its antibiofilm activity alone and in combination with HPMC or P407 of 5:1 polymer to drug ratio. Concentrations of 250 µg/mL to 0.98 µg/mL (serially double diluted) were examined on (4, 24 and 72 hours) *C. albicans* biofilms. Although there was a reduction in the metabolic activity at a thymol concentration of ≥62.5 against 4-h biofilm (Figure 2.6-a), the effect was fluctuating with no certain pattern for all tested compounds. Similar results were found for the 24-h biofilm (Figure 2.6-b) and at 250 µg/mL an increase in the absorbance to 120% for thymol, followed by a loss in its value to 75% at 62.5 and 125 µg/mL.

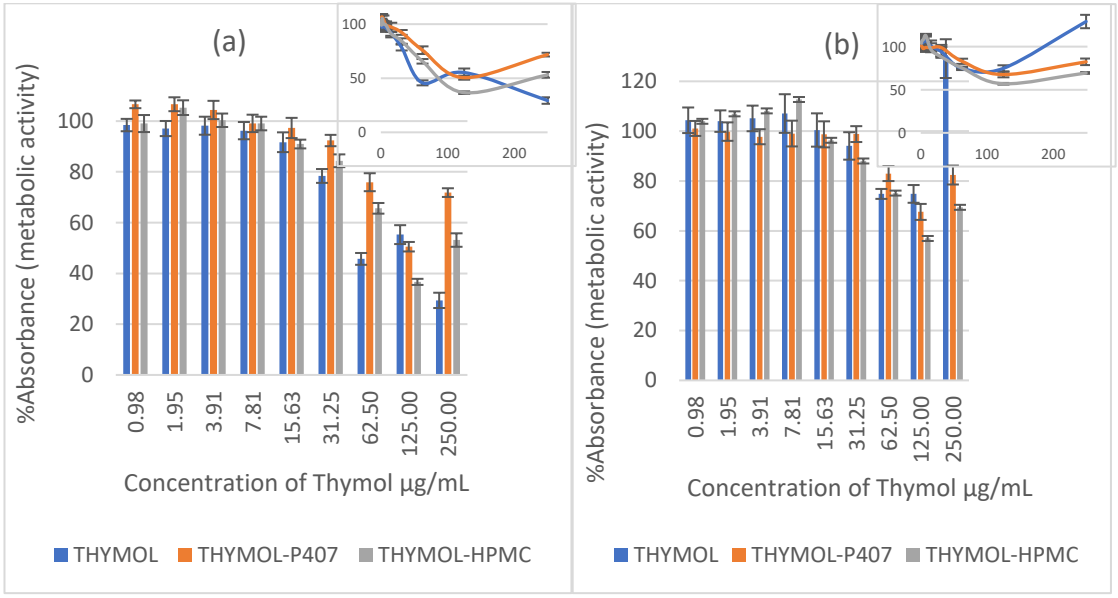

Figure 2.6 Effect of thymol on initial C. albicans biofilm (a)4-h and (b) 24-h for 2 hours at 37°C using XTT assay. Data are expressed as mean percentage ± SE, n = 12.

There was a concentration-dependent loss in the metabolic activity of the biofilm which grown for 72 hours (Figure 2.7). Due to the visual loss of the 72-h biofilm mass as mentioned earlier with CHD results, 72-h biofilm investigations will be omitted from future experiments.

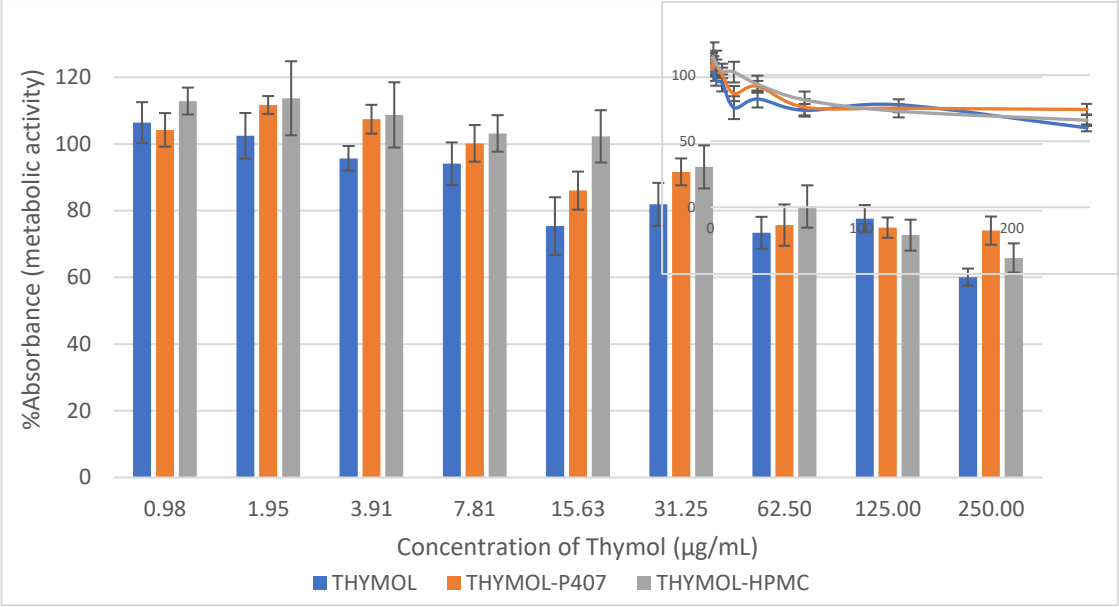

Figure 2.7 Effect of thymol on C. albicans biofilm 72-h, for 2 hours at 37°C using XTT assay. Data are expressed as mean percentage ± SE, n = 4.

2.2.5.2 Crystal violet (CV) assay

CV is used to measure the biomass of the biofilms (Peeters *et al*., 2008). Biofilms grown for 4 and 24 hours were treated with CHD, CHD-P407 and CHD-HPMC at concentrations from 160 to 1.25 µg/mL for two hours at 37°C. The percentage of the absorbance of treated to untreated cells represents the biomass per cent remained after treatment. The biomass for 4-h biofilms treated with concentrations of ≥10 µg/mL had approximately an absorbance percentage ranging from 30±5 % for CHD and CHD-polymer combinations (Figure 2.8-a). At 5 µg/mL, the loss was approximately 50% which was decreased with decreasing CHD concentration and no 100% biomass was noticed even at the lowest concentration of 1.25 µg/mL.

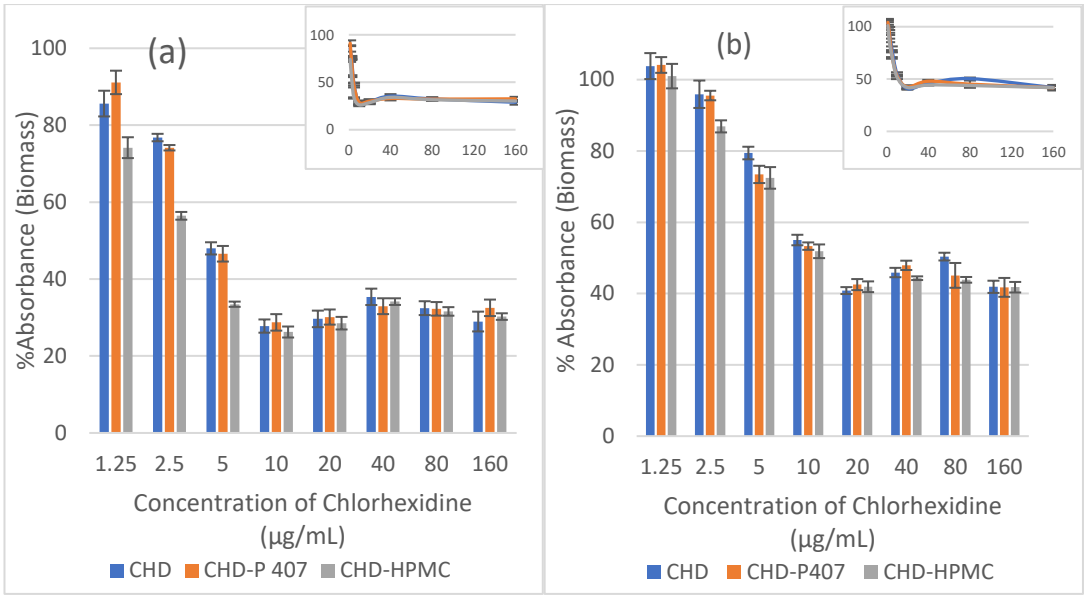

Figure 2.8 Effect of CHD on initial C. albicans biofilm (a) 4-h, (n = 6), (b)24-h, (n = 8), for 2 hours at 37°C using CV assay. Data are expressed as mean percentage ± SE.

In contrast, the biomass of 24-h biofilm showed slightly less reduction (45±5%) at the concentrations of ≥20 µg/mL and at 10 µg/mL was 55%. The loss was less with the lower concentrations and at 1.25 µg/mL no loss was detected (Figure 2.8-b). Moreover, HPMC and P-407 had no pronounced effect on CHD activity at ≥10 µg/mL for both biofilms, at lower CHD concentrations the effects of the polymers were unpredictable.

Light microscopy images for 24-h biofilm (Figure 2.9), showed that the intensity of the colour and the thickness of the mycelium stained with CV decreases with the increase in the concentration of CHD, compared to the control and indicates a loss in the biomass.

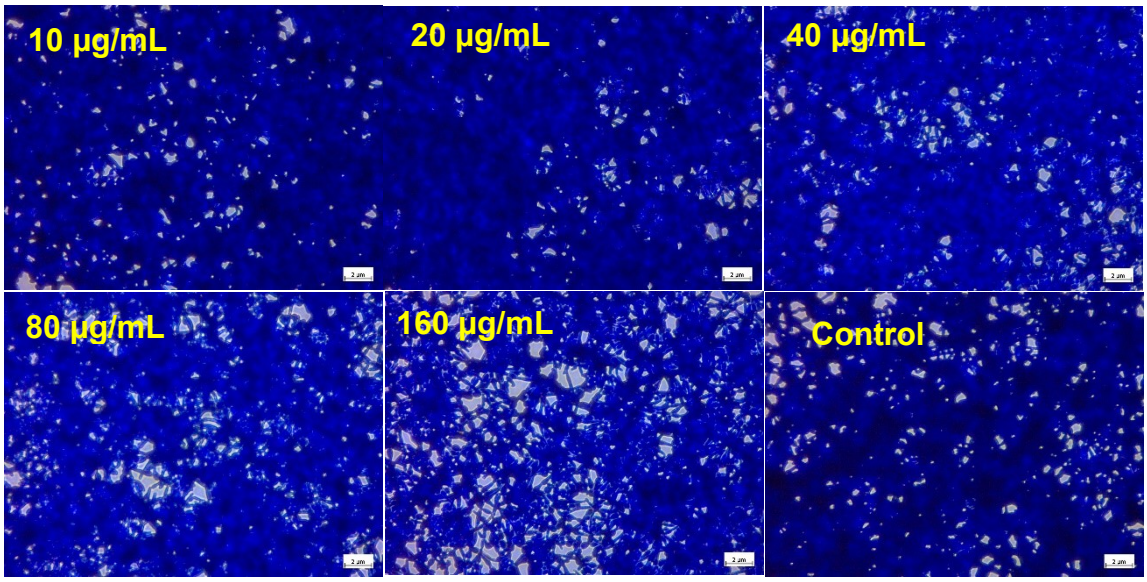

Figure 2.9 Images of C. albicans biofilm 24-h treated with CHD and stained with CV (x400).

The effect of thymol on the biomass of *C. albicans* was investigated using CV at the concentrations from 250 to 1.95 µg/mL. Biomass loss was increased with the increase in thymol concentration, the effect of both MBC and MIC on the biomass of the 4-h biofilm, is presented in (Figure 2.10-a). The absorbance percentages were 29% and 48% respectively and increased to 65% at 62.5 µg/mL, this followed by a gradual increase in biomass with the decrease in thymol concentration and no loss was recorded at 3.91 µg/mL. However, the 24-h biofilm was less affected; the percentages increased to 63% and 68% at MBC and MIC, respectively (Figure 2.10-b). Moreover, at concentrations of ≥7.81, there was 100% retaining of the biomass. This indicates that the sensitivity to the drug is affected by the maturity of the biofilm.

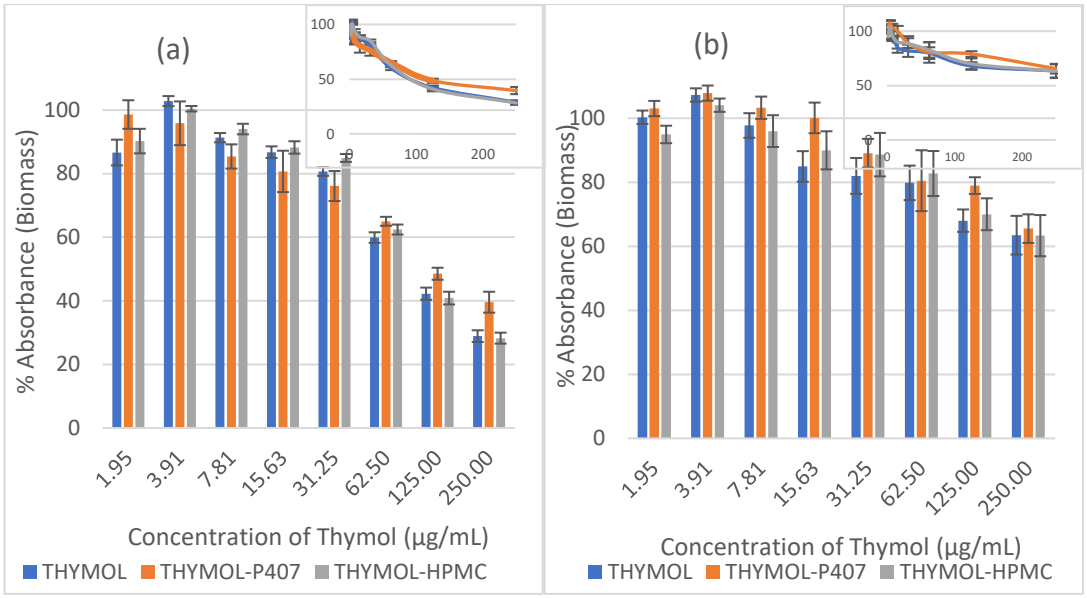

Figure 2.10 Effect of thymol on the biomass of initial C. albicans biofilm (a) 4-h, (n = 8), (b) 24-h, (n = 8) for 2 hours at 37°C. Data are expressed as mean percentage ± SE.

Light microscopy studies showed that the effect of thymol on 24-h biofilm was not distinct compared to the control (Figure 2.11) indicating the low effect of thymol on the biomass of *Candida* biofilm.

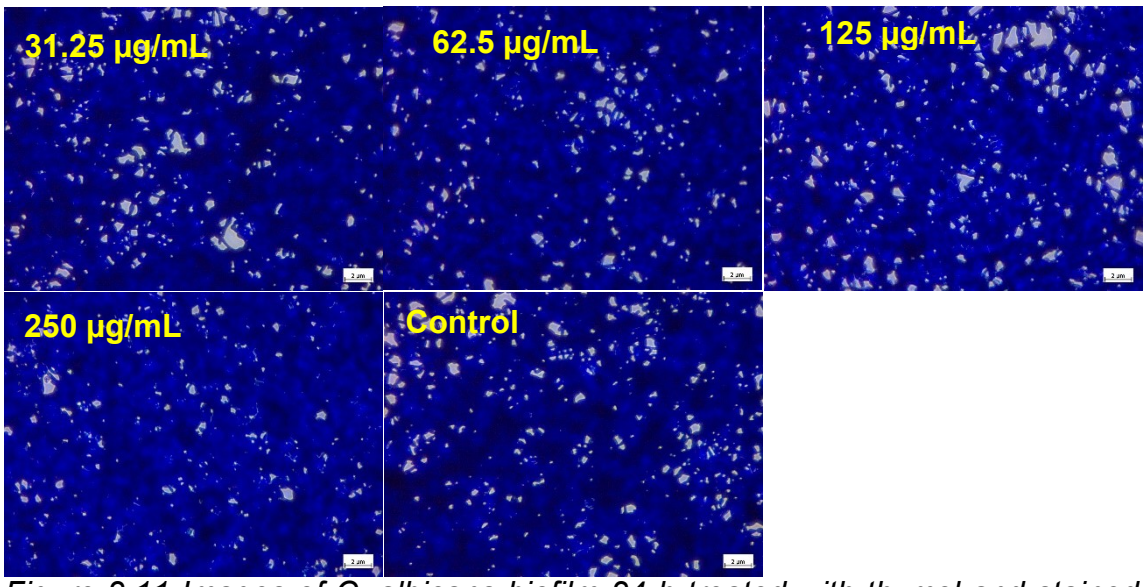

Figure 2.11 Images of C. albicans biofilm 24-h treated with thymol and stained with CV (x400).

2.2.5.3 Neutral red (NR) uptake assay

NR is a basic dye retained by the lysosomes of viable cells (Repetto *et al.*, 2008). This assay is widely applied to measure the cytotoxicity for human cell lines, and depending on the same principle, since the pH of the vacuoles is around 5.5 (Patenaude *et al.*, 2013), the assay was applied to *C. albicans* cells. Washed biofilms were incubated for two hours with CHD at concentrations of 160-1.25 µg/mL. The biofilms were then washed, incubated with the NR, and after washing and fixation the stain was extracted and measured. The percentage absorbance of CHD treated biofilm to untreated is an indicator of cell viability. The results (Figure 2.12-a) show the observed viability based on the vacuolar staining of the biofilm cells. NR uptake was decreased with increasing CHD concentration and that at ≥10 µg/mL was around 10% with a considerable effect of 40% retaining in activity at 5 µg/mL and around 100% at ≤2.5 µg/mL.

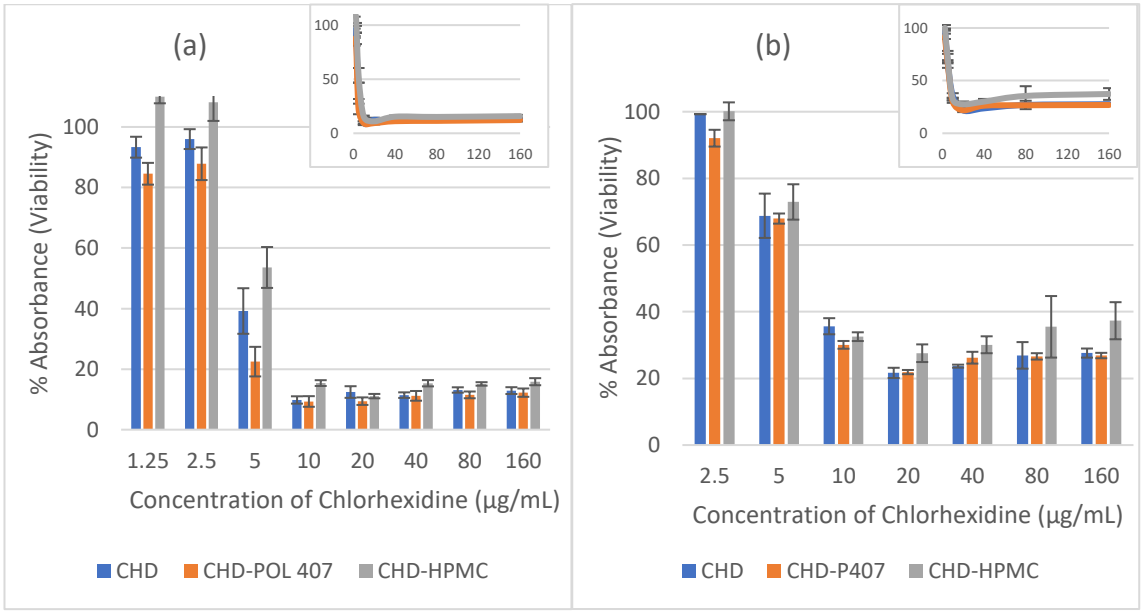

Figure 2.12 Effect of CHD on initial C. albicans biofilm using NR assay (a) 4 hours, (n = 9), (b) 24-h, (n = 5), for 2 hours at 37°C. Data are expressed as mean percentage ± SE.

A similar effect was seen on 24-h biofilm (Figure 2.12-b) at ≥20 µg/mL, with apparent viability only reduced to 21-27% and 36% at 10 µg/mL and no effect recorded at 2.5 µg/mL. CHD-HPMC showed slightly higher absorbance for almost all concentrations, whereas CHD-P407 was similar to that of CHD alone. The effect of HPMC may be attributed to the mucoadhesive nature of the polymer which might form a barrier against the change in the pH and the release of the NR from *Candida* or interfere with the mechanism of the assay.

Microscopical analysis of stained cells showed that the colour intensity of NR in the vacuoles. Colour intensity is decreased with increasing CHD concentration. This is due to the loss of the vacuolar activity and pH gradient (Figure 2.13), which in agreement with the colourimetric assay. The hazy appearance of the image may be due to the presence of the extracellular material in the growing biofilm (Chandra *et al*., 2001)

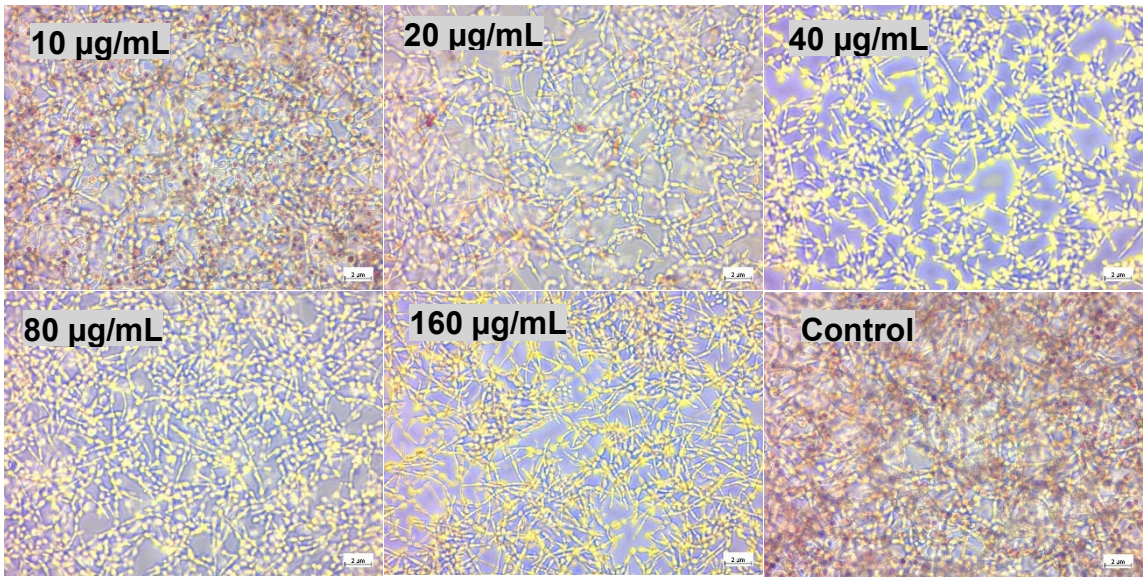

Figure 2.13 Images of C. albicans biofilm 24-h treated with CHD and stained with NR (x400).

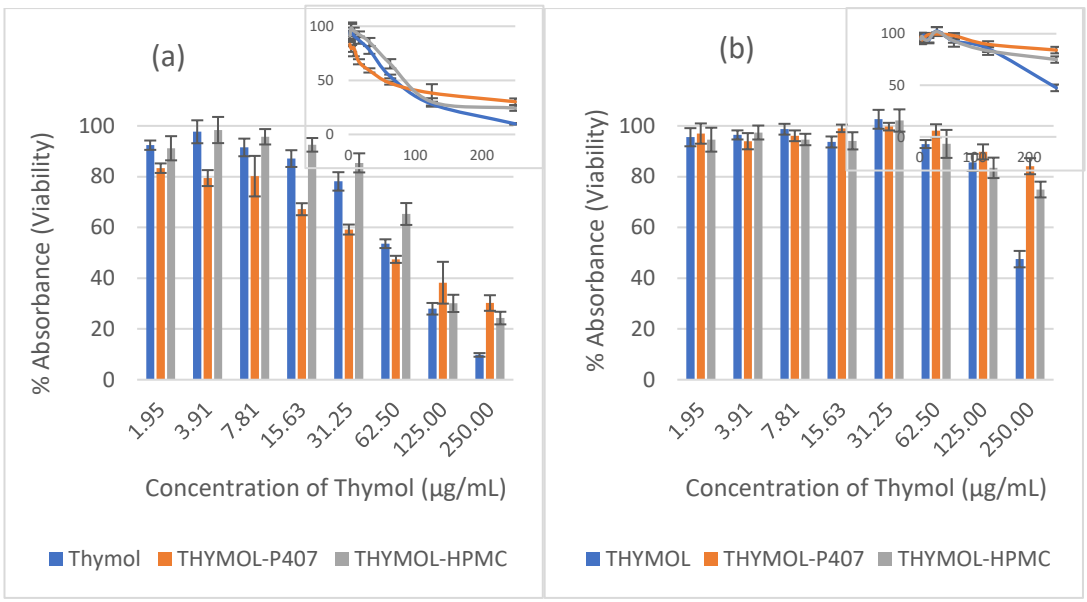

Figure 2.14 Effect of thymol on initial C. albicans biofilm using NR assay (a) 4-h, (n = 6) (b) 24-h, (n = 5) for 2 hours at 37°C. Data are expressed as mean percentage ± SE.

The effect of thymol upon vacuolar activity (viability) of *C. albicans* 4-h biofilm are presented in Figure 2.14-a. It can be seen, that thymol at concentrations > 15.63 µg/mL have decreased the apparent viability, for instance at 125 and 250 µg/mL the viability was 28% and 10%, respectively. There was a clear antagonistic effect of P407 on thymol activity at 125 and 250 µg/mL, which was similar to the finding on planktonic cells as it affected the MIC and the MBC. On the contrary, P407 showed an increase in thymol activity at a concentration of ≥62.5 µg/mL. HPMC has a similar antagonistic effect at 250 µg/mL.

Thymol activity against C. albicans 24-h biofilm was substantially reduced (Figure 2.14-b) compared to 4-h biofilm in which loss of cell viability occurred only at concentrations ≥125 µg/mL. Both polymers exerted an antagonistic effect on thymol antimicrobial activity at 250 µg/mL. Microscopical images for the effect of thymol on 24-h biofilm (Figure 2.15) agreed with the CV images reflecting the low

potency of thymol against *C. albicans* biofilm even at high concentration (250 µg/mL).

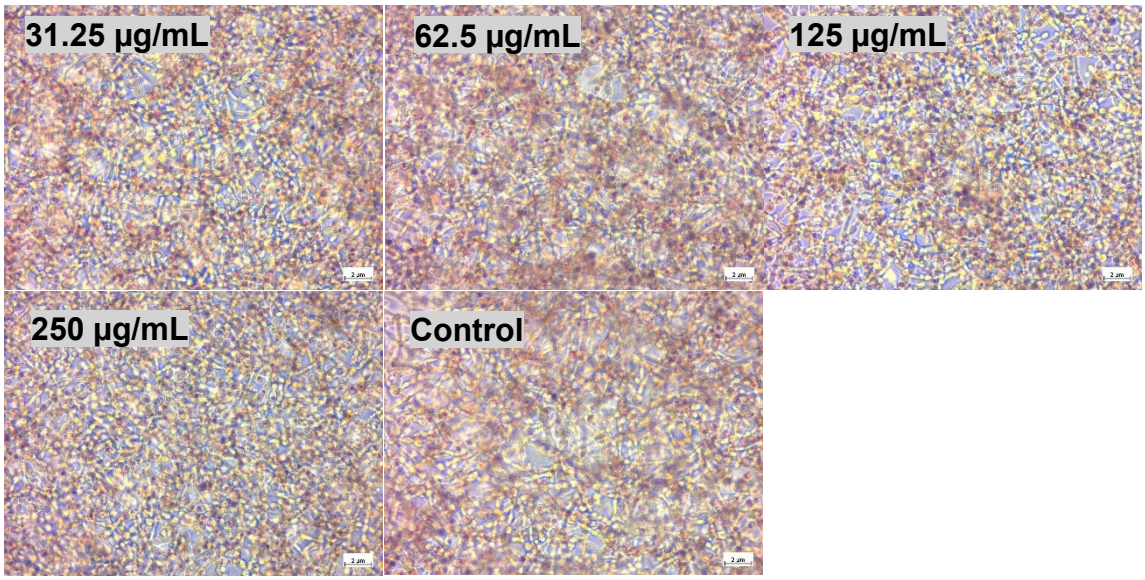

Figure 2.15 Images of C. albicans biofilm 24-h treated with thymol and stained with NR (x400).

2.2.6 Recovery of biofilm after treatment

Biofilm cells' recovery was performed to check if the cells have lost their viability after treatment with the drugs and if the damage is reversible or permanent. Based on the previous analyses using XTT, NR uptake and CV assays, although the behaviour of the drug was the same, but the values were different for instance treating 24-h biofilm with CHD at concentration of ≥40 µg/mL showed ~100% inhibition of mitochondrial activity, ~60% loss of biomass and ~80% loss of vacuolar activity. Accordingly, the recovery experiment is to check if the biofilm maintained its viability.

2.2.6.1 CV and NR assays

Biofilm cell viability recovery was performed for 24-h biofilm treated with CHD or thymol for 2 hours, followed by washing and re-incubating in a fresh medium for

another 24 hours. The viability was assessed using CV and NR assays (Figure 2.16).

The test was not reproducible due to the damage of the biofilms, uneven growth with floating of non-adherent pieces of the biofilms was noticed visually after 24 hours of recovery, in most of the wells. Moreover, for both drugs, unlike the previous results, the biomass results were lower than the vacuolar activity. It can be concluded that the cells were viable, but the accuracy of these results is questionable.

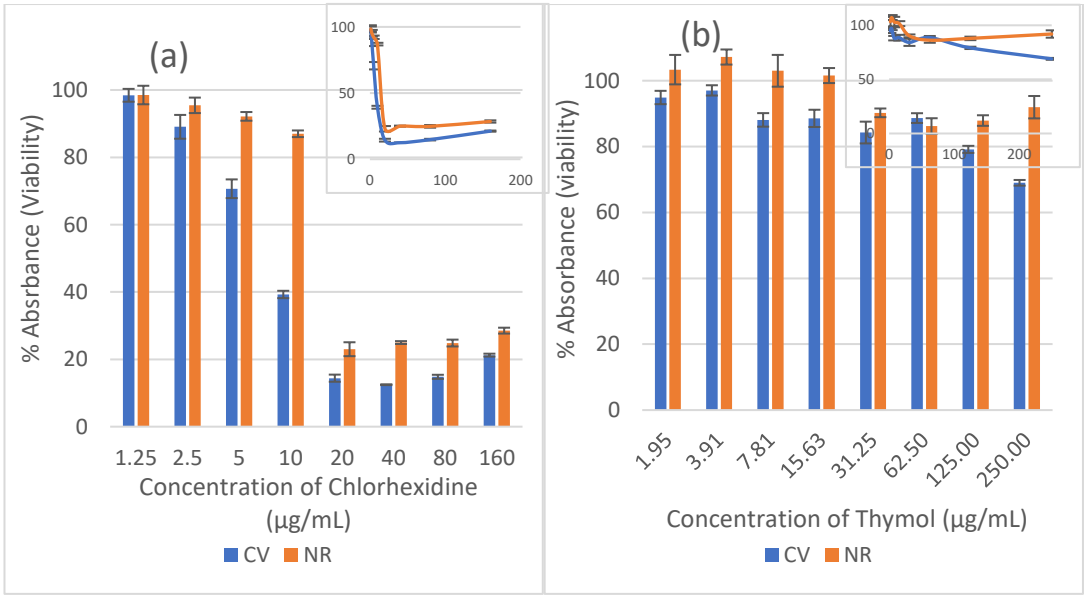

Figure 2.16 Recovery of C. albicans biofilm for 24hours after treatment with different concentrations of (a) Chlorhexidine (b) thymol using NR uptake and CV assays at 37°C, Data are expressed as mean percentage ± SE, n = 6.

2.2.6.2 Viable count

Based on the previous analysis, the quantitative value of biofilm recovery was inconclusive. Therefore, the need for another experiment with a minimum washing and treating steps were necessary. By using viable count, these steps were kept to a minimum.

Viable count for 24-h biofilms treated with CHD was performed and *Candida* was grown on SDA plates (Figure 2.17). It was noticed that the viability is decreased with increasing CHD concentration. The viability was 0.02%, 1.06% and 4.3% at 160, 80 and 40 µg/mL, respectively and 100% recovery with 2.5 µg/mL.

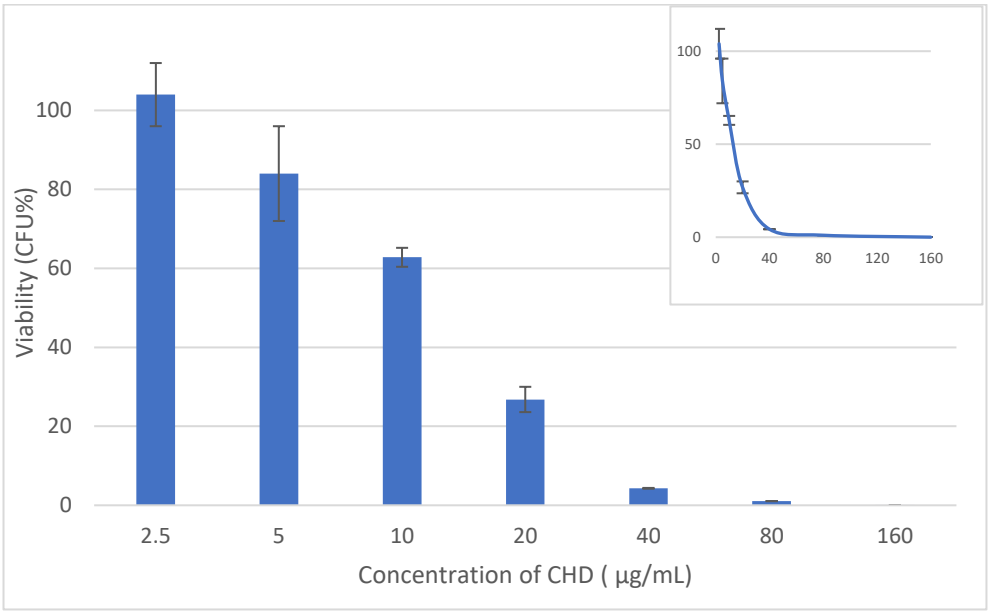

Figure 2.17 viable count of C. albicans biofilm after treatment with CHD at 30°C, Data are expressed as mean percentage ± SE, n = 3.

2.2.7 Effect of CHD and Thymol combination on *C. albicans* biofilms

Thymol and CHD affect the cell wall of *C. albicans* in different ways. Therefore, the combined effect of CHD and Thymol was investigated to check the possibility of synergistic or additive effect against *Candida* biofilm. The investigated concentrations were chosen based on the previous analysis and the results were evaluated using CV and NR uptake assays. The XTT assay excluded due to the reducing activity of thymol.

Crystal violet assay

CV assay was used to detect the combined effect of the drugs on the biomass of the biofilm grown at 4-h and 24-h. CHD concentrations were 5, 10 and 20 µg/mL, whereas thymol concentrations were 31 and 62 µg/mL.

It was found that the addition of thymol to CHD had a limited additive effect (Figure 2.18). Statistical analysis was performed individually between CHD and CHD combinations at the same concentration. There was a significant difference for both treatment groups. At 5 µg/mL CHD and 62.5 µg/mL thymol, there was a 10 and 15% decrease in the biomass compared to CHD alone for 4-h and 24-h biofilms, respectively. Although other statistical analysis showed significant differences, the effect was ≤10%.

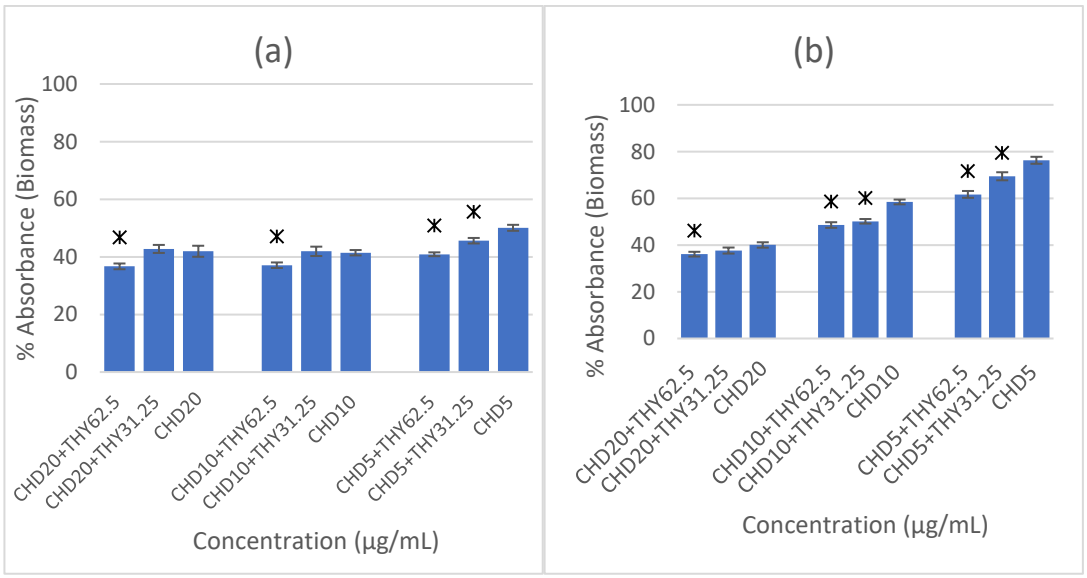

Figure 2.18 Effect of the combinations of CHD and thymol on C. albicans biofilm (a) 4-h and (b) 24-h for two hours treatment at 37°C using CV assay. Data are expressed as mean percentage ± SE, n = 12, p>0.05.
**Asterisks represent values significantly different from CHD alone of the same concentration.*

Neutral red uptake assay

Using the NR uptake assay to examine the effect of antifungal combinations on vacuolar activity in 4 and 24 hrs biofilms, revealed significant differences at 5 µg/mL CHD. The greatest effect was seen for 62.5% thymol on the 4 hrs biofilm with a 20% reduction in vacuolar activity, followed by the 5 µg/mL CHD and 31.25 % thymol combination which was 15% higher than CHD alone (Figure 2.15).

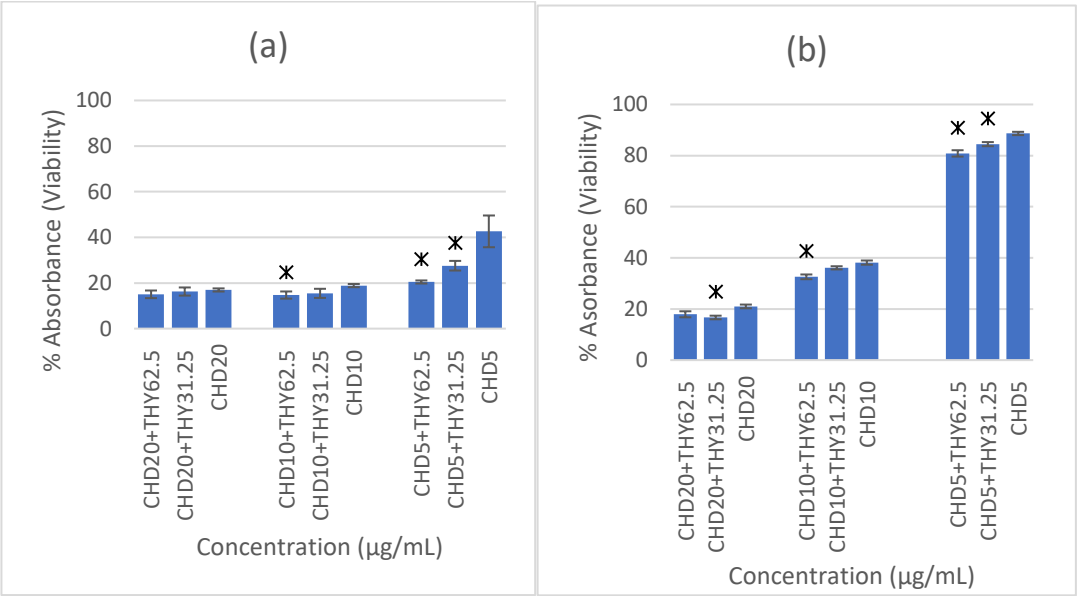

Figure 2.19 Effect of the combinations of Chlorhexidine and thymol on C. albicans biofilm (a) 4-h and (b) 24-h for two hours treatment at 37°C using NR uptake assay. Data are expressed as mean percentage ± SE, n = 12, p>0.05.
**Asterisks represent values significantly different from thymol alone of the same concentration*

2.3 Discussion

The effects of CHD on both planktonic and biofilm cells are of equal importance. Although the pathogenicity of *C. albicans* is mainly attributed to biofilm formation, the first stage of its initiation starts with the surface adhesion of yeast cells; the

final stage of a developed biofilm is the dispersal stage where yeast cells are liberated from the biofilm to invade new sites (Gulati and Nobile, 2016).

The MIC of CHD were 1.25 and 2.5 µg/mL and MBC 2.5 and 5 µg/mL for NCYC 854and ATCC 10231 strains, respectively. This finding is comparable with a previous work, in which MIC and MBC values for thirty-two *C. albicans* species were found to be 3.125 and 6.25 µg/mL, respectively (Salim *et al*., 2013). Time-kill studies were performed to check the antimicrobial activity with respect to time, due to its importance for future formulations which are intended to be applied in the oral cavity for two hours. The antimicrobial effect of CHD was time and concentration dependent (Table 2.3 and Table 2.4), and at a concentration of 10 µg/mL, the fungicidal effect was achieved within 40-60 minutes for both strains. The fungicidal effect of the MBC was recorded at the 4th hour, and there was 1 log reduction in the growth of Candida after 2.5 hours (Figure *2.1*). Moreover, there was no change in cells viability for the first 30 minutes, i.e. the onset of action of CHD appeared after 30 minutes, which was attributed to its concentration and time-dependent activity (Bobichon and Bouchet, 1987).

The effect of CHD on *Candida* biofilm was concentration-dependent when using XTT, CV and NR assays. A 100% loss of the mitochondrial activity (XTT assay) was found at a concentration of ≥10 and ≥40 µg/mL for 4-hr and 24-h biofilms, respectively (Figure *2.4*). The result of the 4-h biofilm was comparative to the time kill assay for planktonic cells (Table 2.3), all cells were killed after one hour at a concentration of 10 µg/mL. Surpriµy, the 24-h biofilm finding is equivalent to the MBC of CHD in the presence of farnesol against planktonic cells, and there is no evidence that farnesol release by the biofilm had a direct effect on CHD activity.

Bobichon and Bouchet (1987) reported that *C. albicans* exposure to 1 µg/mL of CHD gluconate (MIC for the chosen strain) resulted in mitochondrial swelling after only 2 hours. In the current work, there was a complete loss of the mitochondrial activity at a concentration of ≥10 and ≥ 40 µg/mL, and the residual biomass for the same concentrations was around 30% and 45% for 4-h and 24-h biofilms, respectively. It therefore appears that because CHD damaged the cells or even made them detached from the biofilm, there were cells residues or stressed cells that can interact with CV staining. This is accompanied by a substantial loss in the vacuolar activity leaving 4-h biofilm with 10% and 24-h with around 24% activity. Accordingly, the *C. albicans* cells suffer a complete loss of metabolic activity, a significant loss of pH gradient and to a lesser extent, a reduction in biomass. The microscopical images are shown in Figure 2.9 and Figure 2.13 are in agreement with the colourimetric assays, that visually it shows the intensity of colour decreasing with increasing the concentration.

Moreover, based on these analyses, there is no evidence whether the loss is permanent or temporary, so NR, CV assay and viable count were used to assess the damage by leaving the treated cells to grow for another 24 hours. Using viable count, almost 100% fungicidal activity was recorded at 160 µg/mL, the viability increased with decreasing the concentration (Figure 2.17) and all concentration above the MIC (2.5 µg/mL) of planktonic cells showed a reduction in the viability. Furthermore, by comparing XTT, CV and NR, XTT has a better comparison to viable count than CV and NR assays. Although XTT results were lower than the viable count, this might be attributed to the sensitivity of colourimetric absorbance assay.

Previous investigations (Chandra *et al*., 2001) were performed using CHD against planktonic cells and biofilm of *C. albicans.* It was found that the resistance of *C. albicans* biofilm of pathogenic strains increased towards different antifungals compared to planktonic cells including CHD, the MIC increased from 16 to 256 µg/mL for ~4-h and 72-h biofilms, respectively. The increase in resistance might be due to the extracellular material, genetic or biochemical changes in the cells (Chandra *et al*., 2001). Furthermore, Chlorhexidine might be more effective against planktonic cells than biofilm due to the uniform concentration of the drug in the medium in the former. In the latter, there would be a concentration gradient for both extrinsic and intrinsic material, attributable to the uneven thickness and cell density in the biofilm (Suci and Tylor, 2002).

The MIC of thymol was identical to a previous study (Braga *et al*., 2007a) and it is equal to 125 µg/mL against *C. albicans* ATCC 10231, and the MBC was 250 µg/mL. Although both polymers are mucoadhesive, HPMC did not affect the MBC of thymol, while P407 increased it to ≥250 µg/mL and the effect was concentration-dependent and that might be explained by its surfactant activity. Rhee *et al*. (2006) found there is an interaction between P407 and thymol by changing the gelling temperature and thermal behaviour of P407 by thymol. Moreover, it was found that the effect of thymol against *Salmonella typhimurium* was counteracted by the non-ionic surfactant Tween 80, and this effect increased with the increase in Tween concentration. The authors assumed that by the addition of the surfactant, thymol became more soluble in the aqueous medium leading to decrease its solubility in the cell membrane of the microorganism (Juven *et al*., 1994). Thymol fungicidal activity at the MBC was only found at 24

hours (Table 2.5). Moreover, time-kill studies showed continuous loss of cell viability from 30 minutes leading to a 1 log reduction in viable cells, by 2.5 hours (Figure *2.2*) indicating a slow rate of kill.

Similar to CHD, the effect of thymol on Candida biofilm was investigated using XTT, CV and NR assay. The XTT results were inconsistent, at 24-h biofilm and 250 µg/mL, the mitochondrial activity was 120% (Figure 2.6). This can be explained by the reducing activity of thymol (Ozen *et al*., 2011) which gave false positive results by increasing the reduction of XTT by thymol itself and masks the real mitochondrial activity of live cells. The effects of thymol on the biomass and vacuolar activity were concentration dependent, and the effectiveness of the thymol decreased with the increase in maturity of the biofilm. The maximum effect on the biomass was with 250 µg/mL leaving the biofilm with a biomass of 29% and 63% for 4-h and 24-h, respectively (Figure 2.10). Lower thymol concentrations led to a lower reduction of biomass. Furthermore, the effect upon the vacuolar activity at 250 µg/mL left the remaining biofilm with 10% and 47% vacuolar activity for 4-h and 24-h biofilm, respectively (Figure 2.14). Braga *et al*., (2007b) found that thymol interacted with *C. albicans* and changed the morphology of the cell envelop and the permeability and fluidity of the cell wall.

Thymol was previously investigated by Braga *et al*., (2008) against *C.albicans.* ATCC 3153A and ATCC MYA 2876 biofilm grown for 24 hours and treated with different concentrations of thymol for 6,12 and 24 hours at concentrations of 250 to15 µg/mL. The effect was measured using XTT assay and the results were concentration and time-dependent, and at 250 µg/mL, there was ~40% reduction in the mitochondrial activity. Another investigation showed 80% inhibition of *C.*

albicans biofilm after 24 hours treatment with 0.06% of thymol (Dalleau *et al*., 2008).

The reducing activity of thymol was measured by Deng *et al*., (2016) using Ferric reducing antioxidant potential, its effect on the XTT assay cannot be exempted, especially after the viability of 24-h biofilm treated with 250 µg/mL showed 129% of metabolic activity and based on the CV and NR assay the activity was 68% and 47%, respectively.

From the results, it can be confirmed that CHD has more potent *anti-Candida* activity than thymol. Other research work compared the activity of chlorhexidine gluconate and thymol mouthwashes, also found that CHD was more potent than thymol mouthwash against planktonic cells and biofilms of *C. albicans* clinical isolates (Shrestha *et al*., 2011 and Ramage *et al*., 2011).

The effect of the polymers on the activity of CHD and thymol was variable between XTT, CV and NR assays. No distinctive effect of both HPMC and P407 on CHD activity was observed with the XTT assay. Using CV assay, HPMC increased the effect of CHD on the 4-h biofilm at concentrations <10 µg/mL (Figure 2.8-a). Generally, using NR assay, HPMC decreased the activity of CHD (Figure 2.12). However, P407 did not show a clear effect on CHD activity. By comparing the three methods the effect was not consistent and it can be assumed that none of the polymers has a direct effect on the activity of CHD.

On the other hand, HPMC decreased the activity of thymol at 250 µg/mL and neutral red assay this effect diminished at lower concentrations (Figure 2.14). This effect was dictated neither on planktonic cells nor using CV analysis and it was noticed with CHD-HPMC and NR assay, the mucoadhesive nature of HPMC

might have resulted in the inconsistency of the results. P407 had no effect on thymol assessed by CV assay which might be attributed to the measurement of both dead and live cells. However, it decreased thymol activity, assessed by NR assay at 250 µg/mL thymol for 4-h and 24-h biofilm, similar to planktonic cells. Accordingly, there is no effect of HPMC on thymol activity while P407 at high concentration decreased the activity of thymol.

Farnesol inhibited the filamentation of *C. albicans* (Figure 2.3). The effect of farnesol was previously investigated by other researchers who found complete inhibition of filamentation at 300 µM (Ramage *et al*., 2002). The *anti-Candidal* activity of CHD and thymol was decreased in the presence of farnesol. Shirtliff *et al*., (2009) studied the effect of farnesol on *C. albicans* and they found that farnesol at a concentration of 200 µM causes upregulation of proteins involved in oxidative stress, protein folding and protection against the environment. This might explain the decreased activity of CHD and thymol, which have their direct effect on the cell wall. The effect of farnesol on the MIC of amphotericin B, fluconazole, itraconazole and caspofungin was studied, and it was found that there is a synergistic effect between the tested antifungals and farnesol with FIC < 0.5 (Cordeiro *et al*., 2013). The authors also found that the potentiation was more with azoles, which was attributed to the involvement of both compounds in sterol pathway of *Candida* and they assumed the activity increased due to the accumulation of intermediate toxic metabolites. A similar investigation was performed by Katragkou *et al*., (2015), by studying the combined effect of farnesol with micafungin, fluconazole or amphotericin B on *C. albicans* biofilm.

Amphotericin B showed no interaction while both micafungin and fluconazole showed a synergistic effect with an FIC value of 0.49 and 0.5, respectively.

CHD-thymol combination showed a decrease in the MIC of the planktonic cells, although no MBC reduction was registered, the MIC for the combination was 1.25 µg/mL CHD and 31.25 µg/mL thymol. The combined effect was more influential at lower concentrations of CHD and thymol (Figure 2.18 and Figure 2.19).

Previous researchers investigated chlorhexidine–thymol combinations against different microorganisms. They found that it was more effective against biofilms of *Streptococcus mutans and Lactobacillus plantarum* than their planktonic cells, and *S. mutans* biofilm was more sensitive toward the combination (Filoche *et al*, 2005).

2.4 Conclusion

Chlorhexidine showed a promising effect at a low concentration compared to thymol, with MIC and MBC against planktonic cells of 2.5 and 5 µg/mL for CHD and 125 and 250 µg/mL for thymol, both drugs showed concentration dependant antifungal effect. Farnesol is not a suitable candidate to be added to the formulation due to its negative effect on the activity of the drugs, it increased the MBC of CHD and Thymol. The effect of CHD on the 24-h mature biofilm was more than 50% reduction at concentrations of ≥20 µg/mL, however, thymol at the highest concentration of 250 µg/mL was around 50%. P407 and HPMC did not have a negative impact on the activity of CHD while on thymol the antagonistic effect of p407 was only at high concentration. Combination of CHD and thymol did not show any synergistic effect. To select the proper formulation further

investigations on human cells, need to be conducted for CHD, thymol and the combination.

Chapter Three

Cytotoxic effect of CHD and Thymol on HEK293 cell line

Chapter 3 : Cytotoxic effect of CHD and Thymol on HEK293 cell line

In this chapter, the cytotoxicity of CHD and thymol will be examined both individually and in combination together with any potentiating effects of HPMC and P407. Accordingly, the effective concentration will be considered in the buccal tablet. In the previous chapter, an additive effect of the drugs against *C. albicans* biofilm was not observed, however, the addition of thymol was as an attempt to overcome the oxidative stress produced by CHD. To our knowledge, the cytotoxic effect of CHD-thymol in combination has not been investigated to date.

3.1 Materials and Methods

3.1.1 Preparations of HEK293 cells cultures

HEK293 cells (Human embryonic kidney cells) were used to test *in vitro* cytotoxicity of CHD, thymol, HPMC and P407.

3.1.1.1 Reagents and medium preparation

Preparation of DMEM (Dulbecco's modified Eagle's medium):

Dulbecco's Modified Eagle's Medium - high glucose powder (DMEM), Foetal Bovine Serum (FBS), L-Glutamine solution (200 mM), Antibiotic-Antimycotic Solution (10,000 U penicillin, 10 mg streptomycin and 25 µg amphotericin B per mL), Sodium bicarbonate (Sigma Aldrich, UK)

DMEM was prepared as instructed by the manufacturer, the powdered medium was dissolved in 900 mL of RNase, DNase free sterile ultrapure water, then 3.7

g of sodium bicarbonate was added and the pH was adjusted to 7.4 with 1 M HCl, followed by completing the volume to one litre. To prepare DMEM complete, 50 mL of FBS, 5mL of L-Glutamine solution and 5 mL of Antibiotic antimycotic solution were added to 500mL of DMEM then it was filter sterilised and stored at 4°C.

Gelatine solution: Gelatine (Sigma Aldrich, UK) was prepared at a concentration of 0.1% in ultrapure water, autoclaved and stored at 4°C.

Sorensen's glycine buffer: Glycine and sodium chloride (Sigma Aldrich, UK) were prepared at a concentration of 0.1 M and the pH was adjusted to 10.5 using 5 M NaOH.

Phosphate buffered saline (PBS) pH 7.2-7.6: was prepared by diluting PBS 10x (Sigma Aldrich, UK) to 1x with ultrapure water (RNase and DNase free)

3.1.1.2 HEK293 cells culture

Tissue culture flask (T75) was coated with 5 mL of 0.1% gelatine solution and incubated for 10-15 minutes, then gelatine was aspirated followed by the addition of 10 mL of DMEM complete. HEK293 cells were recovered from liquid nitrogen storage (-180 °C), defrosted in a water bath. Cells were added to the flask and incubated to subconfluency at 37°C in a humidified 5% CO2 incubator. Cells subculture was performed by aspirating the medium, washing the cells with 10 mL of PBS, followed by cells detachment with the aid of 2 mL of 0.25% trypsin-EDTA (Sigma-Aldrich, UK) which left for 3-4 minutes. Cells detachment can be seen visually, then 6 mL of DMEM complete was added to deactivate trypsin-EDTA. Then cells were ready for subculturing, cytotoxicity study and freezing.

HEK293 cells for cryopreservation

Trypsinized cells were centrifuged at 1650 g for 3 minutes, the medium was discarded, and the pellets were resuspended in 0.95 mL FBS and 0.05 mL DMSO and transferred to cryovials. The vials were stored for 5-6 hours at -80°C and then transferred to -180°C.

3.1.2 Cytotoxicity studies

Cytotoxicity studies were performed to test the effect of the drugs on human cells. The effect of the polymers on HEK293 cells were tested individually and with CHD or thymol. The treatment was performed for two hours which is the time that intended to apply the tablet in the oral cavity. Cells were treated first with the tested solutions followed by measuring the cytotoxicity using MTT, NR uptake and SRB assays.

Determination of cell seeding density (calibration curve)

Seeding density was investigated to choose the proper number of the cells to be seeded in each well for the cytotoxicity assay. Trypsinized Hek293 cells were counted using haemocytometer, then serially diluted in DMEM complete and transferred to 96 well plate at a cell number range from 2.0×10^5 to 781 cells/well and incubated for 24 hours. MTT assay was performed to find the optimum number of cells.

Cell treatment for cytotoxicity studies

Based on the result of the calibration curve, 4.0 x 10^4 cells were placed in each well of the 96 well microtiter plate, the latter was incubated for 24 hours at 37°C and humidified 5% CO_2. The cytotoxic effect of CHD, CHD-HPMC and CHD-P407 was studied at 5:1 polymer to CHD ratio. Concentrations of 160 µg/mL of CHD in DMEM alone or with the polymer were serially double diluted in the same medium. For thymol, thymol-P407 and thymol-HPMC, a concentration of 250 µg/mL of thymol in DMEM were serially double diluted. The ratio of polymers to thymol was 5:1 similar to CHD. The medium of overnight cells culture was replaced with the serial dilution of the investigated drug solutions and incubated for two hours. The latter were aspirated, and cell viability was dictated using MTT, NR uptake and SRB assays.

3.1.2.1 MTT assay

MTT reduction assay was used to measure the metabolic activity of human cells. It is a water-soluble salt and converted to insoluble formazan by the cleavage of the tetrazolium ring by succinate dehydrogenase within the mitochondria. Formazan is impermeable through the cell membrane. Consequently, it accumulates inside the metabolically active cells (Fotakis and Timbrell, 2006).

MTT stock solution: MTT 3-(4,5-Dimethyl-2-thiazolyl)-2,5-diphenyl-2H-tetrazolium bromide (Sigma Aldrich, UK) was dissolved in PBS at a concentration of 5 mg/mL and stored at 4°C in the dark.

MTT working solution was prepared freshly prior the addition to the cells, by diluting the stock solution in DMEM complete to a concentration of 0.5 mg/mL, then 100 µL was added to each well and incubated for two hours. The medium

was aspirated, and formazan salt was dissolved using 80 µL of dimethyl sulfoxide (Alfa Aesar, UK) and 20 µL of glycine buffer, and the absorbance was measured at λ_{540nm}. The viability was calculated as a percentage of the absorbance of treated cells to untreated cells. DMSO was added to dissolve formazan and glycine buffer to shift the pH to 10.5, at this pH formazan gives one peak, however at pH 7, it gives two peaks at λ_{500} and λ_{570} which underestimates the amount of formazan (Plumb, 2004).

3.1.2.2 Neutral red uptake (NR) assay

As mentioned in chapter three, Neutral red is a weekly basic dye, it penetrates cells by diffusion and accumulates in the lysosomes due to its low pH compared to the cytoplasm. In healthy or live cells, pH gradient was maintained, upon cells death, lysosomes will not be able to retain the dye (Repetto *et al*., 2008). NR stock solution was prepared using RNase, DNase free sterile ultrapure water at a concentration of 4 mg/mL and stored in the dark for 1-2 months at room temperature. A working solution was prepared freshly in DMEM complete at a concentration of 80 µg/mL, incubated at 37°C for 24 hours, then filtered through a 0.45 µm filter to remove precipitated dye crystals. Aliquots of 100 µL were added to each well, and the plate was incubated for two hours. NR was removed, washed with 150 µL PBS, followed by fixation with 100 µL of 5% glutaraldehyde for 2 minutes. After removing the fixative solution, 150 µL of de-stain solution (50% absolute ethanol, 48% ultrapure water and 2% glacial acetic acid) was added to each well, and the plate left for 30 minutes on an orbital shaker to extract NR from cells. The optical density was measured at λ_{540nm}, and the cytotoxicity was measured as a percentage of untreated cells.

Imaging of HEK293 cells

Microscopical images were used to study the morphological changes in the treated cells. Each well of the 6 well plate was seeded with $2.0X10^5$ / 2mL and incubated for 24 hours. For CHD 2mL of 160, 80, 40, 20, 10 µg/mL were tested. For thymol 250 and 125 µg/mL with and without P407 and a negative control.
Cell imaging was performed after staining with NR and SRB using a phase contrast microscope (Nikon Eclipse TS100, UK). The Images of SRB stained cells were further investigated using fluorescence microscopy (EVOS FL, UK).

3.1.2.3 Sulforhodamine B (SRB) assay

SRB is a water-soluble dye, used to measure the cellular density based on cellular protein content. Under acidic condition it binds to the basic amino acid residue in proteins (Skehan *et al*., 1990), it is used to measure both dead and live cells, the method was adopted from Vichai and Kirtikara (2006). SRB (Alfa-easer, UK) stock solution was prepared at a concentration of 0.057% in 1% acetic acid. Treated cells with CHD and thymol solutions were fixed with 100 µL of cold 10% TCA (Trichloroacetic acid, Sigma Aldrich, UK) and stored for 1 hour at 4°C. TCA was removed under a low stream of running tap water and the plate was left to dry at room temperature. SRB (100 µL) solution was added to each well and left at room temperature for 30 minutes, then the dye was removed, and the microtiter was washed quickly with 1% acetic acid to remove the excess dye. SRB was extracted with 200 µL of 10 mM Tris base solution (Sigma-Aldrich, UK), pH of 10.5, the absorbance was measured at $\lambda_{540nm.}$ The viability was calculated as the percentage of the absorbance of treated to untreated cells.

3.1.2.4 Statistical Analysis

Tow-way ANOVA (analysis of variance) was obtained using Microsoft Excel to test the significant difference between the tested compounds.

3.2 Results

3.2.1 Determination of cell seeding density

The calibration curve was performed to choose the proper number of cells for cytotoxicity studies. As presented in Figure 3.1 there is a linear relationship between the number of cells and the absorbance using MTT assay up to cell density of 10^5. Therefore, to perform the cytotoxicity assay, $4.0x10^4$ was chosen as a seeding density with a relative absorbance of ~0.7.

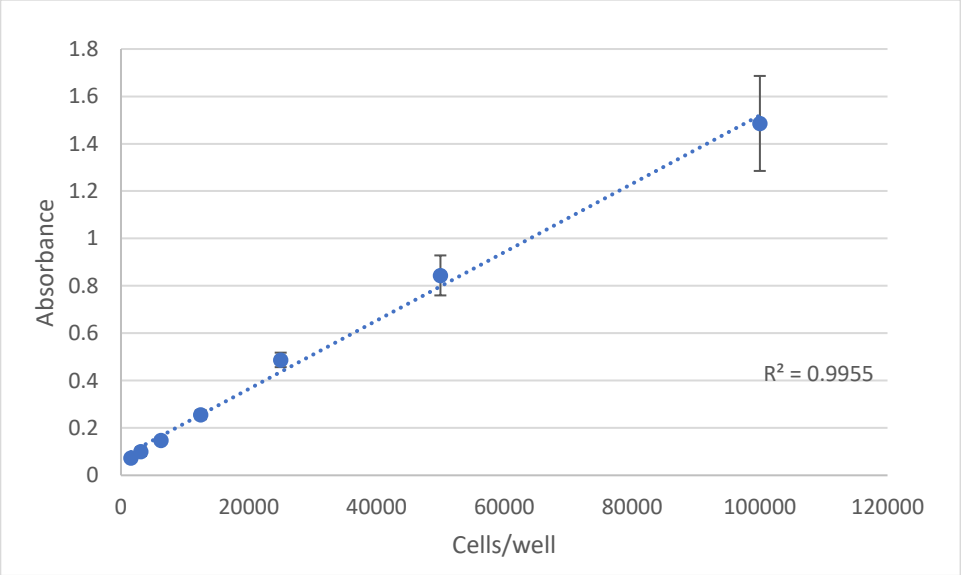

Figure 3.1 Absorbance of different numbers of HEK293 cells grown for 24 hours using MTT assay. Data are expressed as mean absorbances ± SD, n = 18.

3.2.2 Cytotoxicity assay

3.2.2.1 MTT assay

MTT reduction assay was used to measure the oxidative stress of human cells and consequently the cytotoxic effect of the drugs on HEK293 cells. The cytotoxic effect of CHD, HPMC, P407, CHD-HPMC and CHD-P407 were tested at a concentration range from 160 to 1.25 µg/mL of CHD. The absorbance of the dissolved formazan was recorded, and the mitochondrial activity was calculated as a percentage of the average absorbances of treated to untreated cells, the results were displayed in Figure 3.2.

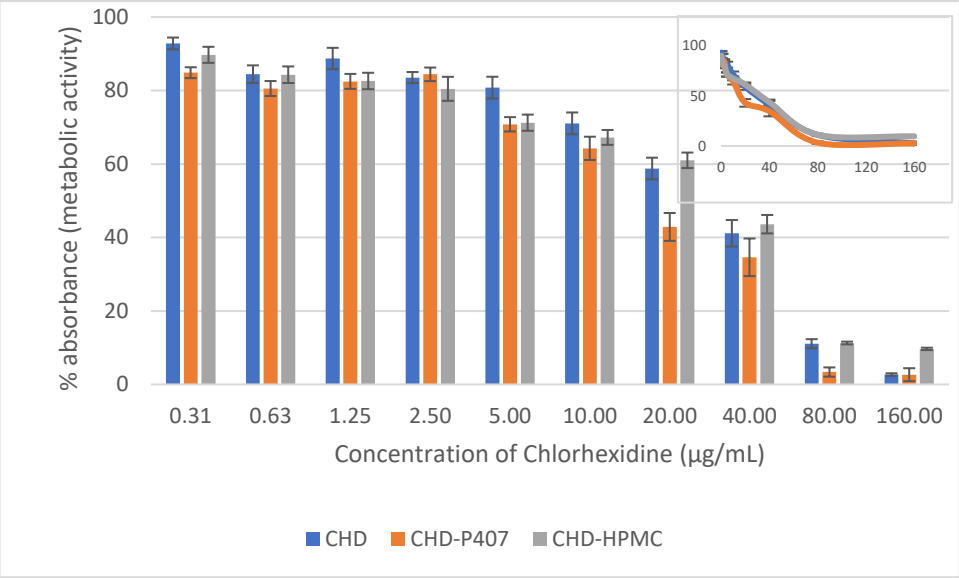

Figure 3.2 The effect of two hours exposure to different concentrations of CHD, on the viability of HEK293 cells measured using an MTT assay. Data are expressed as mean percentage ± SE, n = 34.

The effect of HPMC and P407 were tested individually, at a concentration range from 1.25 to 0.02 mg/mL. Both polymers had no effects on cell viability.

The inhibitory effect of CHD on the mitochondrial activity of HEK293 cells (Figure *3.2*) was increased progressively with the increase in CHD concentration and

becoming more pronounced at CHD concentrations of P407 at ≥ 20 µg/mL. Here, cytotoxic effect was greater than an equivalent concentration of CHD and CHD HPMC.

Similarly, MTT assay was tested for thymol, thymol-P407 and thymol-HPMC at a concentration range from 250 to 0.49 µg/mL of thymol. Figure *3.3*, shows a considerable inhibitory effect of thymol on HEK293 cells at a concentration of ≥ 125 µg/mL. At 250 µg/mL, both thymol and thymol-HPMC had an almost complete inhibitory effect. However, P407 showed an intensive protective effect against thymol, resulted in maintaining the viability to around 46% and 83% at concentrations of 250 and 125 µg/mL, respectively.

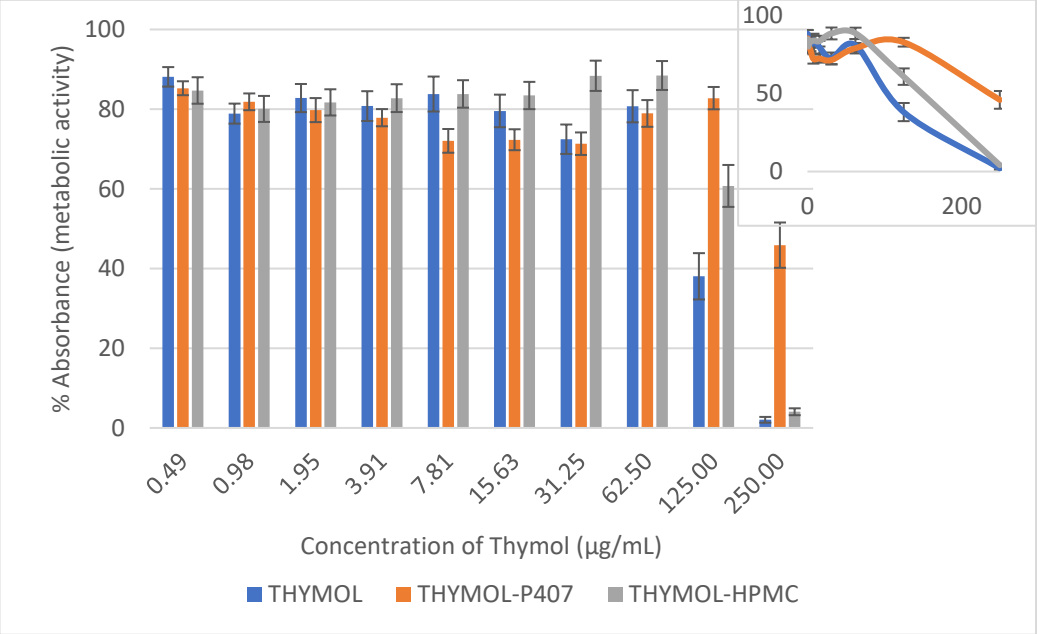

Figure 3.3 The effect of two hours exposure to different concentrations of thymol, on the viability of HEK293 cells measured using an MTT assay. Data are expressed as mean percentage ± SE, *n = 34.*

3.2.2.2 Neutral red uptake (NR) assay

NR assay was used to measure the lysosomal activity of human cells and consequently, it estimates the cytotoxic effect of the drugs.

The cytotoxic effect of CHD, HPMC, P407, CHD-HPMC and CHD-P407 were tested at a concentration range from 1.25 to 160 µg/mL of CHD. After staining with NR and de-staining, the absorbance of the de-stain solution was measured, and the results were displayed in Figure 3.4. The retained lysosomal activity was ~20% at 80 and 160 µg/mL and 85% at 40 µg/mL.

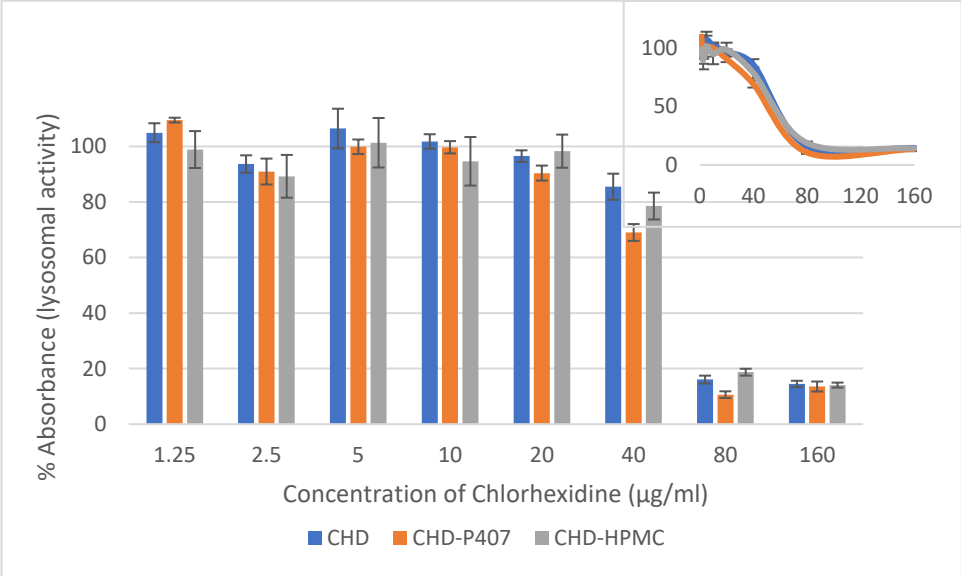

Figure 3.4 The effect of two hours exposure to different concentrations of CHD, on the viability of HEK293 cells measured using an NR uptake assay. Data are expressed as mean percentage ± SE, *n = 9.*

For further investigation, images were obtained for cells treated with a concentration range from 10 to 160 µg/mL and the positive control. Visually, at 160 µg/m no NR stain detected in the cells and at 80 µg/mL, few cells were stained compared to the lower concentrations (Figure 2.13).

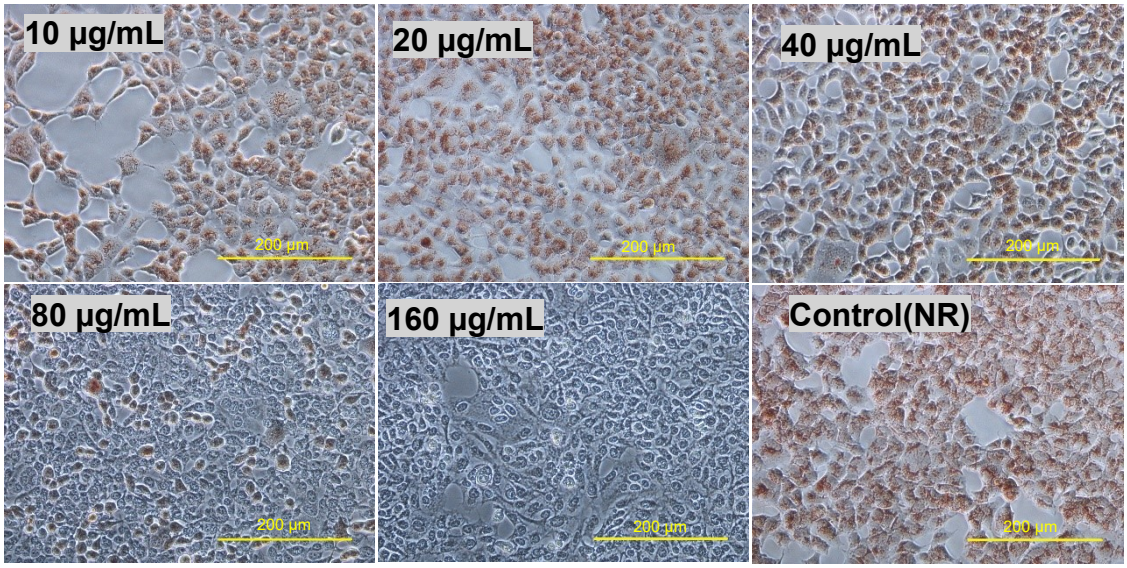

Figure 3.5 Images of HEK293 cells treated with CHD and stained and with NR, x200.

Images of living untreated and treated HEK293 cells with 160 µg/mL of CHD were examined under the microscope to investigate the morphological changes. Treated cells show chromatin condensation and cell shrinkage (Figure *3.6*).

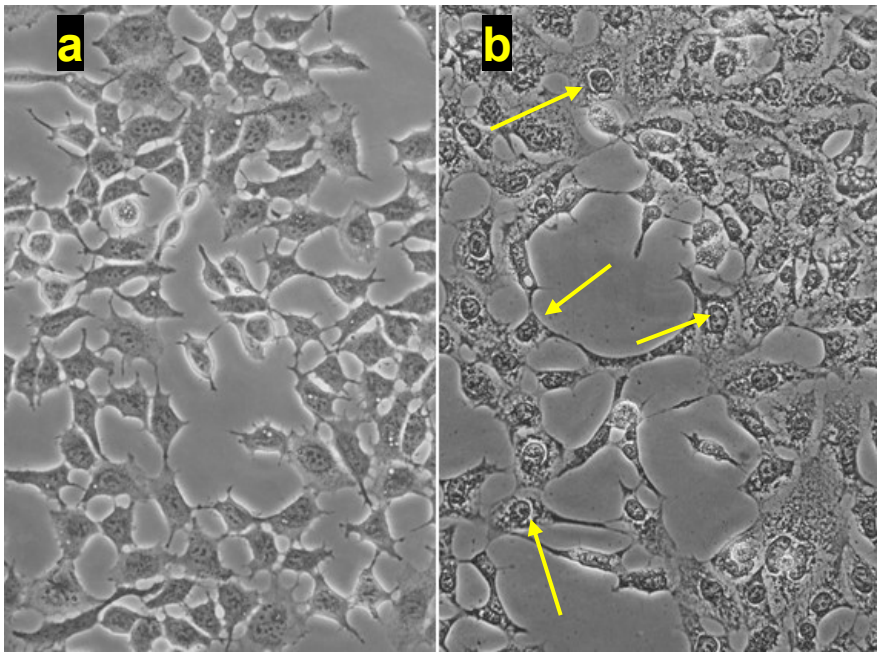

Figure 3.6 microscopical images of live HEK293 a) non-treated and b) treated with 160 µg/mL CHD (x200), (arrows showing chromatin condensation).

NR assay results for thymol, thymol-P407 and thymol-HPMC are presented in Figure *3.7*, at a concentration range from 1.95 to 250 µg/mL of thymol. Thymol and thymol-HPMC showed nearly 100% loss of lysosomal activity, however, thymol-P407 preserved 25% of the activity. Furthermore, both polymers thymol combinations have nearly double the activity compared to thymol alone at a concentration of 125 µg/mL.

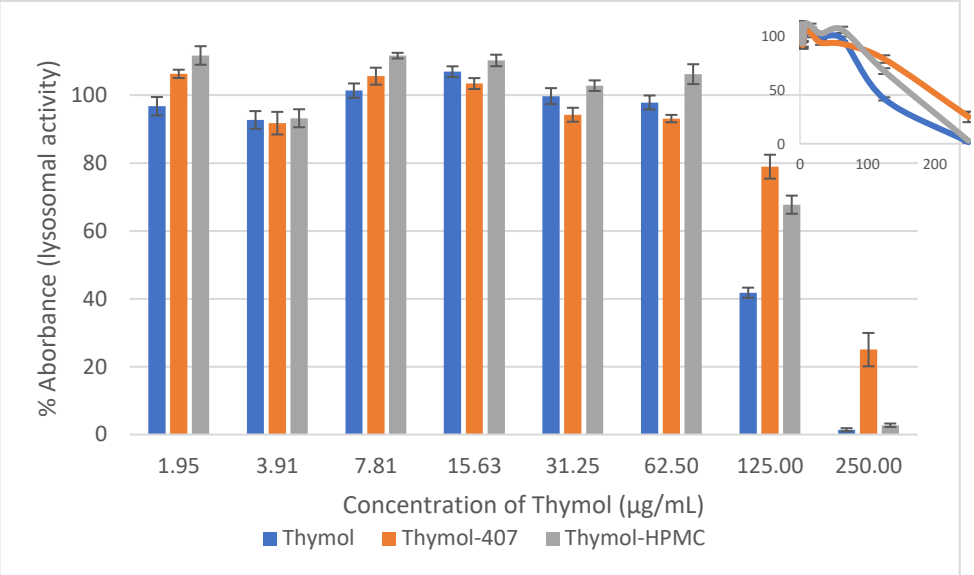

Figure 3.7 The effect of two hours exposure to different concentrations of Thymol, on the viability of HEK293 cells measured using an NR uptake assay. Data are expressed as mean percentage ± SE, *n = 6.*

Microscopical images were obtained for cells treated with 125 and 250 µg/mL of thymol and thymol-P407. At 125 µg/mL images do not show a significant difference between thymol and thymol-P407. However, at 250 µg/mL, no cells are shown in the image due to their detachment after the treatment with thymol and staining with NR (Figure 3.8). On the other hand, cells treated with thymol-P407 are visualised in the well. Although by comparing it to the positive control image, it shows vacuolizations of the cytoplasm (Figure 3.9).

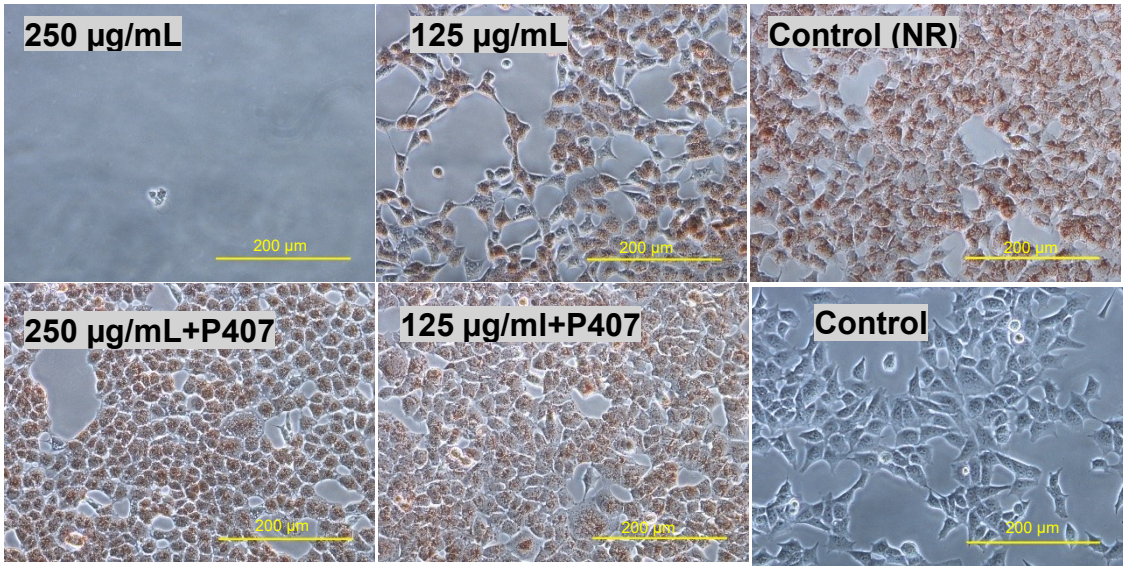

Figure 3.8 Images of HEK293 cells treated with thymol and thymol-P407 and stained and with NR, (x200).

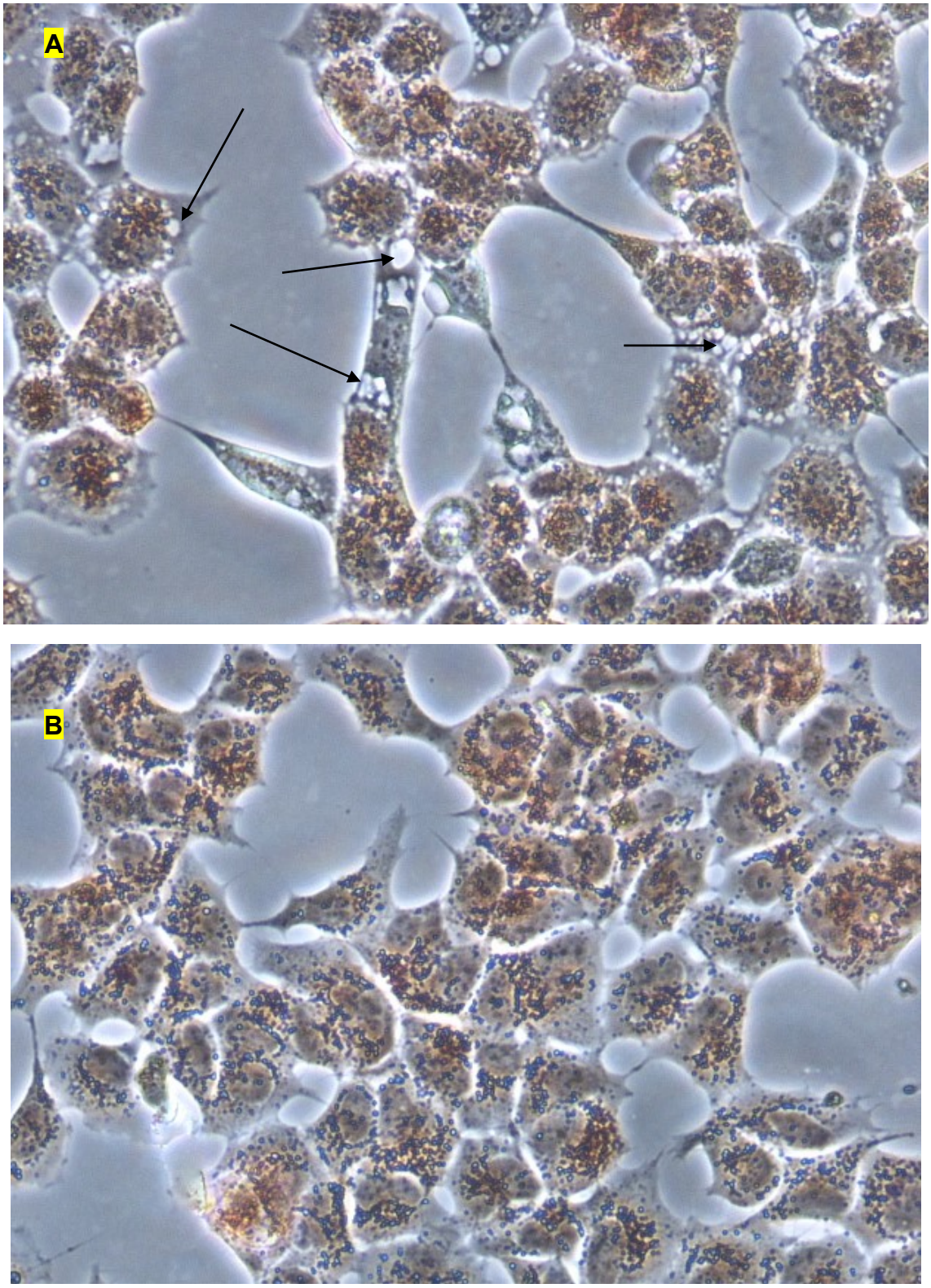

Figure 3.9 Images of HEK293 (A)cells treated with thymol-P407 250 µg/mL (B) HEK293 control and stained with NR (x200), (arrows showing vacuolization)

3.2.2.3 Sulforhodamine B (SRB) assay

SRB assay was used to measure cells density based on the protein content of dead and live cells, this method is used to measure the degree of cytotoxicity. Solutions of CHD, CHD-HPMC and CHD-P407 were tested at a concentration range from 1.25 to 160 µg/mL of CHD. After staining the cells with SRB, the absorbance of the extracted stain was measured, and the results are displayed in Figure 3.10. There was a 40% loss in cellular density at a concentration of 80 and 160 µg/mL, the polymers showed no clear effect on the activity of CHD. The microscopical images show an agreement with the absorbance% of the extracted stain, visually the density of the colour for cells treated at 80 and 160 µg/mL was less intense than the control and cells treated at lower concentrations (Figure 3.11).

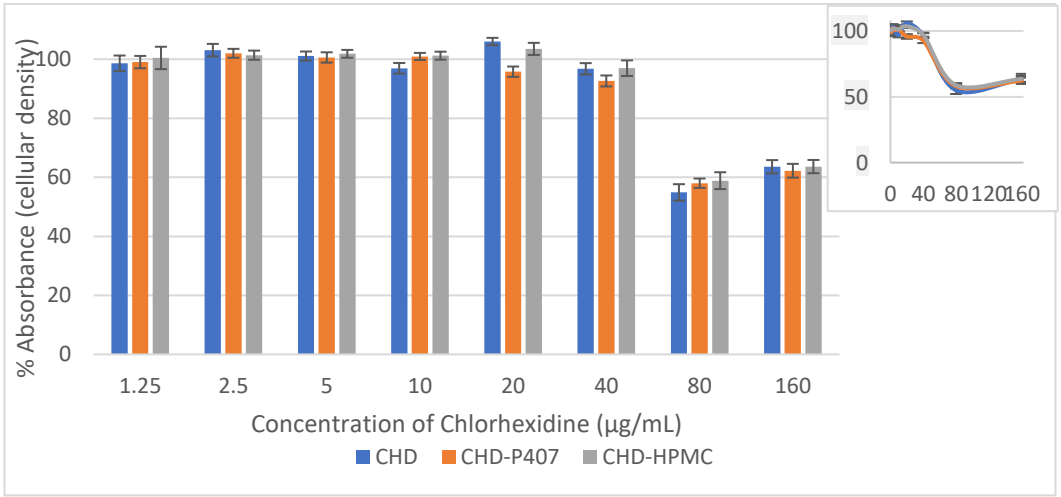

Figure 3.10 The effect of two hours exposure to different concentrations of CHD on the viability of HEK293 cells measured using an SRB assay. Data are expressed as mean percentage ± SE, (*n = 9).*

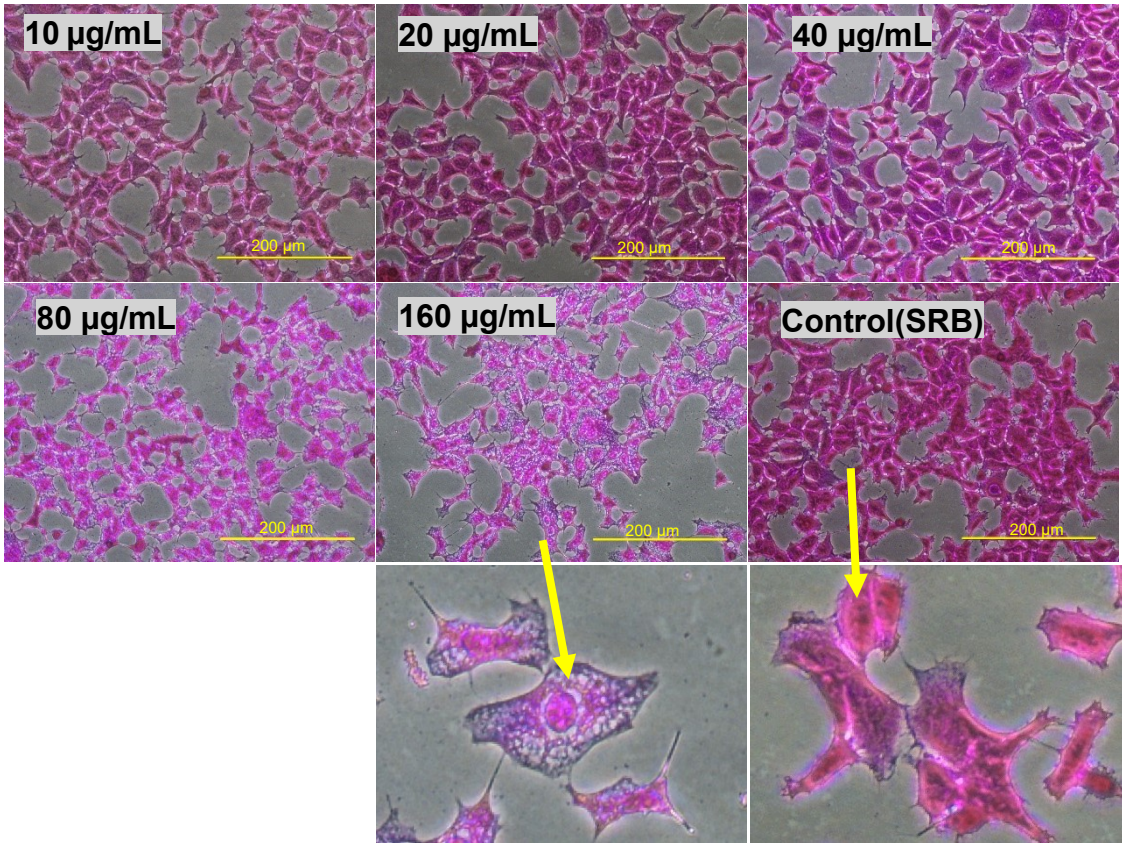

Figure 3.11 microscopical images of HEK293 cells treated with different concentrations of CHD for two hours at 37°C and stained with SRB. (x200), (arrows showing the difference between chromatin condensation in a treated cell and normal cell).

The same cells were examined using fluorescence microscopy, the results confirmed the previous finding shown in Figure *3.6*. HEK293 cells attaining were homogenous due to the interaction of SRB to the cellular proteins, while cells treated with 160 µg/mL showed chromatin condensation, cell shrinkage, and vacuolization resulted in the loss of proteins and consequently cell membrane damage (Figure 3.12). This effect was seen to a lesser extent at 80 µg/mL, no morphological changes were noticed for lower concentrations (results not shown).

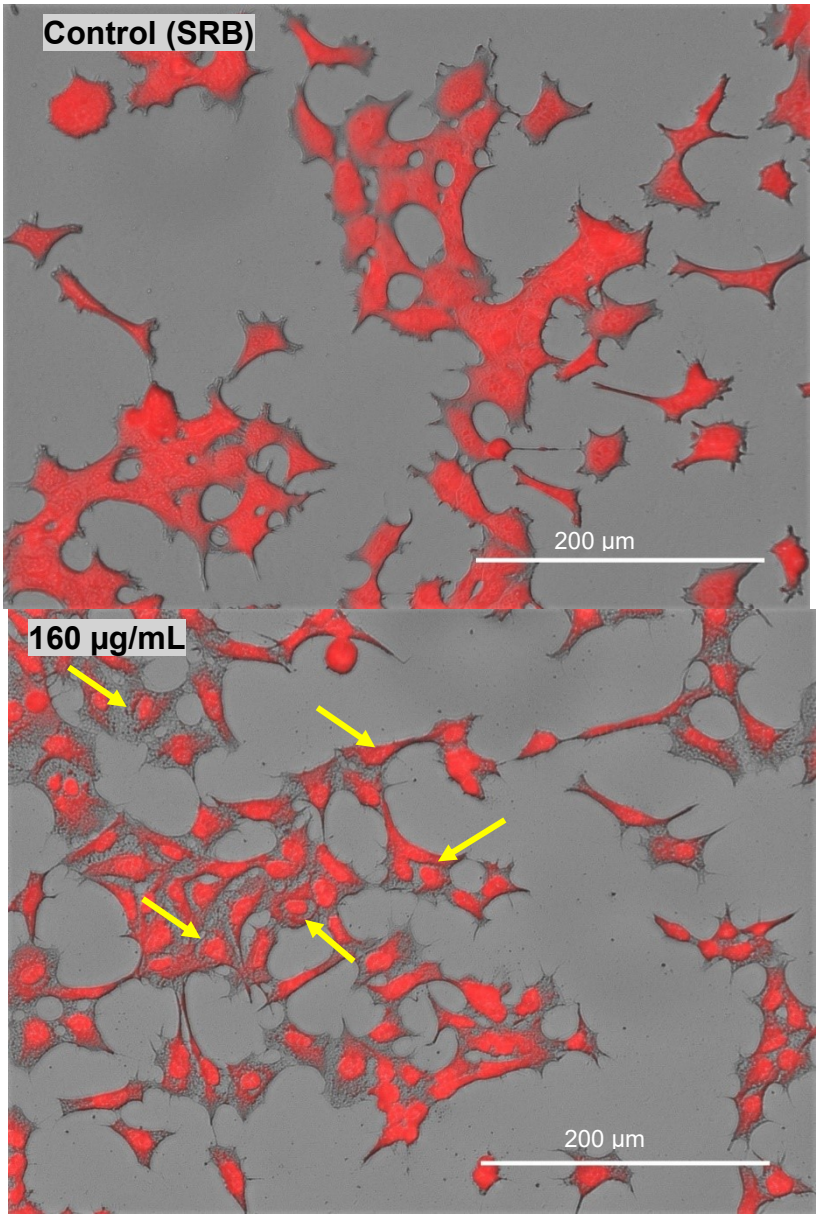

Figure 3.12 Fluorescence microscopy images for HEK293 a) non-treated and b) Treated with CHD 160 µg/mL and stained with SRB stain, (x400), (arrows showing chromatin condensation).

SRB assay was performed to detect the effect of thymol, thymol-P407 and thymol-HPMC at a concentration range from 1.95 to 250 µg/mL of thymol. The effect of thymol on the cells was obvious at 250 µg/mL, however, P407 protected the cells from the effect of thymol, this result agreed with the NR assay (Figure *3.13*).

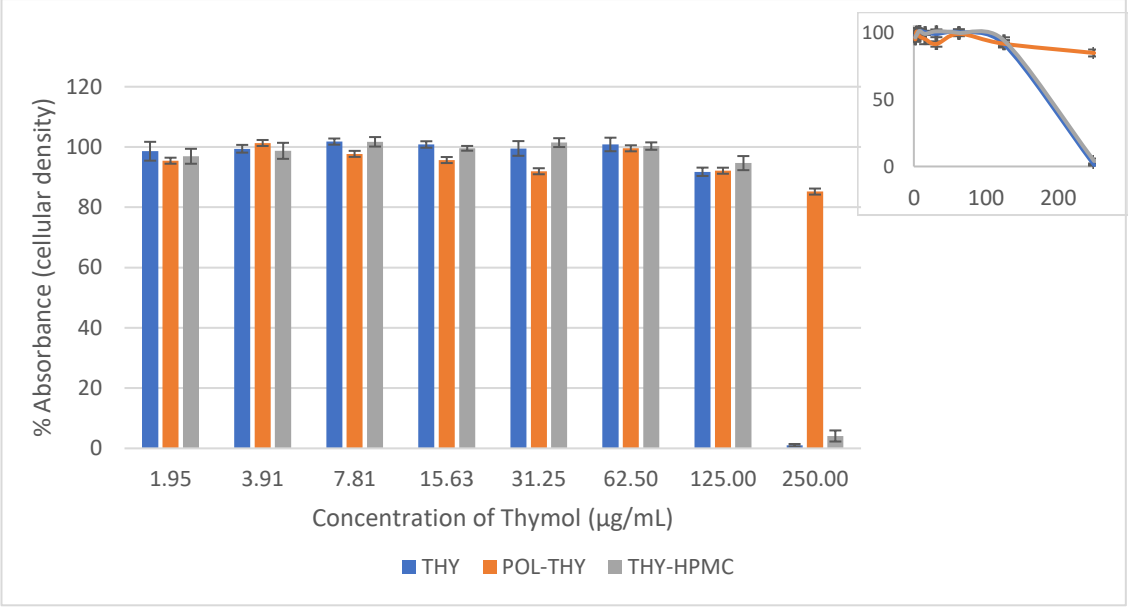

Figure 3.13 The effect of two hours exposure to different concentrations of Thymol, on the viability of HEK293 cells measured using an SRB assay. Data are expressed as mean percentage ± SE, *n = 9.*

Figure 3.14 shows the microscopical images of the cells treated with Thymol and thymol-P407 at 125 and 250 µg/mL, no morphological changes were detected between different treatments accept the loss of the cells treated with 250 µg/mL of thymol.

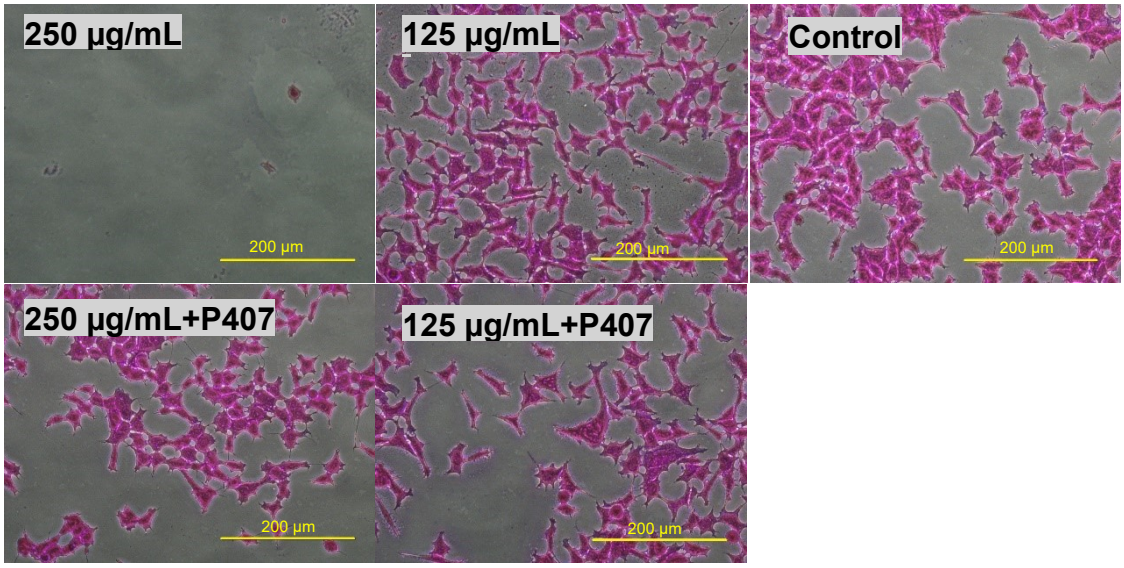

Figure 3.14 microscopical images of HEK293 cells treated with Thymol and Thymol-P407 at a concentration of 125 and 250 µg/mL for two hours at 37°C and stained with SRB (200x).

3.2.3 Cytotoxic effect of CHD and Thymol on HEK293

The combined effect of CHD and thymol were investigated at concentrations of 5, 10 and 20 µg/mL for CHD with 31.25 and 62.5 µg/mL of thymol. The tested concentrations were chosen based on the cytotoxicity studies and the feasibility of incorporation into the buccal tablet. The effect was investigated using NR uptake and SRB assays.

NR uptake assay

The lysosomal activity of the cells was affected more by the combined drugs and the effect was concentration-dependent. For instance, CHD 20 µg/mL with thymol 31.25 µg/mL has decreased the activity to 67% compared to 94% for CHD alone (Figure 3.15). One-way ANOVA results show that CHD has a significant difference when combined with thymol at 62.5 µg/mL, and at CHD 10 µg/mL with thymol at 31.25 µg/mL, this effect resulted in an increase in the cytotoxic effect of CHD in the presence of thymol.

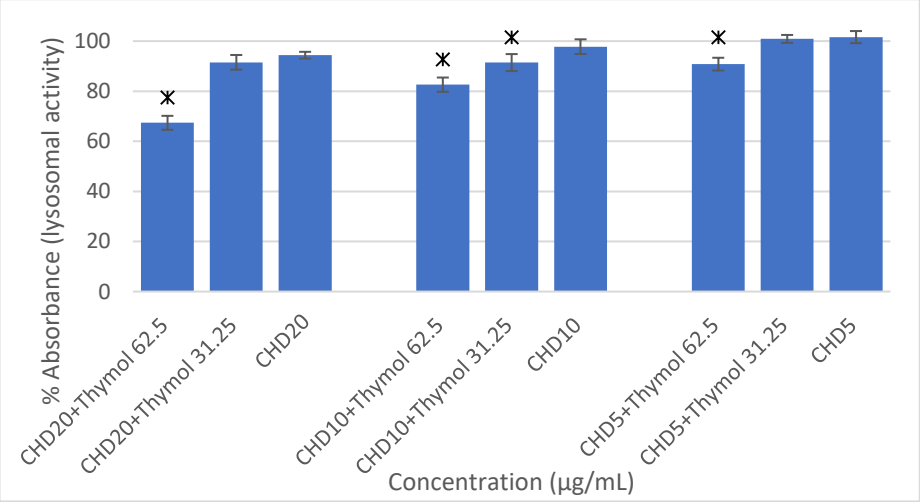

Figure 3.15 The effect of two hours exposure to selected concentrations of CHD and Thymol, on the viability of HEK293 cells measured using an NR uptake assay. Data are expressed as mean percentage ± SE, *n = 12.*
**Asterisks represent values significantly different (p<0.05) from CHD alone of the same concentration.*

SRB assay

The same combinations of thymol and CHD were tested using SRB assay. A similar effect was noticed with a less decrease in cellular density compared to the lysosomal activity (Figure 3.16) statistically, the results are identical with the NR assay results.

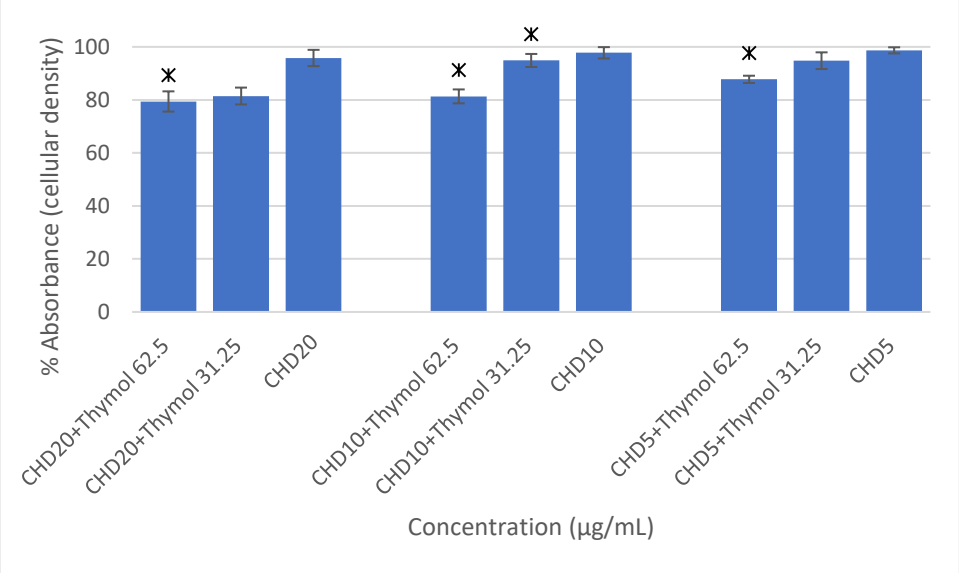

Figure 3.16 The effect of two hours exposure to selected concentrations of CHD and Thymol, on the viability of HEK293 cells measured using an SRB assay. Data are expressed as mean percentage ± SE, *n = 12.*
**Asterisks represent values significantly different (p<0.05) from thymol alone of the same concentration.*

3.3 Discussion

Different methods were used to inspect the cytotoxic effect of CHD and thymol. Based on the MTT assay, the exposure of HEK293 cells to different concentrations of CHD resulted in dose-dependent mitochondrial inhibitory effect. Treating the cells at a concentration of 160 µg/mL left the cells with 2.6% mitochondrial activity this was increased to 92.8% at 0.315 µg/mL. The effect aggravated by the addition of P407 at a concentration of ≥20 µg/mL, which might

be attributed to the surfactant activity of P407, led to increased cellular penetration of CHD and consequently, its toxicity (Figure 3.2).

In a previous work on human fibroblast cells, which were exposed to different concentrations of CHD for three hours and analysed using XTT assay, 100% suppression was found for concentrations of ≥ 0.005% which is equivalent to 50 µg/mL (Hidalgo and Dominguez, 2001). Another investigation was performed on odontoblast cell line MDPC-23 and treated with 0.02%, 0.004% and 0.0024 CHD, the effect was analysed using MTT assay, the results showed a concentration-dependent inhibitory effect. The loss of viability for 0.04% (= 40µg/mL) was 29.9%. Moreover, the morphology of the cells for 0.004% and 0.0024 was similar to the control. However, cells treated with 0.02% CHD showed a change in the morphology to a round shape (Souza *et al*., 2007). In this work at a concentration of 40 µg/mL showed around 60% loss in the viability of cells.

By comparing the current results to *C. albicans* antibiofilm results in chapter 2, using XTT assay, *C. albicans* showed more sensitivity toward CHD than HEK293. CHD showed nearly 100% suppression of the metabolic activity on the biofilm at a concentration of ≥ 40µg/mL.

Whereas, the cytotoxicity of thymol was pronounced at 125 and 250 µg/mL, and it was greatly antagonised by P407 (Figure 3.3). Although, there was no effect against neuronal cells as reported by García *et al*., (2006). They investigated the effect of thymol at a concentration of 150 µg/mL on neuronal cells for 30 minutes and 24 hours and MTT assay, no effect on the mitochondrial activity was recorded. However, Türkez and Aydın (2013) studied the effect on human blood cells at a concentration range from 0 to 200 µg/mL for 24 hours and using MTT

assay, the finding was a reduction in the viability to around 60% at concentrations of 150 and 200 µg/mL.

To further investigate the effect of CHD and thymol on HEK 293 cells, NR assay was used to test its effect on the lysosomal activity. Although the effect of CHD at a concentration of ≥80µg/mL was comparable to the result obtained by the MTT assay, the cytotoxicity was much less at lower concentrations. For instance, at 40µg/mL the viability was 40% using MTT and 85% using NR assay (Figure 3.2 and Figure 3.4). Images obtained for cells stained with NR confirm the colourimetric results and the morphological changes were represented by cell shrinkage and chromatin condensation (Figure *3.6*).

Cells treated with 125 and 250 µg/mL of thymol and tested using NR showed a high agreement with MTT result with nearly 100% suppression of activity at 250 µg/mL and around 40% remaining of activity at 125 µg/mL and P407 showed a similar protective behaviour with less viability (Figure 3.7). This observation confirms a previous finding, in which P407 decreased the toxicity of tramadol by approximately 2-fold when tested using MTT and NR uptake assays (dos Santos, *et al*., 2015). In the current work, the micrographs (Figure 3.8) of cells treated with 250 µg/mL of thymol show the disappearance of the cells resulted from their detachment by thymol, which might be explained by anoikis (Kroemer *et al*., 2009). Using the same concentration of thymol combined with P407 led to protecting the cells from detaching and this might be attributed to the mucoadhesive properties of P407, preventing the cells from detachment. It seems that P407 protect the cells from detaching, but not from vacuolization (Figure 3.9). The latter agreed with a previous work performed by Llana-Ruiz-

Cabello *et al*. (2014), Caco-2 cells were treated with 37.5 µg/mL of thymol for 48 hours, cells showed vacuolization, which is one of the features related to apoptosis. In the same work cell detachment was shown with carvacrol but not thymol and this attributed to the lower concentration of thymol investigated in the work. Both carvacrol and thymol have the same chemical formula $C_{10}H_{14}O$ and they found in the oil of thyme.

Another research group found that the effect of thymol was antagonised by the non-ionic surfactant Tween 80, and this effect increased with the increase in Tween concentration. The assumption was, by the addition of the surfactant, both proteins and thymol became more hydrophilic, this resulted in decrease the degree of binding between them. Moreover, the addition of bovine serum albumin showed a similar effect (Juven *et al*., 1994). Dušan *et al*., (2006) tested the cytotoxicity of thymol against Caco-2 cells and based on the morphology, cells treated with 120 µg/mL led to cell necrosis at ~10 and 15% after 1 and 24 hours treatment respectively, with less than 1% of apoptosis.

However, based on the morphology, no sign of necrosis was seen, and apoptosis is the mechanism of cell death based on anoikis and vacuolization, and this effect is concentration dependent and it was found at 250 µg/mL and for two hours exposure.

Protein mass was investigated using SRB assay, cells exposed to CHD at 80 and 160 µg/mL preserved a 60% of total protein after treatment, lower concentrations have no effect on the protein mass based on SRB assay (Figure 3.10). Microscopical images (Figure 3.11 and Figure 3.12) show chromatin condensation and confirm the previous images (Figure *3.6*). Regarding thymol

treated cells the major loss in proteins was found with cells treated with thymol and thymol-HPMC at a concentration of 250 µg/mL and this attributed to their detachment. CHD produces metabolic stress which might be overcome by the antioxidant activity of thymol, the combination of CHD and thymol were tested as an attempt to minimise the cytotoxic effect of CHD. However, CHD and thymol combination showed an increase in the cytotoxicity of CHD and that effect was higher with increasing concentrations of thymol.

3.4 Conclusion

CHD is toxic toward HEK293 cells within a concentration range 80 and 160 µg/mL, while thymol at 250 µg/mL for two hours exposure with a decrease in cellular density reflecting irreversible cellular damage. However, at lower concentrations there were effects on the mitochondrial and lysosomal activity with no changes in the microscopical morphology. The cytotoxicity of CHD and thymol at the highest concentrations might lead to apoptosis through the mitochondrial pathway, further investigations need to be performed to investigate the mechanism of cell death.

Furthermore, there is no advantage to design a tablet with CHD and thymol, due to the increase in the toxicity of the drug combination. Moreover, the anti-candidal activity of these combinations has neither a synergistic nor an additive effect. Generally, polymers showed no negative impact on the cytotoxicity of CHD and thymol, although, there was a clear protection activity of P407 against thymol cytotoxicity. Based on the results achieved in this chapter and on *C. albicans* planktonic and biofilms, it is recommended to prepare the tablets with CHD only. Dosage adjustment will be performed to control the release of the drug at a

concentration of 20 μg/mL for two hours. This concentration has an effective (and therefore possibly therapeutic) anti-candidal activity and low cytotoxicity.

Chapter Four

Tablet Design, Formulation and Analysis

Chapter 4 : Tablet Design, Formulation and Analysis

The aim of this investigation was to develop and evaluate mucoadhesive buccal tablets based on hydroxypropyl methylcellulose (HPMC) and Poloxamer 407 (P407) for the controlled release of CHD over two hours. HPMC is widely investigated for the preparation of controlled release hydrophilic matrices, due to its water solubility, ease of manufacturing, low cost, not affected by the pH and nontoxic (Ghori and Conway, 2015). In the current chapter is an attempt to control the release for two hours which might not achieve by HPMC, accordingly, P407 was added to increase the hydrophilicity and maintaining the hydrogel network structure. P407 forms a three-dimensional network structure at a concentration >20% at 25°C (Ruel-Gariepy and Leroux, 2004).

Two different sources of HPMC were investigated to assess whether there were any physicochemical differences between the polymers that could affect drug release individually and also in the presence of P407.

4.1 Materials and method

Tablet formulations were prepared using CHD, P407, HPMC and HPMC-S, as previously investigated in chapters 2 and 3.

4.1.1 Characterization of raw materials

4.1.1.1 Solubility of CHD

CHD solubility was investigated to find a suitable solubilising and dissolution medium. The solubility of CHD was determined by adding excess CHD to 3 mL

of water or phosphate buffer saline (PBS) solution at pH 6.8. The samples were shaken at 37 ± 0.1 °C for 24 hours. The suspensions were filtered through a 0.45µm Millipore membrane filter (Merck Millipore Ltd, Ireland), the filtrates diluted, and CHD concentration determined at λ_{254} nm (Biochrom WPA Biowave II UV- Spectrophotometry, UK) in triplicate. The concentration of CHD was obtained from the calibration curve of pre-prepared standard solutions of CHD.

4.1.1.2 Particle size analysis

Particle size distribution of CHD, HPMC, HPMC-S, P407 and Magnesium stearate (MgSt) was assessed by laser diffraction using a Malvern Mastersizer 3000 with Aero S dry dispersion unit system (Malvern Instruments, Malvern, U.K.). Cumulative particle sizes at 10, 50 and 90 % were displayed as $D_{0.1}$, $D_{0.5}$ and $D_{0.9,}$ respectively. The particle size distribution (span) was calculated using Equation 1.

$$Span = \frac{D_{0.9} - D_{0.1}}{D_{0.5}} \qquad \textit{Equation 1}$$

4.1.1.3 Morphology of the ingredients of the tablets

Scanning electron microscopy (SEM) images were obtained for a small amount of the samples, which were mounted onto standard pin stubs using a double-sided adhesive tape and then loaded on a universal specimen holder, followed by gold sputter coating of each sample under low vacuum (Zeiss Evo® 50EP SEM, Germany).

4.1.2 Formulations and characterisation of the tablets

Three different groups of formulations with CHD were prepared based upon different drug to polymer (CHD to HPMC-S) ratios; different HPMC-S to P407 and HPMC to P407 ratios.

4.1.2.1 Tablet formulations

Formulations of CHD mucoadhesive tablets were formulated as shown in Table 4.1. The powders were blended for 5 minutes in a V-shaped powder blender (CapsulCN®).

Table 4.1 Formulations of CHD mucoadhesive buccal tablets.

Formulations	Weight (mg)/tablet				
	CHD	HPMC-S	HPMC	P407	Tablet Weight
F1	5	25 mg	-	-	30
F2		45 mg	-	-	50
F3		65 mg	-	-	65
F4		85 mg	-	-	90
F5		23.5	-	1.5	30
F6		20.5	-	4.5	30
F7		17.5	-	7.5	30
F8		14.5	-	10.5	30
F9		11.5	-	13.5	30
F10		6.25	-	18.75	30
F11		-	25	-	30
F12		-	20.5	4.5	30
F13		-	17.5	7.5	30
F14		-	11.5	13.5	30
F15		-	6.25	18.75	30

4.1.2.2 Dry granulation

Dry granules were prepared using the slugging method (Tuğcu-Demiröz *et al.,* 2004) which involved formulations being manually pressed to form slugs

(diameter = 4 cm, weight = 5.5 ± 0.5 g) using a manual hydraulic hand press. Slugs prepared using HPMC-S and HPMC were formed with 1 and 4 tons compression force, respectively. The slugs were granulated using a Sinopham, YK60 Mini Lab Rotary Granulator (China) in which granules were passed through 1 mm screen (mesh no. 18). The granules were collected and characterised similar to powder blends. MgSt was added prior to compression of the granules into tablets.

4.1.2.3 Powder Flow properties and compressibility

Powder and granule bulk and tapped volumes were assessed using a Tapped Density tester (Varian, U.K.). Tapped volumes were obtained by subjecting the powders to 200 taps each time until a constant volume was achieved. Carr's (compressibility) index (CI) and Hausner ratio (HR) were calculated using Equation 2 Equation 3:

$$Carr's\ Index = \left(1 - \frac{V_t}{V_0}\right) \qquad \textit{Equation 2}$$

$$Hausner\ ratio = \frac{V_0}{V_t} \qquad \textit{Equation 3}$$

Where V_0 is bulk volume and V_t is the tapped volume.

4.1.2.4 Preparation of CHD buccal tablets

Dry granules (10 ± 2 g) and 0.5% (w/w) of MgSt were blended for 3 minutes using a mini V-shaped powder Mixer (CapsulCN, China). Tablets were pressed using a ZPS heavy duty mini rotary tablet machine (Shanghai, China) at 8.6 RPM speed

of compression and tablets with a biconvex 6 mm diameter round shape punch, the setting of the tablet press was thickness of 0.3 mm and weight of approximately 30 mg (F1, F5-15), which resulted in compression force of 1-2 KN. F2, F3 and F4 were pressed using the same punch, tablet weight 50, 70 and 90 mg respectively, with the same compression force of 1-2 KN.

4.1.2.5 Friability

A sample of approximately 1 g of each formulation was placed in the drum of the friability tester (Charles Ischi AG, AE-1, U.K.), and rotated 100 times at 25 rpm. The tablets were dedusted, reweighed and percentage weight lost calculated according to Equation 4.

$$Friability = \frac{W_i - W_f}{W_i} \times 100 \qquad \textit{Equation 4}$$

Where W_i is the initial weight and W_f is the final weight.

4.1.2.6 Tensile strength

The mechanical strength of the biconvex tablet is calculated based on Equation 5 (Pitt *et al*., 1988).

$$\sigma_x = \frac{10\,F}{\pi D^2}\left[\frac{2.84H}{D} - \frac{0.126H}{W} + \frac{3.15W}{D} + 0.01\right]^{-1} \qquad \textit{Equation 5}$$

Where σ_x is the tensile strength, *F* is tablet hardness (Newtons), *D* is tablet diameter, *H* is tablet thickness, and *W* is central cylinder thickness (tablet wall height), with all tablet dimensions in mm.

Tablet hardness was measured using a Varian VK 200 (U.K.) hardness tester (*n* = 10).

4.1.2.7 Content Uniformity and mass variation

To maintain the consistency of the formulations within the acceptable level, the content uniformity and mass variation were investigated.

Mass Variation

Mass variation was measured to evaluate the consistency of the weight of the prepared tablets. For the investigated tablets, the weight of 20 tablets of each formulation was measured; acceptance criteria of ± 10% of average tablet weight were determined. Not more than two tablets should deviate with more than 10% and one tablet with more than 20%. Although, for the investigated formulations this test is not a mandatory requirement according to the BP due to a drug content of <25% (BP, 2018 a).

Content uniformity

According to the BP, content uniformity is mandatory for tablet dosage forms with active ingredients <25% (BP, 2018 a). The content was analysed by taking 10 tablets, each was dissolved individually in 100 mL of distilled water, the concentration was calculated from the absorbance at $\lambda_{245.}$ The formulation is considered a fail if more than one tablet deviates from the range of 85-115% or if one tablet deviates from the range of 75-125% of the average content.

4.1.2.8 *Ex Vivo* Mucoadhesion

Mucoadhesion was measured to estimate the adherence of the tablets in the oral cavity and was it measured by two means; duration and force of adhesion.

Duration of mucoadhesion

The mucoadhesion was determined as a function of dosage form residence time using a modified protocol adopted from Nafee *et al*. (2003). Freshly harvested chicken pouches were carefully washed to remove food residue and were subsequently stored at -80 °C. The pouches were defrosted before use, cut into small pieces (1 cm x 2 cm) and fixed to a glass slide using cyanoacrylate glue. The tissue was hydrated using one drop of ultrapure water before a CHD tablet was placed on top and weighed down with a 4 g weight for 20 seconds to aid the adhesion process. The glass slide was then placed into the disintegration apparatus tubes (Varian VK 100, U.K.), prefilled with 37 ± 0.2°C ultrapure water. The test was performed for 120 minutes at 50 rpm and samples examined every 15 minutes. Each tablet formulation was assessed in triplicate.

Force of detachment

The force of detachment was measured using the modified two-arm balance method adopted from Parodi, *et al*. (1996) with a slight modification of putting the sample inside a jacketed beaker to maintain the temperature at 37°C.

The tablet was fixed with cyanoacrylate glue to a disc and fixed on an inverted container hung on one side of the balance (Figure 4.1). It was then left to adhere

to the chicken pouch for 5 minutes, with the aid of a 4 g weight. The chicken pouch was previously fixed on a top of a container and placed in a jacketed beaker which was maintained at 37°C. On the other side of the balance, a small beaker was placed to collect the water received from a peristaltic pump at a rate of 1mL/min. Once the tablet had adhered to the chicken pouch the pump was switched on, the amount of the water in the beaker was increased until the tablet detached from the chicken tissue. The weight of the collected water was then measured.

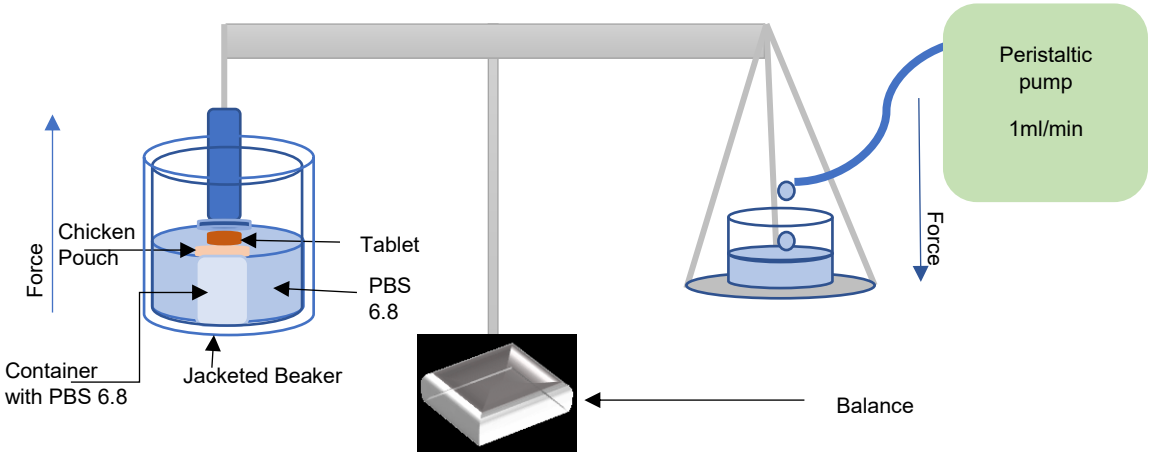

Figure 4.1 Diagram illustrating the measurement of the force of mucoadhesion.

4.1.2.9 Swelling Index

Swelling index was determined by weighing an individual CHD tablet (W_0) and sticking it to a previously weighed glass coverslip using a single water droplet and allowing it to equilibrate for 30 s. The coverslip was then placed vertically in a beaker in a 37 ± 0.2 °C water bath (Clifton, Nickel-Electro Ltd, UK). The weight of the swollen tablet (W_s) was recorded at 30, 60, 90 and 120 minutes. Swelling index (SI) was calculated using Equation 6 (Kassem *et al.*, 2014).

$$SI = \frac{W_s - W_0}{W_0}$$ *Equation 6*

4.1.2.10 Tablet morphology (SEM)

Tablet morphology was investigated for aqueous media swollen tablets. They were prepared by adding 0.5 mL distilled water to each tablet unit in a 5 mL test tube and left until it swollen, and then freeze-dried using Beta 1-8 LSC Freeze Dryer, (Christ, UK). Tablets were cut in half and analysed by SEM as previously described (4.1.1.3).

4.1.2.11 *In Vitro* Dissolution of CHD (Apparatus I)

The dissolution was performed in a BP Dissolution Apparatus type I basket method (BP, 2018 b) using Varian 705 DS (Varian, U.K.). One tablet of each formulation was placed in 500 mL Ultrapure distilled water at 37 ± 0.1 °C, with the basket rotating at 50 ± 1 rpm. At predetermined time intervals, 4 mL was withdrawn from the dissolution medium and replaced with the same volume of fresh media. CHD concentration was determined spectrophotometrically by measuring the UV- Absorbance at λ_{254} (Biochrom WPA Biowave II UV-Spectrophotometry, UK).

4.1.2.12 Similarity (f_2) and Difference (f_1) factors

Both factors Were investigated to check the similarity and the difference for drug release from the formulations of the same polymer ratios.

i. Similarity factor(f_2)

This analysis is applied to the dissolution profile of more than three-time points (except zero point) and not more than one value above 85% of the drug released. The difference at each time point should be less than 10%, and 12 individual value for each time point. The results of this analysis lie between 0-100%, and f_2 ≥ 50 suggests a similarity between the standard and the test (CPMP, 2000). Similarity factor is calculated by applying Equation 7.

$$f_2 = 50 \times log\left\{\left[1 + (1/n)\sum_{t=1}^{n}(R_t - T_t)^2\right]^{-0.5} \times 100\right\} \qquad \textit{Equation 7}$$

Where n is the number of time points, R_t is the per cent release of the standard and T_t is the per cent release of the test.
In the current work, we will apply f_2 on each 2 replicates of the triplicate.

ii. Difference factor (f_1)

Difference factor is defined as the cumulative difference between the two tested replicates (equation 3). Values between 0-15 indicate the difference between the samples is acceptable. When f_1 = 0, this means the two samples (n = 12) are identical.

$$f_1 = \left\{\left[\sum_{t=1}^{n}|R_t - T_t\right] / \left[\sum_{t=1}^{n} R_t\right]\right\} \times 100 \qquad \textit{Equation 8}$$

When applying Equation 8, and interchange the standard with the test, the values of f_1 will be changed (O'hara *et al*., 1998). To overcome this limitation, Equation 9 was used to test the difference between a pair of pharmaceutical products (Costa and Lobo, 2001).

$$f_1 = \left\{\left[\sum_{t=1}^{n} |R_t - T_t\right] / \left[\sum_{t=1}^{n} (R_t + T_t)/2\right]\right\} \times 100 \qquad \textit{Equation 9}$$

4.1.2.13 Kinetics of drug release

The kinetics of CHD release was investigated to further understand the mechanism of CHD release and the effect of the different ratios of the polymers. Five models (Costa and Lobo, 2000) were used to analyse the release of CHD from the tablet matrices, namely zero order (Equation 10), first order (Equation 11), Higuchi equation (Equation 12), Hixon-Crowell model (Equation 13) and Korsmeyer-Peppas equation (Equation 14) as follows:

$$Q = Q_0 - K_0 t \qquad \textit{Equation 10}$$

$$\log Q = Log Q_0 - \frac{K_1 t}{2.303} \qquad \textit{Equation 11}$$

$$Q_t = K_H t^{1/2} \qquad \textit{Equation 12}$$

$$Q^{1/3} = Q_0^{1/3} - K_c t \qquad \textit{Equation 13}$$

$$Q_t / Q_\infty = K t^n \qquad \textit{Equation 14}$$

Where Q is the amount of drug released or dissolved at time t; Q_0 is the amount of drug release or dissolved at time t (usually $t = 0$); Q_t/Q_∞ is the fraction of drug released at time t; K is constant, and n indicates the release mechanism.

4.1.2.14 Drug polymer interaction (FTIR and DSC)

Fourier Transform Infrared Spectroscopy (FTIR)

FTIR was used to investigate the possibility of interaction between the polymers and CHD. Spectra were obtained using a Bruker Alpha spectrometer (Germany) scanning from 4000-400 cm^{-1}.

Differential Scanning Calorimetry (DSC)

DSC analysis was performed to investigate the interaction between CHD and the polymers during the processing steps. Samples of 5.0 ± 0.2 mg of each CHD, HPMC, P407, F15 Physical mix, F15 granules and F15 tablet were investigated. Each was heated in an aluminium pan under a nitrogen flow of 40 mL/min from 25°C to 300°C at a scan rate of 10°C/min. The analysis was performed using DSC (Mettler Toledo DSC823e, Switzerland).

4.2 Results

4.2.1 Charectarisation of raw materials

The physical properties of the CHD, HPMC, HPMC-S and P407 were investigated to evaluate their impact on tablet preparation and characterisation.

4.2.1.1 Solubility of Chlorhexidine diacetate salt

CHD solubility was investigated to determine the dissolution medium to achieve sink condition. Its solubility in water and phosphate buffer saline (PBS) at pH 6.8 was 23.069 ± 1.928 and 0.047 ± 0.0124 mg/mL, respectively. The solubility in water agreed with the British Pharmacopoeia (BP, 2018 c), which classifies CHD solubility as “sparingly soluble” in water. However, it can be described as “practically insoluble” in PBS and based on the British Pharmacopeia the volume of the dissolution media should be 3-10 times of the saturated volume. Accordingly, PBS will not attain the sink condition.

4.2.1.2 Particle size analysis

All powders are classified as fine powders according to the British Pharmacopoeia with a different degree of fines (BP, 2018 d). Particle size and particle size distribution of CHD and the excipients are shown in Figure 4.2 and Table 4.2, CHD and MgSt show a bimodal particle size distribution with a span value of 3.04 and 3.15. Both HPMC and HPMC S showed bigger particle size.

Table 4.2 Particle size distribution of CHD, HPMC, HPMC-S, P407 and MgSt.

Raw material	D 0.1 (µm)	D 0.5 (µm)	D 0.9 (µm)	Span (µm)
CHD	5.14	21.00	69.00	3.04
HPMC S	33.00	84.60	172.00	1.64
HPMC	26.50	70.80	202.00	2.48
P 407	11.50	34.50	74.30	1.82
MgSt	1.17	6.27	20.90	3.15

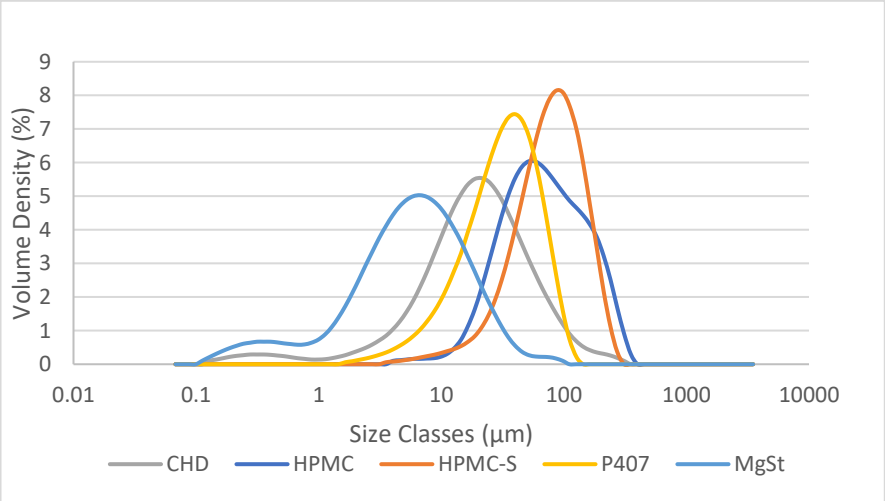

Figure 4.2 Particle size distribution of CHD, HPMC, HPMC-S, P407 and MgSt.

SEM analysis (Figure 4.3) confirmed the previous results, both CHD and P407 have smaller particle sizes and the latter tend to be more spherical, however,

HPMC and HPMC-S possess larger particle size with irregular and rod shape, respectively.

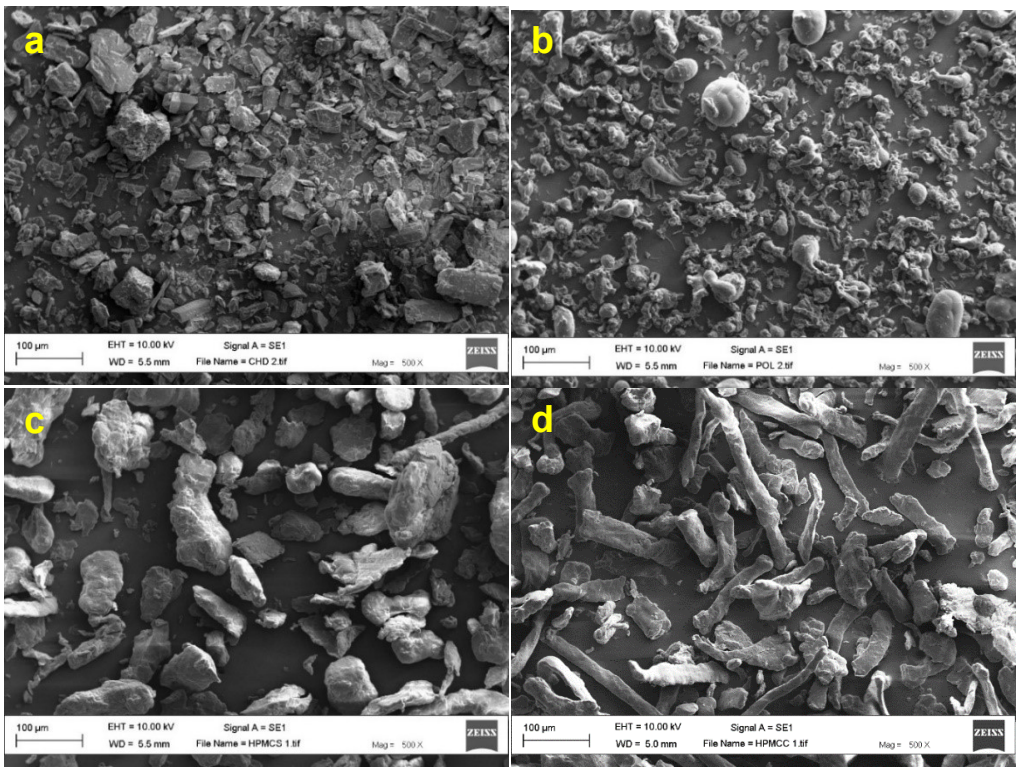

Figure 4.3 SEM images of (a) CHD (b) P407, (c) HPMC-S and (d) HPMC, x500

4.3.1 Characterisation of the tablets and tablet blends

The flowability of the various powder formulation blends was found 'very poor' and 'very, very poor' (Table 4.3). Dry granulation improved the flow properties of all formulation. Increasing the ratio of polymer to drug from 5:1 to 17:1 had no effect on the flow properties of the various granules, and P407 content of 25% or more improved the flowability to poor flowability with CI and HR, especially in HPMC formulations.

Table 4.3 Compressibility index (CI%) and Hausner ratio for tablet bend before and after granulation (descriptive terms are those used by BP).

Formulations	Powder Blends			Granules		
	CI%	Flow Character	HR	CI%	Flow Character	HR
F1	36.59 ± 4.00	Very poor	1.58 ± 0.10	29.41 ± 1.03	poor	1.42 ± 0.02
F2	35.00 ± 1.25	Very poor	1.54 ± 0.03	28.57 ± 0.25	poor	1.40 ± 0.01
F3	35.00 ± 0.81	Very poor	1.54 ± 0.02	21.43 ± 0.35	Passable	1.27 ± 0.01
F4	36.84 ± 1.50	Very poor	1.58 ± 0.04	25.00± 0.00	poor	1.33 ± 0.00
F5	35.71 ± 2.71	Very poor	1.56 ± 0.07	33.95 ± 1.67	Very poor (CI) | Poor (HR)	1.38 ± 0.07
F6	42.31 ± 1.61	Very, very poor	1.73 ± 0.05	32.38 ± 1.58	Very poor	1.50 ± 0.06
F7	42.86 ± 1.55	Very, very poor	1.75 ± 0.02	32.29 ± 1.47	Very poor	1.50 ± 0.03
F8	41.38 ± 1.50	Very, very poor	1.71 ± 0.02	25.93 ± 0.00	poor	1.36 ± 0.00
F9	31.43 ± 2.91	Very poor	1.46 ± 0.03	26.38 ± 0.00	poor	1.35 ± 0.00
F10	34.21 ± 3.62	Very poor	1.52 ± 0.05	27.92 ± 0.92	poor	1.43 ± 0.02
F11	43.74 ± 1.32	Very, very poor	1.78 ± 0.19	34.92 ± 1.37	Very poor	1.54 ± 0.03
F12	39.28 ± 2.24	Very, very poor	1.65 ± 0.11	34.85 ± 0.00	Very poor	1.53 ± 0.00
F13	41.36 ± 2.12	Very, very poor	1.69 ± 0.06	30.33 ± 3.21	poor	1.43 ± 0.07
F14	38.45± 4.43	Very, very poor	1.63 ± 0.06	27.50 ± 0.87	poor	1.38 ± 0.02
F15	42.36 ± 5.81	Very, very poor	1.75 ± 0.04	26.83 ± 0.76	poor	1.37 ± 0.01

407	0%	5%	15%	25%	35%	45%	62.5%
PMC-S	F1	F6	F6	F7	F8	F9	F15
PMC	F11	-	F12	F13	-	F14	F15

Figure 4.4 shows the morphology of the granules for selected HPMC and HPMC-S formulations with the same ratio of P407 (0%, 25%, 45% and 62.5% P407). Dry granulation showed a limited improvement of the flowability, this may be attributed to the generation of fine particles fraction (Herting and Kleinebudde, 2007).

P407	0%	5%	15%	25%	35%	45%	62.5%
HPMC-S	F1	F6	F6	F7	F8	F9	F15
HPMC	F11	-	F12	F13	-	F14	F15

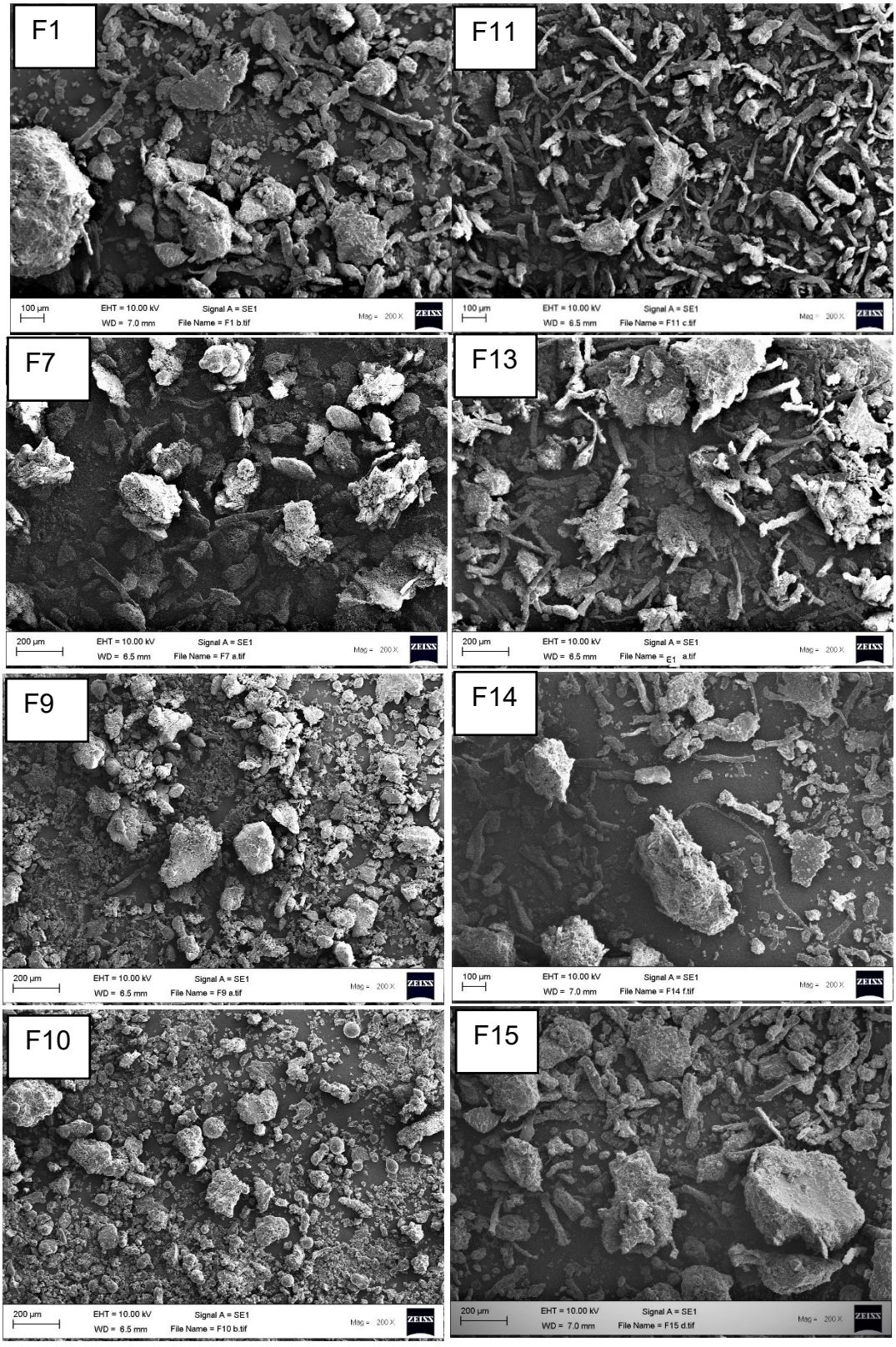

Figure 4.4 SEM images of selected tablet formulations of HPMC-S and HPMC, x200.

P407	0%	5%	15%	25%	35%	45%	62.5%
HPMC-S	F1	F6	F6	F7	F8	F9	F15
HPMC	F11	-	F12	F13	-	F14	F15

4.3.1.1 Physical properties of the tablets

The physical properties of the prepared tablet formulations are presented in Table 4.4. All the tablets showed tensile strength less than 1 MP, and HPMC formulations showed higher tensile strengths than HPMC-S formulations which might be due to the higher force used in the granulation for the former. All had acceptable levels of friability of less than 1%. Moreover, the resultant tablets showed acceptable weight variation 90-110%. Although F11 showed one tablet out of this range, it is still acceptable based on the BP (BP, 2108 a) the content uniformity was within the acceptable range 85-115% (Table 4.4).

In conclusion, all the tablet formulations exhibited acceptable physical characteristics for further study.

P407	0%	5%	15%	25%	35%	45%	62.5%
HPMC-S	F1	F6	F6	F7	F8	F9	F15
HPMC	F11	-	F12	F13	-	F14	F15

*Table 4.4 Physical characteristics of the tablets (n = 10), * n=20, ** Friability was performed with 1g of tablets.*

Formulations	Weight (mg)*	Min% and Max% tablet weight	Diameter (mm)	Height (Edge) (mm)	Thickness (Centre) (mm)	Hardness (N)	Tensile strength (MPa)	Friability (%)**	Min% and Max% tablet content
F1	30.3 ± 0.7	98-105	6.03 ± 0.02	1.54 ± 0.03	0.91 ± 0.03	7.64 ± 1.95	0.67 ± 0.18	0.48	94-105
F2	50.2 ± 0.9	94-102	6.01 ± 0.16	2.21 ± 0.14	1.45 ± 0.48	10.29 ± 1.06	0.56 ± 0.13	0.44	97-103
F3	67.6 ± 1.3	97-102	6.02 ± 0.02	2.79 ± 0.07	2.21 ± 0.07	18.91 ± 2.74	0.76 ± 0.11	0.30	96-104
F4	87.7 ± 1.7	98-102	6.01 ± 0.01	3.44 ± 0.08	2.88 ± 0.10	22.74 ± 3.09	0.67 ± 0.09	0.59	97-102
F5	29.1 ± 1.0	95-106	5.99 ± 0.04	1.49 ± 0.04	0.98 ± 0.04	5.68 ± 1.01	0.49 ± 0.09	0.68	92-104
F6	30.2 ± 1.0	93-104	6.01 ± 0.01	1.50 ± 0.02	0.99 ± 0.07	6.57 ± 1.91	0.56 ± 0.18	0.28	94-109
F7	29.7 ± 1.2	95-108	5.99 ± 0.01	1.46 ± 0.05	0.99 ± 0.07	6.66 ± 1.72	0.58 ± 0.17	0.12	93-109
F8	29.5 ± 1.5	93-108	5.98 ± 0.01	1.42 ± 0.04	0.92 ± 0.07	7.45 ± 1.97	0.69 ± 0.20	0.24	97-103
F9	29.6 ± 1.0	95-105	5.98 ± 0.04	1.43 ± 0.04	0.90 ± 0.06	9.11± 2.62	0.83 ± 0.23	0.09	97-103
F10	29.2 ± 1.9	92-109	5.98 ± 0.03	1.42 ± 0.06	0.90 ± 0.07	7.74 ± 1.87	0.72 ± 0.16	0.36	98-102
F11	28.3± 1.1	88-108	5.99± 0.01	1.47 ± 0.04	0.97 ± 0.05	10.19 ± 1.86	0.88 ± 0.17	0.04	96-105
F12	31.1 ± 1.1	93-107	5.98 ± 0.05	1.49 ± 0.04	0.92 ± 0.30	6.03 ± 1.92	0.80 ± 0.15	0.02	97-103
F13	30.6 ± 1.2	93-106	5.99 ± 0.04	1.45 ± 0.05	1.02 ± 0.08	5.00 ± 2.61	0.73 ± 0.24	0.01	97-114
F14	31.4 ± 1.5	94-111	5.96 ± 0.05	1.47 ± 0.04	1.02 ± 0.10	4.60 ± 3.47	0.83 ± 0.32	0.06	96-113
F15	32.6 ± 1.1	94-106	5.95 ± 0.03	1.50 ± 0.04	1.10 ± 0.08	4.60 ± 2.62	0.96 ± 0.22	0.25	90-106

P407	0%	5%	15%	25%	35%	45%	62.5%
HPMC-S	F1	F6	F6	F7	F8	F9	F15
HPMC	F11	-	F12	F13	-	F14	F15

4.3.1.2 *Ex vivo* mucoadhesion

Tablets of 30 mg weight were tested for Ex vivo mucoadhesion. All tablets successfully adhered to the chicken pouch while repeatedly immersed in the aqueous media for two hours using the disintegration tester, which represents the ideal residence time of a tablet in the buccal cavity.

The modified balance method was performed for selected formulations (Figure 4.5). As presented below, the force of detachment was not affected by the type of HPMC or the ratio of P407, results are ranging from ~11-18 gm/cm^2.

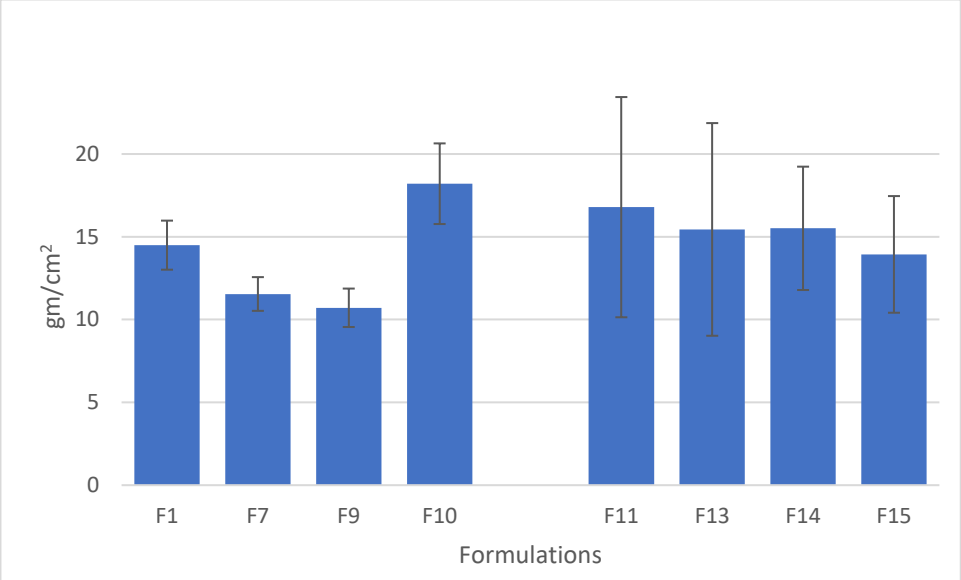

Figure 4.5 Average force of detachment of HPMC-S and HPMC formulations at 37°C, Data are expressed as mean ± SD, n = 3.

4.3.1.3 Swelling index (SI)

The swelling index for both HPMC and HPMC-S formulations (Figure 4.6 and Figure 4.7) increased with time. Formulations with higher drug-to-polymer ratio showed higher SI when compared with lower ratios, possibly because of the higher surface area versus volume for increasing total tablet weights. However, statistical analysis (two-way ANOVA with replication) revealed no statistical

P407	0%	5%	15%	25%	35%	45%	62.5%
HPMC-S	F1	F6	F6	F7	F8	F9	F15
HPMC	F11	-	F12	F13	-	F14	F15

significance (p>0.05) of tablet SI between HPMC and HMPC-S (formulations F1 and F11). There was a significant difference between the tested tablets (p<0.001), for HPMC-S (F1 and F5 – F10) and HPMC (F11 – F15) formulations.

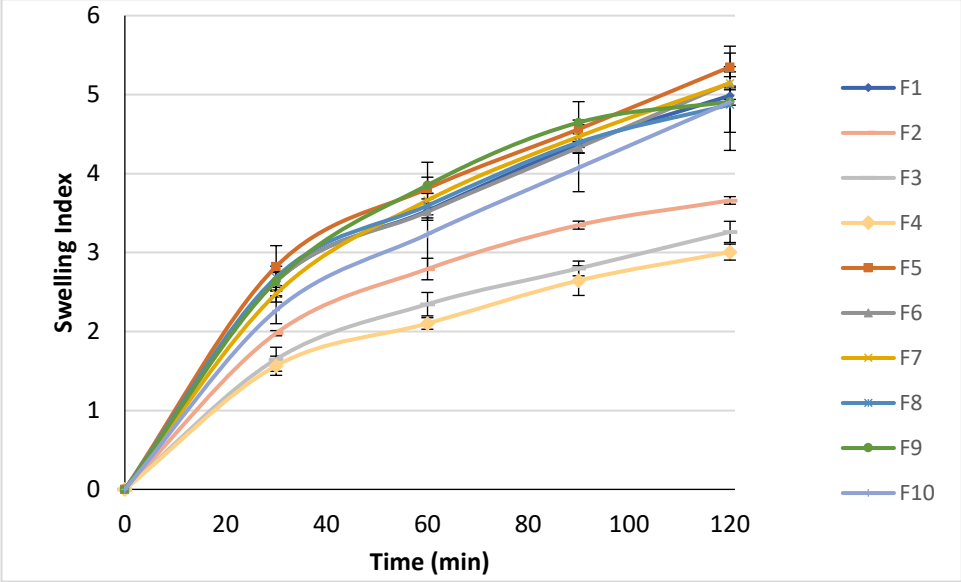

Figure 4.6 swelling index of tablets prepared using HPMC Sigma in ultrapure water and at 37 °C, Data are expressed as mean ± SD, n = 3.

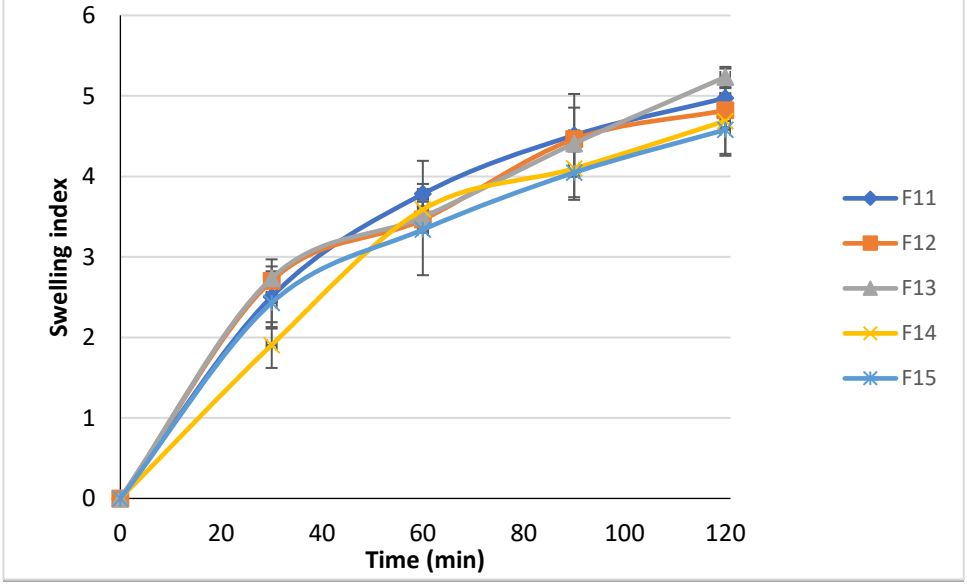

Figure 4.7 Swelling index of tablets prepared using HPMC Colorcon in ultrapure water and 37 °C, Data are expressed as mean ± SD, n = 3.

P407	0%	5%	15%	25%	35%	45%	62.5%
HPMC-S	F1	F6	F6	F7	F8	F9	F15
HPMC	F11	-	F12	F13	-	F14	F15

4.3.1.4 The morphology of the swollen tablets

The internal morphology of swollen tablets was investigated using SEM. The SEM images (Figure 4.8) shows the swollen tablet formulations form a sponge-like, porous network. The pores of F1 and F6 are smaller and more spherical compared to F11, F12 and F13. For instance, the average pores cross-sectional surface area of F1 and F11 were 0.46±0.86 and 1.86±2.95 mm^2, respectively. Increasing P407 changes their morphology to small and irregular pores, and the tablets after freeze-drying was fragile, this may have affected the shape of the pores during sample cutting.

P407	0%	5%	15%	25%	35%	45%	62.5%
HPMC-S	F1	F6	F6	F7	F8	F9	F15
HPMC	F11	-	F12	F13	-	F14	F15

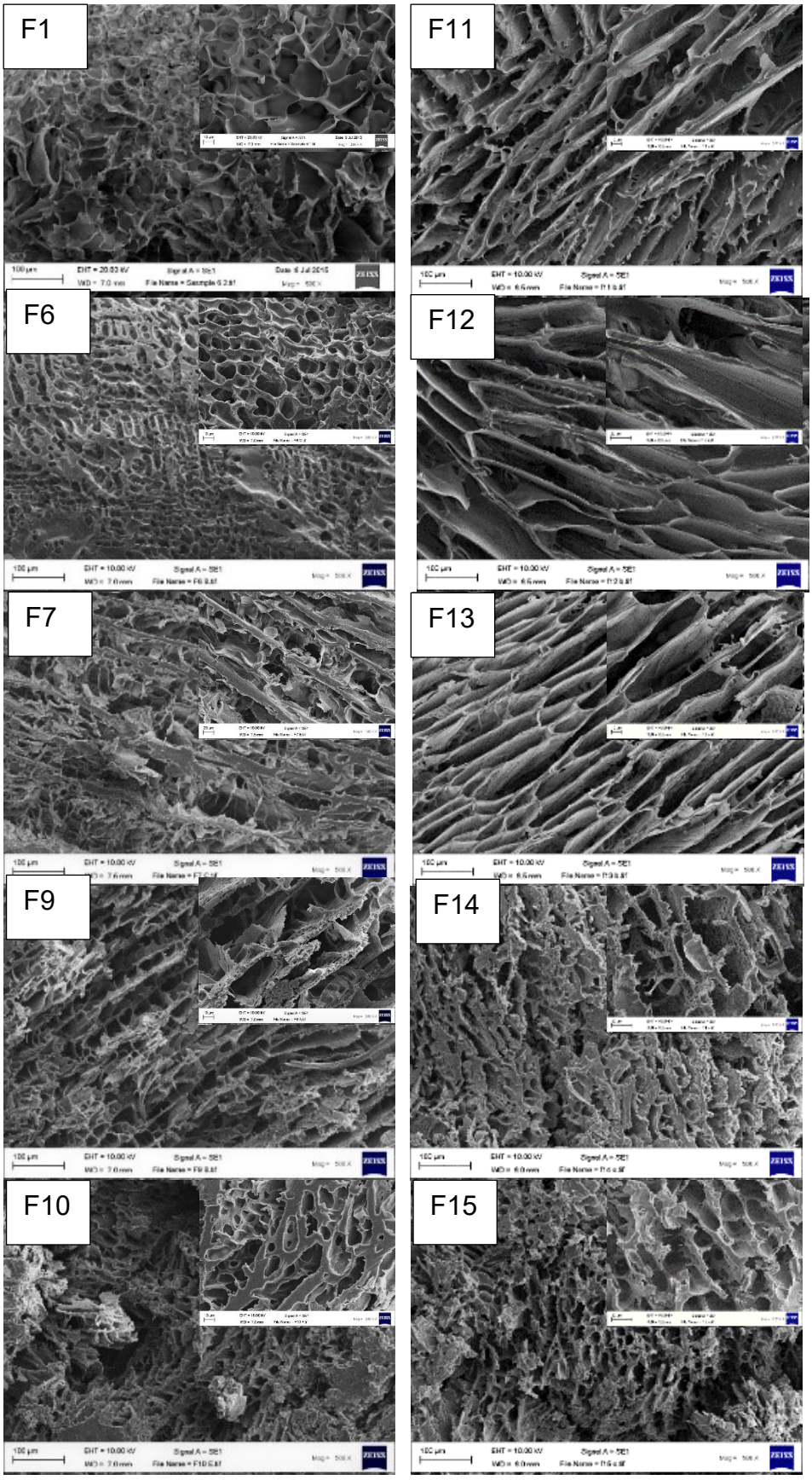

Figure 4.8 SEM images for swollen tablets of selected formulations.

P407	0%	5%	15%	25%	35%	45%	62.5%
HPMC-S	F1	F6	F6	F7	F8	F9	F15
HPMC	F11	-	F12	F13	-	F14	F15

4.3.1.5 *In vitro* dissolution of CHD

The release of CHD from HPMC-S matrix tablets (Figure 4.9) increased with time for all formulations and was affected by the drug/polymer ratio: Increasing the polymer content from 5:1 (F1) to 17: 1 (F4) decreased drug release by approximately 40% after two hours.

Cumulative CHD release from HPMC-S tablets, with the same drug/polymer ratio and weight, but varying P407 ratios indicated that increasing P407 content could elevate drug release by as much as 30%. For example, 60.53% CHD was released from F1 (25.00 mg HPMC-S and no P407) compared to 94.27% CHD release from F10 (6.25 mg HPMC-S and 18.75 mg P407). Moreover, cumulative CHD release from HPMC formulations F11 and F15 with the same composition of F1 and F10 were 57.77% and 94.58%, respectively (Figure 4.10). HPMC and HPMC-S formulations are similar in terms of cumulative drug release based on similarity factor (f_2) and difference factor (f_1) values of 79.62% and 7.05, respectively. F1 and F11 showed a cumulative release after two hours of 60.5% and 57.7%, respectively and F10 and F15 showed 94.3% and 94.6%, respectively. Both F10 and F15 considered similar with f_2 of 72.67% and f_1 of 7.87.

P407	0%	5%	15%	25%	35%	45%	62.5%
HPMC-S	F1	F6	F6	F7	F8	F9	F15
HPMC	F11	-	F12	F13	-	F14	F15

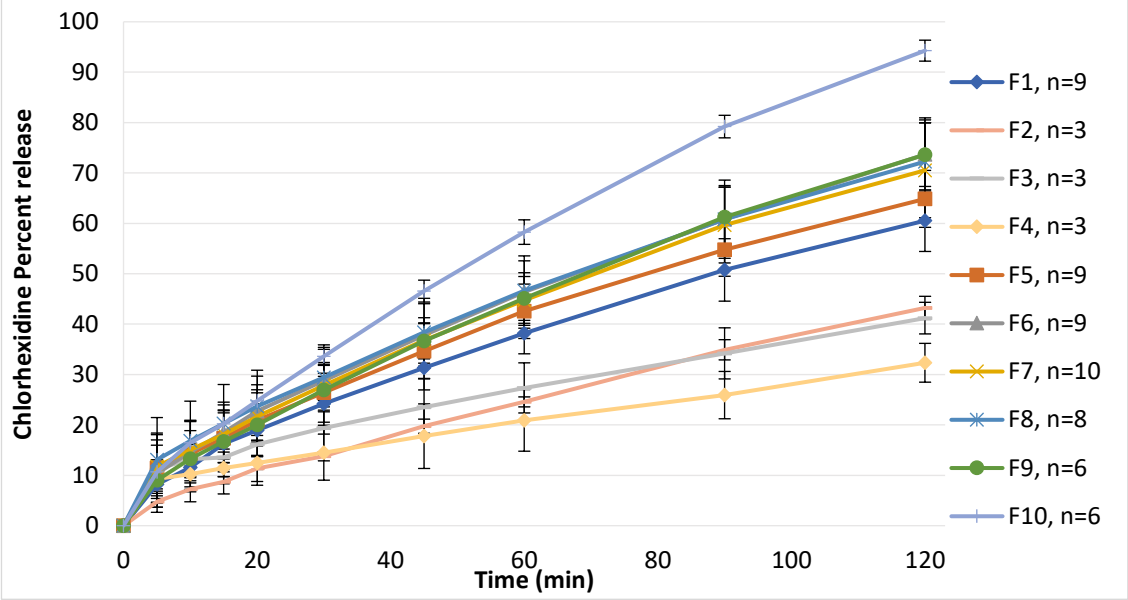

Figure 4.9 Cumulative percent release of chlorhexidine diacetate salt from tablets with different drug polymer ratios in ultrapure water at 37±0.1 °C and 50 rpm, results represent the average ± SD.

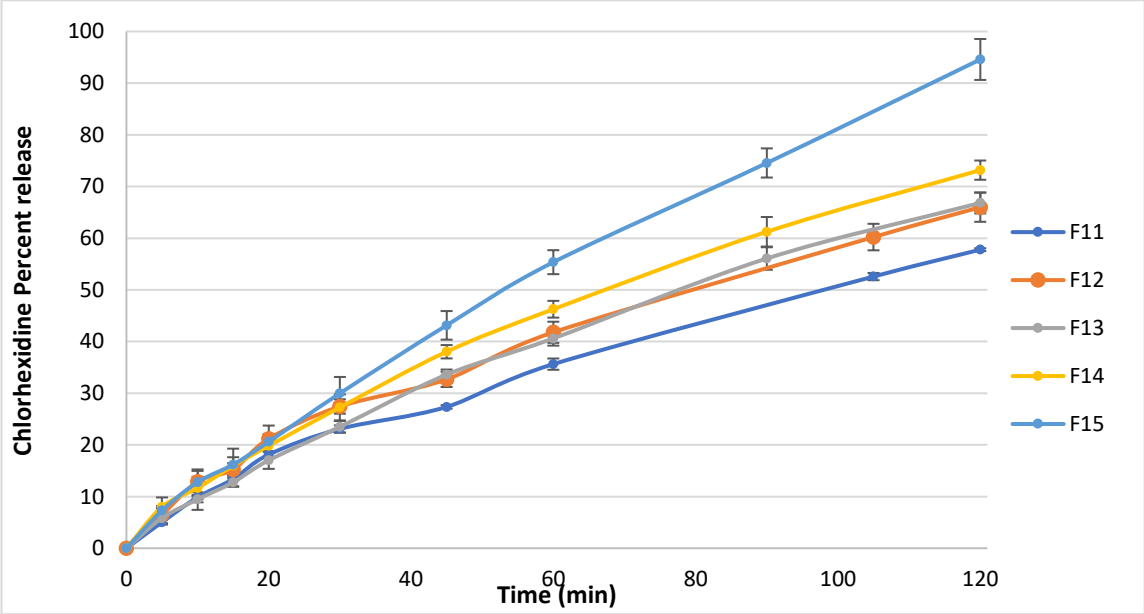

Figure 4.10 Cumulative percent release of chlorhexidine diacetate salt from tablets with HPMC Colorcon and different P 407 content in ultrapure water at 37±0.1 °C and 50 rpm, n = 3 ± SD.

P407	0%	5%	15%	25%	35%	45%	62.5%
HPMC-S	F1	F6	F6	F7	F8	F9	F15
HPMC	F11	-	F12	F13	-	F14	F15

4.3.1.6 Kinetics of drug release

The kinetics of CHD release was investigated by fitting the release data to zero and first order, Higuchi, Hixson-Crowell and Korsmeyer-Peppas models (Table 4.5). For zero order, drug release is constant per unit time (drug concentration has no effect on the percentage of drug release). In the first order model, drug release rate decreases with time and it is concentration dependent. The Higuchi model predicts the mechanism of drug release from a matrix occurs by diffusion according to Fick's law. In the Hixson-Crowell model, drug release is governed by dissolution in planes parallel to the surface of the dosage form but assumes that the geometric shape stays constant. Korsmeyer-Peppas equation (power low) is a semi-empirical equation in which the exponent *n* is used to characterise ~60% drug release. Using the correlation coefficient (R^2) values, 30 and 50 mg CHD tablets fitted closest with the Korsmeyer-Peppas and for these formulations $0.45<n<0.89$. This indicating that drug release is anomalous from cylindrical tablets (0.45 representing diffusional control and 0.89 indicating case-II transport which corresponds to zero order kinetic); thus CHD release is anomalous (Siepmann and Peppas, 2012).

P407	0%	5%	15%	25%	35%	45%	62.5%
HPMC-S	F1	F6	F6	F7	F8	F9	F15
HPMC	F11	-	F12	F13	-	F14	F15

Table 4.5 CHD release kinetics using different models.

	Zero Order (R^2)	First order(R^2)	Higuchi (R^2)	Hixon Crowel (R^2)	K-Peppas (R^2)	K-Peppas (n)
F1	0.9540 ± 0.0533	0.9323 ± 0.1307	0.9695 ± 0.0140	0.9114 ± 0.1583	0.9942 ± 0.0085	0.672 ± 0.156
F2	0.9879 ± 0.4940	0.9813 ± 0.0268	0.9563 ± 0.0042	0.9758 ± 0.0307	0.9946 ± 0.0079	0.772 ± 0.079
F3	0.9125 ± 0.0585	0.7478 ± 0.1826	0.9731 ± 0.0191	0.7101 ± 0.2077	0.9856 ± 0.0054	0.510 ± 0.162
F4	0.9127 ± 0.0612	0.7215 ± 0.1817	0.9612 ± 0.0183	0.6929 ± 0.2071	0.9706 ± 0.0181	0.503 ± 0.118
F5	0.9542 ± 0.0376	0.9401 ± 0.0829	0.9755 ± 0.0124	0.9151 ± 0.1093	0.9936 ± 0.0061	0.651 ± 0.173
F6	0.9672 ± 0.0202	0.9693 ± 0.0283	0.9762 ± 0.0174	0.9581 ± 0.0422	0.9958 ± 0.0035	0.676 ± 0.155
F7	0.9587 ± 0.0358	0.9407 ± 0.0780	0.9727 ± 0.0084	0.9223 ± 0.1025	0.9886 ± 0.0151	0.650 ± 0.148
F8	0.9487 ± 0.0462	0.9227 ± 0.1118	0.9731 ± 0.0116	0.8976 ± 0.1397	0.9907 ± 0.0137	0.623 ± 0.188
F9	0.9809 ± 0.0052	0.9703 ± 0.0565	0.9732 ± 0.0064	0.9851 ± 0.0116	0.9981 ± 0.0012	0.718 ± 0.045
F10	0.9819 ± 0.0047	0.9797 ± 0.0033	0.9697 ± 0.0064	0.9908 ± 0.0043	0.9968 ± 0.0039	0.739 ± 0.060
F11	0.9712 ± 0.0054	0.9833 ± 0.0067	0.9736 ± 0.0063	0.9483 ± 0.0128	0.9965 ± 0.0007	0.698 ± 0.033
F12	0.9663 ± 0.0025	0.9854 ± 0.0028	0.9796 ± 0.0019	0.9714 ± 0.0042	0.9959 ± 0.0005	0.671 ± 0.018
F13	09791 ± 0.0107	0.9972 ± 0.0010	0.9606 ± 0.0071	0.9942 ± 0.0030	0.9983 ± 0.0015	0.796 ± 0.009
F14	0.9727 ± 0.0117	0.9952 ± 0.0012	0.9703 ± 0.0105	0.9894 ± 0.0081	0.9981 ± 0.0015	0.740 ± 0.044
F15	0.9907 ± 0.0079	0.9700 ± 0.0143	0.9475 ± 0.0190	0.9872 ± 0.0059	0.9987 ± 0.0005	0.870 ± 0.113

P407	0%	5%	15%	25%	35%	45%	62.5%
HPMC-S	F1	F6	F6	F7	F8	F9	F15
HPMC	F11	-	F12	F13	-	F14	F15

4.3.1.7 Drug polymer interaction (FTIR and DSC)

FTIR analyses were performed (Figure 4.11) to evaluate possible interactions during the granulation and tabletting process, which might have resulted from the low melting point of P407. CHD displayed peaks at 3325 and 3119 cm^{-1} (asymmetric and symmetric NH stretching vibrations), 2938 and 2886 cm^{-1} (asymmetric and symmetric CH stretching), 1624 cm^{-1} (CN stretching vibration of imine group), 1522,1483 cm^{-1} (NH bending vibration of secondary amine and imine groups), 1406 cm^{-1} (C=C stretching vibrations of aromatic rings), 1290 and 1245 cm^{-1}CN stretching, 819 cm^{-1} out of plane vibration of the aromatic ring and the CCl group's spectra at 718 cm^{-1} (Holešová *et al*., 2014 and Yang *et al*., 2007). The characteristic peaks of HPMC are at 3445 cm^{-1} (OH stretching) and 2897 cm^{-1} (CH stretching), 1375 cm^{-1} (asymmetric CH_3 bending vibration), 1049 cm^{-1} (C-O asymmetric stretching vibration) and 942 cm^{-1} (C-O symmetric stretching vibration (Ding *et al*., 2015). P407 is characterised by principal peaks at 2875 cm^{-1} (CH stretching), 1346 cm^{-1} (OH bending) and 1094 cm^{-1} (CO stretching) (Vyas *et al*., 2009). Analyses of tablet formulations F1, F6, F7, F9 and F10 and the (F11-F15) (Figure 4.11 a and c) reveal that increasing the concentration of P407 leads to a decreased intensity of CHD and the disappearance of hydrogen bonding peaks at 3325 and 3119 cm-1, this is prominent for F10 and F15. In contrast, F1, F6, F11 and F12 show a combination of the peaks of all ingredients. The concentration-dependent interaction between CHD and P407 is attributed to the steric hindrance properties of P407 resulted in the shielding of CHD (Göppert and Müller, 2005). Whilst HPMC peaks overlap with P407, with the CO stretching of HPMC and P407 combined into one peak at

P407	0%	5%	15%	25%	35%	45%	62.5%
HPMC-S	F1	F6	F6	F7	F8	F9	F15
HPMC	F11	-	F12	F13	-	F14	F15

around 1097 cm^{-1} in F6, F8 and F10 and F13-F15; however, in F1 and F11, this peak shift to 1049 cm-1. Further investigation was performed to analyse F10 and F15, physical mix, granules and tablets (Figure 4.11 b and d). All FTIR spectra have identical peaks, this means that during the mixing process of the excipient, hydrophobic interactions occur between CHD and P407 ending in steric hindrance by the latter. Although this interaction is more common in liquid formulations, in the current formulation the interaction is aggravated by the small particle size of both CHD and P407.

P407	0%	5%	15%	25%	35%	45%	62.5%
HPMC-S	F1	F6	F6	F7	F8	F9	F15
HPMC	F11	-	F12	F13	-	F14	F15

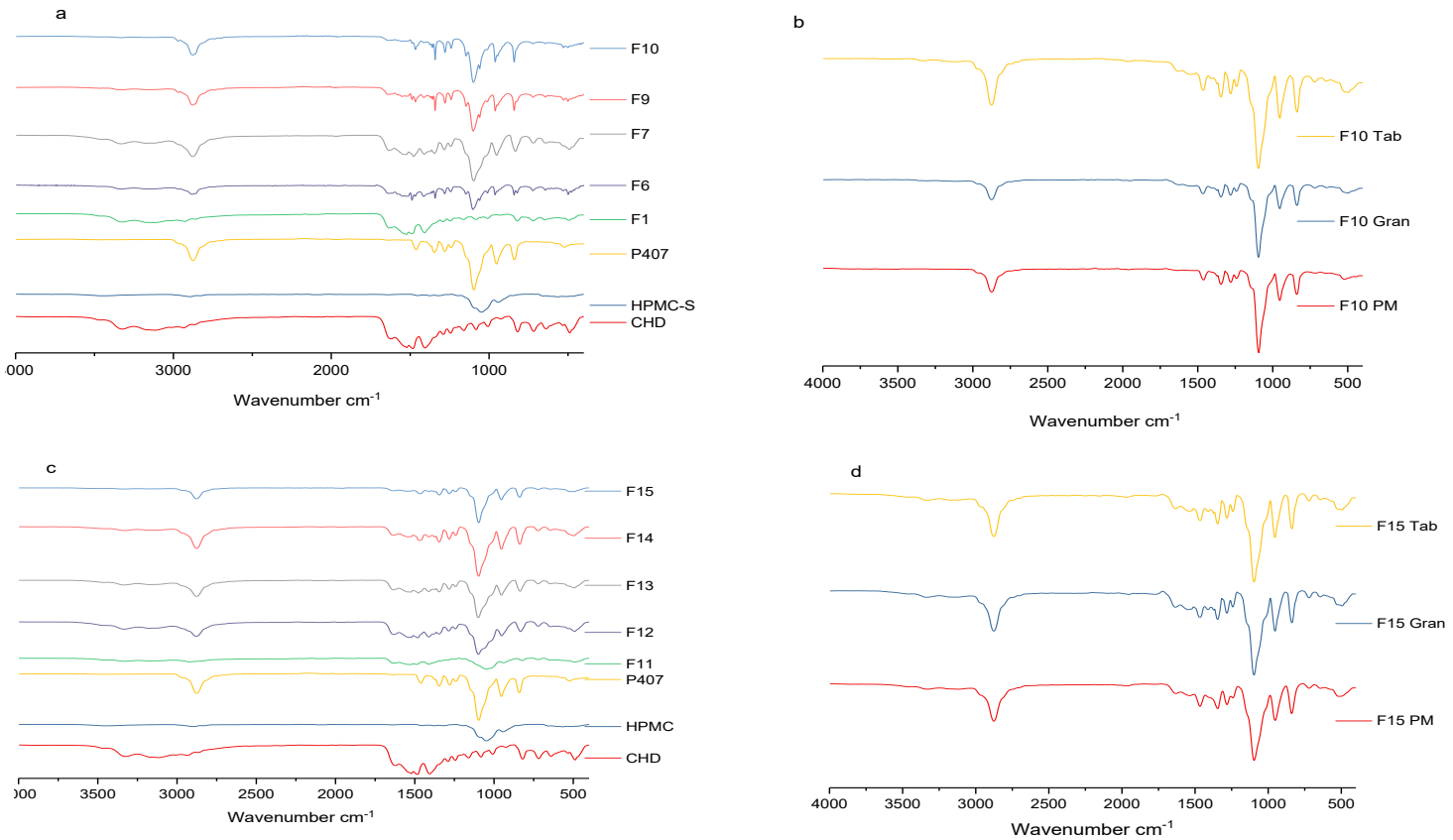

Figure 4.11 FTIR spectra of a) HPMC-S formulations b) F10 physical mix (PM), granules (Gran) and tablet (Tab), c) HPMC formulations and d) F15 PM, Gran and Tab.

P407	0%	5%	15%	25%	35%	45%	62.5%
HPMC-S	F1	F6	F6	F7	F8	F9	F15
HPMC	F11	-	F12	F13	-	F14	F15

DSC analysis

DSC thermograms for raw materials, physical mixture, granules and tablet of F15 formulation which showed the highest drug release, are depicted in (Figure 4.12) CHD has two melting peaks at 158 and 176ºC which indicates its polymorphic nature, HPMC reflects its amorphous nature while P407 has a melting peak at 57ºC. F15 physical mix, granules and tablet thermograms showed the endothermic peak of poloxamer around the same temperature. The first melting peak of CHD was shifted to 156ºC in the physical mix and to 153ºC for the granules and of the compressed tablet, this was accompanied by the disappearance of the small melting peak in the physical mix and granules and shifted to 173ºC in the tablet. Shifting and disappearance of the melting peaks in the physical mix and the granules indicates there is an interaction between the chlorhexidine and P407 However, the re-appearance of the second endothermic peak in the tablet is attributed to phase separation resulted from tablet compression (Singh *et al*., 2016).

P407	0%	5%	15%	25%	35%	45%	62.5%
HPMC-S	F1	F6	F6	F7	F8	F9	F10
HPMC	F11	-	F12	F13	-	F14	F15

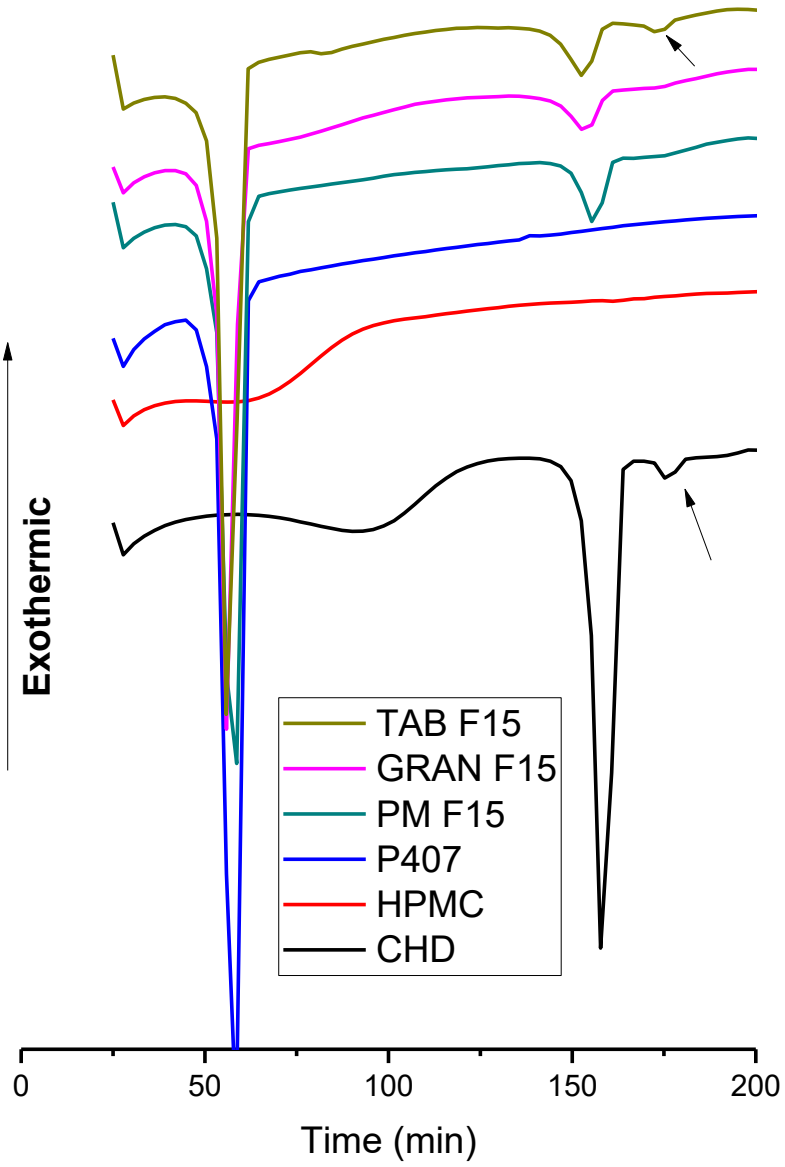

Figure 4.12 DSC thermograms of F15 physical mix (PM), Granules (GRAN), tablet (TAB), CHD HPMC and P407.

P407	0%	5%	15%	25%	35%	45%	62.5%
HPMC-S	F1	F6	F6	F7	F8	F9	F10
HPMC	F11	-	F12	F13	-	F14	F15

4.4 Discussion

Three groups of formulations with CHD were prepared based on different CHD to HPMC-S ratios, different HPMC-S to P407 ratios, and different HPMC to P407 ratios (detailed in Table 4.1).

Pre-formulation analyses were performed for particle size, distribution, morphology and flowability and all the tested powders were classified as fine powders according to BP criteria (BP, 2018 d). CHD and MgSt showed a bimodal particle size distribution, which is most likely due to the agglomeration of powders (Li *et al*., 2004) with adhesion of fine to coarse particles. Particle size analysis of HPMC showed a broadening of the distribution peak and a higher span value compared to HPMC-S (Figure 4.2) that can be attributed to the rod-like shape of the particles seen under SEM (Figure 4.3). Particle size distribution of HPMC-S approximates a nearly normal distribution with SEM revealing more spherical or irregular spheres for HPMC-S particles.

The morphology of both HPMC samples (Figure 4.3) strongly influences their flow behaviour; HPMC-S displays “passable” powder flow (CI of 21.67 and HR of 1.28), whereas HPMC has “poor” flow (CI of 33.33, HR of 1.50) (BP, 2018e). This finding was not unexpected as Hassan and Lau (2009) reported the impeded flow of needle-shaped calcium carbonate particles (CI of ≈40), that resulted from inter-particulate interactions and aggregation. Moreover, the span value of HPMC is higher than HPMC-S which resulted in a decrease in the flowability. This is confirmed by a previous finding by Liu *et al*., (2008) who found that the flowability effected by both particle size and distribution. Particle size (Table 4.2) below 100 µm resulted in increased cohesiveness and decreased flowability (Liu *et al*.,

P407	0%	5%	15%	25%	35%	45%	62.5%
HPMC-S	F1	F6	F6	F7	F8	F9	F10
HPMC	F11	-	F12	F13	-	F14	F15

2008) with the narrower distribution showing better flowability. The flowability of the various powder formulation blends was found to be not flowable (Table 4.3) and may be due to the smaller mean particle size population of the formulations, which results in a relatively high surface area and the potential for increased inter-particulate interactions that can decrease flowability. Dry granulation improved the flow properties of all formulation blends with most of improving from ‘very, very poor’ to ‘very poor’, or from ‘very poor’ to ‘poor’ based on the BP.

The applied force used to prepare HPMC-S granules was 1 ton. In contrast, HPMC granules were initially prepared at 1 and 4 ton, but the 1 ton samples were rejected due to no improvement in flowability. This may be attributed to the rod-like shape of HPMC-C particulates, which result in a weak granule compact, unable to maintain its shape. The flowability of granulated formulations prepared by both forces (1 or 4 tons) was similar. Increasing the ratio of polymer to drug from 5:1 to 17:1 had no effect on the flow properties of the various formulation blends. All these formulations had ‘very poor’ flowability with CI and HR values of 35-37 and 1.54-1.58, but these improved after granulation to 25-29.41 and 1.27-1.42, respectively. Similarly, increasing the P407 content has decreased the flowability of the powder blends most likely because of the irregular shape, small particle size and cohesive properties of P407, which increases inter-particulate interactions and decreases packing efficiency as evidenced by relatively high CI and HR values (40 and >1.7, respectively). Again, flow properties were improved after granulation, possibly as a result of the low melting point and the waxy nature of the P407, which has decreased inter-particulate interactions and improved the packing efficiency. Granulated formulations with a high P407 ratio, demonstrated C.I. and HR values of 27 and 1.4, respectively. Granules flowability did not show

P407	0%	5%	15%	25%	35%	45%	62.5%
HPMC-S	F1	F6	F6	F7	F8	F9	F10
HPMC	F11	-	F12	F13	-	F14	F15

a high improvement, this due to the generation of fine particles using dry granulation as confirmed using SEM images (Figure 4.4).

To overcome the poor flowability, tablets were pressed at the lowest turret speed at 8.6 RPM. The resultant tablet gave acceptable friability, weight variation and content uniformity. Moreover, all tablets successfully adhered to the chicken pouch, as a model tissue, using the modified disintegration tester. Successful mucoadhesion of tablets containing both HPMCs and P407 may be due to chain entanglement and physical interlinking interaction with the chicken pouch mucous membrane; neither polymer is capable of interacting with the mucin component of mucous as they are both uncharged (Sosnik *et al*., 2014). In the modified balance method, the measured force of detachment was not affected by the ratio of the polymers. Using HPMC-S showing no significant difference ($p < 0.05$) among the tested formulations (F1, F7, F9 and F10), however the increase in P407 in HPMC formulations (F11, F13, F14 and F15) showed a significant decrease in the force of detachment ($p > 0.05$). Furthermore, there is no evidence that the source or the morphology of the particles influences the force of detachment. This variation might be attributed to the poor reproducibility using biological membrane (chicken pouch) due to the inter-individual variation of the tissue, as was previously highlighted by Khutoryanskiy (2011). Attempts have been made to replace the use of animal tissue in mucoadhesion tests. For instance, Hall *et al*., (2011) successfully developed a synthetic three-dimensional crosslinked hydrogel with hydroxyethyl methacrylate polymer and acryloyl glucosamine monomers, they found that mucoadhesion results of the synthetic membrane are in agreement with the porcine buccal mucosa results.

P407	0%	5%	15%	25%	35%	45%	62.5%
HPMC-S	F1	F6	F6	F7	F8	F9	F10
HPMC	F11	-	F12	F13	-	F14	F15

The swelling profiles of the tablet formulations (Figure 4.6 and Figure 4.7) in ultrapure water for two hours showed that tablets with a CHD to polymer ratios 1:17 to 1:9 had a lower swelling index range from 3.0 to 3.6. This is possibly because of the higher surface area to volume ratio. Source of HPMC does not show any impact on the swelling index, however increasing P407 led to decreasing swelling index significantly ((p<0.001), for both sources.

Upon hydration the mobility the macromolecules of HPMC and HPMC-S increases along with the rate of water movement (Siepmann and Peppas, 2012). Moreover, hydrated P407 arranges itself into micellar structures that subsequently adopt a cubic shape once the hydrogel is formed. Intriguingly, the presence of HPMC in some of these formulations might facilitate the formation of a network of interconnected P407 micelles (Koffi *et al*., 2006).

Swollen SEM tablet morphology (Figure 4.9) has a strong relationship with particles morphology of HPMC and HPMC-S polymers (Figure 4.3) and their ratios in the formulations. F1 and F6 show clear spherical pores while F11, F12 and F13 have elongated pores, the effect is prominent when the ratio is greater than 50% in the tablet. Increasing P407 lead to the formation of irregular pores which might be due to its surfactant properties which increase the solubility of other polymers and distorting their shapes. Another possibility is that it might be affected by thermosensitive properties of P407, which melts at low temperature, and so pore damage may occur during the freeze-drying process.

The release of CHD from HPMC-S matrix tablets was affected by the CHD/polymer ratio, increasing the polymer content led to increased resistance to the release of CHD (Figure 4.9). The higher mass of F4 (90 mg) compared to F1 (30 mg) would require more time to fully hydrate (data not presented), thus

P407	0%	5%	15%	25%	35%	45%	62.5%
HPMC-S	F1	F6	F6	F7	F8	F9	F10
HPMC	F11	-	F12	F13	-	F14	F15

resulting in decreased CHD release; furthermore, swelling index data (Figure 4.6), for F1 and F4 were 4.98 and 3.00, respectively. Based on these results F1 was selected for further investigation as it released more CHD and would be a more convenient size for patients to administer as a buccal dosage form. Cumulative CHD release from HPMC-S tablets, with the same drug/ polymer ratio and weight, but varying P407 ratios indicated that increasing P407 content could elevate drug release by as much as 30%. The increase in drug release was attributed to the solubilising activity of P407 (Figure 4.9). The copolymer P407 is a surfactant which is widely used to improve the aqueous solubility of poorly soluble drugs (Dumortier *et al*., 2006), and can also form a hydrogel at body temperature. Although different compression forces of 1 ton for HPMC-S formulations and 4 ton for HPMC formulations were used to prepare the granules, this should not affect drug release. Velasco *et al*., (1999) reported that compression force has a minimal effect on drug release or the kinetics of release but can influence initial matrix porosity (before hydration).

Using the correlation coefficient (R^2) values, tablets fitted closest with the Korsmeyer-Peppas kinetic model and the exponent n was found to be $0.45<n<0.89$, Indicating that drug release is anomalous from cylindrical tablets (0.45 representing diffusional control and 0.89 indicating case-II transport which corresponds to zero order kinetic); thus CHD release is anomalous (Siepmann and Peppas, 2012). This concludes that neither drug-polymer ratio nor P407 had an effect on the mechanism of drug release.

The Interaction between excipients and CHD were tested using FTIR and DSC. FTIR spectra revealed increasing in P407 ratio led to decrease the intensity of CHD which was attributed to steric hindrance by P407. Comparing FTIR spectra

P407	0%	5%	15%	25%	35%	45%	62.5%
HPMC-S	F1	F6	F6	F7	F8	F9	F10
HPMC	F11	-	F12	F13	-	F14	F15

for F10 physical mix, granules and tablet showed identical spectra similarly for F15. This indicates that no interaction occurred during the process of tabletting and the source of the polymer showed no difference in behaviour. Moreover, DSC analysis was performed for F15 formulation only, showed no interactions between the drug and the polymers in the prepared table.

4.5 Conclusions

Formulation of buccal tablets using either HPMC-S or HPMC did not affect cumulative CHD release, in spite of their physical properties not being identical. The addition of the thermosensitive hydrogel-forming polymer; P407 to the formulations, improved CHD release from the tablets, whilst not negatively impacting on the time of mucoadhesion. Formulations prepared with HPMC-S and HPMC both showed comparable drug release and kinetics of drug release, although each one had different pore sizes and morphology. Furthermore, based on FTIR and DSC analysis, there was no interaction between CHD and any of the excipients. The results shown in this chapter are promising, although further adjustments are required in terms of a developing a safe and effective concentration under limited availability of salivary dissolution medium.

P407	0%	5%	15%	25%	35%	45%	62.5%
HPMC-S	F1	F6	F6	F7	F8	F9	F10
HPMC	F11	-	F12	F13	-	F14	F15

Chapter Five

Tablet gelling, hydration and drug release

Chapter 5 : Tablet gelling, hydration and drug release

The aim of this work is to investigate the effect of the flow rate of the dissolution media on the behaviour of the matrix tablet in terms of gelling, hydration and drug release. A novel method was used to compare the degree of hydration with different HPMC/P407 ratios using visible spectroscopy, to assess the hydrogel-forming ability using image analysis and exploit polarized microscopy to examine the behaviour of the tablet after swelling. Based upon our knowledge, there is no standard method to assess the effect of different degree of hydration or salivation in the oral cavity upon drug release. In this chapter, the feasibility to design a new method to assess the release of CHD from the mucoadhesive buccal tablets was investigated and the release of CHD was assessed using water as a dissolution medium of different flow rates and compare it with Apparatus I (App1). Mathematical and statistical methods were used to analyze the drug release data.

5.1 Materials and Methods

5.2.1 Materials

Based on the previous results in chapter four, which showed no significant difference in CHD release from mucoadhesive buccal tablets prepared using HPMC or HPMC-S. Formulations F11-F15 prepared with HPMC Dow-Colorcon were further investigated using the methods described below.

5.2.2 Methods

5.2.2.1 Rate of tablet hydration

The rate of hydration or wetting was investigated by testing the rate of water uptake by the tablets, the measurement based on the change in the absorbance

	F11	F12	F13	F14	F15
P407	0%	15%	25%	45%	62.5%

(A) upon hydration, using wideband filters (λ_{405} to λ_{600}), in an automated Bioscreen C spectrophotometric plate reader (Thermo Labsystems, Finland). Tablets were placed in a honeycomb 100 well microtiter plate (one tablet per 0.4 mL well size) 350 µL of distilled water was added to each well, water was used as a negative control. The change in optical density due to tablet swelling over time was recorded every 30 minutes for 24 hours.

To plot the relationship of hydration with time:

All absorbance data were blanked with water. A_0 represents the absorbance of the tablet at time zero. The absorbance of the tablet (A_n) was decreased upon hydration, accordingly, a negative value was obtained by subtracting A_0 from A_n. To calculate the change in the absorbance (ΔA_t) *Equation 15 w*as applied.

$$\Delta A_t = (A_n - A_0) \times -1 \qquad \textit{Equation 15}$$

ΔA_t is the change in the absorbance at time t

Water uptake or hydration (*H*) was calculated using *Equation 16*

$$H_t = \frac{(\Delta A_t \times volume\ of\ water)}{\Delta A_{max}} \qquad \textit{Equation 16}$$

Where (ΔA_{max} is the maximum change in the absorbance at 24 hours), the volume of water is 350 µL.

Hydration curve is obtained by plotting H against time.

Hydration kinetics

Hydration data was fitted to piecewise linear regression 2 (PWL2) and to the exponential model. The AIC (Akaike information criterion) was calculated to find the best fitting model. The analysis was performed using OriginPro software.

	F11	F12	F13	F14	F15
P407	0%	15%	25%	45%	62.5%

5.2.2.2 Image analysis

Image analysis of gelling efficiency

Each tablet was adhered to a glass slide, immersed in a beaker filled with water and placed in a prewarmed water bath at 37°C. Images were acquired for the swollen tablet at 15, 30, 60, 90 and 120 minutes using a digital camera. The area of the gel and the core base were calculated using ImageJ 1.51n software.

Polarized optical microscopy imaging

Tablets were treated similar to section 5.2.2.2 and investigated using polarized microscopy (Primotech-Zeiss, Germany), to monitor the change in tablet morphology upon swelling. Darkfield illumination and retardation plate using 50X magnification were used.

5.2.2.3 *In Vitro* dissolution using controlled flow rate (CFR, Liebig condenser method)

Drug dissolution from F11-F15 was tested at different flow rates of the dissolution medium. The dissolution was performed at 37.0 ± 0.1°C, in a Liebig condenser with circulating warm water (to maintain the temperature around the tablet). The dissolution media was pumped (Watson Marlow 502s peristaltic pump, UK) at 0.48 ± 0.05 and 2 ± 0.05 mL/min over the tablet in the condenser. Then the media was collected in a measuring cylinder, samples were collected every 10 minutes for two hours. Similarly, the dissolution was performed using a fixed speed peristaltic pump (model PP1ML, UK) with a flow rate of 0.9mL/min (Figure 5.1).

	F11	F12	F13	F14	F15
P407	0%	15%	25%	45%	62.5%

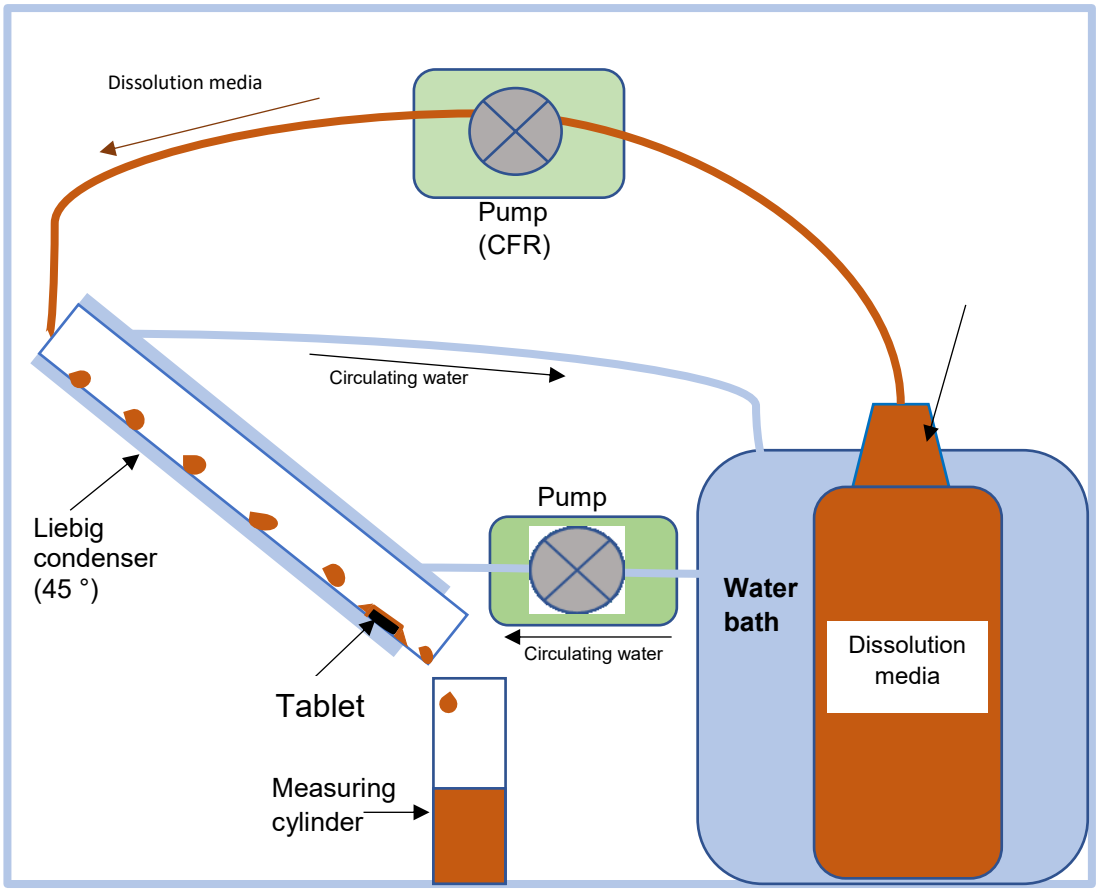

Figure 5.1 Diagram of In-Vitro drug release using controlled rate of flow of dissolution medium over the tablet

5.2.2.4 Analysis of dissolution profiles (statistical and mathematical modelling)

5.2.2.4.1 Dissolution efficiency (D.E.)

D.E. is determined from the percentile ratio of the area under the curve (AUC) of the dissolution data to the AUC of 100% release between time zero to the end of dissolution (Anderson *et al*., 1998). It is obtained using Equation 17 and OriginPro 2017 software were used to calculate the area under the curve.

$$D.E. = \frac{\int_0^t y \times dt}{y_{100} \times t} \times 100\% \qquad \textit{Equation 17}$$

Where *t* is the time, *y* is the percentage of drug dissolved at time t.

	F11	F12	F13	F14	F15
P407	0%	15%	25%	45%	62.5%

5.2.2.4.2 In vitro equivalence analysis (model independent)

Statistical and mathematical methods were applied for each pair of the triplicates of the dissolution testing data to evaluate the degree of equivalence and the applicability of flow rate method compared to standard Apparatus I (Figure 4.10).

i. One-way analysis of variance (ANOVA)

ANOVA was obtained using Microsoft Excel to examine the difference between each triplicate. This test compares the variability in drug release at each time point. However, it doesn't correlate the whole dissolution profile (O'hara *et al*., 1998).

ii. Pairwise model independent methods

Similarity factor (f_2) and Difference factor (f_1) were performed as explained in 4.1.2.12.

iii. Rescigno's indices (ξ_j)

Rescigno Index is used to measure the difference in drug concentration of a sample compared to a reference; it is obtained by applying Equation 18 (O'hara *et al.,* 1998)

$$\xi_j = \left(\frac{\int_0^{t_n} |R_t - T_t|^j d_t}{\int_0^{t_n} |R_t + T_t|^j d_t} \right)^{1/J} \qquad \textit{Equation 18}$$

Where ξ_j is rescigno index, j is the exponent and it is equal to 1 or 2, ξ_1 is the absolute area difference and ξ_2 is the square area difference, n is the number of sampling points, R_t and T_t represent the concentration at time t of the reference and the sample, respectively, the endpoint of the dissolution is denoted as t_n.

ξ_j value ranges between 0 and 1, when the test samples are identical it is equal to zero, however, 1 means there is no release from one of the samples. The

	F11	F12	F13	F14	F15
P407	0%	15%	25%	45%	62.5%

difference between similarity factor and the Rescigno ratio is the former take sampling time in consideration while the latter take spacing between sampling intervals as well (Vertzoni *et al*., 2003). In the current work, DDsolver (Zhang *et al.,* 2010) software was used for the calculation of Rescigno's Indices.

iv. The ratio of the Area Under the Curve (AUC)

The ratio of the AUC is used to measure the bioequivalence of drug release *in vivo*. It is used *in vitro* to compare between a reference and a sample. It is calculated by dividing the AUC of the sample over the AUC of the reference. The ratio should lie between 0.80- 1.25; this limit was selected based on 90% confidence intervals (Morais and Lobato, 2010).

5.2.2.4.3 Model-dependent methods (Kinetics of drug release)

Kinetics of drug release was applied to investigate the effect of the different flow rates of the dissolution medium on the mechanism of drug release and compare it to the standard App I. DDSolver software was used to calculate the Kinetic modelling of drug release, the advantage of this software is the use of non-linear fitting (Zhang *et al.*, 2010) which is more reliable, the same models investigated in chapter four (4.1.2.13) were investigated (Zero order, First order, Higuchi model, Hixon-Crowell model and Korsmeyer-Peppas models).

5.3 Results

5.3.1 Rate of hydration

The rate of water uptake by polymers is varied and it is based upon their properties. The mechanism of drug release from the matrix is mainly controlled

	F11	F12	F13	F14	F15
P407	0%	15%	25%	45%	62.5%

by diffusion and erosion, both of which are affected by the hydration state of the matrix (Colombo *et al.,* 2000). In this work, the hydration rate was measured by the change in the light absorbance with time. Figure 5.2 displays the raw data obtained from the Bioscreen spectrophotometer, showing the decrease in light absorbance with time, which is obtained by the hydration of the tablets.

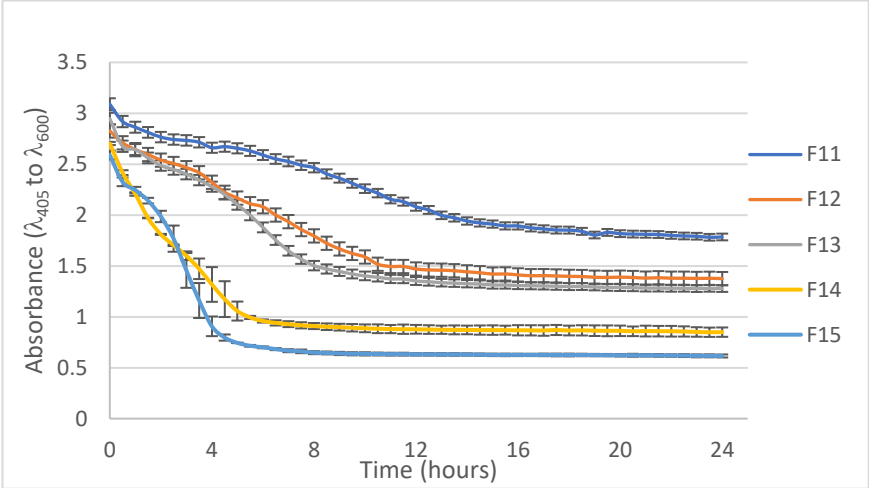

Figure 5.2 original data of the change in the absorbance with time obtained from the Bioscreen spectrophotometer.

Figure 5.3 shows the calculated values of tablets hydration over 24 hours and it was faster for both F14 and F15, they reached the plateau 4 hours faster than other formulations.

	F11	F12	F13	F14	F15
P407	0%	15%	25%	45%	62.5%

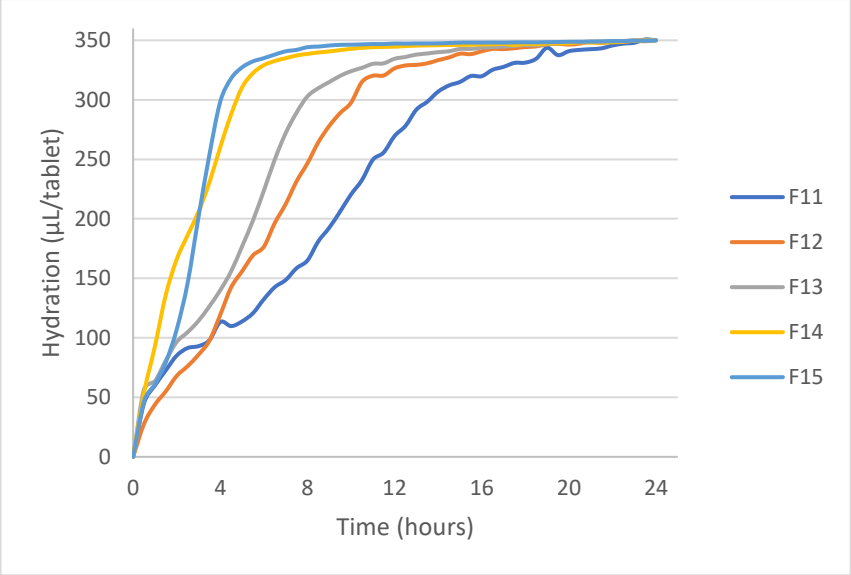

Figure 5.3 Hydration of F11-F15 formulations with time for 24 hours at 37°C, n = 3.

Based on the shape of the graphs, data were fitted to the piecewise linear regression 2 (PWL2) model (Figure A 1) and to the exponential model.

All fitted data showed a high degree of fit (R^2>0.99) to the PWL2 model. K1 and K2 represent the rate constant for tablet hydration in µL/tab (Table 5.1), the rate constant of the first line of the curve showed the rate of water uptake by the tablets, K1 increased from 19.52 µL/tab.hr to 72.64 µL/tab.hr from F11 to F15.

Table 5.1 Rate constants and R2 for fitted hydration curves for F11-F15 using PWL2

Formulations	PWL2			Exponential
	K 1	K2	R^2	R^2
F11	19.52	0.39	0.992	0.974
F12	29.69	0.30	0.998	0.976
F13	34.21	0.69	0.994	0.968
F14	58.53	1.37	0.993	0.989
F15	72.64	1.84	0.992	0.955

	F11	F12	F13	F14	F15
P407	0%	15%	25%	45%	62.5%

OriginPro software was used to compare the best fitting by obtaining AIC values, they were 215 and 299 for PWL2 and exponential fitting, respectively. Which is further confirms the fitting to PWL2 model due to its lower value of AIC.

To further investigate the effect of P407 on the rate of water absorption, the latter was plotted against the ratio of P 407 in the formulations (Figure 5.4).

Interestingly the effect of P407 content in the tablets showed high linearity with the hydration rate constant, which indicates the increase P407 ratio from 0% in F11 to 62.5% in F15, lead to a consistent increase in the hydrophilicity of the formulations and consequently the rate of hydration, which is attributed to the surfactant properties of P407 (Beck-Broichsitter *et al*., 2017).

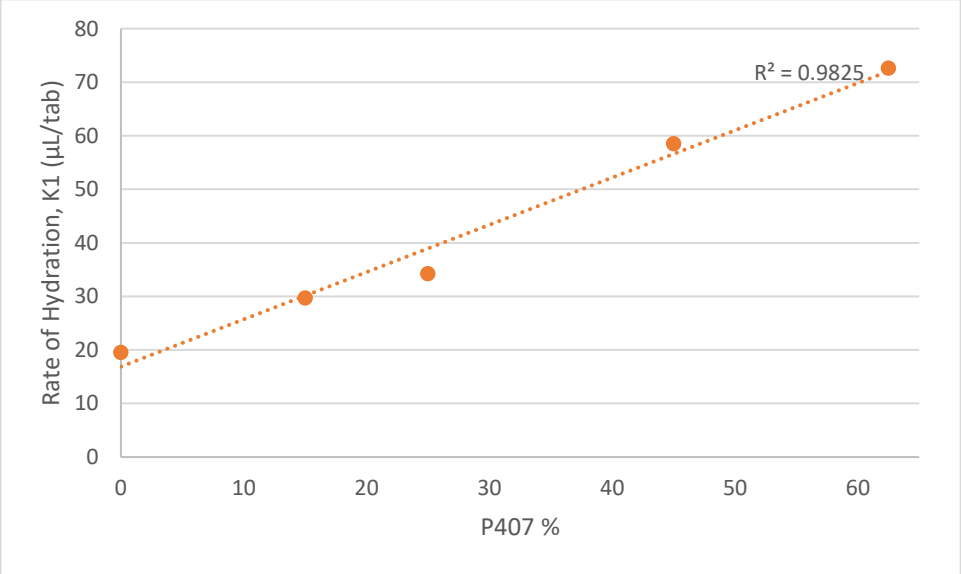

Figure 5.4 relationship between the percentage of P407 and the rate of hydration (K1).

5.3.2 Image analysis

5.3.2.1 Tablet gelling

To investigate tablets gelling, images were acquired using a digital camera at (15, 30, 60, 90 and 120 min) during tablet hydration, and the surface area of the base of the tablet was calculated for both the core (solid glassy material) and the

	F11	F12	F13	F14	F15
P407	0%	15%	25%	45%	62.5%

hydrogel layer. Hence the tablet hydrates radially in all direction, thus the ratio of the hydrogel to the core will be constant in the swollen tablet (Figure 5.5).

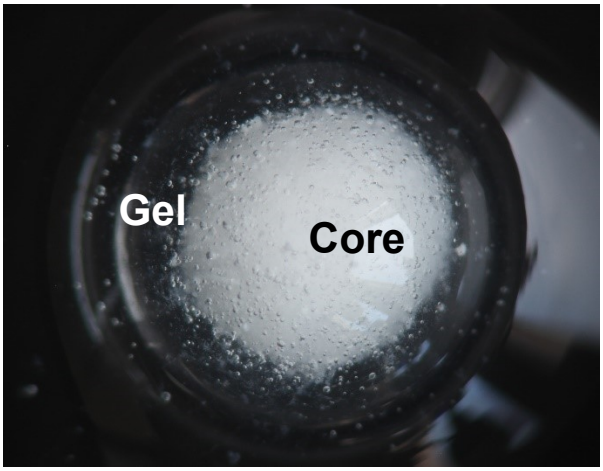

Figure 5.5 Swollen F11 tablet after 1.5 hours showing the two layers of the tablet.

The results show that as the area of the whole tablet increases with time the core area decreases and the hydrogel area increases for all samples (Figure 5.6). The increase in the P407 in the tablets resulted in the increase of hydrogel to core area over time. Finally, the hydration profile in Figure 5.3 and Figure 5.6 is dissimilar, and this is attributed to the difference in the exposed surface area to water. For the former the surface area was constant which is represented by the surface area of the tablet (6mm in diameter and its equal to the surface area of the well). While in Figure 5.6, the surface area was increasing with time due to tablet swelling.

	F11	F12	F13	F14	F15
P407	0%	15%	25%	45%	62.5%

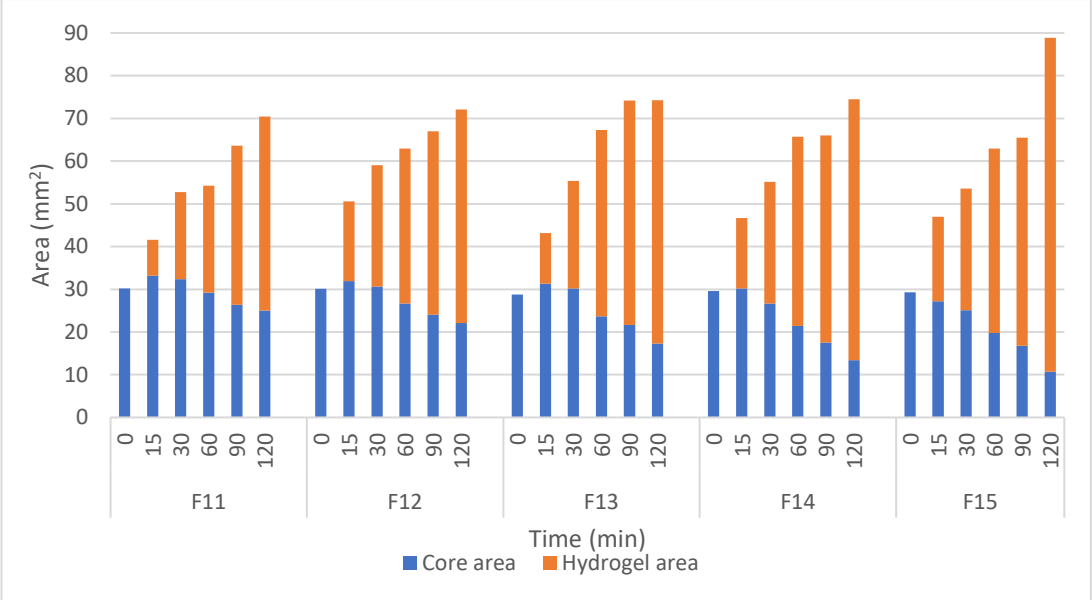

Figure 5.6 image analysis results for F11 - F15 tablet showing the planner area of both the core and the hydrogel layer at 37°C and 2 hours.

5.3.2.2 Polarized microscopy imaging:

Polarized microscopy images were obtained to investigate the behaviour of the tablet during the swelling process, it distinguishes between materials of a different refractive index. The hydrogel layer is transparent under a light microscope and it is difficult to monitor tablet swelling without staining which might affect the property of the tablet. However, the use of cross polarised illumination with the dark field (Figure 5.8) and the retardation plate (Figure 5.9) gave more detailed information.

Figure 5.7 shows the optical properties of the raw materials; CHD, HPMC and P407. They have anisotropic with birefringent properties, CHD and P407 for their crystalline structure and HPMC for its randomly oriented chains resultant from the stress of the manufacturing process (Arruda *et al.,* 1993).

	F11	F12	F13	F14	F15
P407	0%	15%	25%	45%	62.5%

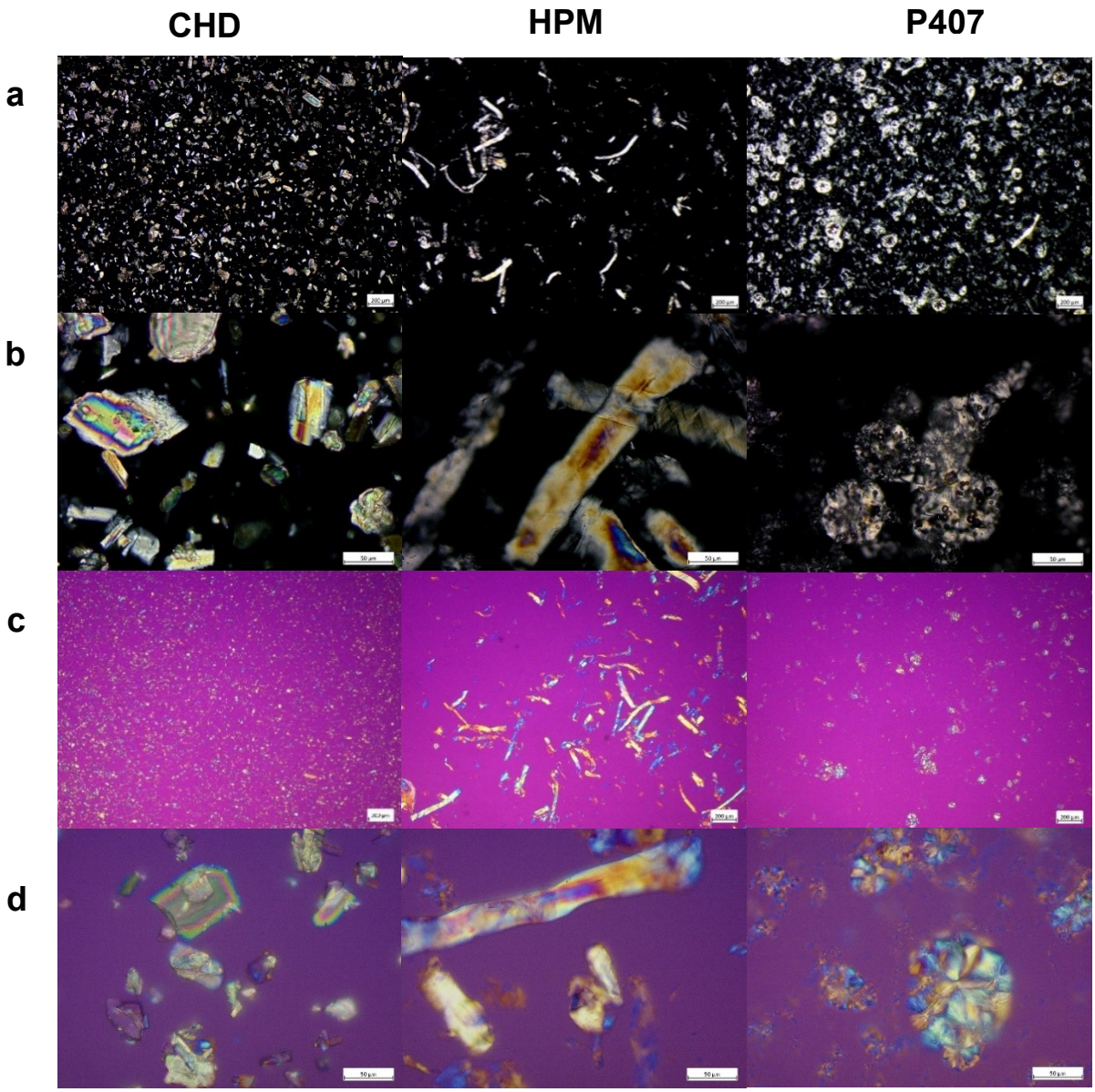

Figure 5.7 CHD, HPMC and P407, using cross polarised microscopy (darkfield) and a retardation plate, 50x and 400x, bars are 200 µm (a and c) and 50 µm (b and d).

Images were obtained at the predetermined time intervals, by examining the core of the tablets within the hydrogel layer (F11, F13, F14 and F15) during their swelling (Figure 5.8). There is some fragments detached from the core of the tablets. The fragments are increased with time and also with P407 ratio.

	F11	F12	F13	F14	F15
P407	0%	15%	25%	45%	62.5%

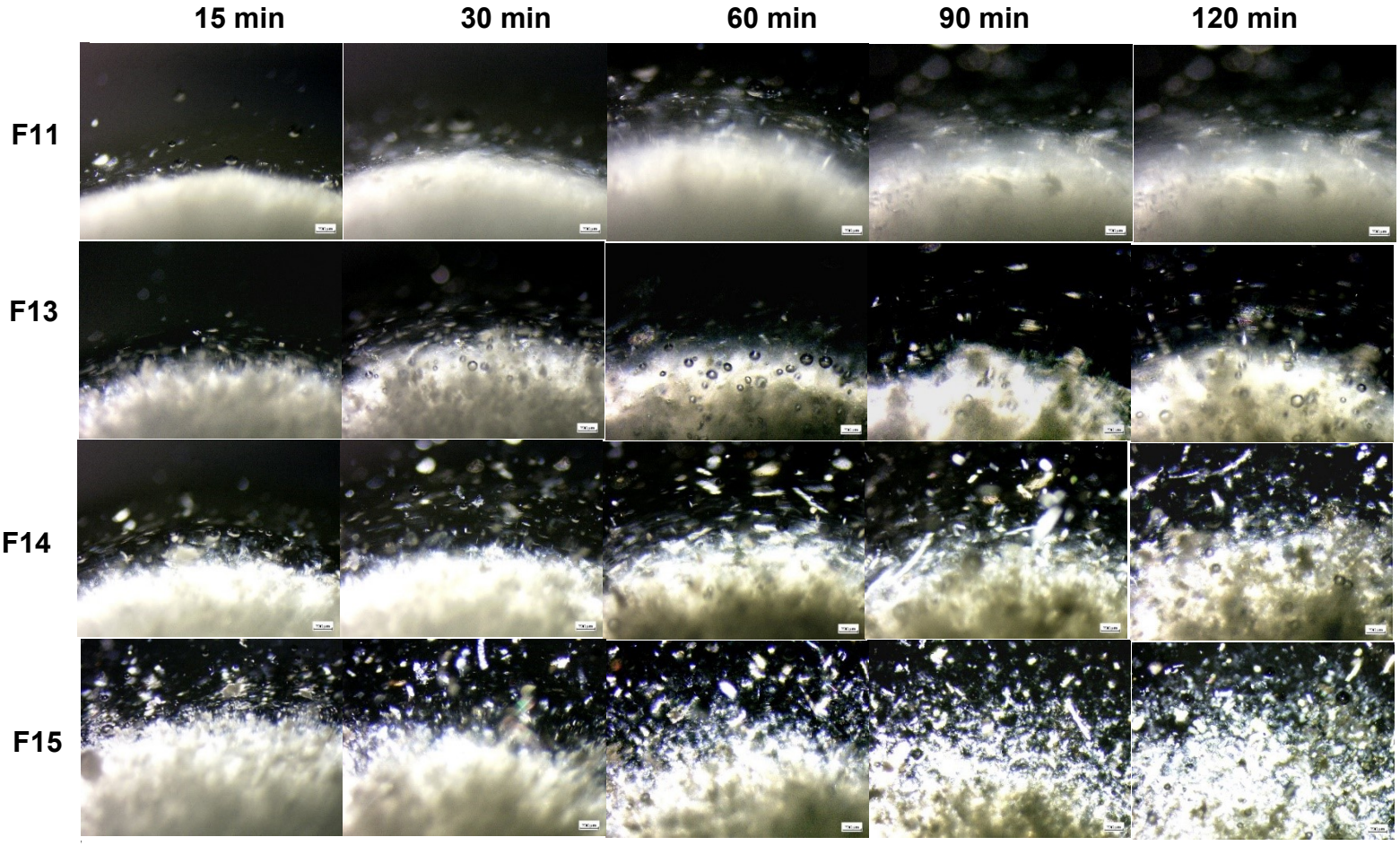

Figure 5.8 F11, F13, F14 and F15 swollen tablets morphology under polarized microscopy (using cross polarised illumination, 50x

	F11	F12	F13	F14	F15
P407	0%	15%	25%	45%	62.5%

Using the retardation plate as shown in Figure 5.9, the fragments are more visible within the hydrogel layer due to their birefringent properties, which is more obvious with F14 and F15. Moreover, rod-shaped particles can be seen in Figure 5.9 that are similar in size and shape to HPMC in Figure 5.7. Furthermore, the gel layer showed dichroic properties upon rotation to 90°.

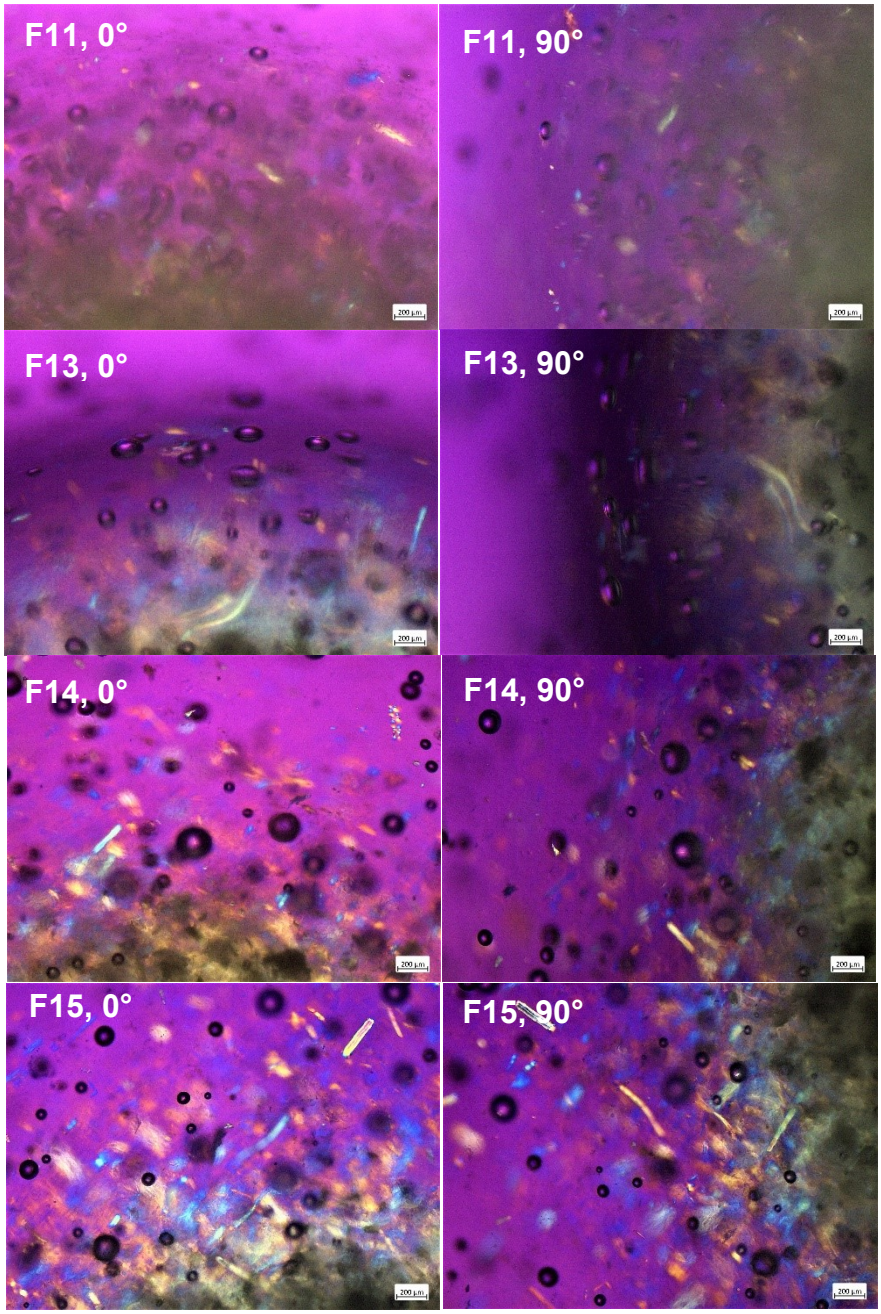

Figure 5.9 F11, F13, F14 and F15 swollen tablets morphology under polarized microscopy (using cross polarised illumination and a retardation plate, 50x).

	F11	F12	F13	F14	F15
P407	0%	15%	25%	45%	62.5%

5.3.3 In Vitro dissolution studies and dissolution efficiency

Drug release studies were investigated using App I (4.3.1.5) and using the novel method of controlling the flow rate over the tablet and the results are presented in (Figure 5.10). Generally, CHD release showed no substantial change in CHD release from F11, which is represented by 24.45%, 21.64% and 28.3% using flow rates of 0.48, 0.9 and 2mL/min, respectively, while the release using App I was 57.78%. On the other hand, almost 40% of CHD released from F15 using flow rates of 0.48 and 0.9 mL/min, by increasing the flow rate to 2 mL/min the release increased to around 68% and using App I it was nearly 95% after 2 hours.
This concludes the variability of the response of the formulations to the different flow rates, although for all formulation using App I showed the highest release.

	F11	F12	F13	F14	F15
P407	0%	15%	25%	45%	62.5%

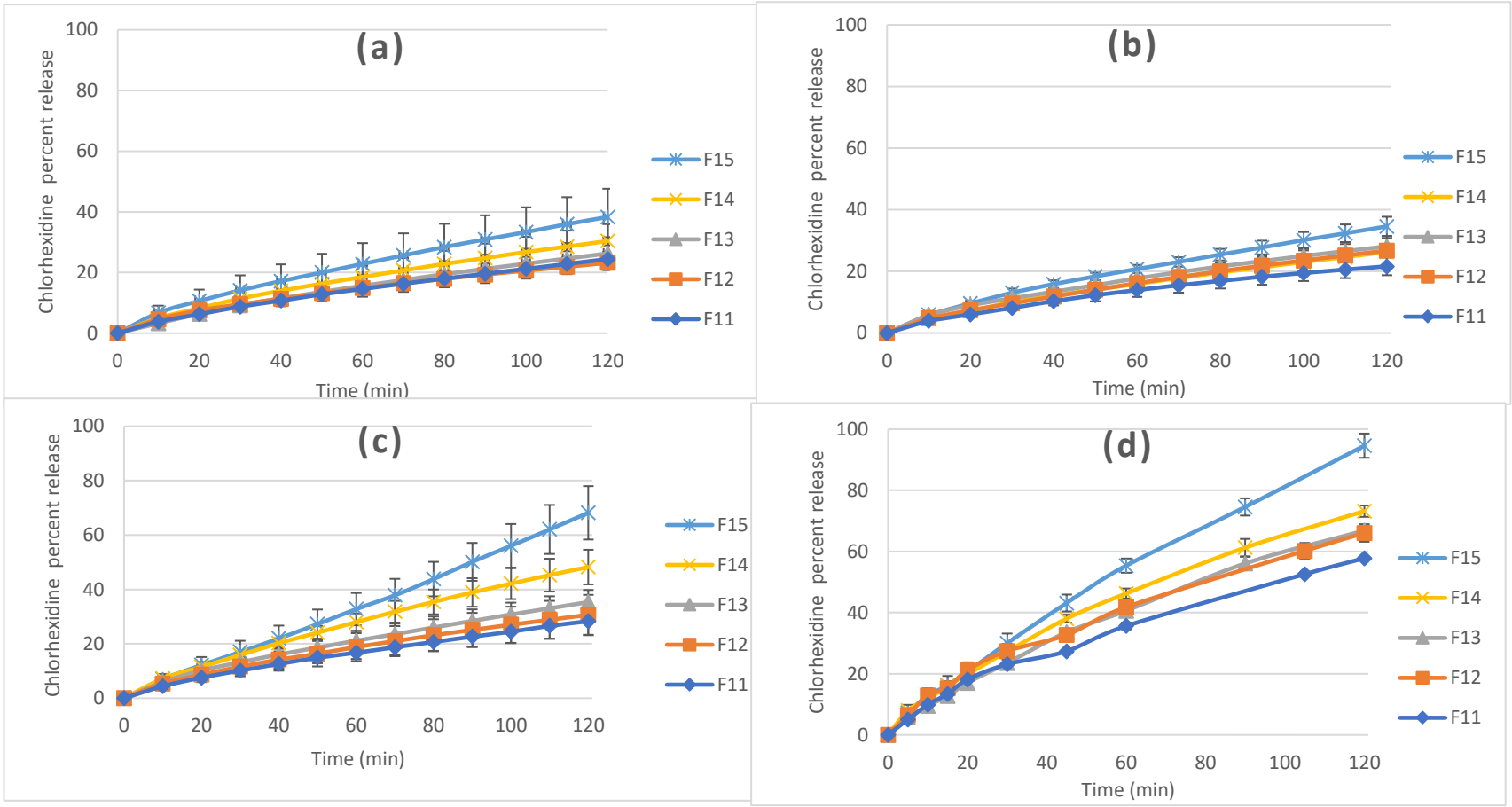

Figure 5.10 Drug release studies of chlorhexidine buccal tablet in a) flow rate 0.48 mL/min, b) 0.9 mL/min flow rate c) 2 mL/min flow rate and d) 500 mL App I (basket method) 50 RPM. Release studies were performed at 37°C for 2 hours. Data are expressed as mean percentage ± SD, n = 3.

	F11	F12	F13	F14	F15
P407	0%	15%	25%	45%	62.5%

D.E. results are displayed in Figure 5.11, highest D.E. value was achieved by using App I, due to the abundant availability of water, however, flow rates of 0.48 and 0.9 mL/min their D.E. values were minimum and comparable. However, at 2 mL/min flow rate the results were higher compared to other flow rates.

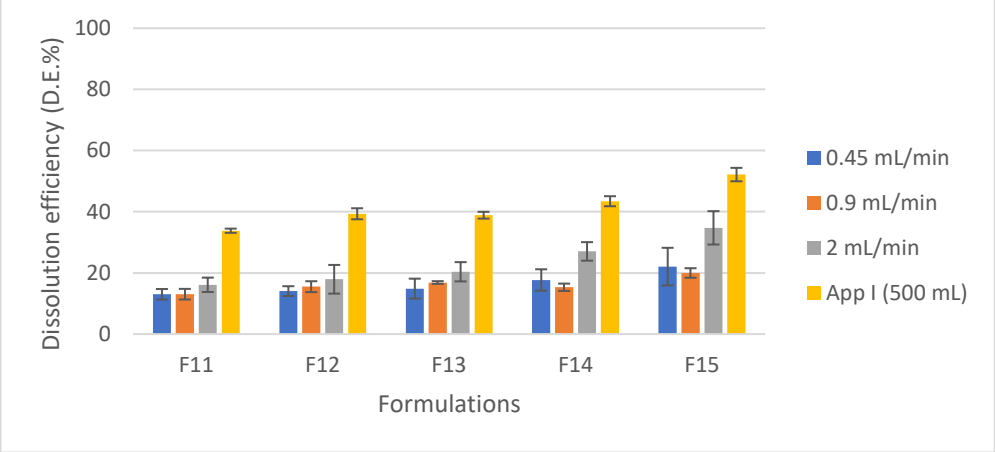

Figure 5.11 Dissolution Efficiency of CHD release using a) flow rate 0.48 mL/min, b) 0.9 mL/min flow rate c) 2 mL/min flow rate and d) 500mL App I (basket method) Data are expressed as mean ± SD, n = 3.

Statistical analysis by ANOVA two factor with replication was conducted between each two consecutive methods; P-values are listed in Table 5.2. There was no significant difference for the same formulations between the flow rate of 0.49 and 0.9 mL/min dissolution; P-Value >0.05. However, for the other two comparisons between (0.9 mL/min, 2 mL/min) and (2 mL/min, App I), there is a significant difference with a P-value < 0.05.

Table 5.2 ANOVA; two-way with replication. Sample: within the same formulation, Columns: between different formulations and the interaction, effect of the volume of the dissolution medium on the different formulations.

Comparison	**P-value**		
	Sample	**Columns**	**Interaction**
0.48 mL/min and 0.9 mL/min	0.848427	0.001102	0.552698
0.9 mL/min and 2 mL/min	7.74E-08	1.51E-08	1.86E-05
2 mL/min and App I	1.51E-15	3.66E-11	0.07217

	F11	F12	F13	F14	F15
P407	0%	15%	25%	45%	62.5%

Comparing formulations (F11-F15) intra and inter dissolution methods (Table 5.2), D.E appears to increase with increasing P407. The statistical analysis shows P-value <0.5 which means different P407 ratio influences the release of the drug for the same method. Finally, the interaction reflects the effect of the flow rate or the volume of the dissolution medium on different content of P407. The only significant difference was between 0.9 mL/mL and 2 mL/min, which means increase the flow rate from 0.9 to 2 mL/min effect differently on CHD release with the increase of P407.

Based on these results, it is concluded that the dissolution efficiency was grouped into 2 groups; group one; 0.48 and 0.9 mL/min and group two; 2 mL/min and App I. each group has the same behaviour regardless the concentration of drug released.

5.3.4 Kinetics of drug release (Model dependent methods)

The kinetics of drug release was calculated using DDsolver software (Zhang *et al.*, 2010). The coefficients of determination (R^2) are listed in Table 5.3. The best linearity was achieved with Korsmeyer-Peppas model, with n value in the range of 0.45 - 0.89. This indicates the release is anomalous which is governed by swelling and diffusion. The only formulation with n value of 0.934 > 0.89 was for F15 and 2 mL/min method, based on this result the release was zero order, and this is confirmed by R^2 of zero order and Korsmeyer-Peppas of 0.9976 and 0.9982, respectively.

	F11	F12	F13	F14	F15
P407	0%	15%	25%	45%	62.5%

Table 5.3 Coefficients of determination, using DDsolver software.

		Zero Order (R^2)	First order (R^2)	Higuchi (R^2)	Hixon Crowel (R^2)	K-Peppas (R^2)	K-Peppas (n)
500 ML	F11	0.9712 ± 0.0054	0.9833 ± 0.0067	0.9736 ± 0.0063	0.9483 ± 0.0128	0.9955 ± 0.0009	0.698 ± 0.033
	F12	0.9663 ± 0.0025	0.9854 ± 0.0028	0.9796 ± 0.0019	0.9714 ± 0.0042	0.9966 ± 0.0004	0.671 ± 0.013
	F13	09791 ± 0.0107	0.9972 ± 0.0010	0.9606 ± 0.0071	0.9942 ± 0.0030	0.9961 ± 0.0040	0.764 ± 0.029
	F14	0.9727 ± 0.0117	0.9952 ±0.0012	0.9703± 0.0105	0.9894 ± 0.0081	0.9973 ± 0.0002	0.718 ± 0.050
	F15	0.9896 ± 0.0086	0.9700 ± 0.0143	0.9475 ± 0.0190	0.9872 ± 0.0059	0.9988 ± 0.0004	0.824 ± 0.087
0.48- ML	F11	0.9809 ± 0.0183	0.9694± 0.0405	0.9678 ± 0.0205	0.9635 ± 0.0448	0.9997 ± 0.0002	0.746 ± 0.115
	F12	0.9653 ± 0.0099	0.9388 ± 0.0189	0.9863 ± 0.0059	0.9288 ± 0.0216	0.9995 ± 0.0002	0.645 ± 0.038
	F13	0.9853 ± 0.0040	0.9871 ±0.0028	0.9639 ± 0.0047	0.9821± 0.0033	0.9984 ± 0.0014	0.774 ± 0.023
	F14	0.9796 ± 0.0099	0.9771 ± 0.0131	0.9736 ± 0.0090	0.9691 ± 0.0164	0.9996 ± 0.0004	0.721 ± 0.050
	F15	0.9816 ± 0.0154	0.9819 ± 0.0185	0.9670 ± 0.0239	0.9737 ± 0.0250	0.9993 ± 0.0006	0.742 ± 0.113
0.9 ML	F11	0.9703 ± 0.0038	0.9556 ± 0.0091	0.9792± 0.0053	0.9477 ± 0.0089	0.9975 ± 0.0037	0.684 ± 0.019
	F12	0.9757 ± 0.0258	0.9559 ± 0.0622	0.9710 ± 0.0218	0.9487 ± 0.0674	0.9994 ± 0.0004	0.718 ± 0.129
	F13	0.9760 ± 0.0300	0.9120 ±0.0744	0.9803 ± 0.0201	0.8977 ± 0.0840	0.9987 ± 0.0006	0.722 ± 0.128
	F14	0.9792 ± 0.0021	0.9698± 0.0050	0.9749 ± 0.0053	0.9624 ± 0.0064	0.9989 ± 0.0017	0.708 ± 0.023
	F15	0.9801 ± 0.0054	0.9765 ± 0.0090	0.9748 ± 0.0058	0.9681 ± 0.0106	0.9992 ± 0.0008	0.710 ± 0.029
2 ML	F11	0.9806 ± 0.0150	0.9713 ± 0.0245	0.9685± 0.0216	0.9650 ± 0.0292	0.9992 ± 0.0008	0.740 ± 0.111
	F12	0.9798 ± 0.0084	0.9765 ± 0.0055	0.9745 ± 0.0078	0.9683 ± 0.0088	0.9997 ± 0.0001	0.715 ± 0.038
	F13	0.9798 ± 0.0111	0.9764 ± 0.0170	0.9716 ± 0.0125	0.9681 ± 0.0202	0.9981 ± 0.0015	0.719 ± 0.069
	F14	0.9883 ± 0.0063	0.9917 ± 0.0102	0.9590 ± 0.0163	0.9882 ± 0.0153	0.9986 ± 0.0013	0.788 ± 0.084
	F15	0.9976 ± 0.0010	0.9779 ± 0.0112	0.9254 ± 0.0176	0.9889 ± 0.0071	0.9982 ± 0.0001	0.934 ± 0.078

	F11	F12	F13	F14	F15
P407	0%	15%	25%	45%	62.5%

5.4 *In vitro* equivalence comparison

5.4.1 One-way ANOVA

One-way ANOVA results were displayed in Table 5.4, for each dissolution triplicate performed for all formulations and all methods, there was no significant difference between the triplicate according to the P-value.

Table 5.4 P-values of One-way ANOVA statistics.

Formulations	P-values			
	0.48 mL/min	0.9 mL/min	2 mL/min	App I
F11	0.97	0.45	0.41	0.99
F12	0.53	0.55	0.06	0.96
F13	0.20	0.91	0.36	0.99
F14	0.17	0.76	0.61	0.97
F15	0.05	0.76	0.45	0.97

5.4.2 Pairwise methods

i. Similarity factor(f_2)

As approved, $f_2 \geq 50$ concludes the two replicates are similar, f_2=50 represents the average of 90% equivalence between different time points of two replicates (Langenbucher, 1999). Figure 5.12 displays the values of f_2, they are equal or greater than 50 except three values, 43.99 for (F15, R2-R3 and 0.49mL/min) and 49,45 and 45,21 for (F12; R1-R3 and F15; R2-R3), respectively using 2 mL/min flow rate. The lowest value achieved between two replicates of 43.99 means the difference was less than 15%.

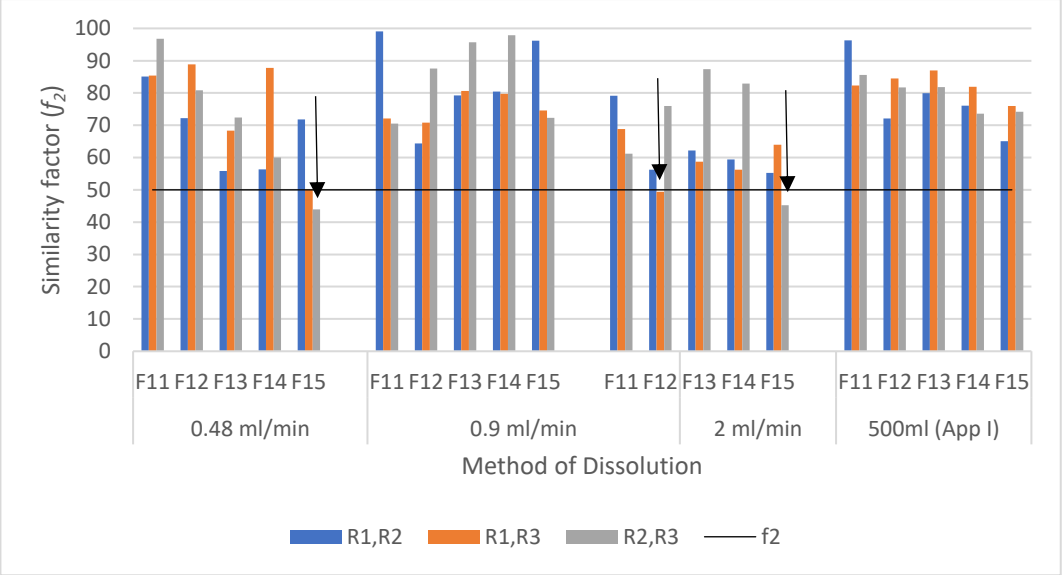

Figure 5.12 Similarity factor between two replicates of each triplicate of the dissolution data.

ii. Difference factor (f_1):

Difference factor values are displayed in Figure 5.13, the minimum difference among the four dissolutions was achieved with the standard App I, all f_1 values lies below 15 except one value of R1-R2; F15 which is equal to 15.73. The highest dissolution data f_1 values were shown for 2 mL/min flow rate, 11 values were above 15, they are ranging from 15.87 to 48.45. This followed by 0.49 mL/min; 8 values above the accepted value ranging from 21.9 to 55.28. While for the flow rate of 0.9 mL/min only 4 values were out of the acceptable range with a highest f_1 value of 23.64.

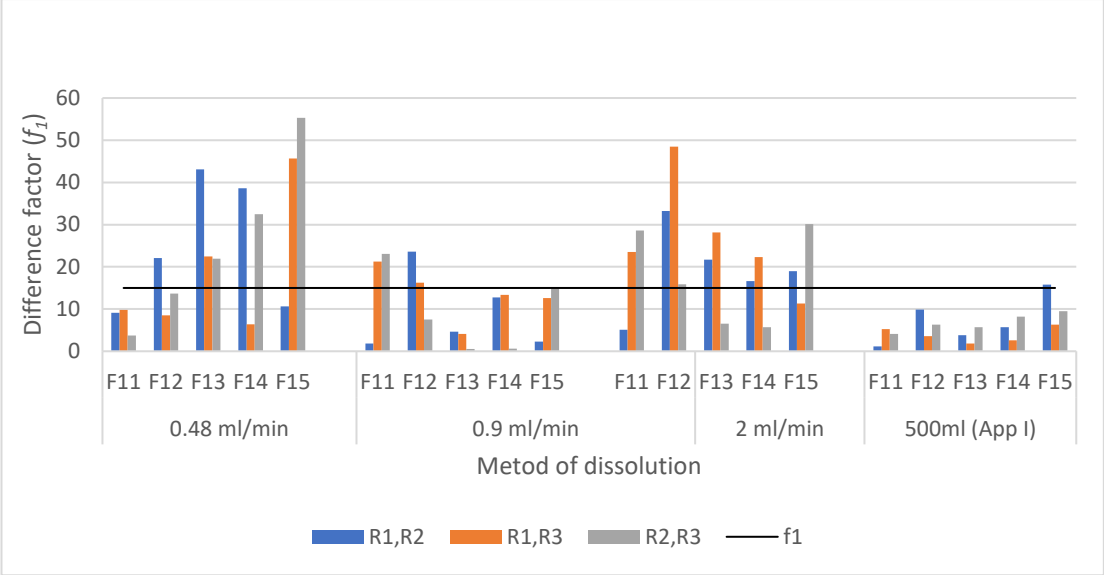

Figure 5.13 Difference factor (f_1) between the replicates of each triplicate of the dissolution data.

iii. Rescigno indices (ξ_j)

Rescigno indices for the studied formulations are displayed in Figure 5.14. There is no cut off value to decide if the two profiles are dissimilar, but the dissimilarity increases while the value approaches 1. All the results were below 0.3 and the lowest error value was shown with the standard dissolution method. Similar to f_2 and f_1 the least difference between the replicates of each formulation was for App1, followed by the 0.9 mL/min.

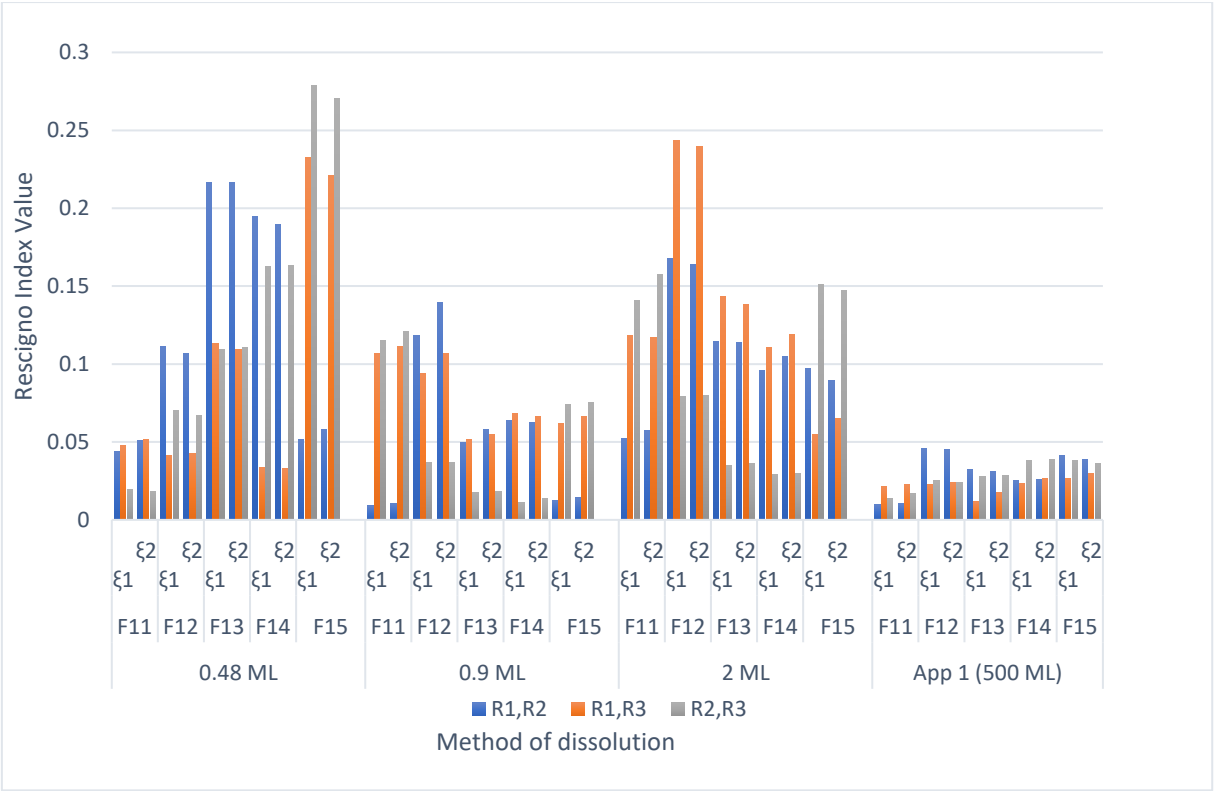

Figure 5.14 Rescigno's indices for the dissolution of the tablet with different volume of Water, R1, R2, and R3 represent the replicates of the triplicate

iv. Ratio of the area under the curve(AUC)

AUC ratios are listed in Table 5.5. The values obtained from the standard dissolution App I lies between 0.8 -1.25, one value (0.79) of 0.9 mL/min flow rate lies out of the acceptable ratio. However, for the other two flow rates, 5 and 7 ratios are out of the acceptable range.

Table 5.5 AUC Ratio for formulations replicates using App I and different flow rates method.

Formulations	0.45 ML/MIN			0.9 ML/MIN			2 ML/MIN			USPI		
	R1-R2	R1-R3	R2-R3	R1-R2	R1-R3	R2-R3	R1-R2	R1-R3	R2-R3	R1-R2	R1-R3	R2-R3
F11	0.95	1.23	1.30	1.02	0.81	0.79	0.96	1.27	1.33	1.02	1.04	1.03
F12	0.80	0.92	1.15	0.80	0.86	1.08	1.40	1.64	1.17	1.10	1.04	0.95
F13	1.55	1.26	0.81	1.04	1.05	1.02	1.25	1.33	1.07	1.05	0.99	0.95
F14	1.48	1.07	0.72	1.14	1.15	1.01	0.85	0.80	0.94	0.97	1.04	1.08
F15	0.91	1.61	1.77	0.98	1.13	1.16	0.82	1.12	1.36	1.07	0.99	0.93

5.5 Discussion

HPMC and P407 are hydrophilic polymers that form transparent hydrogels upon hydration. HPMC is commonly used in swellable hydrophilic matrices (Colombo *et al.,* 2000), while P407 is widely exploited in oral localised drug delivery for its thermo-reversible hydrogel-forming ability due to self-aggregation (Bonacucina *et al.*, 2011). Water uptake was calculated in terms of change in the absorbance of visible light with time at 37°C and hydration data showed an excellent fitting to PWL2 model. All formulations absorbed the same amount of water but at different rates Table 5.1. The fitting to the PWL2 model can be explained by zero order rate of hydration for the first linear part of the graph. The rate of hydration was also observed when measuring the area of hydrogels to the core of the tablet which was also higher for F15 than F11 (Figure 5.6). Currently, swelling index is the only method to measure the water uptake capacity. For water-soluble matrices, this process is accompanied by dissolution or fragmentation of the tablet, accordingly, the rate of water uptake cannot be identified precisely (Kavanagh and Corrigan, 2004). Light transmission was previously applied by Sarkar and Walker (1995) to measure the hydration and dehydration of solutions of HPMC and Methyl cellulose. This infrared light transmission was measured with the change of temperature and this method cannot be applied to tablets.

Based on the analysis of gel to core ratio, the opacity of the tablets decreased with the increase in P407, and this might be attributed to a lower water holding capacity of P407 compared to HPMC. This lower holding capacity might be due firstly, to its low molecular weight of 12,600 compared to 86,000 for HPMC and secondly, to its surfactant properties. The thickness of the gel layer was

previously investigated by Yang *et al.,* (1998) using texture analyser profiling. They found the thickness of the gel layers is affected by the type of the polymer and its molecular weight, for both polyethylene oxide and HPMC when investigated individually. Polarized microscopy images were obtained for the boundary of the core material and within the gel layer. The results showed the fragmentation of the core under cross-polarized illumination (Figure 5.8), which was increased with the increasing of P407 ratio. Retardation plate was applied, to enhance the birefringent properties of the fragments, Figure 5.9 shows the birefringent fragments and presumed HPMC particles embedded in the gel layer. Moreover, the latter had a dichroic property by rotating to 90° the colour and the intensity of the gel layer change from pink to violet which may be attributed to the weak birefringent properties of the gel layer. From polarized microscopy images (Figure 5.8 and Figure 5.9) it is assumed that upon hydration, P407 hydrated first, expanded and formed a gel layer which apparently decreased in the homogeneity with the increase in the P407 ratio. This might also be accompanied by the hydration and swelling of small particles of HPMC. The big particles of the latter take more time to hydrate, due to its lower surface area to particle size ratio and it can be seen clearly in the gel layer. Earlier investigations were used to monitor HPMC matrices swelling using confocal microscopy in the presence of fluorescence markers either embedded in the matrix or added externally to the swelling media. Adler *et al.,* (1999) used non-diffusive latex microspheres loaded with Nile red. They found that the external gel layer continues in expanding even after the core of the tablet is hydrated. Bajwa *et al.,* (2006) used Congo red an external fluorescence stain and monitored HPMC matrix under different NaCl concentration. They found the increase in the salt concentration resulted in the

decrease in the swelling and increase in the erosion. The advantages of polarised microscopy over the confocal microscopy in monitoring the matrices is that no marker is added and the morphology of swollen polymers can be tracked (Figure 5.8Figure 5.9).

The main objective of the *in vitro* dissolution testing is to analyse the release of the drug from the tablets, and this is performed by using conventional dissolution testing (Apparatuses I and II), using 500 -1000 mL of the dissolution media. However, *in vivo* dissolution of buccal tablets is affected by the limited volume of saliva (Azarmi and Löbenberg, 2007). For this reason, three different flow rates were investigated in this work and to the best of our knowledge, the effect of the flow rate on drug release has not been investigated previously.

Dissolution data showed that CHD release from formulations F11 to F15 was sensitive to the flow rate or the volume of the dissolution medium and to the P407 ratio in the tablets. There was approximately 33% and 56% increase in the release from F11 and F15, respectively, using 0.48 mL/min flow rate and App I. Moreover, formulations with high percentages of P407 (F14 and F15) showed greater CHD dissolution in response to the change in flow rate. This is attributed to their higher rate of hydration observed in (Table 5.1 and Figure 5.3). In addition, higher P407 ratio resulted in a looser fragmented core as noticed in polarized microscopy images (Figure 5.9 and Figure 5.9) and facilitating CHD release, this may be due to the high hydrophilic properties of P407 (Dumortier *et al.*, 2006).

Attempts have been made to develop new methods to analyse localised drug release to the oral cavity by using small volumes of dissolution medium. For instance, Mohammed and Khedr (2003) performed the dissolution of

mucoadhesive sustained release buccal tablet in a shaking water bath using 10 mL dissolution medium. A similar study was performed using 22 mL of dissolution medium in a modified Franz diffusion cell (Ìkinci *et al*., 2004). Another (Mumtaz and Ch'ng, 1995), design involved a small cell chamber contains tablet and water recirculated from the dissolution apparatus to the cell at a speed of 4 mL/min. In these methods, tablets were immersed in the dissolution media, unlike the developed flow rate method which simulates drug release in the oral cavity.

Although all formulation showed a similar swelling index after two hours (5.2 to 4.7 for F11 and F15, respectively), there was a greater CHD release with a higher P407 ratio over time, can be explained by increasing tablet erosion or dissolution with continuous swelling associated with higher the P407 ratio (Dürig, and Fassihi, (2002)

To validate drug release based upon different flow rates, statistical equivalence analysis was performed for the drug release using the three different methods and compared with the release using the standard App I (BP, 2018 b). The three different rates were chosen to simulate the release of the drug under different salivary flow rates (Cho *et al*., 2010). The effect of the different flow rates and App I (500 ml) on drug release was investigated using D.E.. By applying ANOVA (2-way with replication), there was no significant difference in D.E. between the flow rates of (0.48 and 0.9 mL/min). However, this is not applicable to other comparisons (9 mL/min with 2 mL/min) and for (2 mL/min with App I) (Table 5.2). This indicates that CHD release was increased by increasing the flow rate >0.9 ml/min. This indicates that patients with xerostomia or of low salivary flow rate will have less drug release compared to the patients with normal salivary flow rate (Cho *et al*., 2010).

Statistical analyses were performed for each triplicate to explore how consistent the drug release was for each formulation using the three different flow rate methods compared to App I. The statistical analysis using two-way ANOVA confirmed that there was no significant difference between each triplicate for the tested formulations and the four methods (Table 5.4). There are dissimilarities when comparing between each two replicates of the tablets using one way ANOVA, the consistency in the dissolution data was ranked as follows App 1> 0.9 mL/min> 0.2 and 0.48 mL/min.

The high consistency of the standard dissolution App I, might be attributed to the full immersion of the tablet in the dissolution medium, accompanied by basket rotation (BP, 2018 b), facilitating tablet swelling, erosion and then dissolution. There was only one value of f_1 out of the acceptable range, and this confirms the uniformity of the tablets.

The results of 0.9 mL/min flow rate; showed a higher equivalence over the other two flow rates, this is explained by the constant flow rate of 9 mL/min with no variation. Out of 15 comparisons per test, there is one value of AUC ratio and four values out of the acceptable values.

While for the 0.48 mL/min and 2 mL/min, the exact flow rates were 0.48 ± 0.5 and 2 ± 0.5 mL/min. Although this has been considered in the calculation of the concentration, it may contribute to the inequivalences between the replicates. The number of values out of range for the AUC ratio, f_1 and f_2 were (5,8,1) and (6,11,2) for 0.48 and 2 mL/min, respectively. Nafee *et al*., (2003) found variability of *in vivo* drug release data resulting in a high standard deviation, which resulted from different salivary flow rate and cheek movement.

Based on the above analyses both the volume and variation of flow rate affect the release of CHD from the matrix tablets. Moreover, the kinetics of drug release was anomalous with a best fitting to a Korsmeyer-Peppas model.

5.6 Conclusion

The study of the rate of water uptake provide a further understanding of the CHD release from the hydrophilic matrix tablets, and it has a strong relationship with the gelling of the tablet which converts the tablet to a porous structure and facilitates CHD release.

Moreover, the use of different methods of dissolution with different flow rates or volume of the dissolution medium affected drug release. The higher flow rate or higher volume increases drug release. Although some of the equivalent analytical methods showed some variation among some formulations, it showed good compliance with other tests. This proves that the rate of CHD release from the hydrogel tablet is likely affected by salivary flow with greater CHD being delivered at a higher flow rate. Furthermore, P407 accelerate hydrogel formation by increasing the rate of water uptake by the tablets, via its faster hydration rate.

Moreover, drug release under a limited volume of dissolution medium as in patients with xerostomia has not been taken into consideration in the standard dissolution method. To our knowledge, there is no method which simulates the release of CHD locally in the oral cavity based on different flow rates. The above attempts showed promising results to investigate drug release for localised oral drug delivery, however, formulations need to be further adjusted to improve CHD release and the dissolution method needs to be further optimised to exclude unfavourable variation.

Chapter Six

Formulation development and dissolution adjustment

Chapter 6 : Formulation development and dissolution adjustment

In the current chapter, sorbitol mannitol and xylitol were added to improve the taste perception of the tablets, especially they have a non-cariogenic properties, and due to their ability to relief oral dehydration. Their effect was investigated on the physical properties and drug release of CHD mucoadhesive buccal tablet. Three groups of formulations were prepared each contains one of the sugars with HPMC and poloxamer.

6.1 Materials and methods

Tablet formulations were prepared using CHD, P407, HPMC, sorbitol, mannitol and xylitol.

6.2.1 The morphology of sorbitol, mannitol and xylitol.

SEM images were performed as explained in 4.2.1.3. for the three polyols.

6.2.2 Formulations and charectarisation of the tablets

Three groups of formulations were prepared, each group had sorbitol or mannitol or xylitol with HPMC and P407. Two different ratios of P407: HPMC and two ratios of the polyols were considered, resulting in four tablets per formulation. The dosage of CHD was 2.5 mg and was based on the microbiology and cytotoxicity studies.

6.2.2.1 Tablet formulations

CHD mucoadhesive tablets were prepared as shown in Table 6.1. The powders were blended for 15 minutes in V-shaped powder blender (CapsulCN). Mg St 0.5% was added and mixed for three minutes before pressing.

Table 6.1 formulation of CHD mucoadhesive tablets with Sorbitol or mannitol or xylitol.

Formulations	Ratio P407: HPMC: Sugar alcohol	CHD	P407	HPMC	Sorbitol or Mannitol or Xylitol	Tablet weight
		mg				
S1, M1, X1	2:2:1	2.5	14	14	7	37.5
S2, M2, X2	2:2:2		14	14	14	44.5
S3, M3, X3	3:1:1		21	7	7	37.5
S4, M4, X4	3:1:2		21	7	14	44.5

6.2.2.2 Melt granulation

The tablet blend was placed in 100 mL beaker and placed in a prewarmed water bath at 57°C and mix with a spatula for 1-3 minutes. Then removed and placed in a high shear mixer for 10 seconds to dismantle the big clumps. The granules were left to cool and then passed through a 1 mm sieve (mesh no. 18). Then collected and characterised for flowability and morphology. Magnesium stearate was added to the granules and mixed for 3 min in the V blender prior pressing into tablets.

6.2.2.3 Powder Flow properties and compressibility

Performed as explained in 4.1.2.3.

Flow through an orifice

The flow rate of the powders and granules was measured by passing 12 g through 10, 15 and 25 mm diameter orifices using ERWEKA Granulate & Powder Flow Tester, Type GTL, Germany, the results were displayed in g/sec.

6.2.2.4 Preparation and characterisation of CHD buccal tablets

Tablets were pressed as explained in 4.1.2.4

Tablets Characterisation has been performed a described earlier; for Friability 4.1.2.5, Tensile strength 4.1.2.6, content uniformity and mass variation 4.1.2.7, Ex-vivo mucoadhesion 4.1.2.8, Swelling Index 4.1.2.9, tablet morphology 4.1.2.10, Dissolution test (type I apparatus) 4.1.2.11, FTIR and DSC 4.1.2.14, Rate of hydration 5.2.2.1, Image analysis 5.2.2.2 and Analysis of dissolution profiles 5.2.2.4.

6.2.2.5 XRD analysis

X-ray diffractometry (PANalytical empyrean X-ray diffractometer, Netherland) was used to analyse the crystallinity of the various tablet ingredients, physical mixture, granules for selected formulations. The samples were analysed from 5-80°, at a 2θ range, and diffraction patterns recorded using Cu-Kα x-ray radiation source.

6.2.2.6 SEM/EDX mapping

Electron dispersive X-ray analysis was conducted to investigate the spatial distribution of the elements on the sample. Images were acquired by SEM equipped with electron dispersive detector which detects the x-ray of the

elements. In the current work, it was performed to show the spatial distribution of nitrogen atoms which is only available in CHD in the investigated formulations. This shows the distribution of the drug on the surface of the tablets.

6.2.2.7 In Vitro dissolution under controlled flow rate (CFR)

CFR method was developed from the previous method described in 5.2.2.3, due to the variation of the achieved results in the latter, the method was further developed aiming to get more reproducible results. In the current work, the dissolution was performed under a constant flow rate (1mL/min) for two hours. The aim of this investigation was to mimic the salivary flow rate in the oral cavity.

Figure 6.1 illustrates the set-up of the CFR method, ultrapure water was used as a dissolution media and placed in a Schott bottle inside a water bath set at 37°C. The flow rate of water was controlled using a peristaltic pump at 1mL/min. The tablet was adhered with one drop of water on a pre-weighed sample holder (the head of a plastic Pasteur pipette cut into two pieces) and placed in a beaker in the water bath, this followed by starting the dissolution experiment for two hours. Samples of 10 mL were collected every 10 minutes and measured using UV-VIS spectrophotometer at λ_{254}.

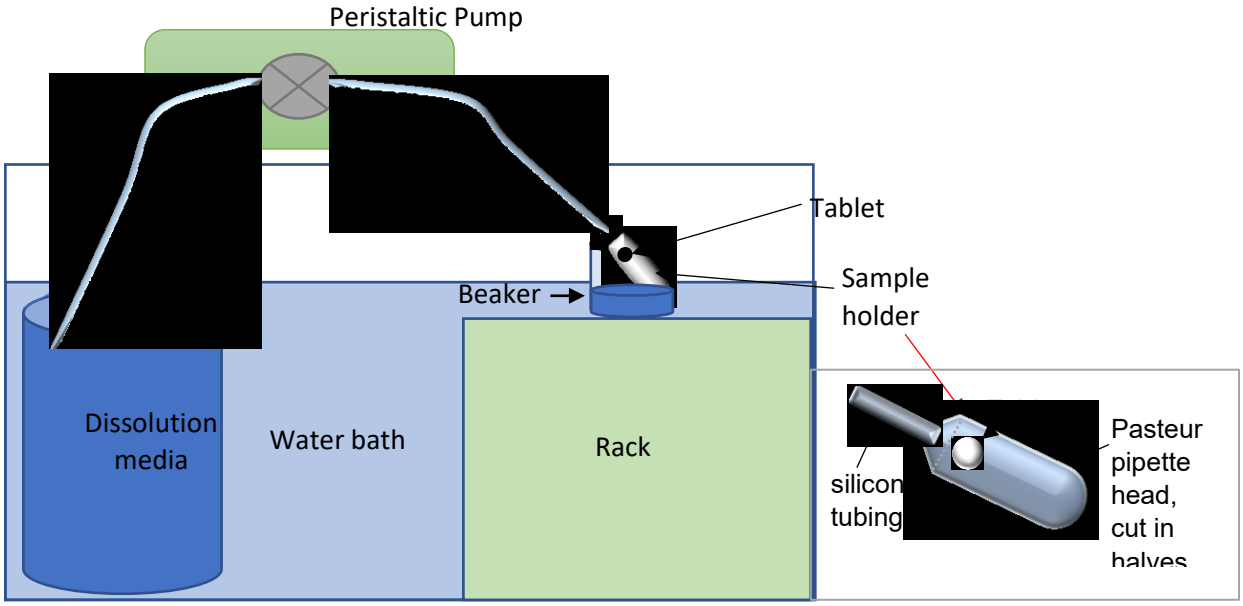

Figure 6.1 Diagram illustrating drug release using CFR method.

6.2.2.8 Tablet erosion

Tablet erosion was investigated to measure the weight of the tablet after swelling and dissolution studies using CFR method, tablets were dried in the oven at 37°C for 24-48 hours and the erosion percentage (*E%)* was calculated based on the following equation

$$E\% = \frac{W_0 - W_e}{W_0} \times 100 \qquad \textit{Equation 19}$$

Where W_0 is the initial weight of the tablet and W_e is the dried weight of the tablet after swelling or dissolution.

6.2.2.9 Kinetics of drug release

Kinetics of drug release was performed as explained in 4.1.2.13 for zero order, first order, second order, Higuchi, Hixon Crowell, Korsmeyer-Peppas models and Hopfenberg model. The latter is an empirical model used to describes drug release from erodible matrices (Costa and Lobo, 2000), it was used to investigate

CHD release from formulation prepared with sorbitol, mannitol and xylitol. Non-linear fitting was performed based on Equation 20 using DDsolver software.

$$F = 100 \times [1 - (1 - K_{Bt} \times t)^n] \qquad \textit{Equation 20}$$

Where F is the fraction per cent of drug released at time t.

K_{Bt} is the combined constant, and it can be obtained from Equation 21

$$K_{Bt} = K_0/(C_0 \times a_0) \qquad \textit{Equation 21}$$

C_0 is the initial concentration of drug in the matrix, and a_0 is the initial radius for a sphere or a cylinder or the half thickness for a slab; n is 1, 2, and 3 for a slab, cylinder, and sphere, respectively.

To examine the best fitting model, the Akaike Information Criterion (AIC) was obtained using DDsolver software, it is used to measure the goodness of fitting, the lowest value of AIC shows the best fitting (Govender *et al*., 2005).

6.2.2.10 Hydration kinetics

Tablet hydration was performed as explained in hydration 5.2.2.1.

Based on the shape of the figures obtained from the Bioscreen C spectrophotometric plate reader, the data were fitted to piecewise linear regression 2 (PWL2) model, exponential and two-phase exponential model. AIC was calculated to find the best fit model. The analysis was performed using Originpro software.

6.3 Result and discussion

6.3.1 Characterization of raw materials

The morphology of CHD, HPMC and P407 was displayed in 4.3.1.2. Figure 6.2 shows the morphology of sorbitol mannitol and xylitol granules. Sorbitol granules were more spherical followed by mannitol then xylitol.

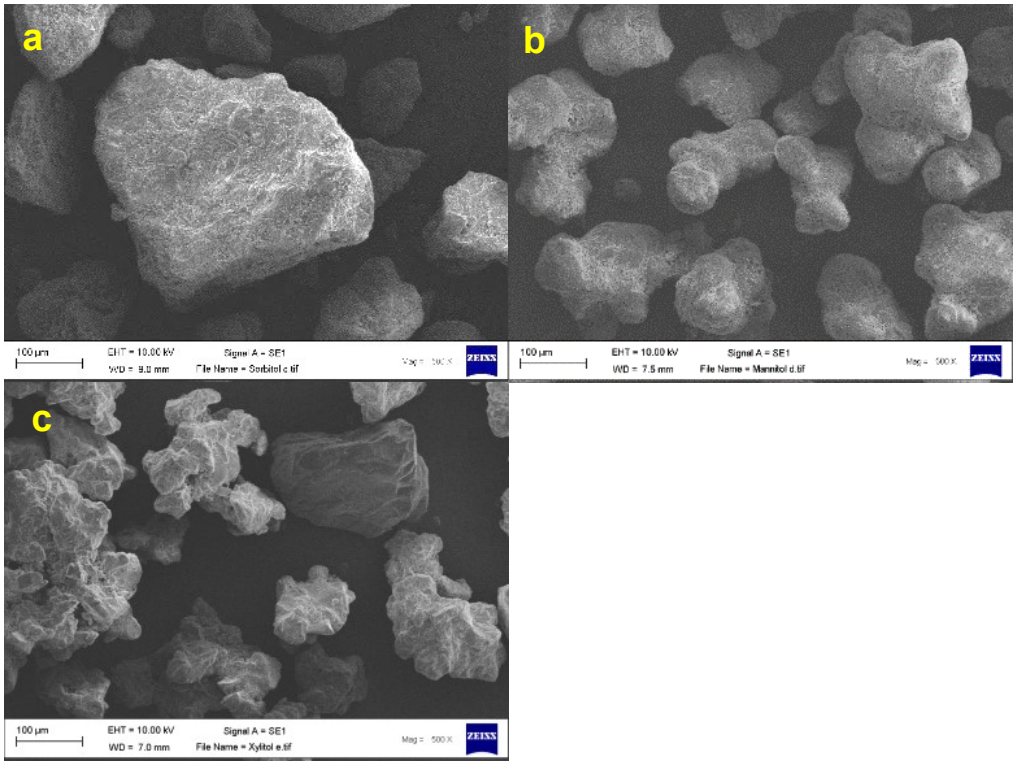

Figure 6.2 SEM images of a- Sorbitol b- mannitol and c-xylitol, x500.

6.3.2 Characterization of tablet blends and granules

The flowability of powder formulation blends varied from ‘poor’ to ‘very very poor’ (Table 4.3). Melt granulation improved the flow properties of all formulations to passable, except X3 showed ‘poor’ flowability and S2 and S4 showed ‘good’ flowability.

Table 6.2 Compressibility index (CI%) and Hausner ratio for tablet bend before and after granulation for sorbitol (S), mannitol (M) and Xylitol (X) formulations,

Formulations	Powder Blends		Granules			
	CI%	Flow Character	HR	CI%	Flow Character	HR
S1	30.81 ± 0.87	Poor	1.45 ± 0.02	20.72 ± 0.61	Fair, passable	1.26 ± 0.10
S2	37.20 ± 0.073	Very poor	1.59 ± 0.02	20.57 ± 2.05	Fair, passable	1.26± 0.03
S3	40.07 ± 0.66	Very very poor	1.67 ± 0.02	12.50 ± 0.00	Good	1.14 ± 0.00
S4	29.60 ± 0.37	poor	1.42 ± 0.01	11.81 ± 0.16	Good	1.13 ± 0.00
M1	39.11 ± 1.32	Very very poor	1.64 ± 0.04	20.86 ± 1.04	Fair, passable	1.26 ± 0.02
M2	34.97 ± 4.23	Very poor	1.54 ± 0.10	22.72 ± 1.09	Passable	1.29 ± 0.02
M3	35.43 ± 3.81	Very poor	1.55 ± 0.09	21.79 ± 1.43	Passable	1.28 ± 0.02
M4	39.47 ± 2.70	Very very poor	1.65 ± 0.08	21.81 ± 1.42	Passable	1.28 ± 0.02
X1	39.50 ± 2.09	Very very poor	1.65 ± 0.06	22.76 ± 1.05	Passable	1.29 ± 0.02
X2	39.87 ± 1.66	Very very poor	1.66 ± 0.02	22.32 ± 1.74	Passable	1.29 ± 0.03
X3	39.32 ± 1.65	Very very poor	1.65 ± 0.04	27.46 ± 1.37	Poor	1.38 ±0.03
X4	41.55 ± 3.57	Very very poor	1.72 ± 0.10	22.88 ± 1.26	Passable	1.30 ± 0.02

	S1, M1, X1	S2, M2, X2	S3, M3, X3	S4, M4, X4
P407: HPMC: polyols	2:2:1	2:2:2	3:1:1	3:1:2

Sorbitol (S), Mannitol (M), Xylitol (X)

The flow of the powders and granules was further investigated using flow through the orifice of different diameter 15, 20 and 25 mm. Powder blends failed to pass through all orifice sizes, however, Figure 6.3 and **Error! Reference source not found.** shows the successful passability of the granules through the three orifice sizes.

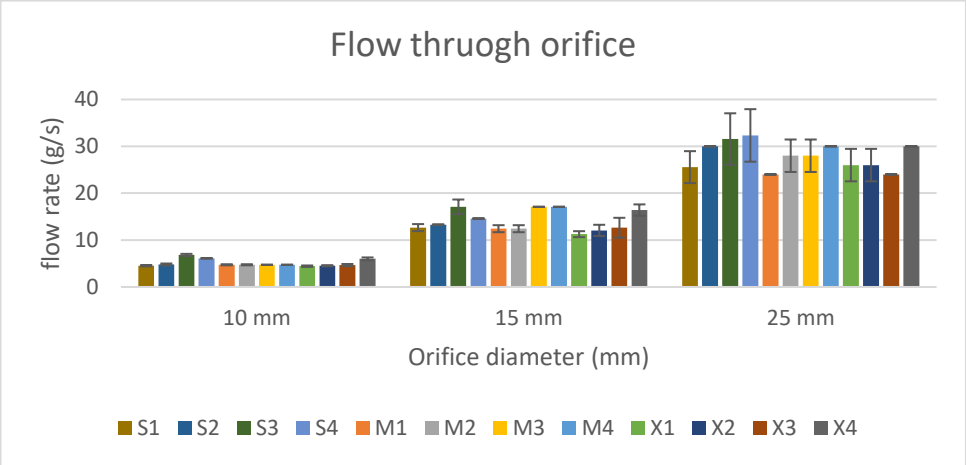

Figure 6.3 Flow rate (g/sec) of sorbitol(S), mannitol (M) and xylitol (X) granules through 10, 15 and 25 mm orifice sizes. Data are expressed as mean ± SD, n = 3.

The morphology and the surface morphology of the granules were depicted using SEM images, and all granules were semi-spherical with HPMC component particles being distinguished by their distinctive rod shape (Figure 6.4). This is also observed in Figure 6.5, which additionally shows the surface of the granules was more smooth at low P407 ratio and the granules with the higher P407 ratio were more grainy in morphology.

	S1, M1, X1	S2, M2, X2	S3, M3, X3	S4, M4, X4
P407: HPMC: polyols	2:2:1	2:2:2	3:1:1	3:1:2

Sorbitol (S), Mannitol (M), Xylitol (X)

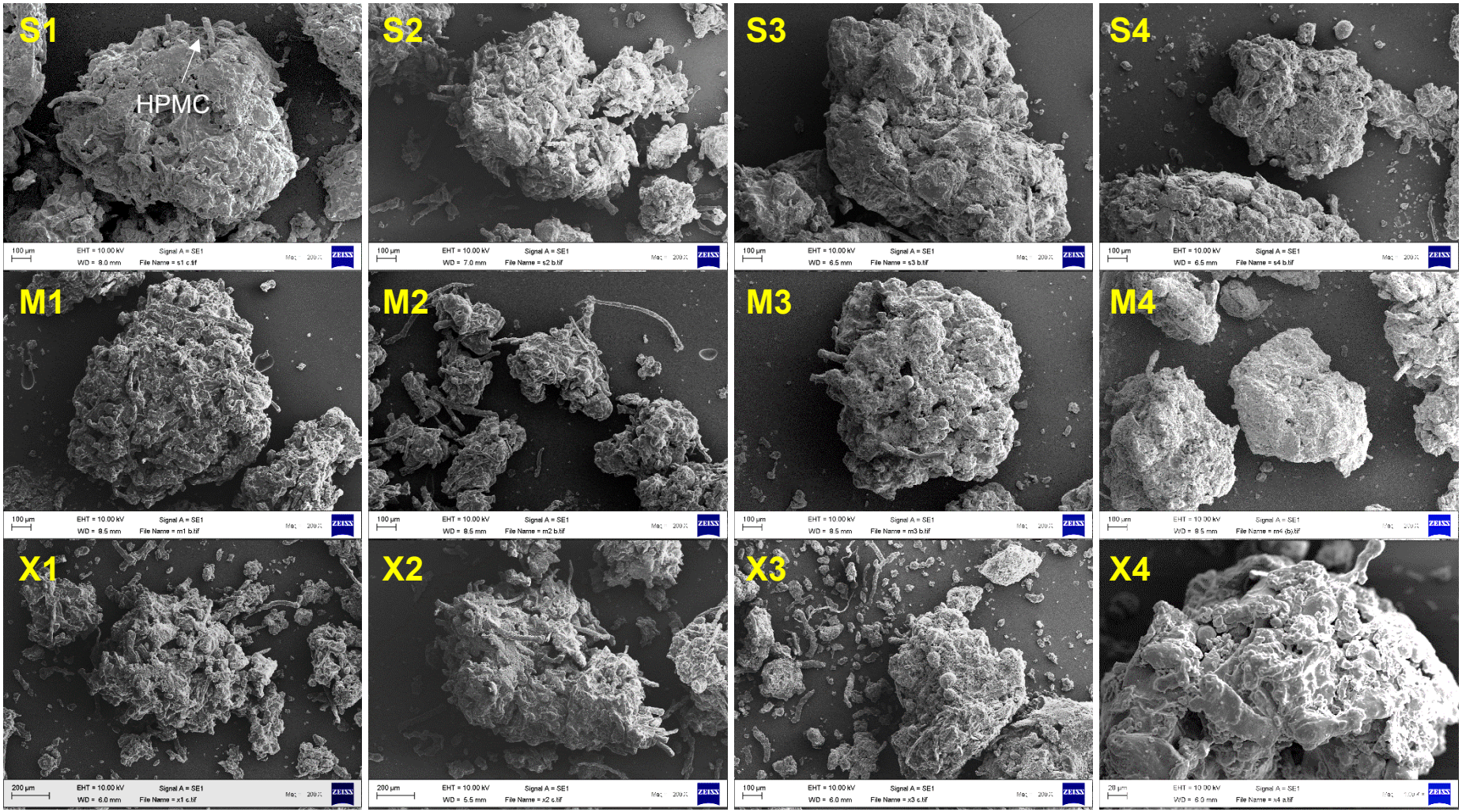

Figure 6.4 SEM images of CHD formulations using sorbitol, mannitol and xylitol, 200x.

	S1, M1, X1	S2, M2, X2	S3, M3, X3	S4, M4, X4
P407: HPMC: polyols	2:2:1	2:2:2	3:1:1	3:1:2

Sorbitol (S), Mannitol (M), Xylitol (X)

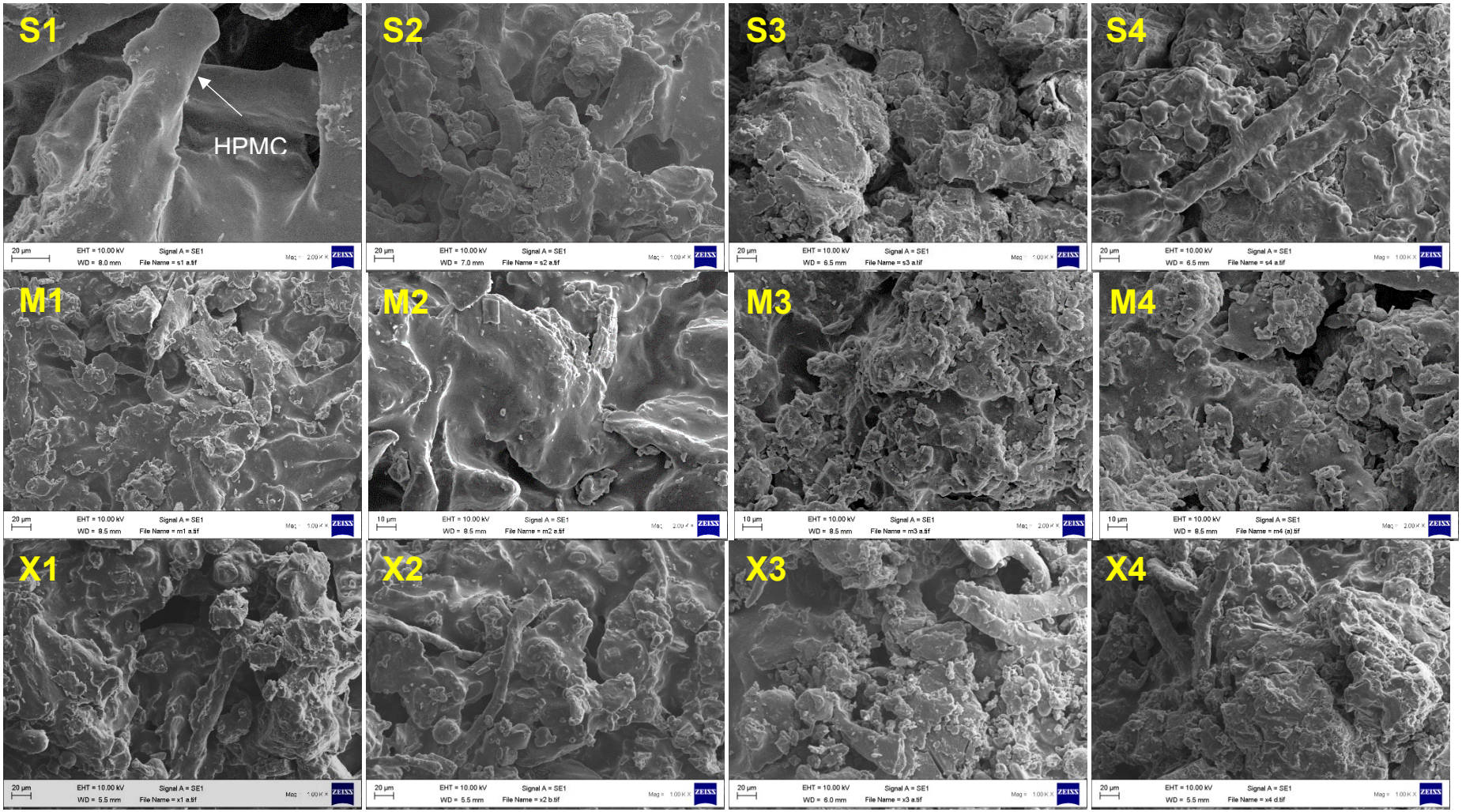

Figure 6.5 SEM images of CHD formulations using sorbitol, mannitol and xylitol, 1000x.

	S1, M1, X1	S2, M2, X2	S3, M3, X3	S4, M4, X4
P407: HPMC: polyols	2:2:1	2:2:2	3:1:1	3:1:2

Sorbitol (S), Mannitol (M), Xylitol (X)

6.3.3 Physical properties of the tablets

The physical properties of the prepared tablets are presented in Table 4.4. The tablets showed an acceptable level of friability; less than 1%, acceptable weight variation (none of the 20 tablets deviate from 90-110% of the average weight) and content uniformity (none of the 10 tablets deviate from 85-115% of the average content). Tensile strength was ≤1, both sorbitol and mannitol showed higher tensile strength than xylitol formulations. Two way-ANOVA with replications showed a significant difference of the tensile strength between each two group of formulations (sorbitol and mannitol, sorbitol and Xylitol, and mannitol and Xylitol) with a p-value <0.5, which means that at the investigated ratios, the type of polyol affect tablet hardness.

	S1, M1, X1	S2, M2, X2	S3, M3, X3	S4, M4, X4
P407: HPMC: polyols	2:2:1	2:2:2	3:1:1	3:1:2

Sorbitol (S), Mannitol (M), Xylitol (X)

Table 6.3 Physical characteristics of CHD mucoadhesive buccal tablets (n = 10 ± SD).

	Average Weight* (mg)	Diameter (mm)	Height (mm)	Thickness (mm)	Hardness (N)	Tensile Strength (MPa)	Friability** (%)	Average Content (mg)
S1	36.77 ± 0.05	5.96 ± 0.03	1.58 ± 0.05	0.99 ± 0.21	12.21 ± 3.54	1.03 ±0.29	0.00	2.38 ± 0.12
S2	44.14 ± 1.44	5.98 ± 0.02	1.77 ± 0.05	1.31 ± 0.07	12.54 ± 3.66	0.80 ± 0.23	0.07	2.49 ± 0.09
S3	36.16 ± 1.45	5.94 ± 0.03	1.57 ± 0.04	0.97 ± 0.12	10.68 ± 3.35	0.90 ± 0.28	0.17	2.23 ± 0.07
S4	43.58 ± 1.16	5.96 ± 0.01	1.77 ± 0.04	1.29 ± 0.09	12.94 ± 2.06	0.85 ± 0.14	0.01	2.50 ± 0.07
M1	38.06 ± 1.16	5.97 ± 0.04	1.72 ± 0.10	1.25 ± 0.24	8.82 ± 4.13	0.63 ± 0.35	0.19	2.58 ± 0.13
M2	43.28 ± 2.14	5.97 ± 0.02	1.82 ± 0.03	1.23 ± 0.11	14.01 ± 2.57	0.94 ± 0.16	0.08	2.46 ± 0.16
M3	36.06 ± 1.47	5.97 ± 0.03	1.60 ± 0.05	1.03 ± 0.60	12.05 ± 2.7	0.96 ± 0.22	0.33	2.46 ± 0.06
M4	43.43 ± 2.24	5.99 ± 0.02	1.84 ± 0.05	1.36 ± 0.08	14.21 ± 3.21	0.88 ± 0.18	0.26	2.64 ± 0.15
X1	38.06 ± 1.16	5.97 ± 0.03	1.73 ± 0.09	1.20 ± 0.08	4.80 ± 1.93	0.37 ± 0.06	0.26	2.64 ± 0.12
X2	42.34 ± 1.57	5.98 ± 0.03	1.76 ± 0.04	1.32 ± 0.07	10.29 ± 1.55	0.67 ± 0.11	0.10	2.47 ± 0.09
X3	37.81 ± 1.25	5.96 ± 0.02	1.68 ± 0.03	1.29 ± 0.15	8.23 ± 2.50	0.56 ± 0.17	0.23	2.38 ± 0.08
X4	42.82 ± 1.31	5.97 ± 0.02	1.77 ± 0.03	1.31 ± 0.07	11.37 ± 3.24	0.74 ± 0.21	0.08	2.44 ± 0.07

*n=20 tablets

** Friability was performed with 1g of tablets

	S1, M1, X1	S2, M2, X2	S3, M3, X3	S4, M4, X4
P407: HPMC: polyols	2:2:1	2:2:2	3:1:1	3:1:2

Sorbitol (S), Mannitol (M), Xylitol (X)

6.3.4 SEM/EDX mapping

Elemental mapping was performed to explore the homogeneity or the distribution of the drug on the surface of the tablet. Since atomic nitrogen is only available in the chemical structure of CHD within the formulation, its availability is linked to CHD molecules. The results (Figure 6.6) show that CHD is distributed over the surface of all tablets and often available as small clusters.

	S1, M1, X1	S2, M2, X2	S3, M3, X3	S4, M4, X4
P407: HPMC: polyols	2:2:1	2:2:2	3:1:1	3:1:2

Sorbitol (S), Mannitol (M), Xylitol (X)

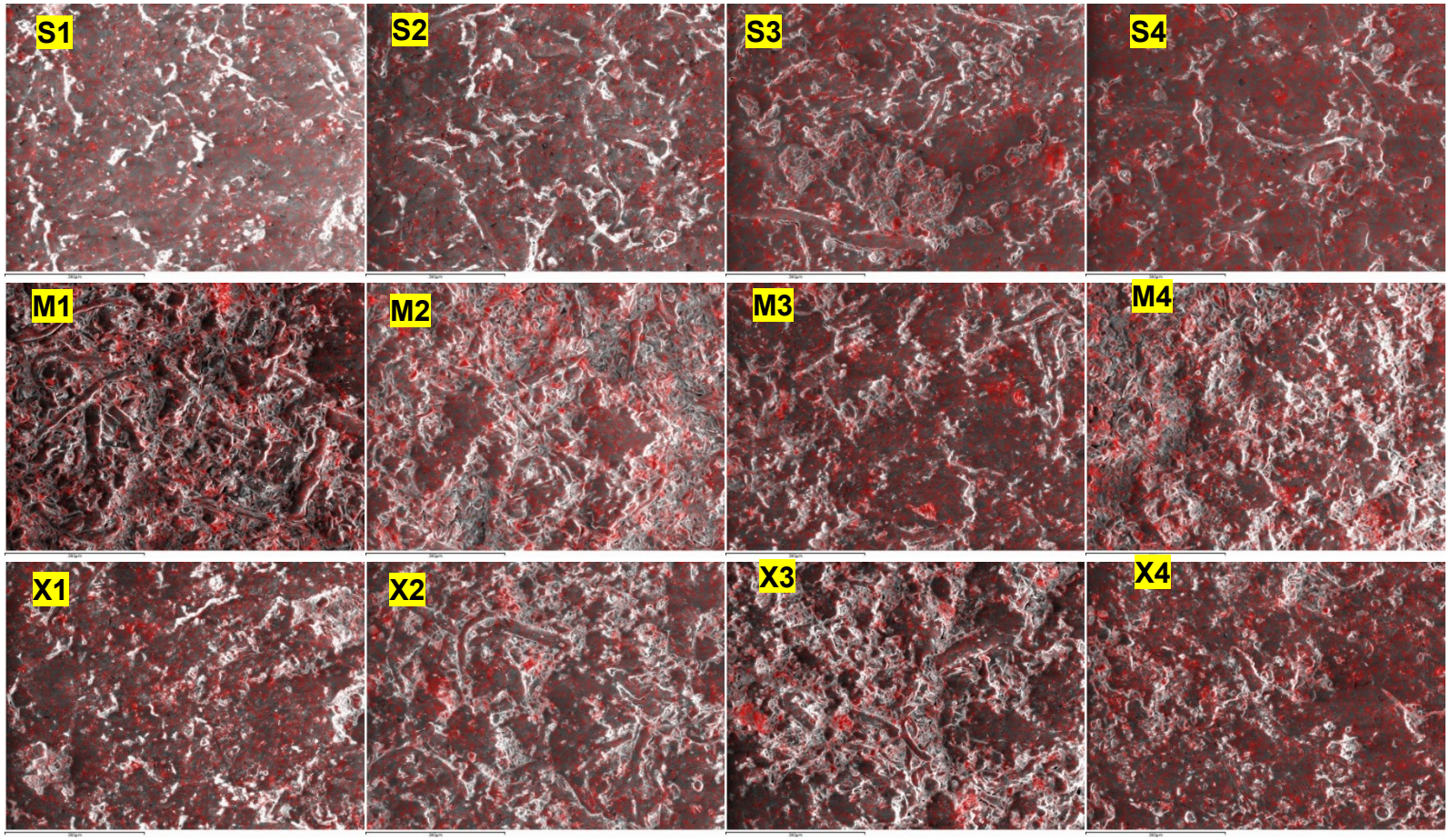

Figure 6.6 SEM/EDX images of CHD mucoadhesive buccal tablets showing the presence of nitrogen (in CHD) in red on the tablets surfaces (x 500), scale bar is 300 µm.

	S1, M1, X1	S2, M2, X2	S3, M3, X3	S4, M4, X4
P407: HPMC: polyols	2:2:1	2:2:2	3:1:1	3:1:2

Sorbitol (S), Mannitol (M), Xylitol (X)

6.3.5 *Ex vivo* mucoadhesion

Initially, the residence time of the tablet on the chicken pouch was tested using the disintegration apparatus. The tested tablets have successfully adhered to the chicken pouch as it was repeatedly immersed in the aqueous media for two hours using the disintegration tester, which represents the ideal residence time of the designed tablets in the buccal cavity. Figure 6.7 shows S4, M4 and X4 tablets after two hours.

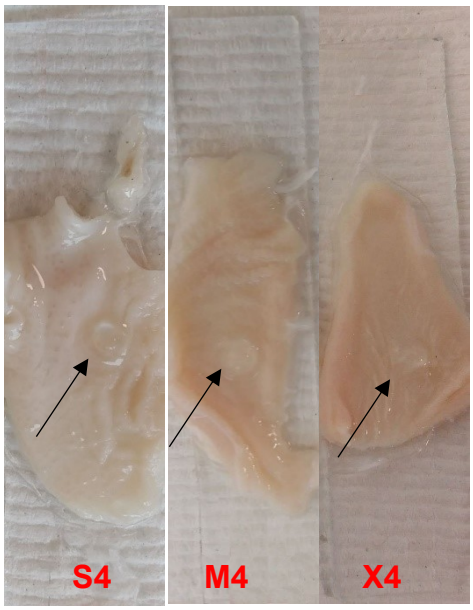

Figure 6.7 S4, M4 and X4 after two-hour Ex-Vivo mucoadhesion using disintegration apparatus, arrows showing the hydrogel tablet after two hours.

Furthermore, the force of detachment of the mucoadhesive tablet was performed to investigate the effect of HPMC, P407 and the polyols ratios on the force of detachment. Generally, mannitol formulations showed a higher force of detachment, whereas increasing xylitol in the formulations showed a negative effect on the mucoadhesion, sorbitol showed a similar effect of xylitol but to a less extent (Figure 6.8). Statistical analysis for each formulation group was performed

	S1, M1, X1	S2, M2, X2	S3, M3, X3	S4, M4, X4
P407: HPMC: polyols	2:2:1	2:2:2	3:1:1	3:1:2

Sorbitol (S), Mannitol (M), Xylitol (X)

using one-way ANOVA. No significant difference was found between mannitol formulations $p>0.05$, however, both sorbitol and xylitol showed a significant difference $p<0.05$.

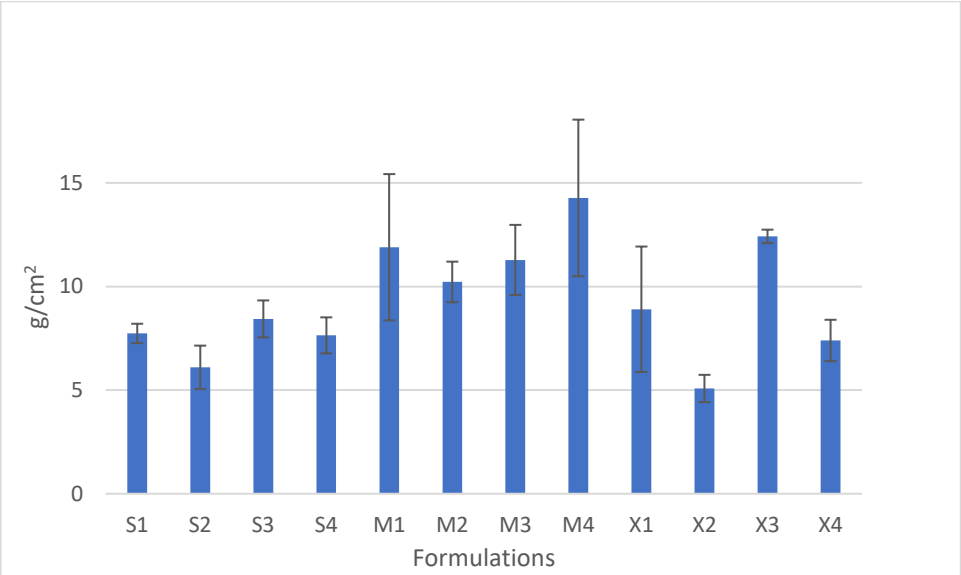

Figure 6.8 Force of detachment of CHD formulations containing sorbitol, mannitol and xylitol from the chicken pouch at 37°C. Data are expressed as mean ± SD, n = 3.

6.3.6 Swelling index (SI)

The swelling of CHD tablets using different polyols is displayed in Figure 6.9, all formulations showed an initial rapid swelling during the first 30 minutes followed by a slower rate of swelling for the followed 90 minutes. S4, M4 and X4 showed SI of 3 after 2 hours, however, S1, M1 and X1 showed swelling of 3.8, 4.2 and 4.4, respectively, which is statistically not significant based on two-way ANOVA analysis. All other formulations showed swelling of 3.4 to 3.6.

	S1, M1, X1	S2, M2, X2	S3, M3, X3	S4, M4, X4
P407: HPMC: polyols	2:2:1	2:2:2	3:1:1	3:1:2

Sorbitol (S), Mannitol (M), Xylitol (X)

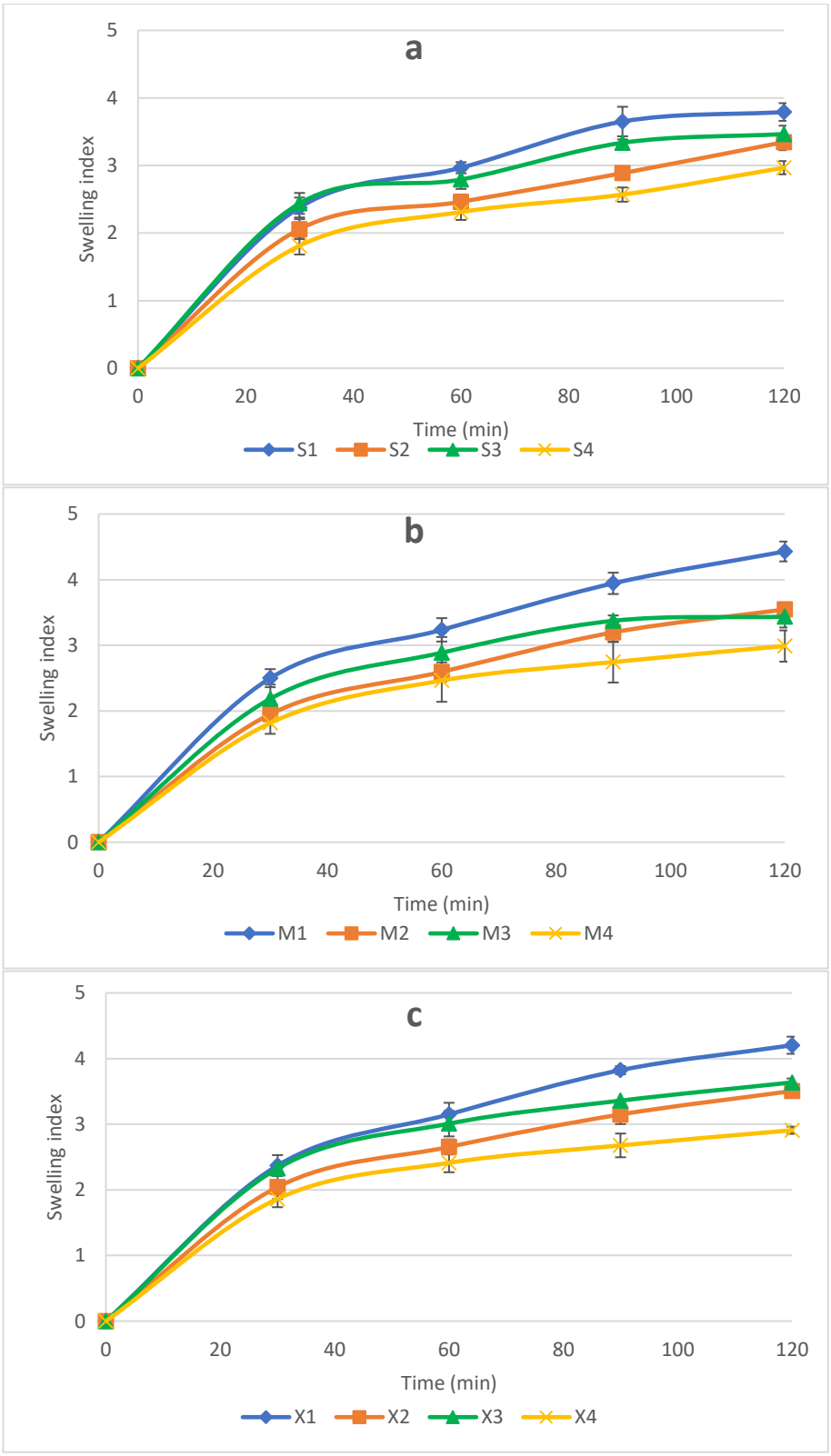

Figure 6.9 Swelling index of CHD containing a-sorbitol, b-mannitol and c-xylitol in ultrapure water and at 37 °C. Data are expressed as mean ± SD, n = 3.

	S1, M1, X1	S2, M2, X2	S3, M3, X3	S4, M4, X4
P407: HPMC: polyols	2:2:1	2:2:2	3:1:1	3:1:2

Sorbitol (S), Mannitol (M), Xylitol (X)

Tablet erosion after swelling

Tablet erosion percentages (*E%)* (Table 6.4) generally increased with the increase of both P407 and sugar alcohol. This can be explained by increasing the solubility attributed to the increase in the hydrophilicity of the tablets.

Table 6.4 Erosion percentage from tablets after two hours swelling, Data are expressed as mean percentage ± SD, n = 3.

Formulations	E%
S1	26.50 ± 0.39
S2	38.43 ± 0.69
S3	50.94± 5. 14
S4	50.36 ± 3.95
M1	28.90 ± 2.55
M2	30.06 ± 2.46
M3	40.81 ± 1.61
M4	43.54 ± 4.71
X1	28.99 ± 4.05
X2	37.42 ± 2.32
X3	39.65 ± 1.56
X4	48.63 ± 1.23

6.3.7 The Internal morphology of the tablets after swelling

All formulations successfully formed a porous structure (Figure 6.10), although formulations with high P407 ratio were very fragile after freeze-drying, and pores were damaged during tablets cutting.

	S1, M1, X1	S2, M2, X2	S3, M3, X3	S4, M4, X4
P407: HPMC: polyols	2:2:1	2:2:2	3:1:1	3:1:2

Sorbitol (S), Mannitol (M), Xylitol (X)

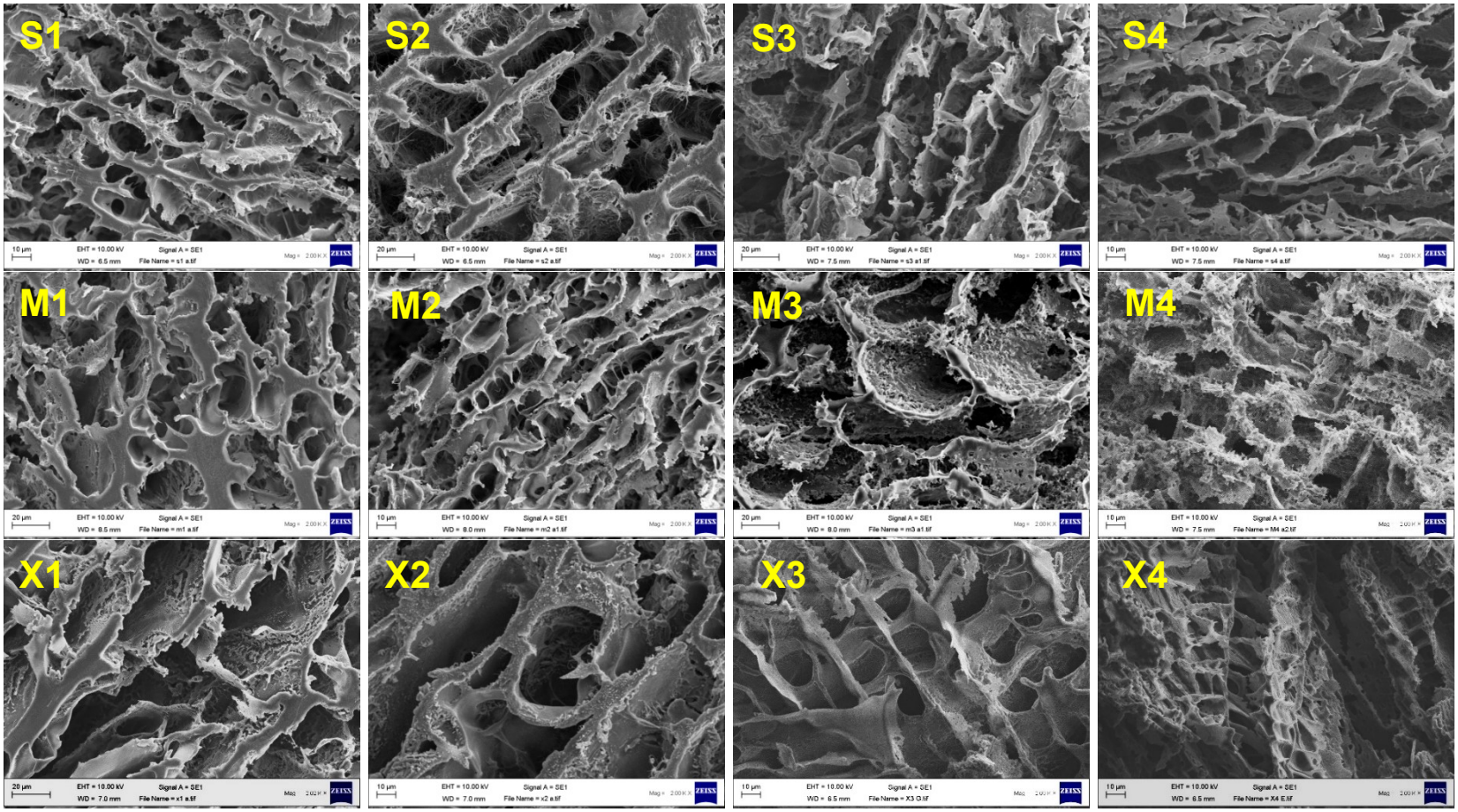

Figure 6.10 SEM images showing the porous structure of the freeze dried swollen tablets containing sorbitol, mannitol and xylitol, 2000x.

	S1, M1, X1	S2, M2, X2	S3, M3, X3	S4, M4, X4
P407: HPMC: polyols	2:2:1	2:2:2	3:1:1	3:1:2

Sorbitol (S), Mannitol (M), Xylitol (X)

6.3.8 Rate of hydration

Tablets hydration was performed using Bioscreen C plate reader, the change in the hydration was recorded as a change in the absorbance, Figure 6.11 shows both the raw data obtained from Bioscreen spectrophotometer and after calculating the water absorbed by the tablets as explained in 5.2.2.1. It is obvious. The results show that tablet hydration was affected mainly by the P407: HPMC ratio rather than the polyols, probably because the polymers turn into hydrogels with different degrees of transparency whereas polyols dissolve to form a colourless solution upon hydration.

	S1, M1, X1	S2, M2, X2	S3, M3, X3	S4, M4, X4
P407: HPMC: polyols	2:2:1	2:2:2	3:1:1	3:1:2

Sorbitol (S), Mannitol (M), Xylitol (X)

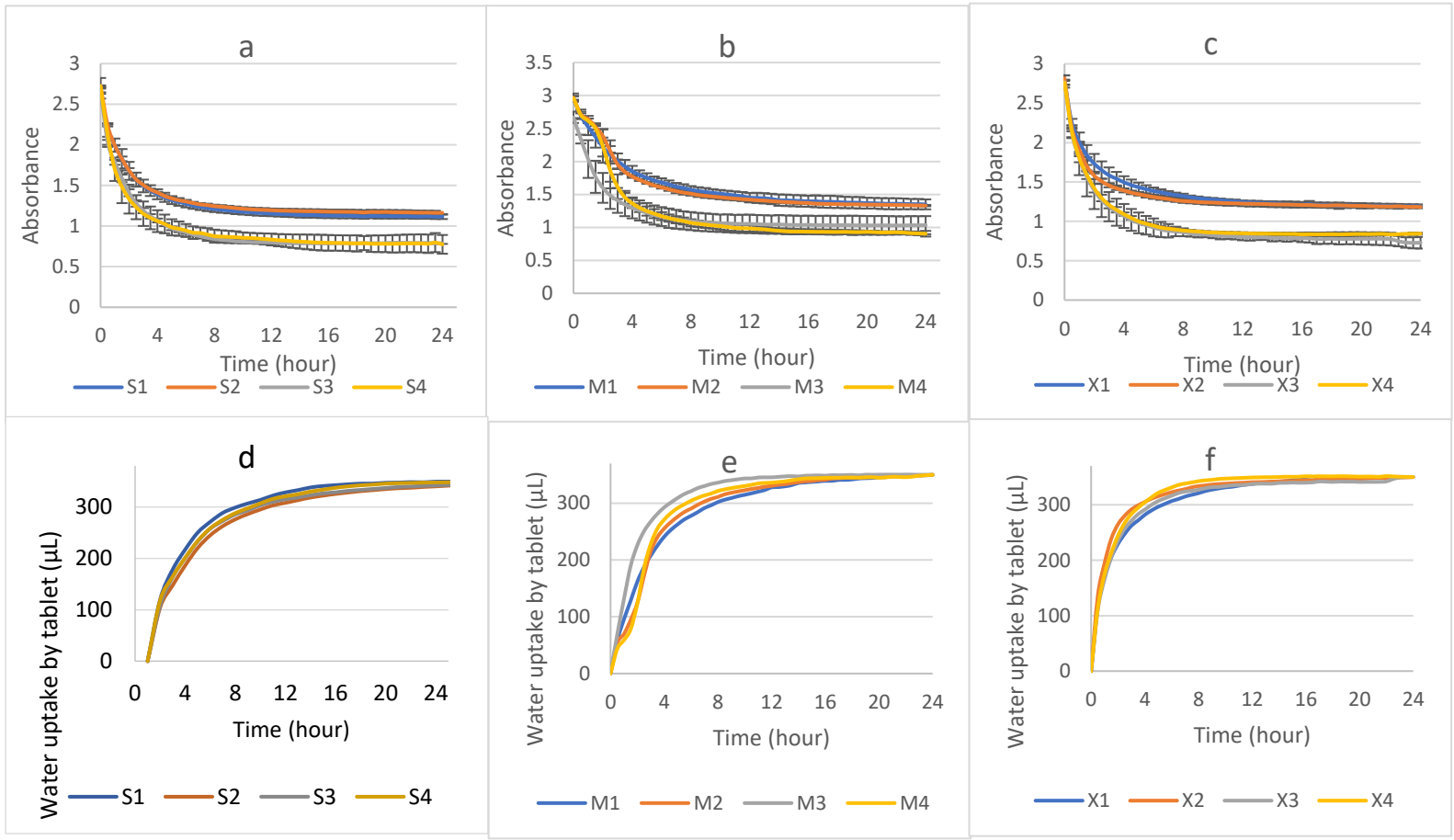

Figure 6.11 Bioscreen C data of optical density change with time, for a- sorbitol, b-mannitol and c-xylitol formulations. Hydration curves of d-sorbitol, e-mannitol and f-xylitol formulations with time for 24 hours at 37°C. Data are expressed as mean ± SD, n = 3.

	S1, M1, X1	S2, M2, X2	S3, M3, X3	S4, M4, X4
P407: HPMC: polyols	2:2:1	2:2:2	3:1:1	3:1:2

Sorbitol (S), Mannitol (M), Xylitol (X)

Three models were used for the fitting of the hydration curve, PWL2, exponential and two-phase exponential, Both PWL2 and two-phase exponential has two rates (Table B 2), however, the exponential model has one rate. The best fitting based on the regression coefficient (R^2) was for the two-phase exponential (Table 6.5), fitted curves are displayed in Figure A 2.

Table 6.5 Hydration data fitting, R^2 using PWL2, exponential, two-phase exponential and biphasic exponential association models.

Formulations	R^2		
	PWL2	**Exponential**	**Two-phase exponential**
S1	0.963	0.991	0.999
S2	0.962	0.991	0.999
S3	0.952	0.992	0.998
S4	0.959	0.984	1.000
M1	0.980	0.996	1.000
M2	0.989	0.991	0.992
M3	0.968	0.997	1.000
M4	0.988	0.983	0.996
X1	0.950	0.975	1.000
X2	0.958	0.980	0.999
X3	0.958	0.989	0.999
X4	0.955	0.994	1.000

AIC was calculated using Originpro software were used to find the best fitting for the exponential and the two-phase exponential model, AIC values were 172 and -18, respectively. This means the best fitting to two-phase exponential due to lower AIC value.

	S1, M1, X1	S2, M2, X2	S3, M3, X3	S4, M4, X4
P407: HPMC: polyols	2:2:1	2:2:2	3:1:1	3:1:2

Sorbitol (S), Mannitol (M), Xylitol (X)

6.3.9 Evaluation of tablet gelation by Image analysis

Gelling efficiency

Photographic images were obtained by a digital camera, they were analysed to monitor the conversion of the glassy tablet to a hydrogel (rubbery) and from these, the core and hydrogel areas were measured/determined (Figure 6.12). Both Sorbitol and xylitol formulations showed a comparable behaviour, 3:1:1 and 3:1:2 formulations, showed complete loss of the integrity of the glassy core and formed hydrogel tablets after 30 minutes. Mannitol formulations took more than 90 minutes for the same ratios. For the lower P407 ratio, all tablets required a longer time ≥90 minutes for the former and ≥120 for the latter to completely, form hydrogels which were influenced by the type of sugar alcohol, although the time decreased with the increase in the sugar ratio.

	S1, M1, X1	S2, M2, X2	S3, M3, X3	S4, M4, X4
P407: HPMC: polyols	2:2:1	2:2:2	3:1:1	3:1:2

Sorbitol (S), Mannitol (M), Xylitol (X)

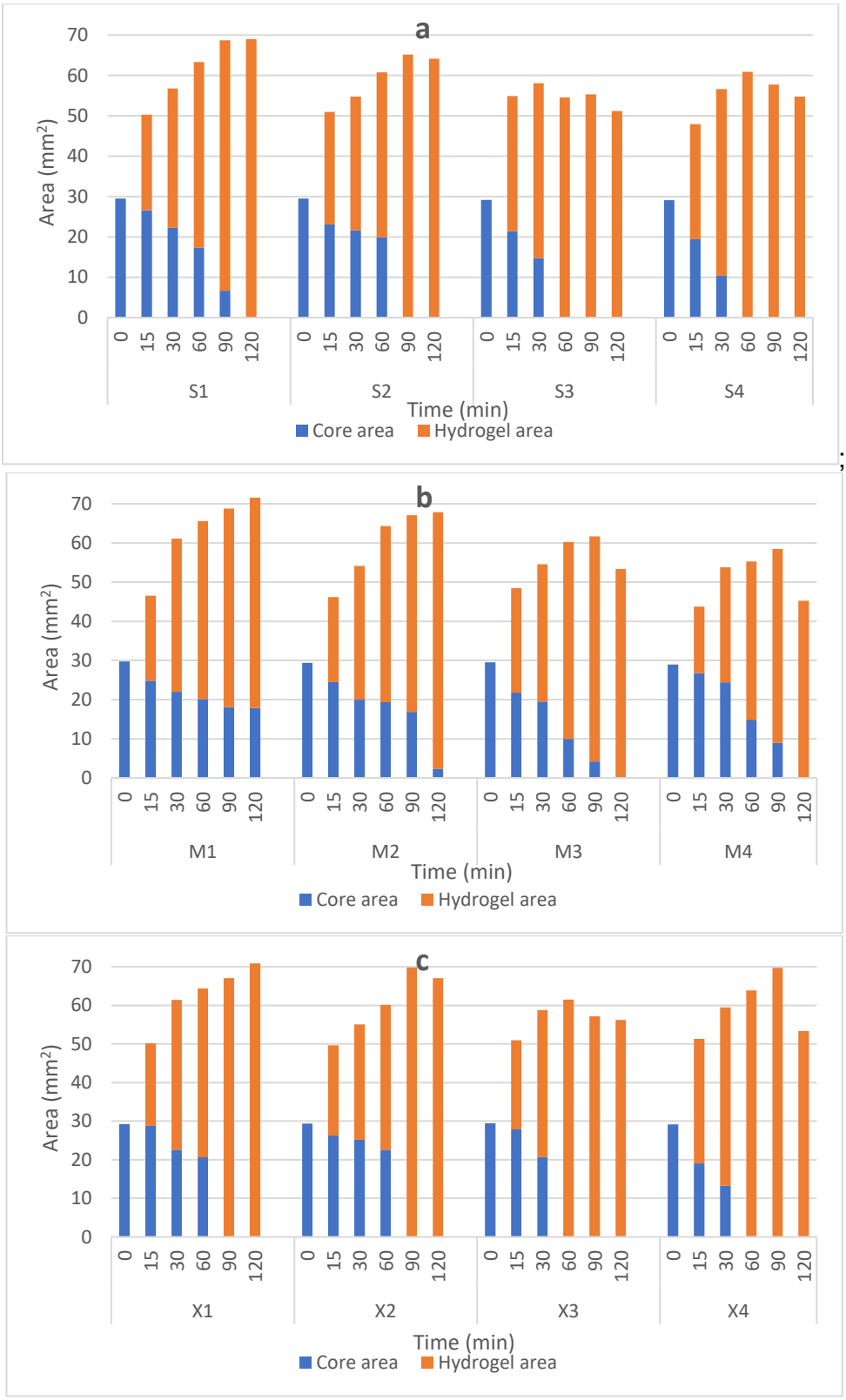

Figure 6.12 Image analysis results for a-Sorbitol (S), b-mannitol(M) and c-xylitol(X) formulations, showing the planner area of both the core and the hydrogel layer at 37°C after 2 hours gelation.

	S1, M1, X1	S2, M2, X2	S3, M3, X3	S4, M4, X4
P407: HPMC: polyols	2:2:1	2:2:2	3:1:1	3:1:2

Sorbitol (S), Mannitol (M), Xylitol (X)

Polarized microscopy imaging

Polarized microscopy was explored for visualising tablet hydration, gelling and fragmentation, in order to potentially interpret gel imagery (and particularly fragments) the components of the tablets were first analysed. Images were obtained for CHD and the excipients, they all have anisotropic birefringent properties (Figure 6.13) under cross polarized light (darkfield), which improved by using a retardation plate or λ (red) quarter waveplate.

	S1, M1, X1	S2, M2, X2	S3, M3, X3	S4, M4, X4
P407: HPMC: polyols	2:2:1	2:2:2	3:1:1	3:1:2

Sorbitol (S), Mannitol (M), Xylitol (X)

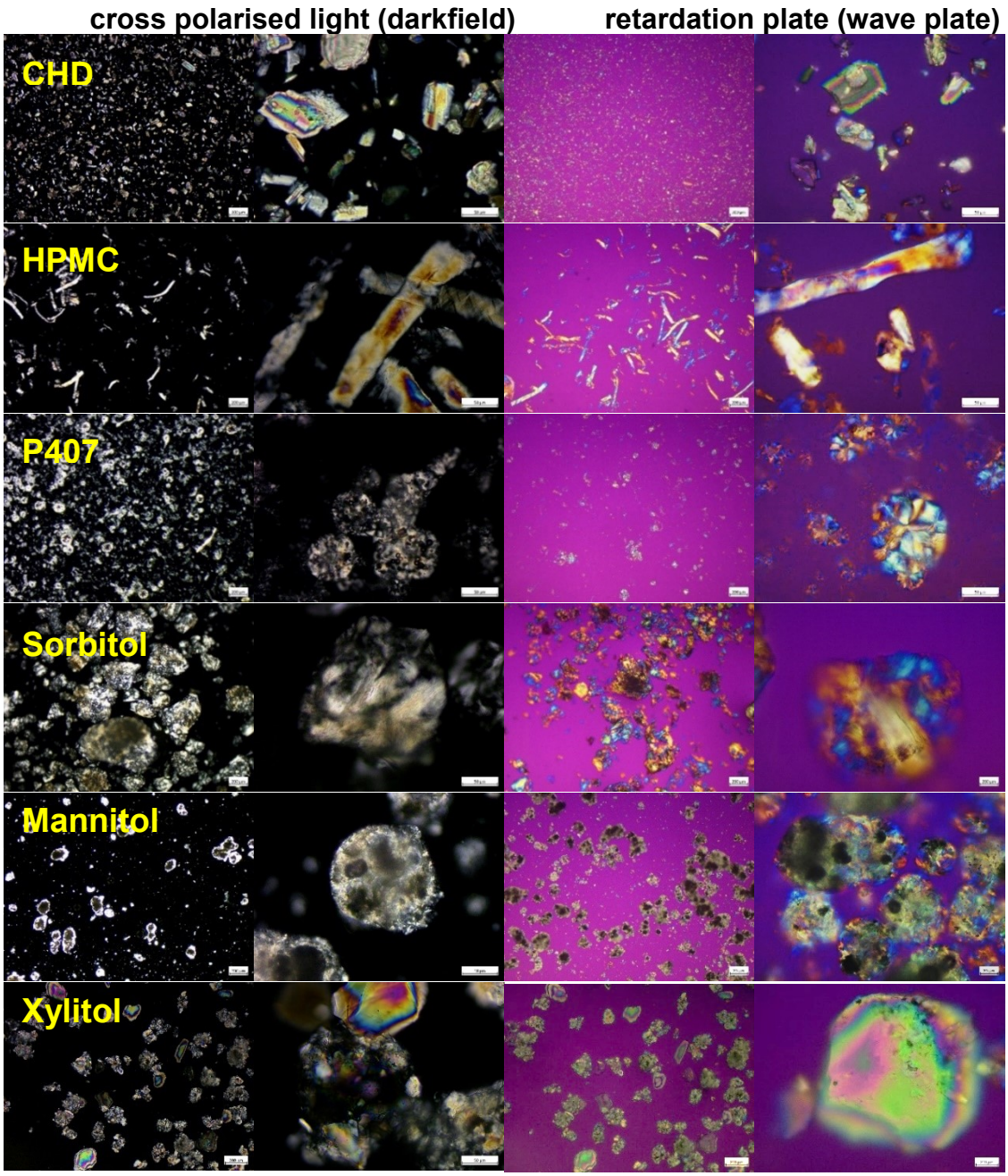

Figure 6.13 CHD, HPMC, P407, sorbitol, mannitol and xylitol using cross polarised light (darkfield) and red plate (purple), 50x and 400x.

Polarized microscopy images were then obtained to investigate the behaviour of the tablet during the swelling process with time. Initially, dark field illumination was used (Figure 6.14 and Figure 6.16). Sorbitol formulations did not show any erosion for the first 15 minutes. Fragments from S4 formulation appeared at 30

	S1, M1, X1	S2, M2, X2	S3, M3, X3	S4, M4, X4
P407: HPMC: polyols	2:2:1	2:2:2	3:1:1	3:1:2

Sorbitol (S), Mannitol (M), Xylitol (X)

minutes, S1, S2 and S3 showed fragmentation at 60 minutes, which increased towards the end of the analysis (Figure 6.14).

Figure 6.15 shows mannitol formulations with more pronounced fragmentation started from the first 15 minutes for M3 and M4. However, xylitol formulations had a similar appearance to sorbitol formulations with more pronounced fragmentation started from the first 15 minutes for X3 and X4 (Figure 6.16), this can be explained by the higher solubility of sorbitol and xylitol compared to mannitol.

	S1, M1, X1	S2, M2, X2	S3, M3, X3	S4, M4, X4
P407: HPMC: polyols	2:2:1	2:2:2	3:1:1	3:1:2

Sorbitol (S), Mannitol (M), Xylitol (X)

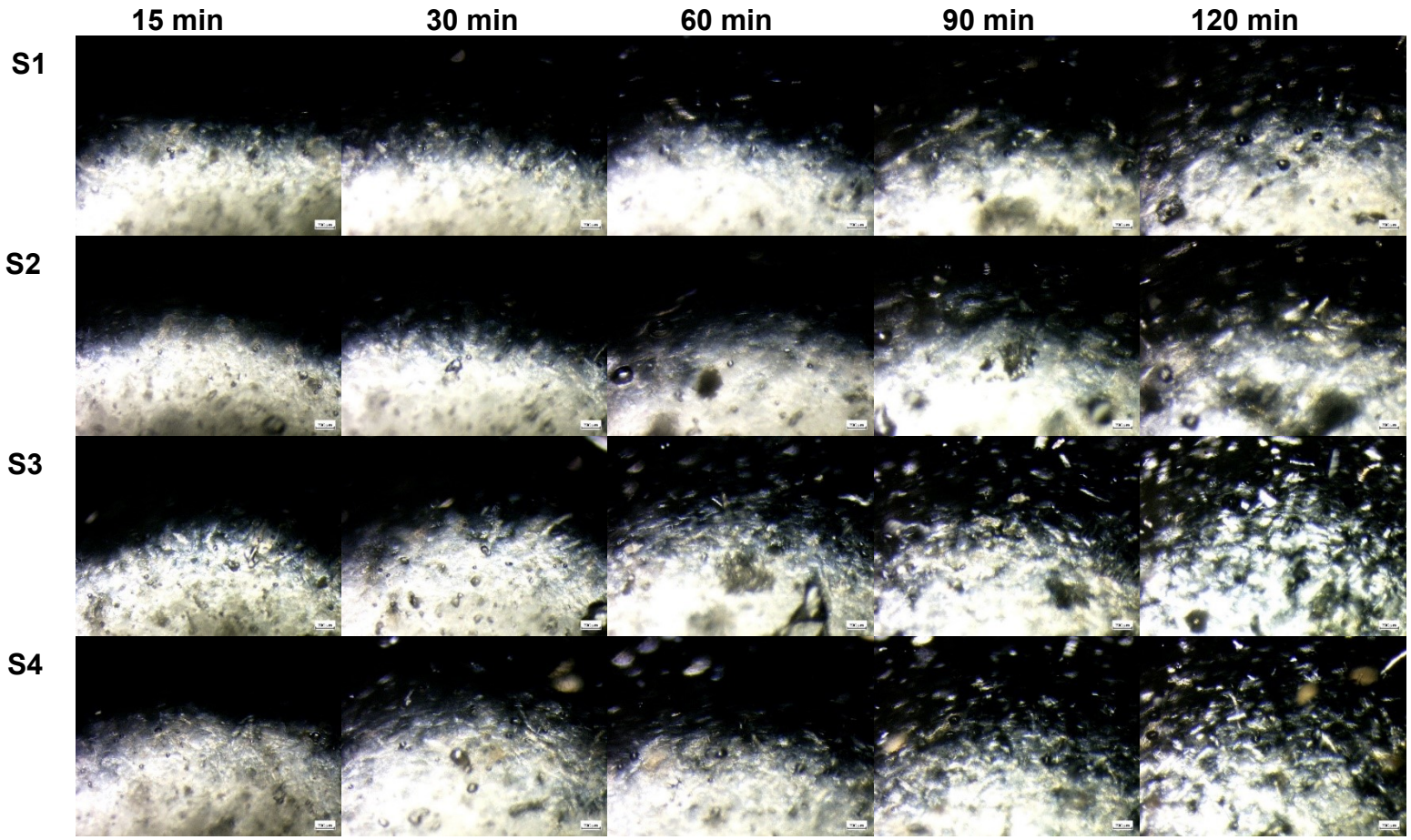

Figure 6.14 Sorbitol formulations morphology changes with time under polarized microscopy (using cross polarised illumination at 50x magnification. Bar marker represents 200 µm).

	S1, M1, X1	S2, M2, X2	S3, M3, X3	S4, M4, X4
P407: HPMC: polyols	2:2:1	2:2:2	3:1:1	3:1:2

Sorbitol (S), Mannitol (M), Xylitol (X)

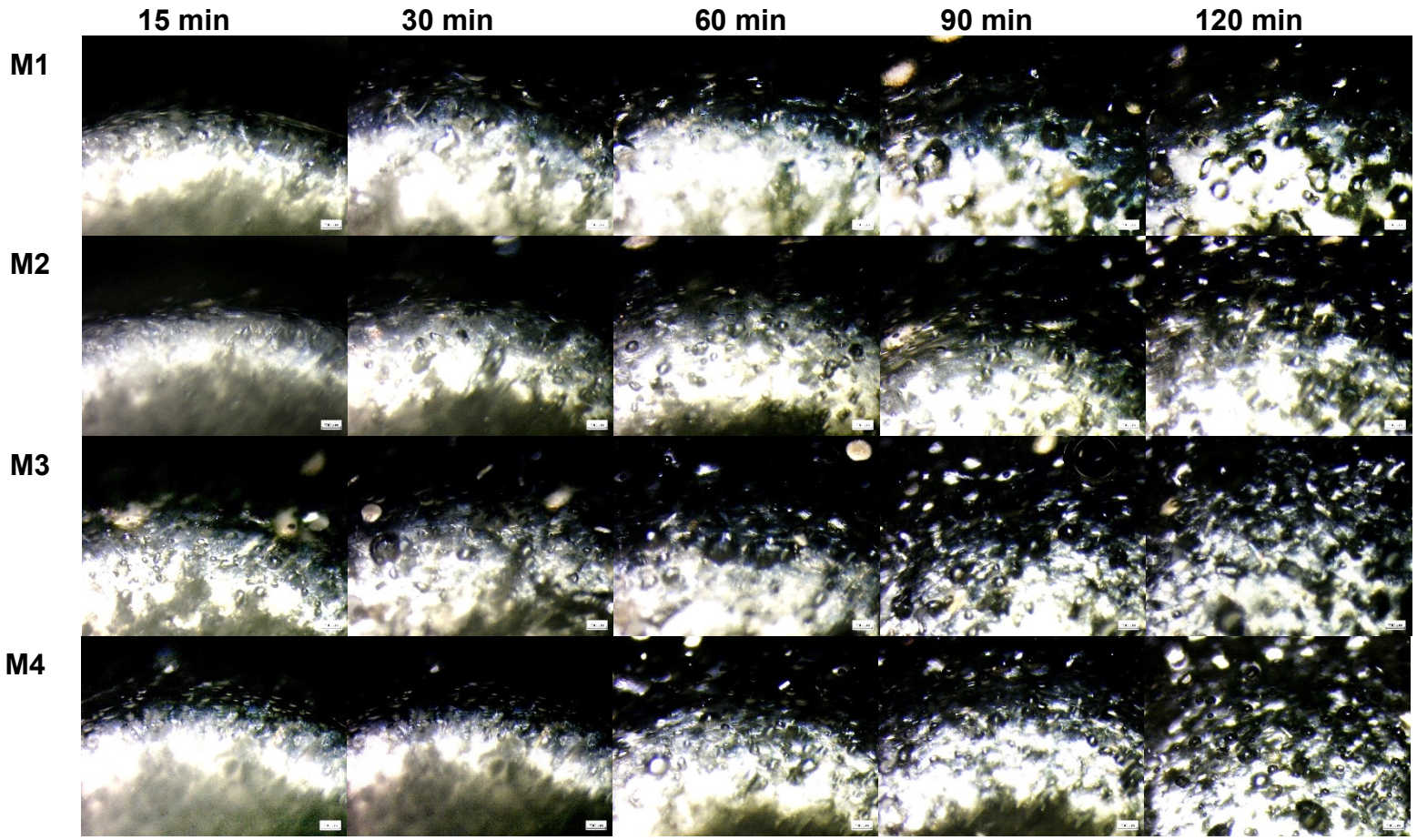

Figure 6.15 Mannitol formulations morphology changes with time under polarized microscopy (using cross polarised illumination at 50xmagnification. Bar marker represents 200 µm).

	S1, M1, X1	S2, M2, X2	S3, M3, X3	S4, M4, X4
P407: HPMC: polyols	2:2:1	2:2:2	3:1:1	3:1:2

Sorbitol (S), Mannitol (M), Xylitol (X)

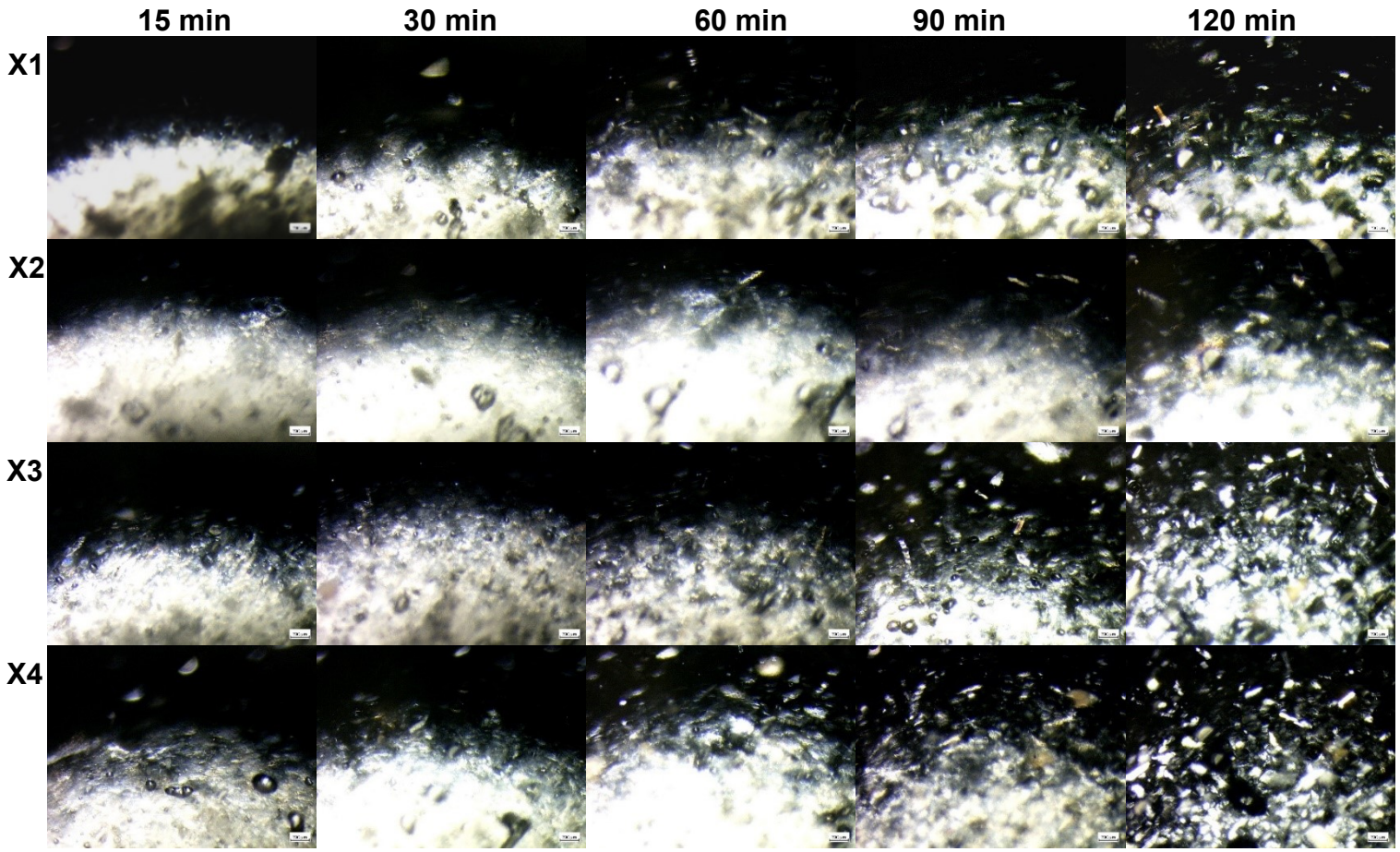

Figure 6.16 Xylitol formulations morphology changes with time under polarized microscopy (using cross polarised illumination at 50xmagnification. Bar marker represents 200 µm).

	S1, M1, X1	S2, M2, X2	S3, M3, X3	S4, M4, X4
P407: HPMC: polyols	2:2:1	2:2:2	3:1:1	3:1:2

Sorbitol (S), Mannitol (M), Xylitol (X)

Additionally, images were obtained for tablets after 2 hours using quarter-waveplate (Figure 6.17) to check the availability of the optical path difference or the birefringent properties of the gel layer. Formulations with ratios of 2:2:1 and 2:2:2 had a clear boundary gel layer preceding the coloured fragments detached from the core indicating the non-homogenous feature of the fragments. Whereas, the gel layer is less distinctive with higher P407 ratio and eroded particles are mixed within the gel layer (Figure 6.17).

	S1, M1, X1	S2, M2, X2	S3, M3, X3	S4, M4, X4
P407: HPMC: polyols	2:2:1	2:2:2	3:1:1	3:1:2

Sorbitol (S), Mannitol (M), Xylitol (X)

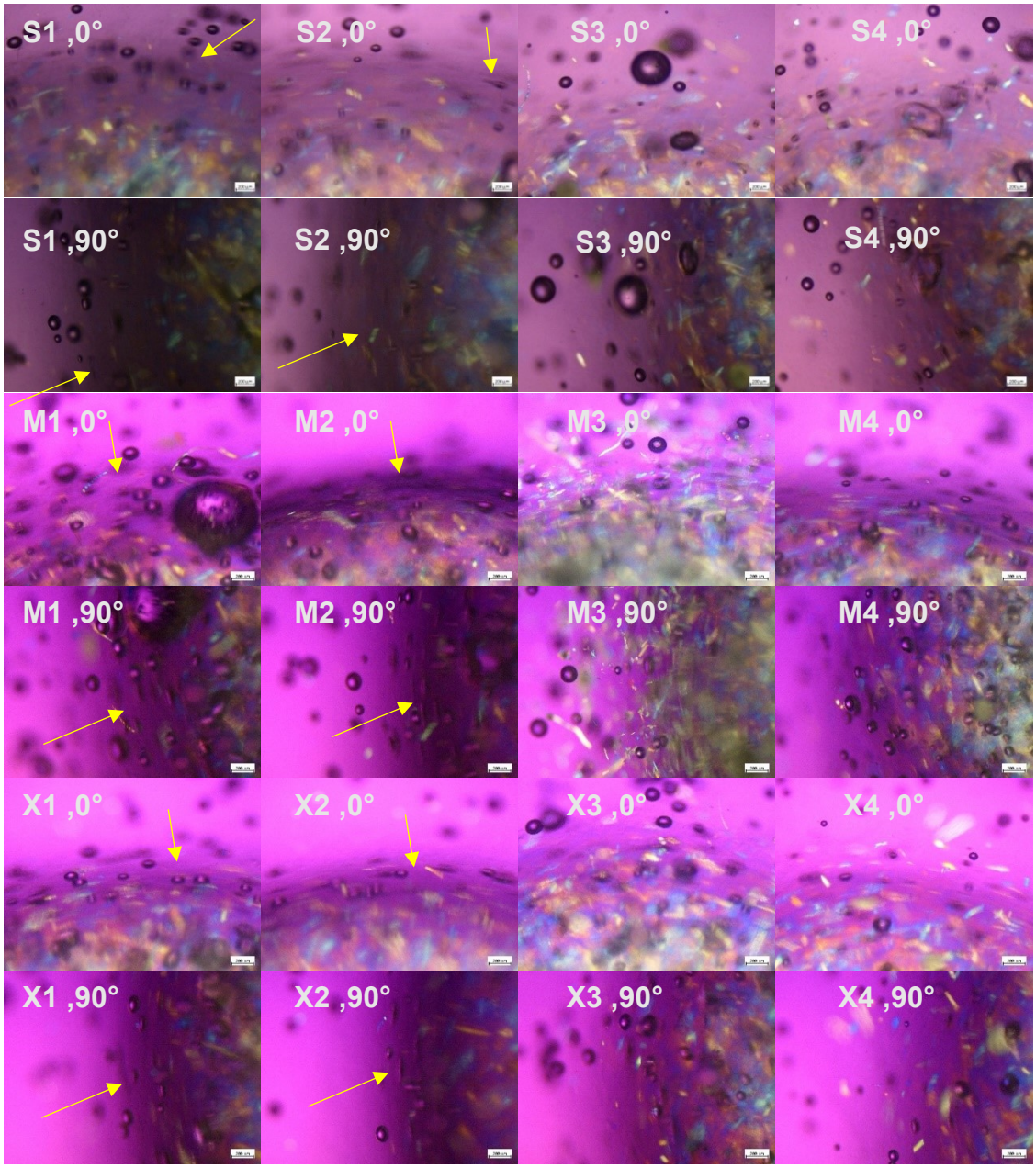

Figure 6.17 CHD formulations morphology under polarized microscopy (using cross polarised illumination and a retardation plate at 0 and 90 degree, (arrows showing the gel layer) 50x and 200 µm scale bar).

6.3.10 Drug release studies:

6.3.10.1 Apparatus I dissolution method

Tablets dissolution was performed using 500 mL of ultrapure water, using App I at 50 rpm, CHD release is displayed in Figure 6.18 a, b and c. For all three set of formulations, CHD release rate was increased with the increase in the ratio of

	S1, M1, X1	S2, M2, X2	S3, M3, X3	S4, M4, X4
P407: HPMC: polyols	2:2:1	2:2:2	3:1:1	3:1:2

Sorbitol (S), Mannitol (M), Xylitol (X)

P407. The highest release was 93% for M4 and X4 of and 87% for S4 after two hours and the lowest was 65% for M1 and X1 and 72% for S1 and S2.

6.3.10.2 Controlled flow rate (CFR) method

The dissolution was performed using the constant flow rate method at 1 mL/min. CHD release from 2:2:1 and 2:2:2 ratios were comparable. Both S1 and S2 showed a release of 34 and 35%, respectively, M1 and M2 of 31% and X1 and X2 of 32%, moreover, this means that the increase in sorbitol, mannitol and xylitol ratios do not have an impact on drug release for these formulations. On the other hand, there was an 11-20% increase in CHD release with the increase of the polyols from S3, M3 and X3 to S4, M4 and X4, respectively, with approximately 90% release after two hours (Figure 6.18 d, e and f).

	S1, M1, X1	S2, M2, X2	S3, M3, X3	S4, M4, X4
P407: HPMC: polyols	2:2:1	2:2:2	3:1:1	3:1:2

Sorbitol (S), Mannitol (M), Xylitol (X)

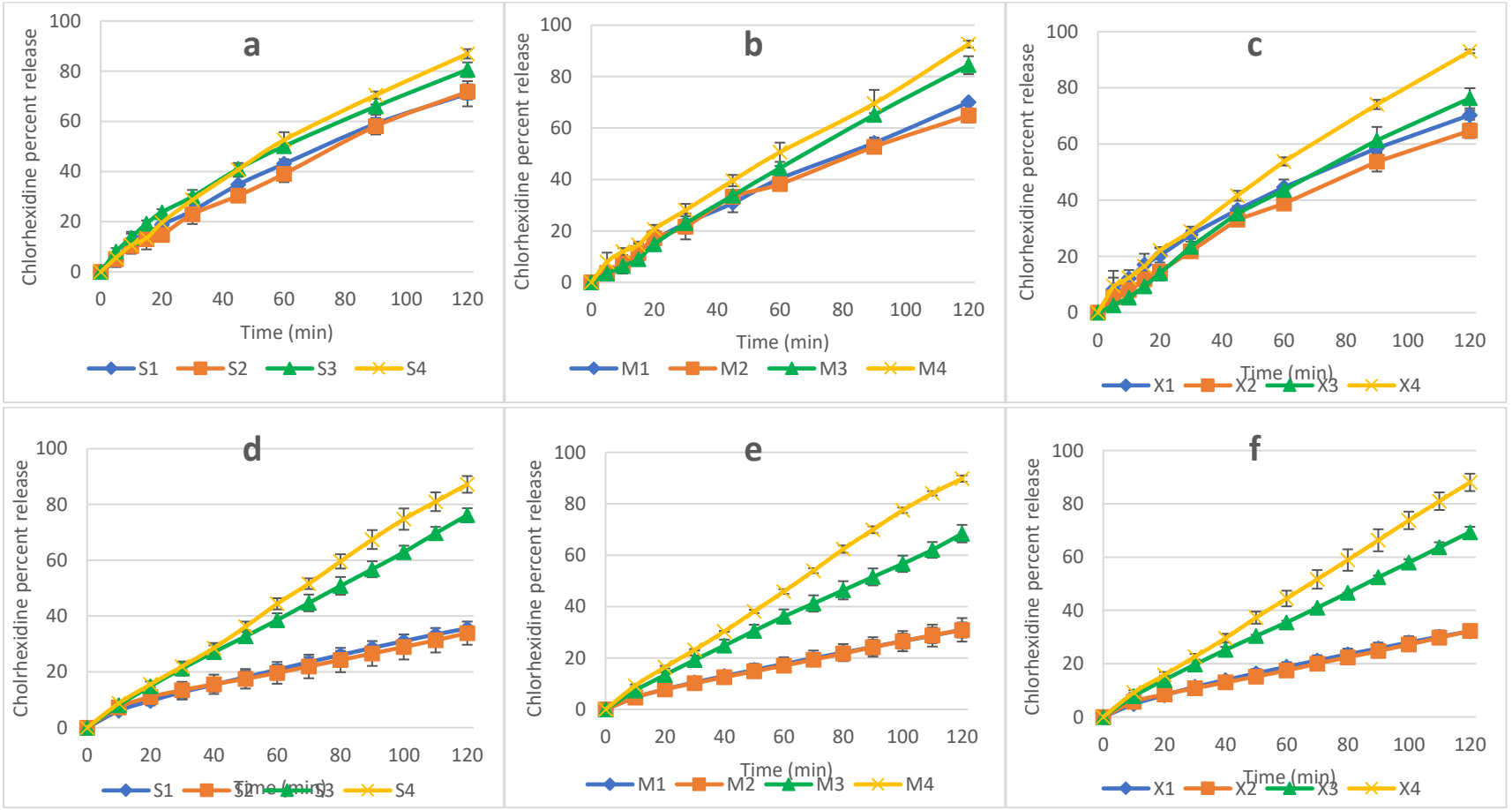

Figure 6.18 CHD release from a-sorbitol, b-mannitol and c-xylitol formulations using App1 and d-sorbitol, e-mannitol and f-xylitol using CFR method. Data are expressed as mean percentage ± SD, n = 3.

	S1, M1, X1	S2, M2, X2	S3, M3, X3	S4, M4, X4
P407: HPMC: polyols	2:2:1	2:2:2	3:1:1	3:1:2

Sorbitol (S), Mannitol (M), Xylitol (X)

Erosion after CFR release

Tablet erosion (%E) was determined for the tablets after two-hour dissolution using the CFR method (Table 6.6). The %E increased with the increase of the hydrophilicity of the formulation (attained by increasing the ratio of P407 and sorbitol, mannitol or xylitol). Furthermore, there are comparable results between %E and CHD dissolution, which might indicate that erosion played a significant role in CHD release.

Table 6.6 Erosion percentage (±SD, n=3) of the tablets after two hours release using CFR method, compared to the release of CHD from the same formulations.

Formulations	% E (2 hours)	% CHD release (2 hours)
S1	36.87 ± 5.88	35.57 ± 0.76
S2	39.70 ± 9.04	33.87 ± 4.16
S3	70.84 ± 10.17	76.14 ± 2.52
S4	88.15 ± 2.62	87.18 ± 2.99
M1	28.43 ± 3.12	30.97 ± 4.58
M2	28.86 ± 1.69	30.92 ± 2.92
M3	69.50 ± 5.65	68.41 ± 3.40
M4	84.63 ± 4.07	89.81 ± 1.22
X1	30.41 ± 5.25	32.14 ± 2.35
X2	36.44 ± 2.54	32.31 ± 1.00
X3	70.41 ± 1.67	69.35 ± 2.03
X4	87.21 ± 5.67	88.05 ± 3.26

6.3.11 Kinetics of drug release

CHD release Data was fitted to zero order, first order, Higuchi, Hixon Crowell, Korsmeyer-Peppas (the power law) and Hopfenberg models. The coefficients of determination R^2 are displayed in Table 6.7 and Table 6.8 for fitted drug release profiles obtained from App I and CFR methods, respectively. Although R^2 for K-

	S1, M1, X1	S2, M2, X2	S3, M3, X3	S4, M4, X4
P407: HPMC: polyols	2:2:1	2:2:2	3:1:1	3:1:2

Sorbitol (S), Mannitol (M), Xylitol (X)

Peppas showed the best fitting for most of the formulations, some of them had a similar or a higher R^2 obtained from other models. For this reason, AIC was calculated to explore the best-fitted models.

	S1, M1, X1	S2, M2, X2	S3, M3, X3	S4, M4, X4
P407: HPMC: polyols	2:2:1	2:2:2	3:1:1	3:1:2

Sorbitol (S), Mannitol (M), Xylitol (X)

Table 6.7 Drug release kinetics using different fitting models for CHD formulation (App1 dissolution)

	Zero Order (R^2)	First order (R^2)	Higuchi (R^2)	Hixon Crowell (R^2)	K-Peppas (R^2)	K-Peppas n	Hopffenberg (R^2)	Hopffenberg n
S1	0.9779 ± 0.0122	0.9907 ± 0.0094	0.9651 ± 0.0029	0.9883 ± 0.0142	0.9918 ± 0.0112	0.771 ± 0.053	0.9918 ± 0.0103	181.82 ± 292.67
S2	0.9917 ± 0.0050	0.9840 ± 0.0032	0.9434 ± 0.0083	0.9907 ± 0.0060	0.9921 ± 0.0064	0.859 ± 0.084	0.9968 ± 0.0029	2.15 ±0.90
S3	0.9790 ± 0.0104	0.9909 ± 0.0031	0.9818 ± 0.0089	0.9864 ± 0.0062	0.9955 ± 0.0031	0.741 ± 0.031	0.9914 ± 0.0036	248.60 ± 368.73
S4	0.9849 ± 0.0022	0.9801 ± 0.0090	0.9531 ± 0.0147	0.9924 ± 0.0045	0.9952 ± 0.0050	0.928 ± 0.162	0.9957 ± 0.0009	1.95 ±0.047
M1	0.9877 ± 0.0078	0.9882 ± 0.0133	0.9504 ± 0.0252	0.9917 ± 0.0056	0.9970 ± 0.0006	0.865 ± 0.136	0.9964 ± 0.0011	6.79 ± 5.92
M2	0.9751 ± 0.0065	0.9908 ± 0.0012	0.9559 ± 0.0084	0.9886 ± 0.0038	0.9893 ±0.0021	0.819 ± 0.078	0.9912 ± 0.0012	291.13 ± 492.32
M3	0.9963 ± 0.0011	0.9600 ± 0.0094	0.9234 ± 0.0053	0.9795 ± 0.0071	0.9968 ± 0.0010	1.047 ± 0.041	0.9975 ± 0.0013	1.12 ± 0.12
M4	0.9932 ± 0.0032	0.9647 ± 0.0093	0.9422 ± 0.0106	0.9823 ± 0.0074	0.9961± 0.0013	0.825 ± 0.064	0.9926 ± 0.0028	1.39 ± 0.25
X1	0.9701 ± 0.0080	0.9832 ± 0.0202	0.9791 ± 0.0113	0.9711 ± 0.0308	0.9971 ± 0.0013	0.694 ± 0.114	0.9833 ±0.0204	1344.84± 1232.74
X2	0.9800 ± 0.0050	0.9942 ± 0.0008	0.9571 ± 0.0076	0.9925 ± 0.0036	0.9909 ± 0.0030	0.826 ± 0.044	0.9948 ± 0.0014	99.49 ± 161.84
X3	0.9880 ± 0.0044	0.9797 ± 0.0128	0.9394 ± 0.0140	0.9907 ± 0.0078	0.9909 ± 0.0050	1.058 ± 0.117	0.9957 ± 0.0027	1.73 ±0.62
X4	0.9920 ± 0.0025	0.9723 ± 0.0073	0.9531 ± 0.0078	0.9887 ± 0.0042	0.9954 ±0.0032	0.815 ± 0.037	0.9952 ± 0.0017	1.62 ± 0.23

Table 6.8 Drug release kinetic using different fitting models for CHD formulation (CFR Method).

	Zero Order (R^2)	First order (R^2)	Higuchi (R^2)	Hixon crowell (R^2)	K-Peppas (R^2)	K-Peppas n	Hopffenberg (R^2)	Hopffenberg n
S1	0.9844 ± 0.0171	0.9804 ± 0.0238	0.9661 ± 0.0195	0.9737 ± 0.0306	0.9985 ± 0.0003	0.756 ± 0.103	0.9803 ± 425.72	425.72 ± 211.64
S2	0.9747 ± 0.0133	0.9515 ± 0.0254	0.9731 ± 0.0179	0.9416 ± 0.0314	0.9932 ± 0.0039	0.677 ± 0.092	0.9515 ± 0.0255	605.60 ± 458.47
S3	0.9980 ± 0.0017	0.9702 ± 0.0128	0.9314 ± 0.0167	0.9852 ± 0.0087	0.9990 ± 0.0006	0.941 ± 0.077	0.9984 ± 0.0007	1.21 ± 0.37
S4	0.9982 ± 0.0007	0.9439 ± 0.0045	0.9207 ± 0.0047	0.9698 ± 0.0027	0.9982 ± 0.0007	0.992 ± 0.023	0.9982 ± 0.0006	1.02 ± 0.03
M1	0.9911 ± 0.0032	0.9896 ± 0.0057	0.9635 ± 0.0075	0.9852 ± 0.0074	0.9995 ± 0.0004	0.783 ± 0.043	0.9896 ± 0.0057	671.80 ± 259 .46
M2	0.9920 ± 0.0079	0.9886 ± 0.0126	0.9553 ± 0.0177	0.9853 ± 0.0162	0.9983 ± 0.0003	0.813 ± 0.089	0.9886 ± 0.0127	177.29 ± 147.62
M3	0.9982 ± 0.0014	0.9844 ± 0.0023	0.9390 ± 0.0073	0.9940 ± 0.0019	0.9998 ± 0.0001	0.895 ± 0.022	0.9989 ± 0.0001	1.39 ± 0.21
M4	0.9990 ± 0.0003	0.9430 ± 0.0054	0.9253 ± 0.0039	0.9704 ± 0.0038	0.9988 ± 0.0004	0.962 ± 0.025	0.9991 ± 0.0002	1.06 ± 0.04
X1	0.9882 ± 0.0039	0.9884 ± 0.0022	0.9669 ± 0.0042	0.9830 ± 0.0026	0.9990 ± 0.0009	0.766 ± 0.014	0.9884 ± 0.0222	495.60 ± 393.71
X2	0.9917 ± 0.0028	0.9858 ± 0.0053	0.9553 ± 0.0081	0.9824 ± 0.0066	0.9956 ± 0.0023	0.792 ± 0.037	0.9857 ± 0.0053	438.59 ± 224.10
X3	0.9982 ± 0.0016	0.9793 ± 0.0083	0.9351 ± 0.0113	0.9903 ± 0.0049	0.9989 ± 0.0010	0.901 ± 0.058	0.9978 ± 0.0022	1.33 ± 0.36
X4	0.9991 ± 0.0005	0.9472 ± 0.0020	0.9242 ± 0.0056	0.9722 ± 0.0013	0.9993 ± 0.0003	0.956 ±0.060	0.9990 ± 0.0005	1.03 ± 0.06

	S1, M1, X1	S2, M2, X2	S3, M3, X3	S4, M4, X4
P407: HPMC: polyols	2:2:1	2:2:2	3:1:1	3:1:2

Sorbitol (S), Mannitol (M), Xylitol (X)

Table 6.9 and Table 6.10 display the AIC for both dissolution methods. The lowest values were obtained with the K-Peppas model, indicating its best fitting accept for S4 formulation analysed by App I, which showed AIC value of 38.8 using Hopfenberg model, compared to 40.7 with K-Peppas model. Thus, the release kinetics from S4 and App I was erosion controlled. This can be explained by the higher solubility of sorbitol compared to xylitol and mannitol.

Table 6.9 AIC values for App I Dissolution data fitted with different kinetics models.

Formulations	Zero Order	First order	Higuchi	Hixon Crowell	K-Peppas	Hoffenberg
S1	49.9	36.4	55.4	37.2	28.1	35.3
S2	40.2	45.7	60.4	39.1	31.8	37.2
S3	49.5	39.7	48.0	43.0	20.7	40.8
S4	51.5	51.6	62.6	41.5	40.7	38.8
M1	42.6	38.1	58.0	37.4	29.6	32.4
M2	50.4	38.7	56.3	40.5	38.5	40.2
M3	36.5	58.6	67.2	51.6	22.9	32.3
M4	43.2	58.1	65.2	50.7	25.1	44.1
X1	53.1	37.4	48.7	44.4	24.4	37.4
X2	48.2	34.1	56.0	35.7	33.8	34.6
X3	46.7	48.8	63.1	39.0	27.5	35.2
X4	45.6	56.1	63.5	46.8	23.4	40.3

Table 6.10 AIC values for CFR Dissolution data fitted with different kinetics models.

Formulations	Zero Order	First order	Higuchi	Hixon Crowell	K-Peppas	Hoffenberg
S1	39.4	38.9	52.4	43.4	16.0	40.9
S2	46.3	52.7	46.5	55.0	30.9	54.7
S3	35.4	70.3	83.9	60.0	8.2	33.9
S4	40.4	84.0	90.5	75.9	21.4	40.9
M1	32.8	31.7	51.7	36.7	-3.3	33.8
M2	27.8	29.5	53.8	32.7	14.0	31.6
M3	31.4	60.0	79.7	47.0	1.7	27.9
M4	34.7	85.0	90.5	76.5	14.4	32.9
X1	38.0	36.1	51.8	41.1	0.4	38.1
X2	32.6	37.5	55.0	40.2	26.0	39.5
X3	30.9	63.4	80.9	53.3	14.2	31.5
X4	30.9	83.0	89.7	74.6	12.1	32.2

	S1, M1, X1	S2, M2, X2	S3, M3, X3	S4, M4, X4
P407: HPMC: polyols	2:2:1	2:2:2	3:1:1	3:1:2

Sorbitol (S), Mannitol (M), Xylitol (X)

Accordingly, using App I, and based on the n value the release was anomalous except for M3 and X3 which shows super case II release. Furthermore, the release kinetics using CFR method were anomalous for formulations with an equal amount of P407 and HPMC (S1, S2, M1, M2, X1 and X2), and formulations with higher P407 the release was super case II.

Based on the drug release studies S4, M4 and X4 showed the best release and the least effect by the volume and the dissolution media and they were further investigated for possible interaction between CHD and the excipients.

6.3.12 Drug polymer interaction (FTIR, DSC and XRD)

FTIR Analysis

FTIR analysis was conducted to explore possible interactions between tablet contents during the granulation process.

FTIR spectra for all tablet contents and physical mix (PM), granules (Gran) for S4, M4 and X4 are displayed in Figure 6.19. FTIR spectra for CHD, HPMC and P407 are explained in 4.3.2.7. The absorption bands of the functional groups of sorbitol, mannitol and xylitol are summarised in Table 6.11, which show agreement with previous work (Wang *et al*., 2012, Bruni *et al*., 2009 and Arafa *et al*., 2016), respectively.

Table 6.11 FTIR spectroscopy absorption bands of the functional groups for sorbitol, mannitol and xylitol.

Functional groups	Sorbitol	Mannitol	Xylitol
O-H stretching	3224	3279	3148, 3289,3355
C-H stretching	2922	2939	2911
C-O stretching	1050, 1093	1077, 1016	1011, 1064,1089, 1117

	S1, M1, X1	S2, M2, X2	S3, M3, X3	S4, M4, X4
P407: HPMC: polyols	2:2:1	2:2:2	3:1:1	3:1:2

Sorbitol (S), Mannitol (M), Xylitol (X)

As discussed in chapter 4 (4.3.1.7), P407 is characterised by principal peaks at 2875 cm^{-1} (CH stretching) and 1094 cm^{-1} (CO stretching). By comparing the spectra of the physical mixes and the granules of each formulation, no difference is observed between each spectrum. Consequently, it is concluded that there is no interaction due to the granulation process. Moreover, all formulations spectra showed the dominant of P407 peaks and this attributed to the steric hindrance or stabiliser effect of P407 which is potentiated by its content in the tablets which constituted approximately 50% of the tablet weight (Beck-Broichsitter *et al*., 2017).

	S1, M1, X1	S2, M2, X2	S3, M3, X3	S4, M4, X4
P407: HPMC: polyols	2:2:1	2:2:2	3:1:1	3:1:2

Sorbitol (S), Mannitol (M), Xylitol (X)

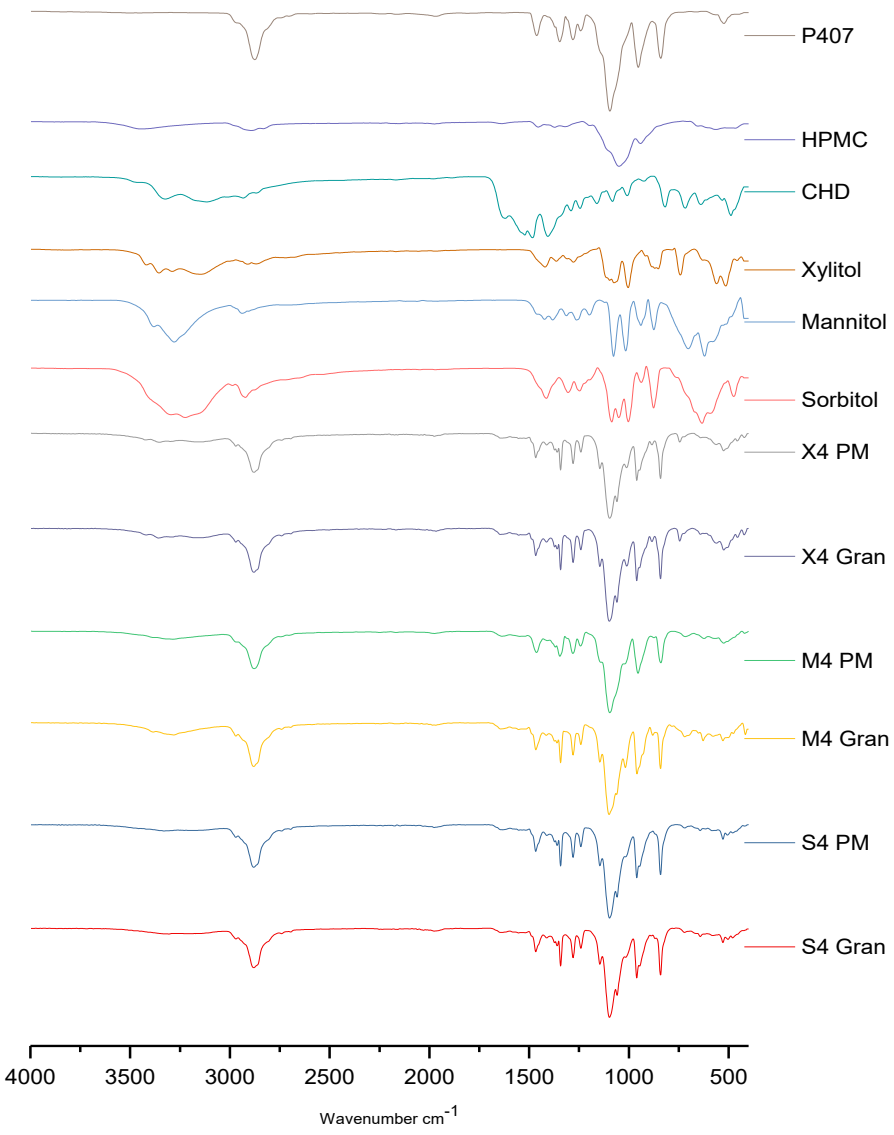

Figure 6.19 FTIR spectra of tablet excipients, CHD, S4, M4 and X4 physical mix (PM) and granules (Gran).

DSC Analysis

DSC analysis was applied for the raw materials CHD, HPMC, P407, Sorbitol, Mannitol and Xylitol, S4, M4 and X4 formulations physical mix, granules and tablets, to investigate possible interactions between CHD and the excipients

	S1, M1, X1	S2, M2, X2	S3, M3, X3	S4, M4, X4
P407: HPMC: polyols	2:2:1	2:2:2	3:1:1	3:1:2

Sorbitol (S), Mannitol (M), Xylitol (X)

during tablets preparation. As shown in Figure 6.20, HPMC is amorphous, whereas the rest of the ingredients are crystalline with distinctive melting peaks. The thermograms indicate no interaction during granulation and tablets pressing. Moreover, the disappearance of the melting peak of CHD in the physical mixes, granules and tablets suggests the dissolution of CHD in P407, the latter has a low melting point ~70. A summary of the melting peaks is presented in Table 6.12.

Table 6.12 Melting peaks obtained from the DSC thermograms of CHD, the excipients, S4, M4 and X4 PM, Gran and Tablets.

Material	Melting Peak (°C)	S1 PM	S1 G	S1 T	M1 PM	M1 G	M1 T	X1 PM	X1 G	X1 T
CHD	156.79	-	-	-	-	-	-	-	-	-
P407	56.79	56.97	57.23	57.38	56.83	57.24	57.43	56.65	57.08	57.07
Sorbitol	99.80	99.54	99.62	99.19	-	-	-	-	-	-
Mannitol	166.31	-	-	-	165.62	165.24	165.10	-	-	-
Xylitol	94.06	-	-	-	-	-	-	93.95	93.32	93.54

	S1, M1, X1	S2, M2, X2	S3, M3, X3	S4, M4, X4
P407: HPMC: polyols	2:2:1	2:2:2	3:1:1	3:1:2

Sorbitol (S), Mannitol (M), Xylitol (X)

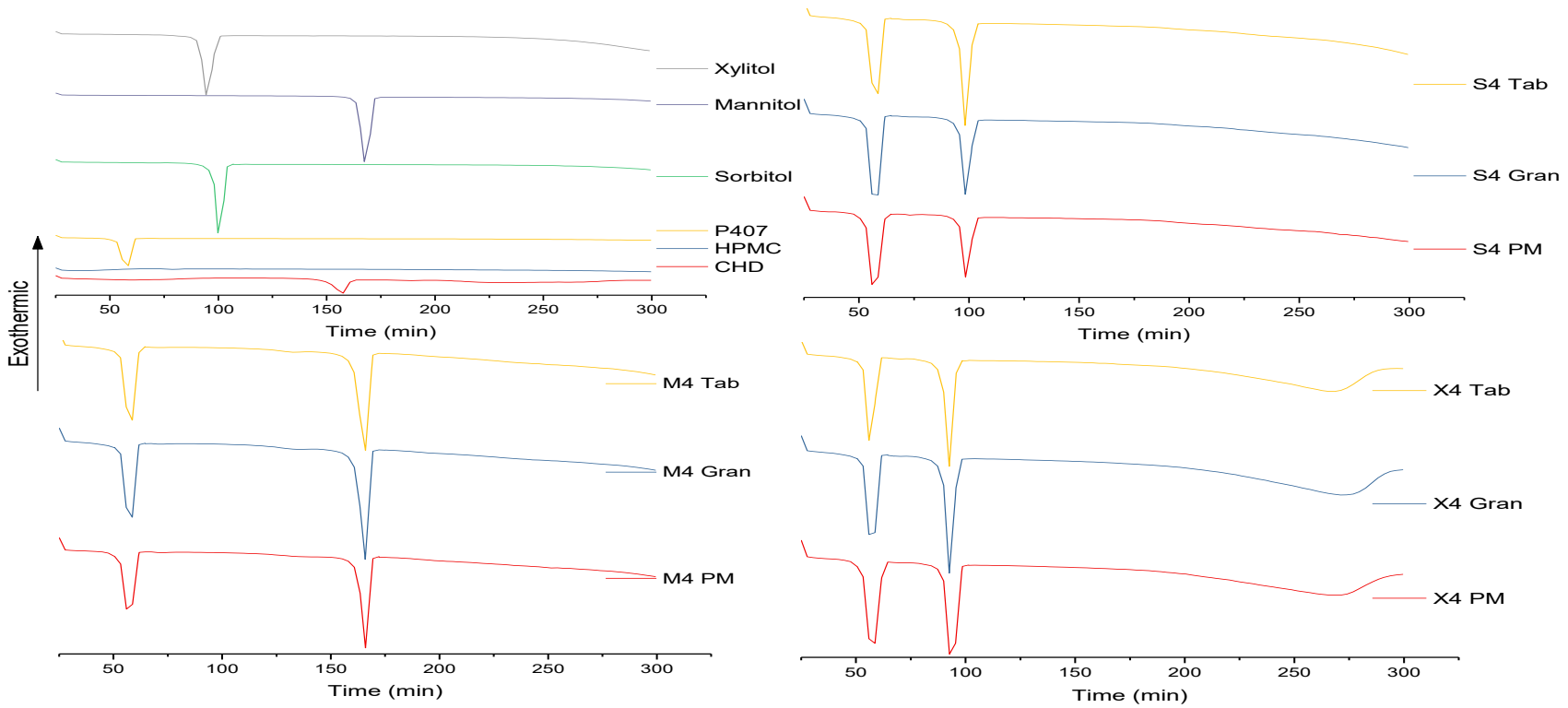

Figure 6.20 DSC thermograms of tablets excipients, CHD, S4, M4 and X4 physical mix (PM) and granules (Gran) and tablets (Tab).

	S1, M1, X1	S2, M2, X2	S3, M3, X3	S4, M4, X4
P407: HPMC: polyols	2:2:1	2:2:2	3:1:1	3:1:2

Sorbitol (S), Mannitol (M), Xylitol (X)

XRD analysis

XRD was used to investigate further a possible interaction resulted from the granulation process. Apart from HPMC, all tablet ingredients showed a crystalline nature (Figure 6.21). The spectra of the physical mixtures and the granules of each formulation show the same XRD pattern which confirms no interaction produced by the granulation process.

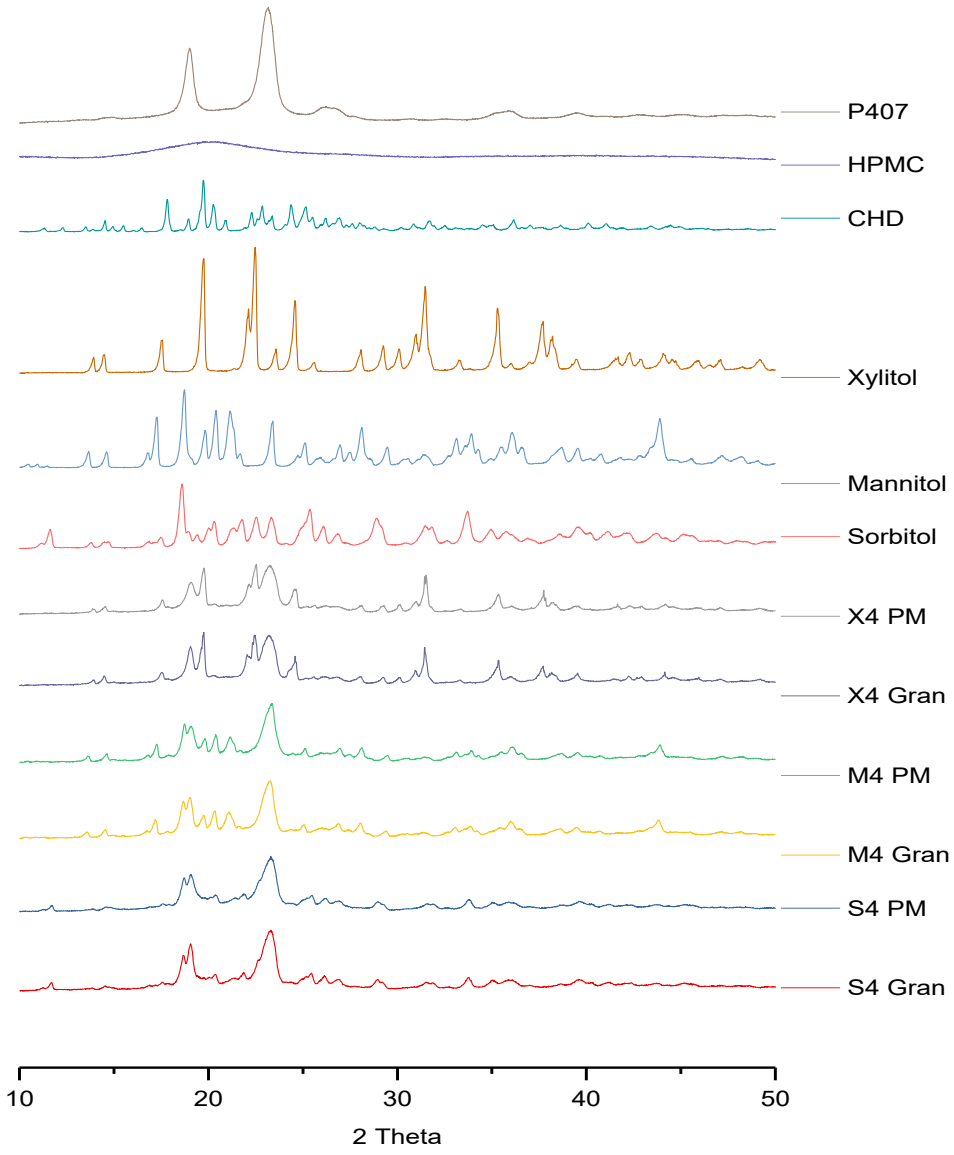

Figure 6.21 XRD patterns of tablets excipients, CHD, S4, M4 and X4 physical mix (PM) and granules (Gran).

	S1, M1, X1	S2, M2, X2	S3, M3, X3	S4, M4, X4
P407: HPMC: polyols	2:2:1	2:2:2	3:1:1	3:1:2

Sorbitol (S), Mannitol (M), Xylitol (X)

6.3.13 Statistical analysis

Dissolution data were analysed statistically for both methods App I and CFR, using Dissolution efficiency (D.E.), Invitro equivalent comparison (model independent) and kinetics of Drug release (model dependent). The analyses were performed to investigate the variation between the replicates of the CFR method and compare it to the standard App 1 method.

Dissolution efficiency (D.E.%)

D.E. is used to compare between different batches, in the current work it was used to compare the different methods of dissolution to investigate the effect of the volume of the dissolution media. D.E. for CHD release using App 1 was higher for all formulation. Moreover, it is double for S1, S2, M1, M2, X1 and X2 than that of the CFR method, and this is attributed to the effect of higher volume of dissolution media. In contrast, the difference was much less for S4, M4 and X4 with a value of 5%, 3% and 7%, respectively (Figure 6.22).

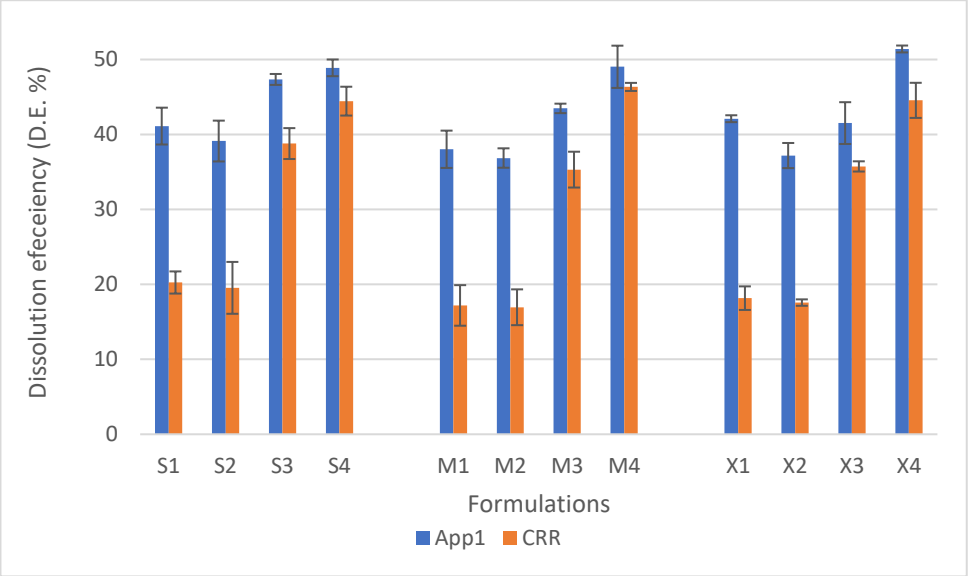

Figure 6.22 Dissolution Efficiency of CHD release using App I and CFR methods. Data are expressed as mean percentage ± SD, n = 3

	S1, M1, X1	S2, M2, X2	S3, M3, X3	S4, M4, X4
P407: HPMC: polyols Sorbitol (S), Mannitol (M), Xylitol (X)	2:2:1	2:2:2	3:1:1	3:1:2

In Vitro equivalence comparison

Single Way ANOVA

Single way ANOVA was performed to investigate the equivalence of each triplicate, the results revealed no significant difference for all formulations and for both methods (Table 6.13).

Table 6.13 P-values of One-way ANOVA statistics.

Formulations	P-value	
	App I	CFR
S1	0.95	0.81
S2	0.90	0.24
S3	0.93	0.92
S4	0.97	0.96
M1	0.89	0.38
M2	0.97	0.58
M3	1.00	0.86
M4	0.96	1.00
X1	0.97	0.74
X2	0.98	0.96
X3	0.95	0.99
X4	1.00	0.92

Pairwise method

Pairwise statistical analysis was used to analyse the equivalence between each two replicates within the triplicates.

i. Similarity factor (f_2)

Based on f_2 values, all replicates considered similar with a value greater than 50 (Figure 6.23).

	S1, M1, X1	S2, M2, X2	S3, M3, X3	S4, M4, X4
P407: HPMC: polyols Sorbitol (S), Mannitol (M), Xylitol (X)	2:2:1	2:2:2	3:1:1	3:1:2

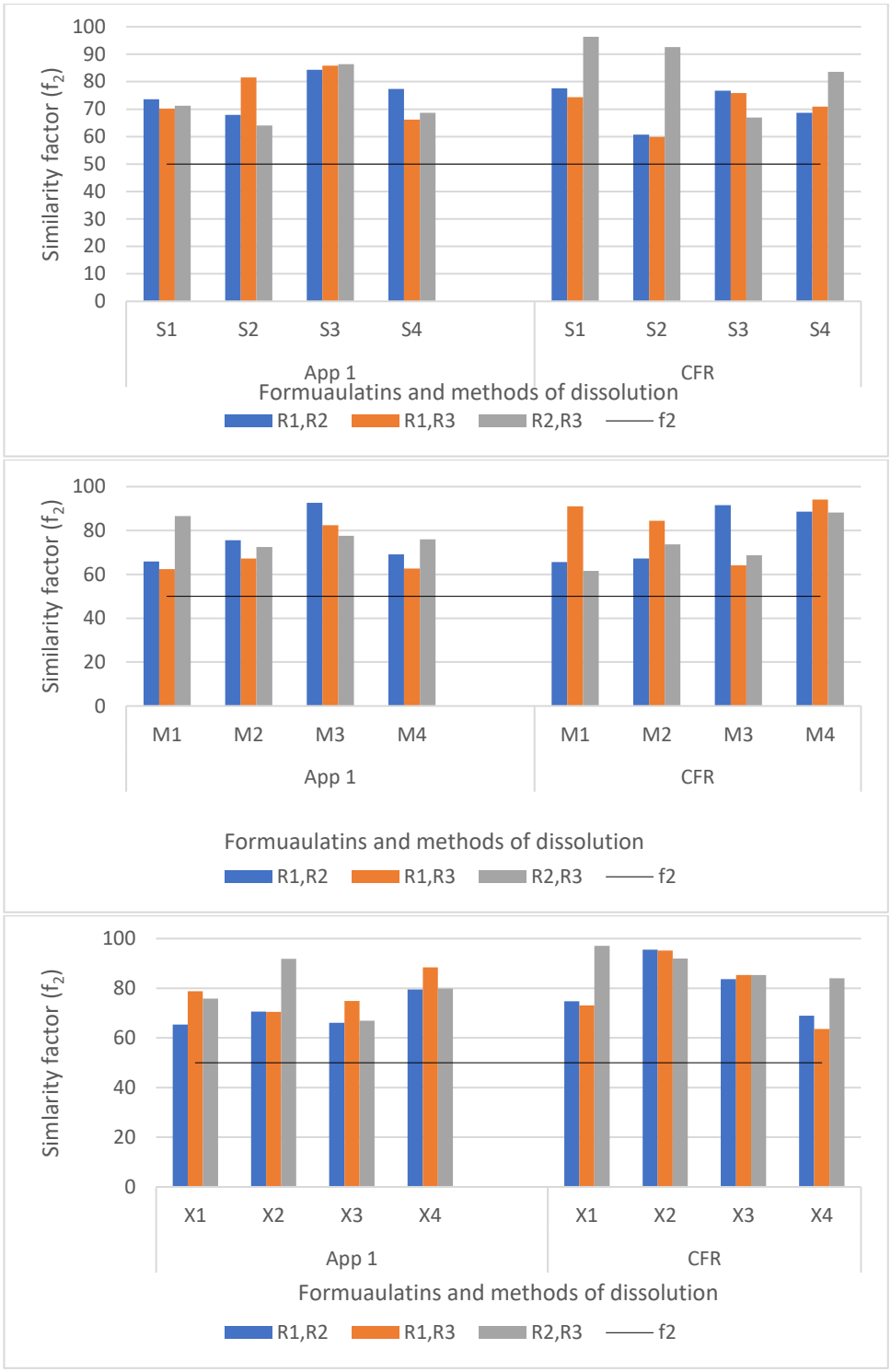

Figure 6.23 Similarity factor (f_2) for the replicates of each triplicate of the dissolution data.

ii. Difference Factor (f_1)

Figure 6.24 illustrates the difference factor (f_1) for the tested formulations. The difference among App I dissolution data are much less than of CFR data. One

	S1, M1, X1	S2, M2, X2	S3, M3, X3	S4, M4, X4
P407: HPMC: polyols Sorbitol (S), Mannitol (M), Xylitol (X)	2:2:1	2:2:2	3:1:1	3:1:2

replicate of S2 and two replicates of M1 with f_1 value less than 20. CFR comparison data showed two values out of three for S1, S2, M1, M2 formulations with 15< f_1<30.

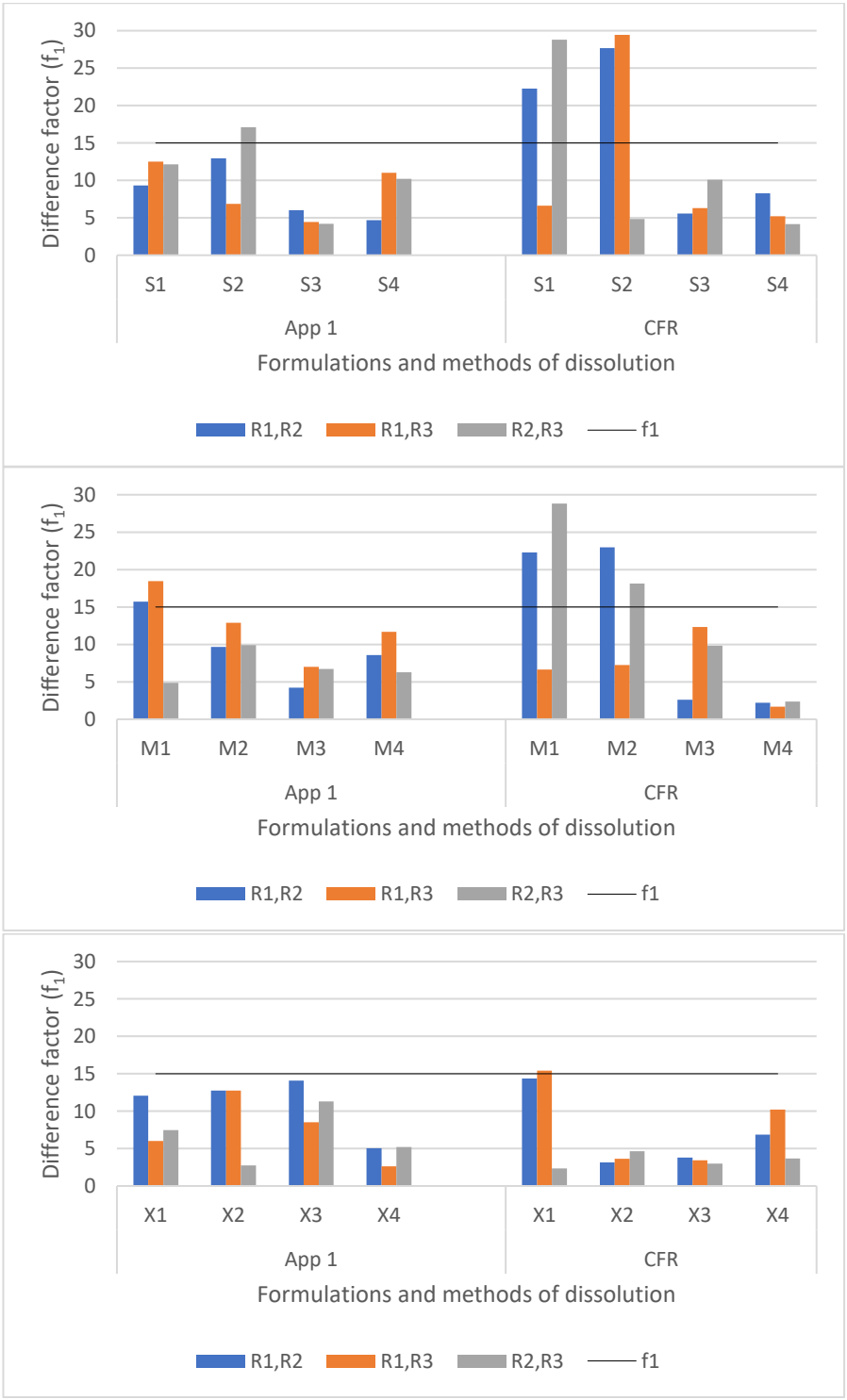

Figure 6.24 Difference factor (f_2) between the replicates of each triplicate of the dissolution data.

	S1, M1, X1	S2, M2, X2	S3, M3, X3	S4, M4, X4
P407: HPMC: polyols Sorbitol (S), Mannitol (M), Xylitol (X)	2:2:1	2:2:2	3:1:1	3:1:2

iii. Resigno's indices

As mentioned earlier (chapter five), there is no cut off value for Resigno's indices, the values are ranging from 0 to 1. The closest to 0 showed the less difference. By comparing both methods most of the formulations have comparable values except S2, M1 and M2, the highest value is 0.15 (Figure 6.25).

Figure 6.25 Resigno's indices for the replicates of each triplicate of the dissolution data.

	S1, M1, X1	S2, M2, X2	S3, M3, X3	S4, M4, X4
P407: HPMC: polyols Sorbitol (S), Mannitol (M), Xylitol (X)	2:2:1	2:2:2	3:1:1	3:1:2

iv. AUC ratio

AUC ratio results are listed in Table 6.14, formulations analysed using App I are within the acceptable range (0.8-1.25), CFR methods show 4 ratios out of the acceptable range. S1 showed two ratios, and one ratio for each M1, M2 out of the acceptable range, although all data using App I are acceptable.

Table 6.14 AUC ratio for formulations replicates using App I and CFR methods

Formulations	App 1			CFR		
	R1-R2	R1-R3	R2-R3	R1-R2	R1-R3	R2-R3
S1	1.05	0.93	0.89	1.11	1.15	1.03
S2	0.90	1.03	1.14	1.33	1.36	1.02
S3	1.03	1.02	0.99	1.05	0.95	0.90
S4	1.03	1.04	1.01	1.09	1.00	0.97
M1	0.90	0.88	0.98	0.80	1.07	1.34
M2	1.02	1.07	1.05	1.26	1.05	0.83
M3	0.97	0.98	1.01	0.98	0.88	0.90
M4	0.93	0.89	0.96	0.98	0.99	1.02
X1	1.01	1.02	1.02	1.15	1.17	1.02
X2	0.93	0.92	0.99	1.01	0.96	0.96
X3	1.13	1.02	0.90	1.01	1.04	1.03
X4	0.99	0.98	0.99	0.93	0.90	0.96

6.4 Discussion

Three groups of CHD hydrogel mucoadhesive buccal tablets were prepared based on the type of the polyol; sorbitol mannitol and xylitol (Table 6.1). Each group had two different ratios of polymers (P407 to HPMC) and two different ratios of polyols. Pre-formulation analysis showed the low flowability of the blends (Table 4.3) ranging from ‘poor’ to ‘very very poor’, and failed to pass through 10, 15 and 25 mm orifices. This is attributed to particle size variation of the drug and the excipients (Figure 6.2 and Figure 6.13) and (as explained in 4.3.3), the percentage of fine particles and the cohesive nature of some of the excipients exerted a negative

	S1, M1, X1	S2, M2, X2	S3, M3, X3	S4, M4, X4
P407: HPMC: polyols	2:2:1	2:2:2	3:1:1	3:1:2

Sorbitol (S), Mannitol (M), Xylitol (X)

effect on the flowability. To improve the flowability of the blends, melt granulation was performed by exploiting the low melting point of P407 which is equal to 57°C as confirmed by DSC analysis (4.3.2.8). Granules flowability displayed remarkable improvement ranging from 'passable' to 'good', and they were successfully passed through 10,15 and 25 mm orifices diameter. Chaturvedi *et al.,* (2018) have compared the flowability of ibuprofen-HPC granules prepared by melt granulation using co-rotating screw extruder and wet granulation using a high shear mixer. Melt granulation gave a superior improvement of flowability from "passable" to "good", whilst for wet granulation, it was only improved from "passable" to "fair".

SEM micrographs (Figure 6.5) show an irregular morphology of the granules, this finding is similar to a previous work performed by Passerini *et al*., (2002) who prepared Ibuprofen-Poloxamer 188 melt granules using a high shear mixer. The surface topography of the granules (Figure 6) depicted that formulations with equal amounts of HPMC and P407 have smoother surfaces compared to the formulations with a higher P407 ratio. Conceivably, in the former P407 melted and formed a layer on the surfaces of other tablet ingredients, however in the latter there was more poloxamer associated into clumps on the surface of the granules. Elemental mapping was performed to check the homogeneity of the CHD on the surface of the tablet. Figure 6.6 shows the distribution of CHD on the surfaces of the tablets, there are some visible clusters which may be attributed to the hand mixing being not optimised during the granulation process. Elemental mapping, of sulphur in spironolactone, was previously applied by Nagy *et al* (2012) to investigate the distribution of spironolactone in melt extruded solid dispersion samples prepared with Soluplus® polymer. Thus SEM-EDX provides a useful tool for evaluating drug distribution issues within particles.

	S1, M1, X1	S2, M2, X2	S3, M3, X3	S4, M4, X4
P407: HPMC: polyols	2:2:1	2:2:2	3:1:1	3:1:2

Sorbitol (S), Mannitol (M), Xylitol (X)

Tablet characterisation was acceptable based on weight variation, content uniformity and friability. Both sorbitol and mannitol showed higher tensile strength than xylitol. The low tensile strength of xylitol is explained by its elastic recovery (Bolhuis *et al*., 2005). On the other hand, sorbitol displays plastic deformation and produced good binding properties (Stoltenberg & Breitkreutz, 2011). Additionally, tablets prepared with granular mannitol produce a porous structure resulting in a higher surface area and increasing bonding and consequently the tensile strength (Westermarck *et al*., 1998)

All formulations successfully adhered to the chicken pouch for two hours using the disintegration tester (Figure 6.7). However, by measuring the force of detachment, it was found that with increasing sorbitol and xylitol ratio the force of detachment decreased, which might be explained by their solubility and hygroscopic property. Sorbitol is highly hygroscopic, whereas xylitol is moderately hygroscopic, and mannitol is considered as non-hygroscopic (Bolhuis *et al.*, 2009). Sorbitol, mannitol and xylitol form hydrogen bonding with water (Yamaguchi *et al.,* 2017), which might be competing with the binding to the chicken mucosa, the lower solubility of mannitol resulted in the higher force of mucoadhesion compared to sorbitol and xylitol (Figure 6.8). On the other hand, the type of sugar does not show a significant effect on the swelling indices, but it does have a clear effect on the erosion percentages. The more the sugar alcohol in the tablet the more is the E% (Table 6.4). The effect was more prominent with xylitol then sorbitol, however, mannitol did not show a similar effect which might be explained by their solubility.

Regarding the hydration data, which was obtained under a constant surface area (the diameter of both the tablet and the well is 6 mm), three models were used.

	S1, M1, X1	S2, M2, X2	S3, M3, X3	S4, M4, X4
P407: HPMC: polyols	2:2:1	2:2:2	3:1:1	3:1:2

Sorbitol (S), Mannitol (M), Xylitol (X)

Firstly; PWL2 which is represented by two regression lines; secondly; one phase exponential change which is a first order process, the rate being proportional to the concentration of the reactant at a specific time; thirdly a two-phase exponential model is used when there are two first order rates, both fast and slow. Data showed the best fitting to the two-phase exponential model based on both R^2 (Table 6.5) and AIC. This can be explained by the different solubility of the excipients in the matrix which resulted in a slow and fast hydration *(Tosun, 2012)*. Upon tablet hydration, it is assumed that highly water-soluble ingredients hydrated faster followed by the less soluble ingredients resulting in a two-phase exponential pattern.

Polyols solubility increased the rate of hydrogel formation within the tablets as detected by the image analysis using a digital camera, in this method tablets were expanded in three-dimensional directions. Both sorbitol and xylitol possess high solubility and humectant properties (Bolhuis *et al.*, 2009), the latter reflects the water holding capacity of both sugars, which clearly has been noticed by the larger gel area compared to that of mannitol formulations (Figure 6.12). Dürig and Fassihi, (2002) found that sugars such as sorbitol and sucrose enhanced water diffusion into the matrix, and the leaching of soluble sugar acts as a changeling agent resulting in improving the release of the drug.

Generally, both sorbitol and xylitol formulations turned to a hydrogel rubbery tablet after 90 minutes for the equal ratio of HPMC and P407, increasing the ratio of P407 decreased the time to after 60 minutes, which is attributed to the increase in the hydrophilicity of the tablets.

Cross polarized microscopy has been used for gel characterization (Hikmet, 1991, Hikmet and Howard, 1993). To our knowledge, this work is the first attempt

	S1, M1, X1	S2, M2, X2	S3, M3, X3	S4, M4, X4
P407: HPMC: polyols	2:2:1	2:2:2	3:1:1	3:1:2

Sorbitol (S), Mannitol (M), Xylitol (X)

to use cross polarized microscopy monitor as part of tablet characterisation during the different swelling stages of the tablet. Using cross polarized microscopy and quarter wave plate, there was no noticeable difference between the formulations based on the type of the sugar (Figure 6.14 to Figure 6.17). The noticed difference is within the same group depending on the polymers ratio, for instance, there were more fragments detaching from the core in S3 and S4 than S1 and S2 which is attributed to the higher ratio of P407. Moreover, both S1 and S2 have a dark boundary of the gel layers which may have resulted from their thickness and/or strength, accompanied by a lower water content due to lower P407 content. P407 plays a significant role in enhancing the hydration of the tablet and the dissolution of CHD. The gel layer in mannitol and xylitol formulations have similar behaviour to sorbitol formulations under polarised microscopy.

Drug release studies were performed using both App I and CFR methods (Figure 6.18). Based on App I, cumulative drug release after two hours was increased with the increase in both sugar and P407 ratio, the increase was limited due to the high volume of the dissolution medium (500 mL), with the greatest difference of 27% from X1 to X4 and M1 to M4. On the other hand, using CFR the release was greatly affected by P407: HPMC ratio, as shown in Figure 6.18 the change of the ratio of P407 to HPMC from 2:2 to 3:1 lead to an increase in the release to around 50%. Moreover, the release for S4, M4 and X4 using 1mL/min CFR method is comparable to the release using App I, this indicates that CHD release from these formulations is not affected by the volume of the dissolution medium. This is attributed to the hydrogel-forming ability with the higher P407 ratio, as indicated by image analysis, and resulted from the fast hydration or water uptake

	S1, M1, X1	S2, M2, X2	S3, M3, X3	S4, M4, X4
P407: HPMC: polyols	2:2:1	2:2:2	3:1:1	3:1:2

Sorbitol (S), Mannitol (M), Xylitol (X)

by the tablets (Figure 6.12). Sorbitol and xylitol formulations formed hydrogel tablets after 30 minutes, while mannitol still had some glassy core up to 90 minutes (Figure 6.12), which is attributed to their higher solubility (Rowe *et al.,* 2005). Dissolution efficiency (D.E.) results confirmed the results of CHD release using both methods. CFR method results showed a difference in the release rate based on polymer ratios, whereas App I did not show the same pattern (Figure 6.22), for instance, there was >20% difference in D.E. for S1, M1 and X1 by comparing the two methods, which decreased to around 5% for S4, M4 and X4. Furthermore, CHD release using the CFR method is more representative for buccal drug delivery by mimicking salivary flow rate with the advantage of an infinite sink condition.

E% for tablets investigated with the CFR method (Table 6.6) has a good agreement with the dissolution data for all formulations which indicates that there is a strong correlation between tablet erosion and CHD release. Kinetics of drug release was studied using six models, the best fitting was with Korsmeyer Peppas and the second best fitting is with Hopfenberg model (Table 6.9 and Table 6.10. Fitting to Hopefenberg model indicates the involvement of erosion mostly for high P407 and polyols content, which is attributed to their high solubility (Dürig and Fassihi, (2002)

In vitro equivalence analysis was performed to investigate the difference within the triplicate of each formulation using CFR method and compare it with the triplicate obtained by App I. Single way ANOVA showed no significant difference within the triplicates for both methods ($p>0.5$), and they were similar based on similarity factor with f_2>50% data. However, difference factor f_1 and AUC ratio did not show the same agreement; interestingly the variation was noticed with few

	S1, M1, X1	S2, M2, X2	S3, M3, X3	S4, M4, X4
P407: HPMC: polyols	2:2:1	2:2:2	3:1:1	3:1:2

Sorbitol (S), Mannitol (M), Xylitol (X)

replicates of 2:2 P407: HPMC ratios. Resigno indices do not have a cut-off value, but it showed a similar comparison. Finally, based on the equivalence analysis, S3, S4, M3, M4, X3 and X4 have similar acceptance to App I data.

The interaction between CHD and the excipients during the granulation and tablet pressing were investigated using FTIR, DSC and XRD (Figure 6.19, Figure 6.20and Figure 6.21). The data showed that there was no interaction between the physical mixtures and the granules for the investigated formulations S4, M4 and X4. This means that the matrix tablet can be applied to control the release of various types of active ingredients to the buccal cavity without being affected by salivary flow rate.

6.5 Conclusions

CHD Mucoadhesive buccal tablets were successfully formulated with the aid of polyols. To overcome poor powder flowability of the excipients, melt granulation showed remarkable improvement in powder flow and no interaction was observed between CHD and the excipients using FTIR, DSC and XRD. Moreover, CFR method preferred over the App I by miming salivary flow rate, although further adjustment needs to be performed to be considered for all buccal formulation drug delivery.

Moreover, S4, M4 and X4 formulations were not affected by the volume of the dissolution media, so they can be considered as a suitable candidate for local buccal drug delivery especially for xerostomia patients and will not be affected by drinking during tablet application. Moreover, due to the successful drug release from these formulations, further investigations on different drugs with different physical properties and for trans buccal applications is required

	S1, M1, X1	S2, M2, X2	S3, M3, X3	S4, M4, X4
P407: HPMC: polyols	2:2:1	2:2:2	3:1:1	3:1:2

Sorbitol (S), Mannitol (M), Xylitol (X)

Chapter Seven

Summary, Discussion and Conclusion

P407: HPMC: polyols	S1, M1, X1	S2, M2, X2	S3, M3, X3	S4, M4, X4
Sorbitol (S), Mannitol (M), Xylitol (X)	2:2:1	2:2:2	3:1:1	3:1:2

Chapter 7: Summary, Discussion and Conclusion

Oropharyngeal candidiasis is a fungal infection caused by *Candida* spp especially *C. albicans.* The targeted population is mostly the immunocompromised patients. CHD, farnesol and thymol were investigated for their anticandidal activity followed by a series of investigations for drug selection, effective and safe concentration. The final goal was to design and prepare mucoadhesive hydrogel buccal tablets and to evaluate the tablets under a condition simulating salivary flow rate in the oral cavity.

7.2 CHD and Farnesol or Thymol

Studies to increase the efficacy of CHD against *Candida*, using thymol and farnesol were investigated. Farnesol showed a negative effect on CHD activity, so it was excluded from the investigation. Thymol showed a minimum enhancement, but the effect was not considered synergistic. Although both CHD and thymol showed concentration and time-dependent biocidal effect on *Candida* (Bobichon and Bouchet, 1987, Braga *et al*., 2008), they showed a concentration-dependent effect on HEK293 cell line as well (Bobichon and Bouchet, 1987, Llana-Ruiz-Cabello *et al*., 2014). However, because the combination of CHD and thymol increased the cytotoxic effect of CHD, accordingly thymol was excluded from future formulations.

Consequently, further studies on combining CHD with farnesol or thymol was discontinued and mucoadhesive buccal tablet formulations only with CHD were developed.

7.3 CHD Dose Selection

Based on the BNF, CHD dosage form for oral application is available in the form of a mouthwash, dental gel and oral spray, none of the formulations has a controlled release effect. In this work, the effect of CHD was investigated for two hours to prolong its activity, which is less than that of the marketed miconazole mucoadhesive buccal tablet (Loramyc®), which is designed to be applied for 6 hours. Although, mucoadhesive buccal tablets are not interfering with eating and drinking (Rahamatullah *et al*., 2011). , the two hours duration for CHD release was chosen to minimise possible poor patient compliance obtained from the repeated and prolonged application of the tablet especially for patients who fears to eat or drink while applying the tablet or due to the lack of its physical flexibility as stated by Salamat-Miller *et al*., (2005).

The effect of CHD was investigated on *C. albicans* planktonic cells, biofilm and on HEK 293 cells. MIC and MBC against *C. albicans* (ATCC 10231) planktonic cells are 2.5 and 5 µg/ml respectively after 24-48 hours. By comparing the effect of CHD on 24-h *Candida* biofilm and HEK 293 cell line, it was found that a concentration of 20 µg/ml and 2 hours treatment effected an 85% and 40% decrease in the oxidative stress, respectively. Furthermore, there was a 78% loss of vacuolar activity and 60% of the protein content of *Candida* biofilm. On the other hand, neither the lysosomal activity nor protein content of HEK 293 cells was affected by the treatment. This concentration (20 µg/ml) was considered as that required to be maintained in the oral cavity for two hours to be effective against *Candida* cells. Consequently, this concentration needs to be considered when designing the buccal mucoadhesive tablet for CHD release. However, this concentration is considered only as a starting point and it might be increased or

decreased depending on the *in vivo* activity. Thus Lilly *et al*., (2006) showed that epithelial cells appear to prevent the growth of *Candida* in the oral cavity by stimulating the release of cytokines. Moreover, salivary antimicrobial proteins prevent overgrowth of *Candida* (Akpan and Morgan, 2002), which might potentiate the anticandidal activity of CHD.

7.4 Tablet Preparation

Formulation development design of mucoadhesive buccal tablets was implemented in three different stages. Firstly, drug: polymer ratio was examined. Secondly: after selecting the proper ratio (1:5) with a tablet weight of 30mg, P407 was introduced to the formulation to improve CHD release, different HPMC: P407 ratios were tested. Finally, to improve drug release and taste perception, sugar alcohol namely sorbitol, xylitol and mannitol (water soluble and non-cariogenic) (Carocho *et al.,* 2017) were investigated.

Tablet blends showed poor flowability, making it unsuitable for direct compression, and this urged the need for blend granulation. Dry granulation and melt granulation was applied, the former showed a limited improvement of the flowability, due to the generation of fine particle fraction, the results showed an agreement with Herting and Kleinebudde, (2007) findings. This was confirmed by dry granules SEM micrographs (Figure 4.4). As a consequence, the low melting point of P407 and the thermal stability of CHD were exploited to prepare melt granules, which showed improvement in the flowability (Table 6.2).

7.6 Tablet physical properties

The subsequently prepared tablet formulations had acceptable physical properties, although they did not show high hardness, they were not friable, which

according to Dugar *et al*. (2016) is due to the waxy nature of P407. Moreover, they all successfully adhered to the chicken mucosa for two hours in the disintegration apparatus, promising an *in vivo* mucoadhesion to the oral mucosa of the patients.

Referring to the kinetics of tablets hydration and by comparing the first group of formulations (Table 5.1 which contain HPMC, P407 and CHD with the second group of formulations with the addition of polyols (Table 6.5), it is noticeable that sorbitol, mannitol and xylitol have increased the rate of hydration. Khan *et al*., (2007) also found that increasing the amount of polyols in the tablets resulted in increasing their wetting. Consequently, this facilitated the conversion of the tablets to form hydrogels. Although the homogeneity of the hydrogel layer is questionable, since by examining the tablets under polarized microscopy, the hydrated tablet showed an anisotropic birefringent appearance which increased with P407 ratio, and to more extent with the added sugar alcohols (sorbitol, mannitol and xylitol). This agrees with the hydration results, which showed faster hydration with the added polyols. The fast hydration of polyols is attributed to their water solubility (Rowe *et al.*, 2006) and considering the humectant property of both sorbitol and xylitol (Ergun *et al.*, 2010). This facilitated the formation of the hydrogel tablet, this would add an advantage of soft texture to improve patients' compliance especially for xerostomia patients.

Drug Excipient interaction was analysed for the selected formulations for a possibility of chemical interaction between the excipients and the drug. It was noticed that P407 produced a steric hindrance (Göppert and Müller, 2005) which might have been obtained from the mixing of the blends and resulted in enveloping of other excipients and CHD. The difference in the DSC thermograms

of CHD between the 5 mg formulation; F15 (Figure 4.12) and the 2.5 mg dosage S4, M4 and X4 (Figure 6.20) is the disappearance of the CHD melting peak, which might be attributed to the low dosage and the higher amount of P407 and HPMC (the former was 18.25 mg and 6.25 mg while the latter was 21 mg and 7 mg, respectively). Another scenario is the availability of polyols in the formulation. Since both sorbitol and xylitol have a lower melting point than CHD, they might affect the disappearance of the CHD peak. However, the mannitol melting point is higher than that of CHD of around 157 and 165°C, respectively, therefore the CHD melting point peak might be masked by the mannitol melting peak.

The formulated tablets were designed to be applied directly to the oral mucosa and the homogeneity of the drug on the surface of the tablet is important to overcome the irritation produced by the drug. The homogeneity of the CHD in the formulations is evidenced in the SEM Nitrogen mapping studies using SEM/EDX imaging, showing CHD is spread evenly over the tablets surfaces

7.7 Drug release conventional versus CFR

The lack of a proper method to analyse drug release from mucoadhesive tablets might result in a non-effective dose or drug activity measurement. Moreover, using conventional dissolution methods, showed a higher percentage of drug released than the CFR method, most likely due to the higher volume of the dissolution media. This highlights the importance to develop an alternative suitable method to analyse drug release in the oral cavity. Three different flow rates were investigated using the CFR method and Liebig condenser, it was found that the higher the flow rate resulted in a higher drug release. This means that in patients with xerostomia or hyposalivation drug release will be less than

that for patients with normal salivary flow rate, and this is confirmed by Bouckaert *et al.,* (1996) finding that buccal drug release is substantially decreased by the low volume of saliva.

Furthermore, due to the statistical inequivalence in some replicates using the Liebig condenser method and to decrease the complexity of the experimental setting, the method was further developed (Figure 6.1), The results obtained were more reliable and showed only minor inequivalence compared to Apparatus I analysis.

Considering the final developed formulations by the addition of polyols with a proper ratio of P407: HPMC the resultant formulations S4, M4 and X4, were not affected by the volume of the dissolution media, and this is of immense importance for the treatment of OPC especially for xerostomic patients. The release kinetics for these formulations was super-case II resultant from the higher rate of water penetration into the tablets faster than polymer relaxation (Bruschi, 2015). CHD Mucoadhesive buccal tablets have been previously investigated by other researchers. Irwin *et al.,* (2003), prepared the mucoadhesive tablet using 75 mg hydroxyethyl cellulose, 25 mg polyacrylic acid and 10 mg CHD. The formulation was tested both *in vitro* using 900 mL of PBS and *in vivo* (n=5). In vitro study showed around 2 mg CHD release from the tablet (20% of the original formulation) which is equivalent to 2.2 µg/ml and this concentration is considered as not effective against *Candida* biofilm, based upon our findings. *In vivo* studies of Irwin *et al* (2003) showed only 0.5-0.8 mg CHD after 4 hours but they did not specify the salivary volume. It did indicate that drug release was affected by the volume of the dissolution media and so there will be individual variations based on salivary flow rates. Finally, neither antimicrobial nor cytotoxicity investigation

was performed in this study to evaluate whether the concentration range used was effective. The size of the prepared tablet was greater than two times bigger than S4, X4 and M4 which might produce patient distress, with more drug loading and less drug release (drug release for S4, X4 and M4 was nearly 90% which is equivalent to 2.25 mg of CHD).

Giunchedi *et al*., (2001) prepared 100 mg buccal tablet using spray dried CHD with chitosan, the drug content was 13 mg and drug release after 12 hours using App I and 300 mL of PBS was (40%). The *in vivo* release was performed in replicate for 4 hours in one volunteer, and the release profile was not comparable to the *in vitro* release as it increased with time reaching a maximum concentration of 20 µg/ml at one hour and then decreases to the end of the analysis at 4 hours. Compared to release studies of our formulations the release was nearly constant over time and volume of the dissolution media did not affect drug release or its profile. In Giunchedi *et al*., (2001), the MIC and the MBC of the prepared CHD: chitosan microspheres against *C. albicans* were 15.6 µg/ml after 24 hours, and no antibiofilm testing was performed. Based upon the antibiofilm activity conducted in our work the successful application of these formulations for the treatment of OPC is doubtful. Moreover, chitosan is practically insoluble in saliva (Savica *et al.,* 2009) compared to our formulation which is completely soluble in saliva. Moreover, there is a lack of information regarding how the tablet was removed from the oral cavity and analysed to see if all of the drug has been released or not.

Another investigation was performed by Ceschel *et al*., (2006). They prepared 60 mg tablets of 2.5 mg CHD and Lactose monohydrate with different ratios of Carbomer 974p to HPMC. They investigated drug release using three dissolution

methods; App II and 900 mL PBS and two *ex vivo* methods. One of the latter was conducted at 1 mL/min flow rate and the second one using 4.8 mL of media in a Franz diffusion cell. The release profile of CHD was erratic and was greatly affected by the volume of the dissolution media. The selected formulation showed a 60% (2.7 µg/ml) burst release from the first few minutes using the puddle method and 900 ml followed by gradual release reaching 90% (1.6 µg/ml) after 6 hours. These concentrations are considered as not effective based upon our anticandidal activity results. The same formulation showed a maximum release of 80% (average of 20 µg/ml) after ~1 hour using an *ex vivo* method and 1 ml/min flow rate. Again, based upon our findings this would not be sufficient to be effective against *C. albicans* biofilm. Moreover, the authors did not investigate the mucoadhesion of their formulations, nor the antimicrobial activity.

Finally, our selected formulations S4, X4 and M4 release studies using CFR at 1mL/min flow rate showed an average release around 19 µg/mL, showed promising results against *Candida* biofilm. Although, the effect on more mature biofilm is not predictable taking into consideration the different factors in the oral cavity which might increase or decrease CHD activity.

7.8 Conclusion and future work

Based on the current findings, CHD hydrogel-forming mucoadhesive buccal tablets were successfully prepared. They showed acceptable properties, good mucoadhesion and drug release which was not affected by the volume of the dissolution media, and consequently by salivary flow rates. Consequently, the tablets are a suitable candidate for the treatment of OPC patients with or without xerostomia and salivary glands hypofunction. Clinical investigation is needed to

be performed to check drug release in the oral cavity, patient perception and acceptance, and the effect on *Candida* biofilm in the oral cavity. Moreover, one of CHD side effects is teeth staining, and this should be tested both *in vitro* and *in vivo,* although the used dosage in this formulation is much less than the dose available in the marketed products. Moreover, regarding the CFR method, a further adjustment needs to be performed to consider different sizes and shapes for local buccal drug delivery. The availability of marketed mucoadhesive buccal tablets, gels and films urged the need for an appropriate method of drug release analysis to mimic the release in the oral cavity. The developed method showed a good start to further adopt other dosage forms.

References

References

Abiko, Y., Nishimura, M. and Kaku, T. (2003). Defensins in saliva and the salivary glands. *Medical Electron Microscopy,* 36: 247-252.

Abu-Elteen, K.H. (2005). The influence of dietary carbohydrates on in vitro adherence of four Candida species to human buccal epithelial cells. *Microbial Ecology in Health and Disease*, 17: 156-162.

Abu-Elteen, K. H., and Whittaker, P. A. (1997). Effect of sub-inhibitory concentration of chlorhexidine on lipid and sterol composition of shape Candida albicans. *Mycopathologia*, *140*: 69-76.

Ai, R., Wei, J., Ma, D., Jiang, L., Dan, H., Zhou, Y., and Chen, Q. (2017). A meta-analysis of randomized trials assessing the effects of probiotic preparations on oral candidiasis in the elderly. *Archives of oral biology*, *83*: 187-192.

Akpan, A., and Morgan, R. (2002). Oral candidiasis. *Postgraduate medical journal*, *78*: 455-459.

Albuquerque, P., and Casadevall, A. (2012). Quorum sensing in fungi–a review. *Medical mycology*, 50: 337-345.

Adler, J., Jayan, A., and Melia, C. D. (1999). A method for quantifying differential expansion within hydrating hydrophilic matrixes by tracking embedded fluorescent microspheres. *Journal of pharmaceutical sciences*, *88*: 371-377.

Amiri, H. M., Frandah, W., Colmer-Hamood, J., Raj, R., and Nugent, K. (2012). Risk factors of Candida colonization in the oropharynx of patients admitted to an intensive care unit. *Journal of Medical Mycology*, 22: 301-307.

Anderson, N. H., Bauer, M., Boussac, N., Khan-Malek, R., Munden, P., and Sardaro, M. (1998). An evaluation of fit factors and dissolution efficiency for the comparison of *in vitro* dissolution profiles. *Journal of Pharmaceutical and Biomedical Analysis*, *17*: 811-822.

Amorim, C. V. G. D., Aun, C. E., and Mayer, M. P. A. (2004). Susceptibility of some oral microorganisms to chlorhexidine and paramonochlorophenol. *Brazilian oral research*, *18*: 242-246.

Ankola, A. V., Hebbal, M. and Mocherla, M. (2008). A review of efficacy of various modes of chlorhexidine delivery. *Journal of Oral Biosciences,* 50: 239-242.

Arafa, M. F., El-Gizawy, S. A., Osman, M. A., and El Maghraby, G. M. (2016). Xylitol as a potential co-crystal co-former for enhancing dissolution rate of felodipine: preparation and evaluation of sublingual tablets. *Pharmaceutical development and technology*, 42: 1-10.

Arruda, E. M., Boyce, M. C., and Quintus-Bosz, H. (1993). Effects of initial anisotropy on the finite strain deformation behaviour of glassy polymers. *International Journal of Plasticity*, *9*: 783-811.

Azarmi, S., Roa, W., and Löbenberg, R. (2007). Current perspectives in dissolution testing of conventional and novel dosage forms. *International Journal of Pharmaceutics*, 328: 12-21.

Baboni, F.B., Barp, D., de Azevedo Izidoro, A.C.S., Samaranayake, L.P., and Rosa, E.A.R. (2009). Enhancement of Candida albicans virulence after exposition to cigarette mainstream smoke. *Mycopathologia*, 168: 227-235.

Bajwa, G. S., Hoebler, K., Sammon, C., Timmins, P., and Melia, C. D. (2006). Microstructural imaging of early gel layer formation in HPMC matrices. *Journal of pharmaceutical sciences*, *95*: 2145-2157.

Baron, A.C., Gansky, S.A., Ryder, M.I., and Featherstone, J.D.B. (1999). Cysteine protease inhibitory activity and levels of salivary cystatins in whole saliva of periodontally diseased patients. *Journal of Periodontal Research*, 34: 437-444

Bastidas, R. J., and Heitman, J. (2009). Trimorphic stepping stones pave the way to fungal virulence. *Proceedings of the National Academy of Sciences*, 106: 351-352.

Beck-Broichsitter, M., Bohr, A., and Ruge, C. A. (2017). Poloxamer-decorated polymer nanoparticles for lung surfactant compatibility. *Molecular pharmaceutics*, *14*: 3464-3472.

Bensadoun, R. J., Daoud, J., El Gueddari, B., Bastit, L., Gourmet, R., Rosikon, A., Allavena, C., Céruse, P., Calais, G. and Attali, P. (2008). Comparison of the efficacy and safety of miconazole 50-mg mucoadhesive buccal tablets with miconazole 500-mg gel in the treatment of oropharyngeal candidiasis. *Cancer*, 112: 204-211.

Bergdahl, M., and Bergdahl, J. (2000). Low unstimulated salivary flow and subjective oral dryness: association with medication, anxiety, depression, and stress. *Journal of Dental Research,* 79: 1652-1658.

Bernauer, U. (2015). Opinion of the scientific committee on consumer safety (SCCS)–2nd Revision of the safety of the use of poly (hexamethylene) biguanide hydrochloride or polyaminopropyl biguanide (PHMB) in cosmetic products. *Regulatory Toxicology and Pharmacology*, *73*: 885-886.

Blanco-Fuente, H., Anguiano-Igea, S., Otero-Espinar, F. and Blanco-Mendez, J. (1996). In-vitro bioadhesion of carbopol hydrogels. *International Journal of Pharmaceutics,* 142: 169-174.

Blanco-Fuente, G.P., Laverty, T.P. and Jones, D.S. (2009). Mucoadhesive polymeric platforms for controlled drug delivery. *European Journal of Pharmaceutics and Biopharmaceutics,* 71: 505-518.

Bobichon, H., and Bouchet, P. (1987). Action of chlorhexidine on budding Candida albicans: Scanning and transmission electron microscopic study. *Mycopathologia,* 100: 27-35.

Bolhuis, G. K., and Anthony Armstrong, N. (2006). Excipients for direct compaction—an update. *Pharmaceutical development and technology*, *11*: 111-124.

Bolhuis, G. K., Rexwinkel, E. G., and Zuurman, K. (2009). Polyols as filler-binders for disintegrating tablets prepared by direct compaction. *Drug development and industrial pharmacy*, *35*: 671-677.

Bonacucina, G., Cespi, M., Mencarelli, G., Giorgioni, G., and Palmieri, G. F. (2011). Thermosensitive self-assembling block copolymers as drug delivery systems. *Polymers*, *3*: 779-811.

Bongomin, F., Gago, S., Oladele, R. O., and Denning, D. W. (2017). Global and multi-national prevalence of fungal diseases—estimate precision. *Journal of Fungi*, *3*: 57.

Both, T., Dalm, V. A., van Hagen, P. M., and van Daele, P. L. (2017). Reviewing primary Sjögren's syndrome: beyond the dryness-From pathophysiology to diagnosis and treatment. *International journal of medical sciences*, *14*: 191.

Bouckaert, S., Vakaet, L., and Remon, J. P. (1996). Influence of the buccal application site of a bioadhesive slow-release tablet on salivary miconazole concentrations in irradiated patients. *International Journal of pharmaceutics*, *130*: 257-260.

Brady, J. Dürig, T. Lee, P.I and Li, J.-X. (2017), Chapter 7 - Polymer Properties and Characterization, Editor(s): Yihong Qiu, Yisheng Chen, Geoff G.Z. Zhang, Lawrence Yu and Rao V. Mantri, Developing Solid Oral Dosage Forms (Second Edition), Academic Press.

Braga, P. C., Alfieri, M., Culici, M., and Dal Sasso, M. (2007a). Inhibitory activity of thymol against the formation and viability of Candida albicans hyphae. *Mycoses*, 50: 502-506.

Braga, P. C., Culici, M., Alfieri, M., and Dal Sasso, M. (2008). Thymol inhibits Candida albicans biofilm formation and mature biofilm. *International journal of antimicrobial agents*, 31: 472-477.

Braga, P. C., Dal Sasso, M., Culici, M., and Alfieri, M. (2007b). Eugenol and thymol, alone or in combination, induce morphological alterations in the envelope of Candida albicans. *Fitoterapia*, 78: 396-400.

Brilhante, R.S.N., Caetano, É.P., de Lima, R.A.C., de Farias Marques, F.J., Castelo, D.D.S.C.M., de Melo, C.V.S., de Melo Guedes, G.M., de Oliveira, J.S., de Camargo, Z.P., Moreira, J.L.B. and Monteiro, A.J., (2016). Terpinen-4-ol, tyrosol, and β-lapachone as potential antifungals against dimorphic fungi. *Brazilian Journal of Microbiology*, 47: 917-924.

British Pharmacopoeia (2018 a). Appendix XII C. Consistency of Formulated Preparations (Online). Available from https://www-pharmacopoeia-com.ezproxy.wlv.ac.uk/bp-2018/appendices/appendix-12/appendix-xii-c--consistency-of-formulated-preparations.html?date=2018-01-01andtext=Consistency+of+Formulated+++Preparations (Accessed 31/01/18)

British Pharmacopoeia (2018 b). Appendix XII B. Dissolution (Online). Available from: https://www-pharmacopoeia-com.ezproxy.wlv.ac.uk/bp-2018/appendices/appendix-12/appendix-xii-b--dissolution.html?date=2018-01-01andtext=Dissolution+ (Accessed 31/01/18).

British Pharmacopoeia (2018 c). Chlorhexidine Acetate (Online). Available from: https://www-pharmacopoeia-com.ezproxy.wlv.ac.uk/bp-2018/monographs/chlorhexidine-acetate.html?date=2018-01-01andtext=Chlorhexidine+Acetate (Accessed 31/01/18).

British Pharmacopoeia (2018 d). Appendix XVII A. Particle Size of Powders Online). Available from: https://www-pharmacopoeia-com.ezproxy.wlv.ac.uk/bp-2018/appendices/appendix-17/appendix-xvii-a--particle-size-of-powders.html?date=2018-01-01andtext=Particle+Size+of+Powders+ (Accessed 31/01/18).

British Pharmacopoeia (2018 e). Appendix XVII N. Powder Flow (Online). Available from: https://www-pharmacopoeia-com.ezproxy.wlv.ac.uk/Search/bp-2018?text=Powder+Flowanddate=2018-01-01 (Accessed 31/01/18).

Brown, C.G., and Wingard, J. (2004). Clinical consequences of oral mucositis. *Seminars in Oncology Nursing*, 20: 16-21

Bruni, G., Berbenni, V., Milanese, C., Girella, A., Cofrancesco, P., Bellazzi, G., and Marini, A. (2009). Physico-chemical characterization of anhydrous D-mannitol. *Journal of thermal analysis and calorimetry*, *95*: 871-876.

Bruschi, M. L. (2015). *Strategies to modify the drug release from pharmaceutical systems;* Elsevier: Amsterdam,The Netherlands.

Bruschi, M.L. and De Freitas, O. (2005). Oral bioadhesive drug delivery systems. *Drug Development and Industrial Pharmacy,* 31, 293-310.

Buhl, R. (2006). Local oropharyngeal side effects of inhaled corticosteroids in patients with asthma. *Allergy*, 61: 518-526.

Bulacio, L., Paz, M., Ramadán, S., Ramos, L., Pairoba, C., Sortino, M., Escovich, L. and López, C. (2012). Oral infections caused by yeasts in patients with head and neck cancer undergoing radiotherapy. Identification of the yeasts and evaluation of their antifungal susceptibility. *Journal of Medical Mycology*, 22: 348-353.

Burgess, J., and Lee, P. (2012). XyliMelts time-release adhering discs for night-time oral dryness. *International journal of dental hygiene*, 10: 118-121.

Calderone, R. A., and Fonzi, W. A. (2001). Virulence factors of Candida albicans. *Trends in Microbiology*, 9: 327-335.

Campisi, G., Paderni, C., Saccone, R., Fede, O., Wolff, A. and Giannola, L. (2010). Human buccal mucosa as an innovative site of drug delivery. *Current Pharmaceutical Design,* 16: 641-652.

Campoy, S., and Adrio, J. L. (2017). Antifungals. *Biochemical pharmacology*, *133*: 86-96.

Cardot, J. M., Chaumont, C., Dubray, C., Costantini, D., and Aiache, J. M. (2004). Comparison of the pharmacokinetics of miconazole after administration via a bioadhesive slow release tablet and an oral gel to healthy male and female subjects. *British journal of clinical pharmacology*, 58: 345-351.

Carocho, M., Morales, P., and Ferreira, I. C. (2017). Sweeteners as food additives in the XXI century: A review of what is known, and what is to come. *Food and Chemical Toxicology*, *107*: 302-317.

Carrijo-Carvalho, L. C., Sant'ana, V. P., Foronda, A. S., de Freitas, D., and de Souza Carvalho, F. R. (2017). Therapeutic agents and biocides for ocular infections by free-living amoebae of Acanthamoeba genus. *survey of ophthalmology*, *62*: 203-218.

Ceschel, G. C., Bergamante, V., Calabrese, V., Biserni, S., Ronchi, C. and Fini, A. (2006). Design and evaluation in vitro of controlled release mucoadhesive tablets containing chlorhexidine. *Drug Development and Industrial Pharmacy,* 32: 53-61.

Chandra, J., Kuhn, D. M., Mukherjee, P. K., Hoyer, L. L., McCormick, T., and Ghannoum, M. A. (2001). Biofilm formation by the fungal pathogen *Candida albicans*: development, architecture, and drug resistance. *Journal of bacteriology*, 183: 5385-5394.

Chaturvedi, K., Gajera, B. Y., Xu, T., Shah, H., and Dave, R. H. (2018). Influence of processing methods on physico-mechanical properties of

Ibuprofen/HPC-SSL formulation. *Pharmaceutical development and technology*, 1-9.

Cho, M.A., ko, J.Y., kim, Y.K. and kho, H.S. (2010), Salivary flow rate and clinical characteristics of patients with xerostomia according to its etiology. *Journal of Oral Rehabilitation*, 37: 185–193

Codd, J.E. and Deasy, P. (1998). Formulation development and in vivo evaluation of a novel bioadhesive lozenge containing a synergistic combination of antifungal agents. *International Journal of Pharmaceutics,* 173: 13-24

Colombo, P., Bettini, R., Santi, P., and Peppas, N. A. (2000). Swellable matrices for controlled drug delivery: gel-layer behaviour, mechanisms and optimal performance. *Pharmaceutical science and technology today*, *3*: 198-204.

Committee for proprietary medicinal products (2000). Note for Guidance on the Investigation of Bioavailability and Bioequivalence*, CPMP/EWP/QWP/1401/98. European Medicines Agency (EMA),* London.

Cordeiro, R. A., Teixeira, C. E., Brilhante, R. S., Castelo-Branco, D. S., Paiva, M. A., Giffoni Leite, J. J., Lima, D.T., Monteiro, A.J., Sidrim, J.J. and Rocha, M. F. (2013). Minimum inhibitory concentrations of amphotericin B, azoles and caspofungin against Candida species are reduced by farnesol. *Medical Mycology,* 51: 53-59.

Costa, P., and Lobo, J. M. S. (2001). Modeling and comparison of dissolution profiles*. European Journal of Pharmaceutical Sciences*, 13: 123-133.

Dalleau, S., Cateau, E., Bergès, T., Berjeaud, J. M., and Imbert, C. (2008). In vitro activity of terpenes against Candida biofilms. *International journal of antimicrobial agents*, 31: 572-576.

Davies, G., Francis, J., Martin, A., Rose, F. and Swain, G. (1954). 1: 6-Di-4′-Chlorophenyldiguanidohexane (“Hibitane”). Laboratory Investigation of a New Antibacterial Agent of High Potency. *British Journal of Pharmacology and Chemotherapy,* 9: 192-196.

Degregorio, M. W., Lee, W. M., and Ries, C. A. (1982). Candida infections in patients with acute leukemia: ineffectiveness of nystatin prophylaxis and relationship between oropharyngeal and systemic candidiasis. *Cancer*, *50*: 2780-2784.

Deng, L. L., Taxipalati, M., Que, F., and Zhang, H. (2016). Physical characterization and antioxidant activity of thymol solubilized Tween 80 micelles. Scientific reports, 6: 38160.

Denning, D.W. (2003). Echinocandin antifungal drugs. *The Lancet,* 362: 1142-1151.

Derrien, M., Van Passel, M.W., Van De Bovenkamp, J.H., Schipper, R., De Vos, W. and Dekker, J. (2010). Mucin-bacterial interactions in the human oral cavity and digestive tract. *Gut microbes,* 1: 254-268.

Deshpande, A., and Jadad, A. R. (2008). The impact of polyol-containing chewing gums on dental caries: a systematic review of original randomized controlled trials and observational studies. *The Journal of the American Dental Association*, *139*: 1602-1614.

Ding, C., Zhang, M. and Li, G. (2015). Preparation and characterization of collagen/hydroxypropyl methylcellulose (HPMC) blend film. *Carbohydrate Polymers,* 119: 194-201.

Dodds, M.W., Johnson, D.A. and Yeh, C.K. (2005). Health benefits of saliva: a review. *Journal of Dentistry,* 33: 223-233.

Dongari-Bagtzoglou, A., and Fidel Jr, P. L. (2005). The host cytokine responses and protective immunity in oropharyngeal candidiasis. *Journal of dental research*, *84*: 966-977.

Dos Santos, A. C. M., Akkari, A. C. S., Ferreira, I. R. S., Maruyama, C. R., Pascoli, M., Guilherme, V. A., de Paula, E., Fraceto, L.F., de Lima, R., da Silva Melo, P. and de Araujo, D. R. (2015). Poloxamer-based binary hydrogels for delivering tramadol hydrochloride: sol-gel transition studies, dissolution-release kinetics, in vitro toxicity, and pharmacological evaluation. *International journal of nanomedicine,* 10: 2391-2401.

Dost, F., and Farah, C. S. (2013). Stimulating the discussion on saliva substitutes: a clinical perspective. *Australian Dental Journal*, *58*, 11-17.

Doumas, S., Kolokotronis, A. and Stefanopoulos, P. (2005). Anti-inflammatory and antimicrobial roles of secretory leukocyte protease inhibitor. *Infection and Immunity,* 73: 1271-1274.

Dugar, R. P., Gajera, B. Y., and Dave, R. H. (2016). Fusion method for solubility and dissolution rate enhancement of ibuprofen using block copolymer poloxamer 407. *AAPS PharmSciTech*, *17*: 1428-1440.

Dumortier, G., Grossiord, J. L., Agnely, F. and Chaumeil, J. C. (2006). A review of poloxamer 407 pharmaceutical and pharmacological characteristics. *Pharmaceutical Research,* 23: 2709-2728.

Dürig, T., and Fassihi, R. (2002). Guar-based monolithic matrix systems: effect of ionizable and non-ionizable substances and excipients on gel dynamics and release kinetics. *Journal of controlled release*, *80*: 45-56.

Dušan, F., Marián, S., Katarína, D., and Dobroslava, B. (2006). Essential oils—their antimicrobial activity against Escherichia coli and effect on intestinal cell viability. *Toxicology in vitro*, 20: 1435-1445.

Epstein, J. B., Emerton, S., Le, N. D., and Stevenson-Moore, P. (1999). A double-blind crossover trial of Oral Balance gel and Biotene® toothpaste versus placebo in patients with xerostomia following radiation therapy. *Oral oncology*, *35*: 132-137.

Epstein, J. B., Gorsky, M., and Caldwell, J. (2002). Fluconazole mouthrinses for oral candidiasis in postirradiation, transplant, and other patients. *Oral Surgery, Oral Medicine, Oral Pathology, Oral Radiology, and Endodontology*, 93: 671-675.

Epstein, J.B. and Polsky, B. (1998). Oropharyngeal candidiasis: A review of its clinical spectrum and current therapies. *Clinical Therapeutics,* 20: 40-57.

Ergun, R., Lietha, R., and Hartel, R. W. (2010). Moisture and shelf life in sugar confections. *Critical reviews in food science and nutrition*, *50*: 162-192.

Farah, C. S., Lynch, N., & McCullough, M. J. (2010). Oral fungal infections: an update for the general practitioner. *Australian dental journal*, *55*: 48-54.

Femiano, F., Rullo, R., di Spirito, F., Lanza, A., Festa, V. M., and Cirillo, N. (2011). A comparison of salivary substitutes versus a natural sialogogue (citric acid) in patients complaining of dry mouth as an adverse drug reaction: a clinical, randomized controlled study. *Oral Surgery, Oral Medicine, Oral Pathology, Oral Radiology, and Endodontology*, *112*: 15-20.

Ferreirós, M. P., García-Martínez, F. and Alonso-González, J. (2012). Update on the treatment of superficial mycoses. *Actas Dermo-Sifiliográficas ,* 103: 778-783.

Fidel Jr, P. L. (2006). Candida-host interactions in HIV disease: relationships in oropharyngeal candidiasis. *Advances in dental research*, *19*: 80-84.

Filoche, S. K., Soma, K., and Sissons, C. H. (2005). Antimicrobial effects of essential oils in combination with chlorhexidine digluconate. Molecular Oral Microbiology, 20: 221-225.

Fini, A., Bergamante, V. and Ceschel, G.C. (2011). Mucoadhesive gels designed for the controlled release of chlorhexidine in the oral cavity. *Pharmaceutics,* 3: 665-679.

Fotakis, G., and Timbrell, J. A. (2006). In vitro cytotoxicity assays: comparison of LDH, neutral red, MTT and protein assay in hepatoma cell lines following exposure to cadmium chloride*. Toxicology letters,* 160: 171-177.

Fothergill, A. W. (2006). Miconazole: a historical perspective. *Expert review of anti-infective therapy*, *4*: 171-175.

Fu, X., Huck, D., Makein, L., Armstrong, B., Willen, U., and Freeman, T. (2012). Effect of particle shape and size on flow properties of lactose powders. *Particuology,* 10: 203-208.

García, D. A., Bujons, J., Vale, C., and Suñol, C. (2006). Allosteric positive interaction of thymol with the GABA A receptor in primary cultures of mouse cortical neurons. *Neuropharmacology,* 50: 25-35.

Ghosh, S., and Sudha, M. L. (2012). A review on polyols: new frontiers for health-based bakery products. *International journal of food sciences and nutrition*, *63*: 372-379.

Giannelli, M., Chellini, F., Margheri, M., Tonelli, P., and Tani, A. (2008). Effect of chlorhexidine digluconate on different cell types: a molecular and ultrastructural investigation. *Toxicology in vitro,* 22: 308-317.

Giunchedi, P., Juliano, C., Gavini, E., Cossu, M. and Sorrenti, M. (2002). Formulation and in vivo evaluation of chlorhexidine buccal tablets prepared using drug-loaded chitosan microspheres. *European Journal of Pharmaceutics and Biopharmaceutics,* 53: 233-239.

Gliemmo, M. F., Campos, C. A., and Gerschenson, L. N. (2004). Effect of sweet humectants on stability and antimicrobial action of sorbates. *Journal of food science*, 69: 39-45.

Ghori, M. U., and Conway, B. R. (2015). Hydrophilic matrices for oral control drug delivery. *American Journal of Pharmacological Sciences*, *3*: 103-109.

Gonsalves, W.C., Wrightson, A.S. and Henry, R.G. (2008). Common oral conditions in older persons. *American Family Physician,* 78: 845-52.

Göppert, T. M., and Müller, R. H. (2005). Protein adsorption patterns on poloxamer-and poloxamine-stabilized solid lipid nanoparticles (SLN). *European journal of pharmaceutics and biopharmaceutics*, 60: 361-372.

Govender, S., Pillay, V., Chetty, D. J., Essack, S. Y., Dangor, C. M., and Govender, T. (2005). Optimisation and characterisation of bioadhesive controlled release tetracycline microspheres. *International journal of pharmaceutics*, *306*: 24-40.

Gow, N.A.R. and Hube, B. (2012). Importance of the Candida albicans cell wall during commensalism and infection. Current Opinion in Microbiology 15: 406-412.

Graybill, J. R., Vazquez, J., Darouiche, R. O., Morhart, R., Greenspan, D., Tuazon, C., Wheat, L. J., Carey, J., Leviton, I., Hewitt, R. G. and MacGregor, R. R. (1998). Randomized trial of itraconazole oral solution for

oropharyngeal candidiasis in HIV/AIDS patients. *The American journal of medicine*, 104: 33-39.

Grenier, D. (1993). Reduction of proteolytic degradation by chlorhexidine. *Journal of dental research*, 72: 630-633.

Guggenheimer, J., Moore, P. A., Rossie, K., Myers, D., Mongelluzzo, M. B., Block, H. M., and Orchard, T. (2000). Insulin-dependent diabetes mellitus and oral soft tissue pathologies. II. Prevalence and characteristics of Candida and candidal lesions. *Oral Surgery, Oral Medicine, Oral Pathology, Oral Radiology, and Endodontology*, *89*: 570-576.

Gulati, M., and Nobile, C. J. (2016). Candida albicans biofilms: development, regulation, and molecular mechanisms. *Microbes and infection*, 18: 310-321.

Guo, J. H., Skinner, G. W., Harcum, W. W., and Barnum, P. E. (1998). Pharmaceutical applications of naturally occurring water-soluble polymers. *Pharmaceutical science and technology today*, 1: 254-261.

Hall, D. J., Khutoryanskaya, O. V., and Khutoryanskiy, V. V. (2011). Developing synthetic mucosa-mimetic hydrogels to replace animal experimentation in characterisation of mucoadhesive drug delivery systems. *Soft Matter*, *7*: 9620-9623.

Han, T.L., Cannon, R.D. and Villas-Boas, S.G. (2011). The metabolic basis of Candida albicans morphogenesis and quorum sensing. *Fungal Genetics and Biology,* 48: 747-763.

Hassan, M. S. and Lau, R. W. M. (2009). Effect of particle shape on dry particle inhalation: study of flowability, aerosolization, and deposition properties. *AAPS PharmSciTech,* 10: 1252-1262.

Helms, J.A., Della-Fera, M.A., Mott, A.E. and Frank, M.E. (1995). Effects of chlorhexidine on human taste perception. *Archives of Oral Biology,* 40: 913-920.

Hendry, E. R., Worthington, T., Conway, B. R., and Lambert, P. A. (2009). Antimicrobial efficacy of eucalyptus oil and 1, 8-cineole alone and in combination with chlorhexidine digluconate against microorganisms grown in planktonic and biofilm cultures. *Journal of Antimicrobial Chemotherapy*, *64*: 1219-1225.

Herting, M. G., and Kleinebudde, P. (2007). Roll compaction/dry granulation: Effect of raw material particle size on granule and tablet properties. *International journal of pharmaceutics*, *338*: 110-118.

Hidalgo, E., and Dominguez, C. (2001). Mechanisms underlying chlorhexidine-induced cytotoxicity. Toxicology in vitro, 15: 271-276.

Hikmet, R. A. M. (1991). Anisotropic gels and plasticized networks formed by liquid crystal molecules. *Liquid Crystals*, *9*: 405-416.

Hikmet, R. A. M., and Howard, R. (1993). Structure and properties of anisotropic gels and plasticized networks containing molecules with a smectic-A phase. *Physical Review E*, *48*: 2752.

Hoare, T.R. and Kohane, D.S. (2008). Hydrogels in drug delivery: progress and challenges. *Polymer,* 49: 1993-2007.

Hoepelman, I.M., and Dupont, B. (1996). Oral candidiasis: The clinical challenge of resistance and management. *International Journal of Antimicrobial Agents*, 6: 155-159.

Holešová, S., Valášková, M., Hlaváč, D., Madejová, J., Samlíková, M., Tokarský, J. and Pazdziora, E. (2014). Antibacterial kaolinite/urea/chlorhexidine nanocomposites: Experiment and molecular modelling. *Applied Surface Science,* 305: 783-791.

Holmes, S. (1998). Xerostomia: aetiology and management in cancer patients. *Supportive Care in Cancer*, *6*: 348-355.

Ihalin, R., Loimaranta, V. and Tenovuo, J. (2006). Origin, structure, and biological activities of peroxidases in human saliva. *Archives of Biochemistry and Biophysics,* 445: 261-268.

İkinci, G., Şenel, S., Wilson, C. G., and Şumnu, M. (2004). Development of a buccal bioadhesive nicotine tablet formulation for smoking cessation. *International Journal of Pharmaceutics*, 277: 173-178.

Irwin, C.R., Mccullough, K.C. and Jones, D.S. (2003). Chlorhexidine-containing mucoadhesive polymeric compacts designed for use in the oral cavity: an examination of their physical properties, in vitro/in vivo drug release properties and clinical acceptability. *Journal of Materials Science: Materials in Medicine,* 14: 825-832.

Islam, N. M., Bhattacharyya, I., and Cohen, D. M. (2012). Salivary gland pathology in HIV patients. *Diagnostic Histopathology*, *18*: 366-372.

Jenkinson, H., Lala, H. and Shepherd, M. (1990). Coaggregation of Streptococcus sanguis and other streptococci with Candida albicans. *Infection and immunity,* 58**:** 1429-1436.

Joint Formulary Committee. (2017) British National Formulary (BNF) 74th Ed. (online) London: BMJ Group and Pharmaceutical Press.

Jones, C. G. (1997). Chlorhexidine: Is it still the gold standard? *Periodontology 2000,* 15: 55-62.

Juliano, C., Cossu, M., Pigozzi, P., Rassu, G. and Giunchedi, P. (2008). Preparation, in vitro characterization and preliminary in vivo evaluation of buccal polymeric films containing chlorhexidine. *AAPS PharmSciTech,* 9: 1153-1158.

Juven, B. J., Kanner, J., Schved, F., and Weisslowicz, H. (1994). Factors that interact with the antibacterial action of thyme essential oil and its active constituents. *Journal of Applied Microbiology,* 76: 626-631.

Kabanov, A. V., Batrakova, E. V., and Alakhov, V. Y. (2002). Pluronic® block copolymers for overcoming drug resistance in cancer. *Advanced drug delivery reviews*, *54*: 759-779.

Kadir, T., Gümrü, B., and Uygun-Can, B. (2007). Phospholipase activity of Candida albicans isolates from patients with denture stomatitis: the influence of chlorhexidine gluconate on phospholipase production. *archives of oral biology,* 52: 691-696.

Kaiser, N., Klein, D., Karanja, P., Greten, Z. and Newman, J. (2009). Inactivation of chlorhexidine gluconate on skin by incompatible alcohol hand sanitizing gels. *American Journal of Infection Control,* 37: 569-573

Kamikawa, Y., Nagayama, T., Fujisaki, J., Hirabayashi, D., Kawasaki, K., Hamada, T., Mori, Y., Kamikawa, Y., Mukai, H. and Sato, T. (2013). Clinical study on anti-fungal drug activity against clinically isolated strains of oral Candida species. *Oral Science International,* 10: 87-94.

Kang, S. H., Kim, Y. S., Kim, E. K., Hwang, J. W., Jeong, J. H., Dong, X., Lee, J.W., Moon, S.H., Jeon, B.T. and Park, P. J. (2016). Anticancer effect of thymol on AGS human gastric carcinoma cells. J Microbiol Biotechnol, 26: 28-37.

Kartsonis, N.A., Saah, A., Lipka, C.J., Taylor, A., and Sable, C.A. (2004). Second-line therapy with caspofungin for mucosal or invasive candidiasis: results from the caspofungin compassionate-use study. *Journal of Antimicrobial Chemotherapy*, 53: 878-881.

Kassem, M.A., ElMeshad, A.N. and Fares, A.R., (2014). Enhanced bioavailability of buspirone hydrochloride via cup and core buccal tablets: formulation and in vitro/in vivo evaluation. *International Journal of Pharmaceutics*: 463, 68-80.

Kathiravan, M.K., Salake, A.B., Chothe, A.S., Dudhe, P.B., Watode, R.P., Mukta, M.S., and Gadhwe, S. (2012). The biology and chemistry of antifungal agents: a review. *Bioorganic and Medicinal Chemistry*, 20: 5678-5698.

Katiraee, F., Khosravi, A.R., Khalaj, V., Hajiabdolbaghi, M., Khaksar, A., Rasoolinejad, M., and Yekaninejad, M.S. (2010). Oropharyngeal

candidiasis and oral yeast colonization in Iranian Human Immunodeficiency Virus positive patients. *Journal of Medical Mycology,* 20: 8-14.

Katragkou, A., McCarthy, M., Alexander, E. L., Antachopoulos, C., Meletiadis, J., Jabra-Rizk, M. A., Petraitis, V., Roilides, E. and Walsh, T. J. (2015). In vitro interactions between farnesol and fluconazole, amphotericin B or micafungin against Candida albicans biofilms. *Journal of Antimicrobial Chemotherapy*, 70: 470-478.

Kavanagh, N., and Corrigan, O. I. (2004). Swelling and erosion properties of hydroxypropylmethylcellulose (Hypromellose) matrices—influence of agitation rate and dissolution medium composition. *International journal of pharmaceutics*, *279*: 141-152.

Khan, S., Kataria, P., Nakhat, P., and Yeole, P. (2007). Taste masking of ondansetron hydrochloride by polymer carrier system and formulation of rapid-disintegrating tablets. *AAPS pharmscitech*, *8*: E127-E133.

Kharenko, E., Larionova, N. and Demina, N. (2009). Mucoadhesive drug delivery systems (Review). *Pharmaceutical Chemistry Journal,* 43: 200-208.

Kilian, M., Mestecky, J. and Russell, M. (1988). Defense mechanisms involving Fc-dependent functions of immunoglobulin A and their subversion by bacterial immunoglobulin A proteases. *Microbiological Reviews,* 52: 296-303.

Kleinegger, C.L., Stoeckel, D.C. and Kurago, Z.B. (2001). A comparison of salivary calprotectin levels in subjects with and without oral candidiasis. *Oral Surgery, Oral Medicine, Oral Pathology, Oral Radiology, and Endodontology,* 92: 62-67.

Koburger, T., Hübner, N. O., Braun, M., Siebert, J., and Kramer, A. (2010). Standardized comparison of antiseptic efficacy of triclosan, PVP–iodine, octenidine dihydrochloride, polyhexanide and chlorhexidine digluconate. *Journal of Antimicrobial Chemotherapy*, *65*: 1712-1719.

Koffi, A., Agnely, F., Ponchel, G. and Grossiord, J. (2006). Modulation of the rheological and mucoadhesive properties of thermosensitive poloxamer-based hydrogels intended for the rectal administration of quinine. *European Journal of Pharmaceutical Sciences,* 27**:** 328-335.

Kroemer, G., Galluzzi, L., Vandenabeele, P., Abrams, J., Alnemri, E. S., Baehrecke, E. H., Blagosklonny, M.V., El-Deiry, W.S., Golstein, P., Green, D.R. and Hengartner, M. (2009). Classification of cell death: recommendations of the Nomenclature Committee on Cell Death 2009. *Cell death and differentiation,* 16: 3-11.

Kruppa, M. (2009). Quorum sensing and Candida albicans. *Mycoses*, *52*: 1-10.

Kuipers, M.E., Heegsma, J., Bakker, H.I., Meijer, D.K., Swart, P.J., Frijlink, E.W., Eissens, A.C., Vries-Hospers, H.G.D. and Van Den Berg, J.M. (2002). Design and fungicidal activity of mucoadhesive lactoferrin tablets for the treatment of oropharyngeal candidosis. *Drug Delivery,* 9: 31-38.

Lalla, R. V., and Bensadoun, R. J. (2011). Miconazole mucoadhesive tablet for oropharyngeal candidiasis. *Expert review of anti-infective therapy*, *9*: 13-17.

Lamfon, H., Porter, S. R., McCullough, M., and Pratten, J. (2004). Susceptibility of Candida albicans biofilms grown in a constant depth film fermentor to chlorhexidine, fluconazole and miconazole: a longitudinal study. *Journal of Antimicrobial Chemotherapy*, *53*: 383-385.

Lamster, I. B., Lalla, E., Borgnakke, W. S., and Taylor, G. W. (2008). The relationship between oral health and diabetes mellitus. *The Journal of the American Dental Association*, *139*: 19S-24S.

Langenbucher, F. (1999). IVIVC: Indices for comparing release and response profiles. *Drug Development and Industrial Pharmacy*, *25*: 1223-1225.

Leardand, A. and Addy, M. (1997). The propensity of different brands of tea and coffee to cause staining associated with chlorhexidine. *Journal of Clinical Periodontology,* 24: 115-118.

Leek, H., and Albertsson, M. (2002). Pilocarpine treatment of xerostomia in head and neck patients. *Micron*, 33: 153-155.

Leigh, J. (2004). Saliva composition and flow rates are impacted by early HIV disease irrespective of xerostomic medications. *Journal of Evidence Based Dental Practice*, 4: 246-248.

Leito, J.T., Ligtenberg, A.J., Nazmi, K. and Veerman, E.C. (2009). Identification of salivary components that induce transition of hyphae to yeast in *Candida albicans*. *FEMS Yeast Research,* 9: 1102-1110.

Li, Q., Rudolph, V., Weigl, B. and Earl, A. (2004). Interparticle van der Waals force in powder flowability and compactibility. *International Journal of Pharmaceutics,* 280**:** 77-93.

Li, C. L., Martini, L. G., Ford, J. L., and Roberts, M. (2005). The use of hypromellose in oral drug delivery. *Journal of pharmacy and pharmacology*, *57*: 533-546.

Li, Y. C., Kuan, Y. H., Lee, T. H., Huang, F. M., and Chang, Y. C. (2014). Assessment of the cytotoxicity of chlorhexidine by employing an in vitro mammalian test system. *Journal of Dental Sciences,* 9: 130-135.

Lilly, E.A., Leigh, J.E., Joseph, S.H., and Fidel Jr, P.L. (2006). Candida-induced oral epithelial cell responses. *Mycopathologia*, 162: 25-32.

Lim, K. and Kam, P. 2008. Chlorhexidine--pharmacology and clinical applications. *Anaesthesia and Intensive Care,* 36**:** 502-512.

Lin, J. N., Lin, C. C., Lai, C. H., Yang, Y. L., Chen, H. T., Weng, H. C., Hsieh, L.-Y., Kuo, Y. C., Lauderdale, T. L. and Tseng, F. C. (2013). Predisposing factors for oropharyngeal colonization of yeasts in human immunodeficiency virus-infected patients: A prospective cross-sectional study. *Journal of Microbiology, Immunology and Infection*, 46: 129-135.

Liu, L. X., Marziano, I., Bentham, A. C., Litster, J. D., White, E. T., and Howes, T. (2008). Effect of particle properties on the flowability of ibuprofen powders. *International journal of pharmaceutics*, *362*: 109-117.

Livesey, G. (2003). Health potential of polyols as sugar replacers, with emphasis on low glycaemic properties. *Nutrition Research Reviews*, 16: 163-191.

Llana-Ruiz-Cabello, M., Gutiérrez-Praena, D., Pichardo, S., Moreno, F. J., Bermúdez, J. M., Aucejo, S., and Cameán, A. M. (2014). Cytotoxicity and morphological effects induced by carvacrol and thymol on the human cell line Caco-2. *Food and chemical toxicology*, 64: 281-290.

Lovelace, T. L., Fox, N. F., Sood, A. J., Nguyen, S. A., and Day, T. A. (2014). Management of radiotherapy-induced salivary hypofunction and consequent xerostomia in patients with oral or head and neck cancer: meta-analysis and literature review. *Oral surgery, oral medicine, oral pathology and oral radiology*, 117: 595-607.

Lu, Y., Su, C., Unoje, O., and Liu, H. (2014). Quorum sensing controls hyphal initiation in Candida albicans through Ubr1-mediated protein degradation. Proceedings of the National Academy of Sciences, 111: 1975-1980.

Mata, A.D., Marques, D., Rocha, S., Francisco, H., Santos, C., Mesquita, M.F. and Singh, J. (2004). Effects of diabetes mellitus on salivary secretion and its composition in the human. *Molecular and Cellular Biochemistry*, 261: 137-142.

Matanović, M. R., Kristl, J., and Grabnar, P. A. (2014). Thermoresponsive polymers: insights into decisive hydrogel characteristics, mechanisms of gelation, and promising biomedical applications. *International journal of pharmaceutics*, *472*: 262-275.

Mayer, F. L., Wilson, D., and Hube, B. (2013). Candida albicans pathogenicity mechanisms. Virulence, 4: 119-128.

Mese, H. and Matsuo, R. (2007). Salivary secretion, taste and hyposalivation. *Journal of Oral Rehabilitation,* 34: 711-723.

Mohammadi-Samani, S., Bahri-Najafi, R., and Yousefi, G. (2005). Formulation and in vitro evaluation of prednisolone buccoadhesive tablets. *Il Farmaco*, *60*: 339-344.

Mohammed, F. A., and Khedr, H. (2003). Preparation and *in vitro/in vivo* evaluation of the buccal bioadhesive properties of slow-release tablets containing miconazole nitrate. *Drug Development and Industrial Pharmacy*, *29*: 321-337.

Morschhäuser, J. (2002). The genetic basis of fluconazole resistance development in Candida albicans. *Biochimica et Biophysica Acta (BBA)-Molecular Basis of Disease*, *1587*: 240-248.

Moore, P. A., Guggenheimer, J., Etzel, K. R., Weyant, R. J., and Orchard, T. (2001). Type 1 diabetes mellitus, xerostomia, and salivary flow rates. *Oral Surgery, Oral Medicine, Oral Pathology, Oral Radiology, and Endodontology*,92, 281-291.

Morais, J. A. G., and Lobato, M. D. R. (2010). The new European Medicines Agency guideline on the investigation of bioequivalence. *Basic and Clinical Pharmacology and Toxicology*, *106*: 221-225.

Morales, J. O., and McConville, J. T. (2011). Manufacture and characterization of mucoadhesive buccal films. *European Journal of Pharmaceutics and Biopharmaceutics*, *77*: 187-199.

Mukherjee, P. K., and Chandra, J. (2004). Candida biofilm resistance. *Drug resistance updates*, *7*: 301-309.

Mumtaz, A. M., and Ch'ng, H. S. (1995). Design of a dissolution apparatus suitable for in situ release study of triamcinolone acetonide from bioadhesive buccal tablets. *International Journal of Pharmaceutics*, 121: 129-139.

Musteata, F.M. and Pawliszyn, J. (2005) Assay of stability, free and total concentration of chlorhexidine in saliva by solid phase microextraction. *Journal of Pharmaceutical and Biomedical Analysis,* 37: 1015-1024.

Nafee, N. A., Ismail, F. A., Boraie, N. A. and Mortada, L. M. (2003). Mucoadhesive buccal patches of miconazole nitrate: in vitro/in vivo performance and effect of ageing. *International Journal of Pharmaceutics,* 264: 1-14.

Nagy, Z. K., Balogh, A., Vajna, B., Farkas, A., Patyi, G., Kramarics, Á., and Marosi, G. (2012). Comparison of electrospun and extruded Soluplus®-based solid dosage forms of improved dissolution. *Journal of pharmaceutical sciences*, *101*: 322-332.

Nair, R.G., and Samaranayake, L.P. (1996). The effect of oral commensal bacteria on candidal adhesion to human buccal epithelial cells in vitro. *Journal of Medical Microbiology*, 45: 179-185.

Närhi, T. O., Meurman, J. H., and Ainamo, A. (1999). Xerostomia and hyposalivation. *Drugs and Aging,* 15: 103-116.

Navazesh, M., Wood, G.J., and Brightman, V.J. (1995). Relationship between salivary flow rates and *Candida albicans* counts. *Oral Surgery, Oral Medicine, Oral Pathology, Oral Radiology and Endodontology*, 80: 284-288

Odds, F. C. (2003). Synergy, antagonism, and what the chequerboard puts between them. *Journal of Antimicrobial Chemotherapy*, 52: 1-1.

Odds, F.C., Brown, A.J. and Gow, N.A. (2003). Antifungal agents: mechanisms of action. *Trends in Microbiology,* 11: 272-279.

O'Hara, T., Dunne, A., Butler, J., Devane, J., and IVIVR Cooperative Working Group (1998). A review of methods used to compare dissolution profile data. *Pharmaceutical Science and Technology Today*, 1: 214-223.

Owotade, F.J. and Patel, M. (2014). Virulence of oral Candida isolated from HIV-positive women with oral candidiasis and asymptomatic carriers. *Oral Surgery, Oral Medicine, Oral Pathology and Oral Radiology,* 118: 455-460.

Ozen, T., Demirtas, I., and Aksit, H. (2011). Determination of antioxidant activities of various extracts and essential oil compositions of Thymus praecox subsp. skorpilii var. skorpilii. *Food Chemistry*, 124: 58-64.

Parodi, B., Russo, E., Caviglioli, G., Cafaggi, S., and Bignardi, G. (1996). Development and characterization of a buccoadhesive dosage form of oxycodone hydrochloride. *Drug Development and Industrial Pharmacy*, *22*: 445-450.

Partenhauser, A., and Bernkop-Schnürch, A. (2016). Mucoadhesive polymers in the treatment of dry X syndrome. *Drug Discovery Today*, *21*: 1051-1062.

Pascal, C., Bigey, F., Ratomahenina, R., Boze, H., Moulin, G. and Sarni-Manchado, P. (2006). Overexpression and characterization of two human salivary proline rich proteins. *Protein Expression and Purification,* 47: 524-532.

Passerini, N., Albertini, B., González-Rodríguez, M. L., Cavallari, C., and Rodriguez, L. (2002). Preparation and characterisation of ibuprofen–poloxamer 188 granules obtained by melt granulation. *European Journal of Pharmaceutical Sciences*, *15*: 71-78.

Patenaude, C., Zhang, Y., Cormack, B., Köhler, J., and Rao, R. (2013). Essential role for vacuolar acidification in Candida albicans virulence. Journal of Biological Chemistry, 288: 26256-26264.

Paul, R., Paul, M., Paul, G. and Paul, R. (2011). Saliva-The Sentinel of the Oral Cavity. *Heal Talk,* 3: 17-18.

Peeters, E., Nelis, H. J., and Coenye, T. (2008). Comparison of multiple methods for quantification of microbial biofilms grown in microtiter plates. *Journal of microbiological methods*, 72: 157-165.

Peppas, N., Bures, P., Leobandung, W. and Ichikawa, H. (2000). Hydrogels in pharmaceutical formulations. *European Journal of Pharmaceutics and Biopharmaceutics,* 50: 27-46.

Peppas, N.A. and Sahlin, J.J. (1996). Hydrogels as mucoadhesive and bioadhesive materials: a review. *Biomaterials,* 17: 1553-1561.

Perioli, L., Ambrogi, V., Giovagnoli, S., Blasi, P., Mancini, A., Ricci, M. and Rossi, C. (2008). Influence of compression force on the behavior of mucoadhesive buccal tablets. *AAPS PharmSciTech,* 9: 274-281.

Perioli, L., Ambrogi, V., Rubini, D., Giovagnoli, S., Ricci, M., Blasi, P. and Rossi, C. (2004). Novel mucoadhesive buccal formulation containing metronidazole for the treatment of periodontal disease. *Journal of Controlled Release,* 95: 521-533.

Petrone, D., Condemi, J. J., Fife, R., Gluck, O., Cohen, S., and Dalgin, P. (2002). A double-blind, randomized, placebo-controlled study of cevimeline in Sjögren's syndrome patients with xerostomia and keratoconjunctivitis sicca. *Arthritis and Rheumatism*, *46*: 748-754.

Pitt, K. G., Newton, J. M., & Stanley, P. (1988). Tensile fracture of doubly-convex cylindrical discs under diametral loading. *Journal of materials science*, *23*: 2723-2728.

Pierce, C. G., Uppuluri, P., Tristan, A. R., Wormley, F. L., Mowat, E., Ramage, G., and Lopez-Ribot, J. L. (2008). A simple and reproducible 96-well plate-based method for the formation of fungal biofilms and its application to antifungal susceptibility testing. *Nature protocols*, 3: 1494-1500.

Plemons, J. M., Al-Hashimi, I., and Marek, C. L. (2014). Managing xerostomia and salivary gland hypofunction: executive summary of a report from the American Dental Association Council on Scientific Affairs. *The Journal of the American Dental Association*, 145: 867-873.

Plumb, J. A. (2004). Cell sensitivity assays: the MTT assay. Cancer cell culture: methods and protocols, 165-169.

Public Health of England. (2016). *HIV in the UK: 2016 report.* [online] Gov.uk. Available at:
https://assets.publishing.service.gov.uk/government/uploads/system/uploads/attachment_data/file/602942/HIV_in_the_UK_report.pdf

Rahamatullah Shaikh, T.R.R.S., Garland, M.J., Woolfson, A.D. and Donnelly, R.F. (2011). Mucoadhesive drug delivery systems. *Journal of Pharmacy and Bioallied Sciences,* 3: 89-100.

Ramage, G., Jose, A., Coco, B., Rajendran, R., Rautemaa, R., Murray, C., Lappin, D.F and Bagg, J. (2011). Commercial mouthwashes are more effective than azole antifungals against Candida albicans biofilms in vitro. Oral Surgery, *Oral Medicine, Oral Pathology, Oral Radiology, and Endodontology*, 111: 456-460.

Ramage, G., Saville, S. P., Wickes, B. L., and López-Ribot, J. L. (2002). Inhibition of Candida albicans biofilm formation by farnesol, a quorum-sensing molecule. *Applied and environmental microbiology*, 68: 5459-5463.

Reichhardt, M.P., Jarva, H., De Been, M., Rodriguez, J.M., Quintana, E.J., Loimaranta, V., De Vos, W.M. and Meri, S. (2014). The Salivary Scavenger and Agglutinin in Early Life: Diverse Roles in Amniotic Fluid and in the Infant Intestine. *The Journal of Immunology,* 193: 5240-5248

Repetto, G., Del Peso, A., and Zurita, J. L. (2008). Neutral red uptake assay for the estimation of cell viability/cytotoxicity. *Nature protocols*, 3: 1125-1131.

Revankar, S.G., Kirkpatrick, W.R., Mcatee, R.K., Dib, O.P., Fothergill, A.W., Redding, S.W., Rinaldi, M.G., Hilsenbeck, S.G. and Patterson, T.F. (1998). A randomized trial of continuous or intermittent therapy with fluconazole for oropharyngeal candidiasis in HIV-infected patients: clinical outcomes and development of fluconazole resistance. *The American Journal of Medicine,* 105: 7-11.

Rhee, Y. S., Shin, Y. H., Park, C. W., Chi, S. C., and Park, E. S. (2006). Effect of flavors on the viscosity and gelling point of aqueous poloxamer solution. *Archives of pharmacal research*, 29: 1171-1178.

Riss T.L., Moravec R.A., Niles A.L., Duellman S., Benink H. A., Worzella T. J., and Minor L. Cell Viability Assays. 2013 (Updated 2016). In: Sittampalam G.S., Coussens N.P., Brimacombe K, *et al*., editors. Assay Guidance Manual (Internet). Bethesda (MD): Eli Lilly and Company and the National Center for Advancing Translational Sciences; 2004-. Available from: https://www.ncbi.nlm.nih.gov/books/NBK144065/

Rowe, R. C., Sheskey, P. J., and Weller, P. J. (Eds.). (2006). *Handbook of pharmaceutical excipients* (Vol. 6). London: Pharmaceutical press.

Roy, S., Pal, K., Anis, A., Pramanik, K. and Prabhakar, B. (2009). Polymers in mucoadhesive drug-delivery systems: a brief note. *Designed Monomers and Polymers,* 12: 483-495.

Ruel-Gariepy, E., & Leroux, J. C. (2004). In situ-forming hydrogels—review of temperature-sensitive systems. *European Journal of Pharmaceutics and Biopharmaceutics*, *58*: 409-426.

Salamat-Miller, N., Chittchang, M. and Johnston, T.P. (2005). The use of mucoadhesive polymers in buccal drug delivery. *Advanced Drug Delivery Reviews,* 57: 1666-1691.

Salim, N., Moore, C., Silikas, N., Satterthwaite, J. and Rautemaa, R. (2013) Chlorhexidine is a highly effective topical broad-spectrum agent against Candida spp. *International Journal of Antimicrobial Agents,* 41: 65-69.

Salimi, A., Alami, B., and Pourahmad, J. (2017). Analysis of cytotoxic effects of chlorhexidine gluconate as antiseptic agent on human blood lymphocytes. *Journal of Biochemical and Molecular Toxicology*. 31: 1-8.

Samaranayake, L. and Macfarlane, T. (1982). The effect of dietary carbohydrates on the in-vitro adhesion of Candida albicans to epithelial cells. *Journal of Medical Microbiology, 15:* 511-517.

Sankar, V., Hearnden, V., Hull, K., Juras, D.V., Greenberg, M., Kerr, A., Lockhart, P.B., Patton, L.L., Porter, S. and Thornhill, M. (2011). Local drug delivery for oral mucosal diseases: challenges and opportunities. *Oral Diseases,* 17: 73-84.

Sarkar, N., and Walker, L. C. (1995). Hydration—dehydration properties of methylcellulose and hydroxypropylmethylcellulose. *Carbohydrate polymers*, *27*: 177-185.

Sarode, S.C., Sarode, G.S. and Patil, S. (2014). Role of Statherin in oral carcinogenesis. *Oral Oncology,* 50: 55-56.

Savica, V., Calo, L. A., Monardo, P., Davis, P. A., Granata, A., Santoro, D., and Bellinghieri, G. (2009). Salivary phosphate-binding chewing gum reduces hyperphosphatemia in dialysis patients. *Journal of the American Society of Nephrology*, *20*: 639-644.

Schipper, R.G., Silletti, E. and Vingerhoeds, M.H. (2007). Saliva as research material: biochemical, physicochemical and practical aspects. *Archives of Oral Biology,* 52: 1114-1135.

Şenel, S., Ikinci, G., Kaş, S., Yousefi-Rad, A., Sargon, M. F., and Hıncal, A. A. (2000). Chitosan films and hydrogels of chlorhexidine gluconate for oral mucosal delivery. *International journal of pharmaceutics*, *193*: 197-203.

Seelig, M.S. (1966). Mechanisms by which antibiotics increase the incidence and severity of candidiasis and alter the immunological defences. *Bacteriological Reviews,* 30**:** 442-459.

Shahin, E. S., Meijers, J. M. M., Schols, J. M. G. A., Tannen, A., Halfens, R. J. G., and Dassen, T. (2010). The relationship between malnutrition parameters and pressure ulcers in hospitals and nursing homes. *Nutrition*, *26*: 886-889.

Shettigar, N. B., Das, S., Rao, N. B., and Rao, S. (2015). Thymol, a monoterpene phenolic derivative of cymene, abrogates mercury-induced oxidative stress resultant cytotoxicity and genotoxicity in hepatocarcinoma cells*. Environmental toxicology,* 30: 968-980.

Shiboski, C.H. and Shiboski, S.C. (2013). Smoking Is an Independent Risk Factor for the Development of Oral Candidiasis (OC) in HIV-1 Infected Persons. *Journal of Evidence Based Dental Practice*, 13: 180-182.

Ship, J. A. (2003). Diabetes and oral health: an overview. *The Journal of the American Dental Association*, *134*: 4S-10S.

Shirtliff, M. E., Krom, B. P., Meijering, R. A., Peters, B. M., Zhu, J., Scheper, M. A., Harris, M.L. and Jabra-Rizk, M. A. (2009). Farnesol-induced apoptosis in Candida albicans. *Antimicrobial agents and chemotherapy*, 53: 2392-2401.

Shrestha, A., Rimal, J., Rao, A., Sequeira, P. S., Doshi, D., and Bhat, G. K. (2011). In vitro antifungal effect of mouth rinses containing chlorhexidine and thymol. *Journal of Dental Sciences*, 6: 1-5.

Siepmann, J. and Peppas, N. (2012). Modeling of drug release from delivery systems based on hydroxypropyl methylcellulose (HPMC). *Advanced Drug Delivery Reviews,* 64: 163-174.

Singh, A., Bharati, A., Frederiks, P., Verkinderen, O., Goderis, B., Cardinaels, R., Moldenaers, P., Van Humbeeck, J. and Van den Mooter, G. (2016). Effect of Compression on the Molecular Arrangement of Itraconazole–Soluplus Solid Dispersions: Induction of Liquid Crystals or Exacerbation of Phase Separation? *Molecular pharmaceutics*, 13: 1879-1893.

Skehan, P., Storeng, R., Scudiero, D., Monks, A., McMahon, J., Vistica, D., Warren, J.T., Bokesch, H., Kenney, S. and Boyd, M. R. (1990). New colorimetric cytotoxicity assay for anticancer-drug screening. JNCI: *Journal of the National Cancer Institute,* 82: 1107-1112.

Skiest, D. J., Vazquez, J.A., Anstead, G.M., Graybill, J.R., Reynes, J., Ward, D., Hare, R., Boparai, N. and Isaacs, R. (2007). Posaconazole for the treatment of azole-refractory oropharyngeal and esophageal candidiasis in subjects with HIV infection. *Clinical Infectious Diseases,* 44: 607-614.

Slomiany, B.L., Murty, V.L.N., Piotrowski, J., and Slomiany, A. (1996). Salivary mucins in oral mucosal defense. *General Pharmacology: The Vascular System*, 27: 761-771.

Smart, J.D. (2005). The basics and underlying mechanisms of mucoadhesion. *Advanced Drug Delivery Reviews,* 57: 1556-1568.

Sosnik, A., Das Neves, J. and Sarmento, B. (2014). Mucoadhesive polymers in the design of nano-drug delivery systems for administration by non-parenteral routes: a review. *Progress in Polymer Science,* 39: 2030-2075.

Souza, L. B. D., Aquino, S. G. D., Souza, P. P. C. D., Hebling, J., and Costa, C. A. D. S. (2007). Cytotoxic effects of different concentrations of chlorhexidine. *American Journal of Dentistry*, 20: 400-404.

Soysa, N. and Ellepola, A. (2005). The impact of cigarette/tobacco smoking on oral candidosis: An overview. *Oral Diseases*, 11: 268-273.

Soysa, N. S., Samaranayake, L. P., and Ellepola, A. N. B. (2006). Diabetes mellitus as a contributory factor in oral candidosis. *Diabetic medicine*, *23*: 455-459.

Soysa, N.S., Samaranayake, L.P., and Ellepola, A.N. (2004). Cytotoxic drugs, radiotherapy and oral candidiasis. *Oral Oncology*, 40: 971-978.

Soysa, N.S., Samaranayake, L.P., and Ellepola, A.N.B. (2008). Antimicrobials as a contributory factor in oral candidosis–a brief overview. *Oral Diseases*, 14: 138-143.

Squier, C. (1991). The permeability of oral mucosa. *Critical Reviews in Oral Biology and Medicine,* 2: 13-32.

Sreebny, L. M., and Schwartz, S. S. (1997). A reference guide to drugs and dry mouth–2nd edition. *Gerodontology*, *14*: 33-47.

Sreenivasan, P. and Gittins, E. (2004). The effects of a chlorhexidine mouthrinse on culturable microorganisms of the tongue and saliva. *Microbiological Research,* 159: 365-370.

Steele, C., Leigh, J., Swoboda, R., and Fidel, P.L. (2000). Growth inhibition of Candida by human oral epithelial cells. *Journal of Infectious Diseases*, 182: 1479-1485.

Stoltenberg, I., and Breitkreutz, J. (2011). Orally disintegrating mini-tablets (ODMTs)–a novel solid oral dosage form for paediatric use. *European Journal of Pharmaceutics and Biopharmaceutics*, *78*: 462-469.

Suci, P. A., and Tyler, B. J. (2002). Action of chlorhexidine digluconate against yeast and filamentous forms in an early-stage Candida albicans biofilm. Antimicrobial agents and chemotherapy, 46: 3522-3531.

Sudhakar, Y., Kuotsu, K., and Bandyopadhyay, A. K. (2006). Buccal bioadhesive drug delivery—a promising option for orally less efficient drugs. *Journal of controlled release*, *114*: 15-40.

Sunesen, V. H., Pedersen, B. L., Kristensen, H. G., and Müllertz, A. (2005). In vivo in vitro correlations for a poorly soluble drug, danazol, using the flow-through dissolution method with biorelevant dissolution media. *European journal of pharmaceutical sciences*, *24*: 305-313.

Thompson, G. R., Patel, P. K., Kirkpatrick, W. R., Westbrook, S. D., Berg, D., Erlandsen, J., Redding, S. W. and Patterson, T. F. (2010). Oropharyngeal candidiasis in the era of antiretroviral therapy. *Oral Surgery, Oral Medicine, Oral Pathology, Oral Radiology, and Endodontology,* 109: 488-495.

Torres, S. R., Peixoto, C. B., Caldas, D. M., Silva, E. B., Akiti, T., Nucci, M., and de Uzeda, M. (2002). Relationship between salivary flow rates and Candida counts in subjects with xerostomia. *Oral Surgery, Oral Medicine, Oral Pathology, Oral Radiology, and Endodontology,* 93: 149-154.

Tsibouklis, J., Middleton, A. M., Patel, N., and Pratten, J. (2013). Toward mucoadhesive hydrogel formulations for the management of xerostomia: the physicochemical, biological, and pharmacological considerations. *Journal of Biomedical Materials Research Part A*, 101: 3327-3338.

Tuğcu-Demiröz, F., Acartürk, F., Takka, S., and Konuş-Boyunağa, Ö. (2004). In-vitro and in-vivo evaluation of mesalazine–guar gum matrix tablets for colonic drug delivery. *Journal of drug targeting*, *12*: 105-112.

Türkez, H., and Aydın, E. (2013). In vitro cytotoxicity, genotoxicity and antioxidant potentials of thymol on human blood cells. *Journal of Essential Oil Research,* 26: 133-140.

Tosun, İ. (2012). Ammonium removal from aqueous solutions by clinoptilolite: determination of isotherm and thermodynamic parameters and comparison of kinetics by the double exponential model and conventional kinetic models. *International journal of environmental research and public health*, *9*: 970-984.

Valenti, P. and Antonini, G. (2005). Lactoferrin. *Cellular and Molecular Life Sciences,* 62: 2576-2587.

Van Lancker, A., Verhaeghe, S., Van Hecke, A., Vanderwee, K., Goossens, J., and Beeckman, D. (2012). The association between malnutrition and oral

health status in elderly in long-term care facilities: a systematic review. *International journal of nursing studies*, *49*: 1568-1581.

Van Steijn, G.J., Nieuw Amerongen, A.V., Veerman, E.C., Kasanmoentalib, S. and Overdijk, B. (1999). Chitinase in whole and glandular human salivas and in whole saliva of patients with periodontal inflammation. *European Journal of Oral Sciences,* 107: 328-337.

Van't Hof, W., Blankenvoorde, M.F., Veerman, E.C. and Amerongen, A.V.N. (1997). The salivary lipocalin von Ebner's gland protein is a cysteine proteinase inhibitor. *Journal of Biological Chemistry,* 272: 1837-1841.

Velasco, M. V., Ford, J. L., Rowe, P. and Rajabi-Siahboomi, A. R. (1999). Influence of drug: hydroxypropylmethylcellulose ratio, drug and polymer particle size and compression force on the release of diclofenac sodium from HPMC tablets. *Journal of Controlled Release,* 57: 75-85.

Vertzoni, M., Symillides, M., Iliadis, A., Nicolaides, E., and Reppas, C. (2003). Comparison of simulated cumulative drug versus time data sets with indices. *European Journal of Pharmaceutics and Biopharmaceutics*, *56*: 421-428.

Vichai, V., and Kirtikara, K. (2006). Sulforhodamine B colorimetric assay for cytotoxicity screening. *Nature protocols,* 1: 1112-1116.

Vyas, V., Sancheti, P., Karekar, P., Shah, M. and Pore, Y. (2009). Physicochemical characterization of solid dispersion systems of tadalafil with poloxamer 407. *Acta Pharmaceutica,* 59**:** 453-461.

Wang, Y., Gao, J., Yin, Q., and Hao, H. (2012). Isolation and characterization of a new polymorph of D-sorbitol. *Crystal Research and Technology*, *47*: 409-414.

Westermarck, S., Juppo, A. M., Kervinen, L., and Yliruusi, J. (1998). Pore structure and surface area of mannitol powder, granules and tablets determined with mercury porosimetry and nitrogen adsorption. *European journal of pharmaceutics and biopharmaceutics*, *46*: 61-68.

Williams, D. W., Kuriyama, T., Silva, S., Malic, S., and Lewis, M. A. (2011). Candida biofilms and oral candidosis: treatment and prevention. *Periodontology 2000*, *55*: 250-265.

Williams, D.W., Walker, R., Lewis, M.A., Allison, R.T., and Potts, A.J. (1999). Adherence of Candida albicans to oral epithelial cells differentiated by Papanicolaou staining. *Journal of Clinical Pathology*, 52: 529-531.

Wong, C.F., Yuen, K.H. and Peh, K.K. (1999). An in-vitro method for buccal adhesion studies: importance of instrument variables. *International Journal of Pharmaceutics,* 180: 47-57.

Wu, L., Feng, J., Shi, L., Shen, X., Liu, W., and Zhou, Z. (2013). Candidal infection in oral leukoplakia: a clinicopathologic study of 396 patients from eastern China. *Annals of Diagnostic Pathology*, 17: 37-40.

Xu, T., Levitz, S., Diamond, R. and Oppenheim, F. (1991). Anticandidal activity of major human salivary histatins. *Infection and Immunity,* 59: 2549-2554.

Yamaguchi, A., Muramatsu, N., Mimura, N., Shirai, M., and Sato, O. (2017). Intramolecular dehydration of biomass-derived sugar alcohols in high-temperature water. *Physical Chemistry Chemical Physics*, *19*: 2714-2722.

Yang, D., Yuan, P., Zhu, J., and He, H. (2007). Synthesis and characterization of antibacterial compounds using montmorillonite and chlorhexidine acetate. *Journal of Thermal Analysis and Calorimetry*, 89: 847-852.

Yang, L., Johnson, B., and Fassihi, R. (1998). Determination of continuous changes in the gel layer thickness of poly (ethylene oxide) and HPMC tablets undergoing hydration: a texture analysis study. *Pharmaceutical research*, *15*, 1902-1906.

Yeh, C.-K., Dodds, M.W., Zuo, P. and Johnson, D.A. (1997). A population-based study of salivary lysozyme concentrations and candidal counts. *Archives of Oral Biology,* 42: 25-31.

Yoshijima, Y., Murakami, K., Kayama, S., Liu, D., Hirota, K., Ichikawa, T., and Miyake, Y. (2010). Effect of substrate surface hydrophobicity on the adherence of yeast and hyphal Candida. *Mycoses*, *53*: 221-226.

Zakaria, M. N., Furuta, M., Takeshita, T., Shibata, Y., Sundari, R., Eshima, N., and Yamashita, Y. (2017). Oral mycobiome in community-dwelling elderly and its relation to oral and general health conditions. *Oral diseases*, *23*: 973-982.

Zeng, P., Rao, A., Wiedmann, T. S., and Bowles, W. (2009). Solubility properties of chlorhexidine salts. *Drug development and industrial pharmacy*, *35*: 172-176.

Zhang, Y., Huo, M., Zhou, J., Zou, A., Li, W., Yao, C., and Xie, S. (2010). DDSolver: an add-in program for modeling and comparison of drug dissolution profiles. The AAPS Journal, 12: 263-271.

Appendices

Appendices

Appendix A: Hydration fitted curves

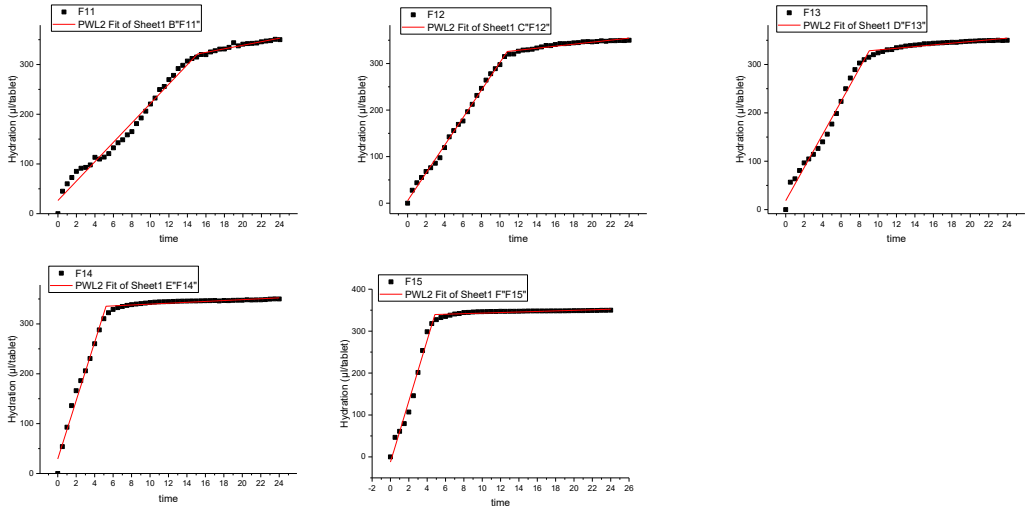

Figure A 1 Hydration curves fitted with PWL2 for F11-F15 (obtained from origin pro software).

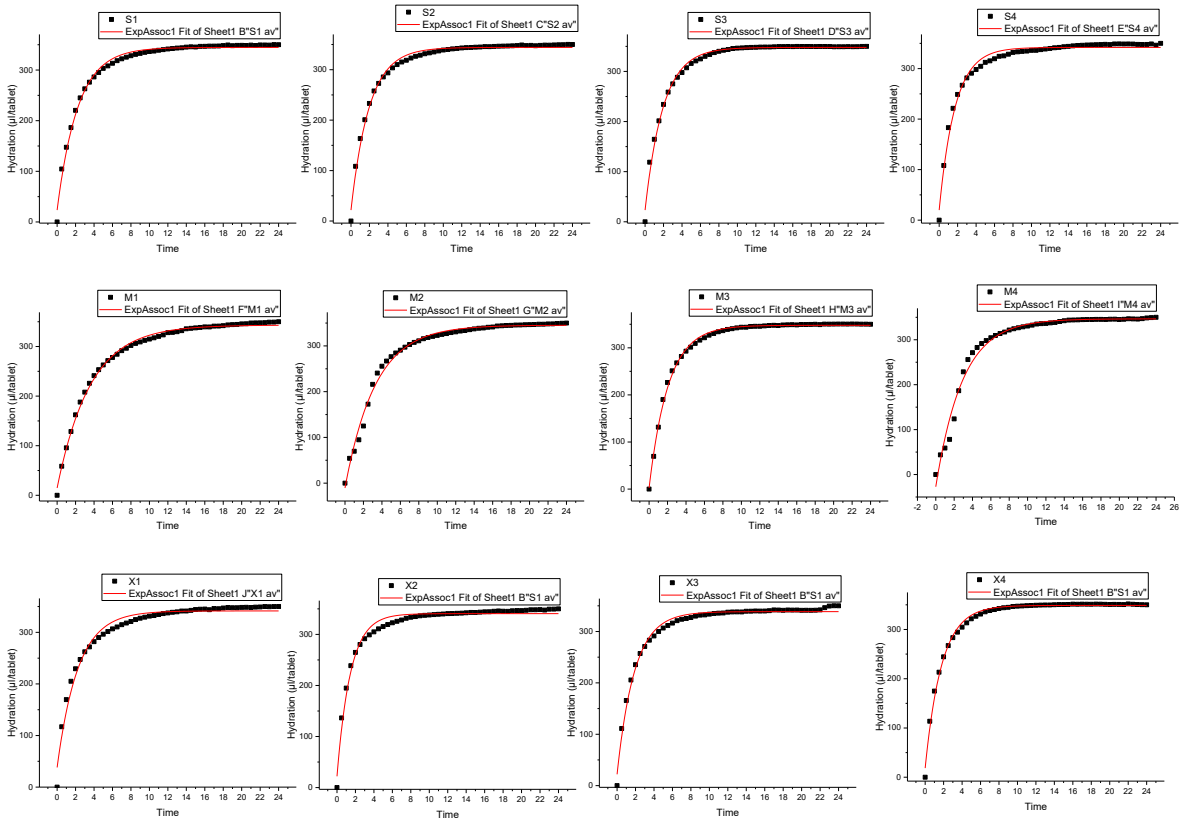

Figure A 2 Hydration curves fitted with two-phase exponential model (ExponAssoc1).

Appendix B: Rate constant of the hydration curves

Table B 1 Rate constant of the hydration curves for Exponential fitted model

Formulations	Exponential (K)
F11	0.06
F12	0.14
F13	0.18
F14	0.36
F15	0.37

Table B 2 Rate constant of the hydration curves for PWL2, EXP and AxpAss2 fitted models.

Formulations	PWL2		Exponential	ExpAss2	
	K1 (µL/tab.hr)	K2 (µL/tab.hr)	K (hr^{-})	K1 (hr^{-})	K2 (hr^{-})
S1	72.64	2.29	0.44	0.99	0.26
S2	84.80	2.15	0.51	1.12	0.29
S3	74.16	1.52	0.51	1.10	0.32
S4	102.58	2.28	0.58	0.23	1.18
M1	54.19	3.85	0.28	0.13	0.46
M2	61.55	3.14	0.30	0.00	0.35
M3	79.94	1.85	0.48	1.00	0.34
M4	68.30	2.30	0.34	0.95	0.44
X1	79.12	2.92	0.44	0.23	1.48
X2	126.34	2.15	0.69	1.35	0.25
X3	83.86	2.07	0.53	1.21	0.30
X4	87.61	1.57	0.56	0.42	1.90